Records of aeolian dust deposition on the Chinese Loess Plateau during the Late Quaternary

J.M. Sun[1, 2], K.E. Kohfeld[1], and S. P. Harrison[1]

[1]Max Planck Institute for Biogeochemistry, Postfach 10 01 64, D-07701 Jena, Germany

[2]Institute of Geology, Chinese Academy of Science, P. O. Box 9825, Beijing 100029, China

Abstract

The Dust Indicators and Records of Terrestrial and MArine Palaeoenvironments (DIRTMAP) data base was established to use geologic records of dust as a means of validating earth-system model simulations of the dust cycle for key times in the past. The DIRTMAP data base originally comprised records from ice cores and marine sediments. However, terrestrial (loess) deposits are a potentially important archive of information about changes in dust accumulation on the continents during the Quaternary period. Their potential as a tool for validating earth-system model simulations of dust has not been explored.

The Chinese Loess Plateau (CLP) contains a 7 million-year record of aeolian deposition. It therefore provides an excellent test case of the potential to use loess records as temporally- and spatially-explicit records of dust accumulation through time. Here we present a synthesis of the data documenting changes in loess and soil accumulation across the CLP during the last 150,000 years (Marine Isotope Stages 1-5). We examined data from 98 sites on the CLP, from several topographically distinct depositional environments. Age models and aeolian mass accumulation rates (MAR) could be determined at 77 of these sites using independent chronologies based on either pedostratigraphy, bulk magnetic susceptibility, radiocarbon or luminescence ages. Comparison of these chronologies suggests that changes in MAR through time are not as well-constrained as might be expected: there are relatively few reliable radiometric or luminescence dates, the magnetic susceptibility records are poorly correlated (<0.5) with the marine isotope stratigraphy at most sites, and the pedostratigraphic age models are based on assumptions that limit their usefulness. Thus, although the CLP represents perhaps the best-studied loess region in the world, there is still much work to be done to quantify changes in the aeolian mass accumulation rates, particularly in terms of developing better and more complete chronologies.

Aeolian MARs for Stage 2 are on average 4.9 times greater than Stage 5 and 3.5 times greater than Stage 1. Stage 5 exhibits the lowest accumulation rates (109 $g/m^2/yr$); Stage 2 exhibits the highest accumulation rates (467 $g/m^2/yr$). MAR values are highest in the northwest of the CLP, and lowest in the southeast, during all Marine Isotope Stages. This observation is consistent with the suggestion that dust for the entire CLP is derived consistently from the northwest. As a corollary to these observations, the largest glacial-interglacial changes in accumulation rates were observed in the southeast CLP.

Both the temporal and spatial patterns are strongly influenced by geomorphological setting. MARs from loess terraces are consistently higher than at non-terrace sites (on average 2-4 times greater for Stages 1, 2, and 4). Glacial-interglacial differences in MAR are therefore greatly amplified at loess terrace sites compared with non-terrace sites. However, the pattern of highest MAR values in the northwestern CLP is more pronounced when only non-terrace sites are considered. This appears to reflect the fact that there is considerably more inter-site variability in accumulation rates at terrace sites, which are heavily influenced by local sources, than at non-terrace sites.

Table of Contents

List of Figures

List of Tables

1. Introduction

Ice core and marine records show that the amount of dust in the atmosphere has varied both spatially and temporally throughout the Quaternary (see e.g. Petit et al., 1981; Hovan et al., 1989; Tiedemann et al., 1989; Petit et al., 1990; Hovan et al., 1991; Rea, 1994; Petit et al., 1999; Kohfeld and Harrison, in press). These changes in the atmospheric dust loading clearly occur in response to climatic and environmental changes. However, dust is not a passive factor in the climate system: earth-system models show that there are significant feedbacks associated with changes in atmospheric dust loading (Andreae, 1995; Tegen et al., 1996; Tegen and Lacis, 1996) and the impact of these feedbacks could have been significant on glacial-interglacial timescales (Overpeck et al., 1996; Harrison et al., in press). The investigation of the role of dust in palaeoclimate changes is a major focus of earth system modelling, largely because such model investigations can be combined with geological data documenting the actual changes in dust loading. The use of geologic data for model validation is greatly facilitated when the data are available in public-access data bases (Kohfeld and Harrison, 2000). The Dust Indicators and Records of Terrestrial and MArine Palaeoenvironments (DIRTMAP) data base was therefore established in 1997 to provide a global palaeoenvironmental data set that can be used to validate earth-system model simulations of the dust cycle for key times during the past 150,000 years (Kohfeld and Harrison, in press).

The DIRTMAP data base originally consisted of records of dust accumulation found in marine and ice core records (see e.g. Mahowald et al., 1999). However, terrestrial (loess) sites could also provide spatially explicit records of dust deposition on the continents. The use of terrestrial records could significantly enhance the spatial coverage of the DIRTMAP database, and hence its usefulness as a validation tool. However, the interpretation of loess deposits as a measure of dust accumulation rates is more difficult than either marine or ice core records. First, loess areas can act both as sources and sinks for mineral dust. Second, the degree to which individual sites acts as sources or sinks, and the overall rate of deposition, can be affected by the geomorphic setting. Third, the possibilities of dating terrestrial loess records are limited by the paucity of datable materials. Finally, in common with most terrestrial records, the recent loess record has the potential to be significantly impacted by human activities. Thus, it can be difficult to determine the modern accumulation rate which would serve as a baseline for assessing changes in accumulation rates at specific sites.

The aim of the present work is to evaluate whether, despite these potential problems, loess records could be used to provide a record of dust accumulation rates during the Late Quaternary and thus to extend the spatial extent of records used to evaluate models of the palaeodust cycle. For this evaluation we have focussed on a single region, namely the Chinese Loess Plateau (CLP). The CLP was chosen because (1) the loess deposits are extensive and there are a very large number of individual sections described in the literature, (2) the record is now believed to extend over the last 7 Ma (e.g. (Ding et al., 1999), and thus provides an opportunity to reconstruct and compare accumulation rates at several different time periods, and (3) the deposits have been intensively studied using a variety of different geological, sedimentological, geochemical and dating methods, and this provides an opportunity to evaluate the usefulness of different approaches. Records from the CLP are considered to provide one of the classic reconstructions of climate change on glacial-interglacial timescales (e.g Liu, 1985;

Kukla, 1987; Ding et al., 1990; An et al., 1991a; 1991b), and our focus on these records is therefore likely to provide the most favourable evaluation of the potential of loess to yield dust accumulation rates.

1.1 Characteristics of Chinese Loess

Chinese loess is distributed in the mid-latitude regions (between 30° and 49° N), and cover an area of ca 440,000 km^2 (Liu, 1985). The loess thickness in the central and southern parts of the CLP ranges from 110-180 m, with maximum thicknesses exceeding 300 m in the northern and northwestern parts of the CLP (Derbyshire, 1984).

Meteorological observations of modern dust storms (Liu et al., 1981) suggest that Chinese loess is derived from the Gobi Desert and the sand deserts in the arid- to semi-arid regions of northwestern China. Dust from these regions is not only deposited directly downwind to form the CLP, but also can be transported across the North Pacific and has been recorded as far as 3600 km away from the source regions (Hovan et al., 1989; 1991).

2. Organisation of this Report

We have made the most comprehensive compilation to date of pedostratigraphic, magnetic susceptibility, and chronological data (radiocarbon, thermoluminescence, and optically stimulated luminescence dates) from individual sections on the CLP. We use these data to determine the changes in the mass accumulation rates (MAR) of aeolian material on the CLP for five time periods (corresponding to Marine Oxygen Isotope Stages 1–5). Standard methods have been developed for the interpretation and evaluation of the stratigraphy and chronological information, and for the calculation of MAR. These methods are described in the next section (Section 3. Methods). The bulk of the report (Section 4. Site Documentation) consists of the description of the primary and derived data from individual sections in the form of summary diagrams and tables. A consistent format is used to facilitate comparison between individual sites. In Section 5 (Summary of Results) these data are summarised in the form of maps and the reconstructed patterns in MAR are briefly discussed. We conclude (Section 6) with a summary of the implications of our analyses.

3. Methods

3.1. Site Selection

We have examined the descriptions of 98 individual sections with sediments covering part or all of the last 150,000 years, from the CLP, the surrounding desert margins, and Tibet (Table 1; Figure 1). The descriptions came from both published and unpublished sources. Where exact site locations were not provided by the original authors, they were estimated using Chinese atlases (Anonymous, 1986; 1992; 1995). Some of these 98 sections were found to be unsuitable for subsequent analyses because they do not provide an adequate record of dust accumulation. There are two sites for which we are unable to provide documentation. A further 19 sections were documented, but omitted from subsequent analyses for one or more of the following reasons:

Figure 1. Site Locations.
Categorised by geomorphic or geographic location (yuan, loess terrace, river terrace, liang or mao, and desert margin or sand dune).

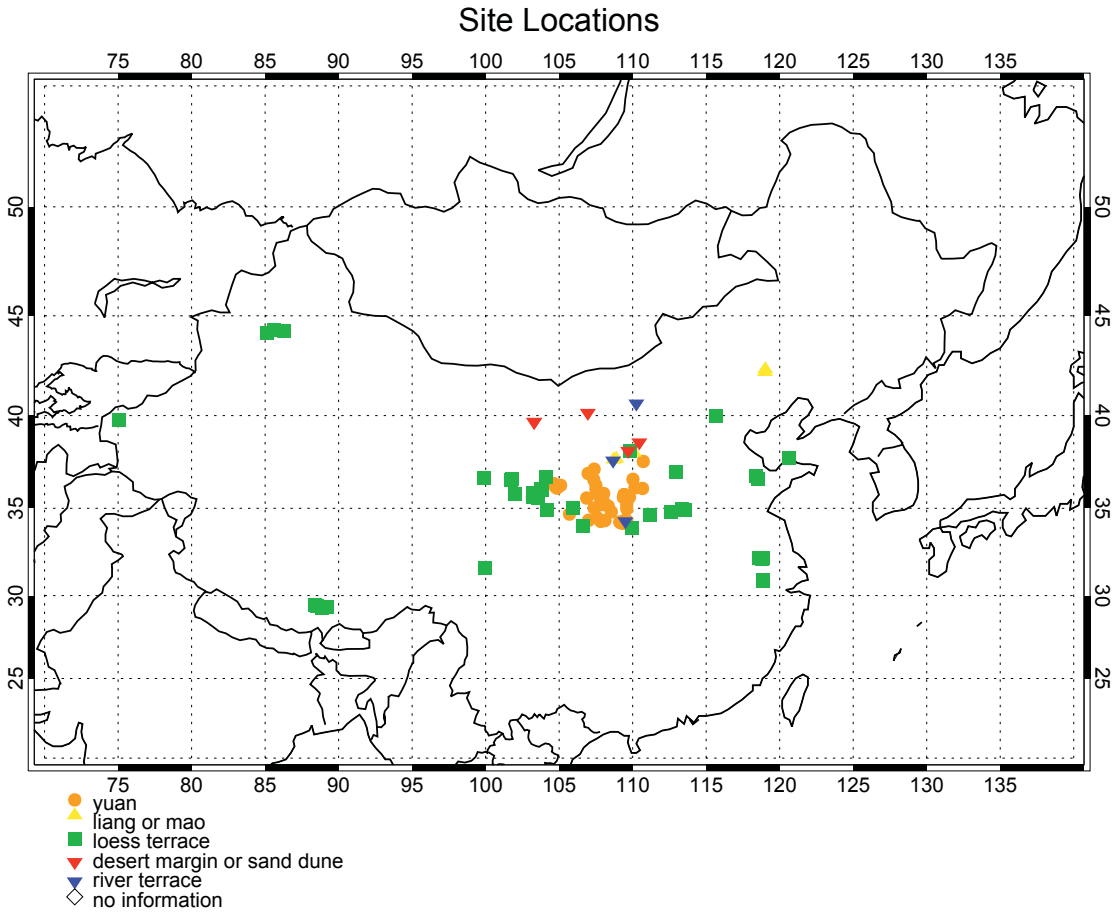

(1) there was insufficient information to erect a chronology (10 sections);

(2) the site was from a region not easily correlated with the CLP stratigraphy (9 sections);

and/or

(3) sand layers, hiatuses, or the absence of information about part of the section prevented estimation of mass accumulation rates (8 sections).

Stratigraphic and chronological data were compiled for the remaining 77 sections. Four sites (Chagelebulu, Heimugou (Luochuan), Liujiapo, and Mangshan) appear twice in the database because more than one stratigraphy has been developed for the same site location. Table 1 summarises the metadata available for the sites in the compilation. The metadata includes information on location (site name, latitude, longitude, elevation), geomorphic setting, the chronological data used to generate mass accumulation rate estimates, the Marine Isotope Stages for which mass accumulation rates were calculated, additional data generated for each site, and the sources of original data.

The continuity and thickness of aeolian deposits are strongly influenced by their geomorphic setting. Thus, accumulation is most likely to be continuous in geomorphically stable settings, such as large sedimentary basins. Sites on hill slopes or in exposed hilltop positions are more likely to be subjected to reworking either by aeolian activity or other geomorphic processes. Loess sections from such a position in the landscape are therefore likely to contain sedimentary hiatuses and thus provide discontinuous records of dust accumulation. Fine-grained material can be produced or concentrated by non-aeolian processes, such as fluvial activity. Proximity to a local source of such material could potentially lead to abnormally thick concentrations of loess. To determine the degree to which the records of dust accumulation derived from the 78 loess sections in our compilation might be affected by local factors, we have classified them according to their geomorphic setting (Figure 1), using a Chinese scheme that recognises 5 basic landform types: yuan, lian, mao, loess terrace, and desert margin sites (Liu, 1964; 1985). Yuan-type landforms develop when loess accumulates in large sedimentary basins (e.g. Heimugou (Luochuan) yuan). Yuan-type sections (42 sections) are most likely to yield thick and continuous records of aeolian accumulation because these settings are geomorphically stable. ‘Liang’ and ‘mao’ type loess deposits are formed on small hills. Liang-type deposits are elongated in form (e.g. Guojialiang), whereas mao-type deposits are round (e.g. Mizhi). Sections from these two landform types frequently contain sedimentary hiatuses. The six sections in the database classified as either liang- or mao-type all occur in the sandy loess belt of the northern CLP. Five of these contain hiatuses. Thick loess deposits, or "loess terraces," occur on high river terraces (e.g. Jiuzhoutai (Lanzhou) section). Forty sections in the database are from loess terraces, six of which contain hiatuses. The lack of hiatuses in the remaining terrace sections is shown by the fact that (1) they do not contain fluvial sand or gravel layers, which would indicate a hiatus in aeolian deposition, and (2) the median particle size is usually less than 20 μm, which suggests that coarser material from the local river channel does not contribute significantly to the deposit. The data compilation contains five marginal desert sites, which occur in or adjacent to deserts and contain loess intercalated with sand deposits. All of the marginal desert sites in the compilation contain sedimentary hiatuses.

A total of eleven sections contain sedimentary hiatuses. These sections are used to document accumulation rates only for those time intervals when deposition is

continuous and there is enough information to erect a chronology. Six of these sections were used to estimate accumulation rates.

3.2. The Calculation of Mass Accumulation Rates

The mass accumulation rate of aeolian sediments (MAR) is estimated in the following manner:

$$MAR_{eol}\ (g/m^2/yr) = AR\ (m/yr)\ \ f_{eol}\ \ BD\ (g/m^3) \qquad (1)$$

Where AR is the accumulation rate, f_{eol} is the mass concentration of aeolian materials within the sample (for loess sediments we assume that all material is aeolian and therefore $f_{eol} = 1$), and BD is the bulk density.

3.2.1 Bulk Density

Pye (1987) suggests that a typical BD for loess sediments is 1.65 g/cm^3. Measurements on last glacial loess (L1, equivalent to Marine Isotope Stages 2, 3, and 4) across the CLP have yielded a range of BDs from 1.281 to 1.632 g/cm^3, with an average BD of 1.48 g/cm^3 (Liu, 1966). BD values within the Heimugou section range from 1.40 to 1.65 g/cm^3 for loesses and soils across the last glacial-interglacial cycle (Liu, 1985). This demonstrates that BDs can vary by as much as 27% within a single stratigraphic unit across the CLP, and by as much as 18% between different stratigraphic units within a single section. Thus, adopting an average BD for the calculation of MAR could lead to errors in the MAR estimates.

Liu (1964; 1965; 1966) divides the CLP into three belts: the sandy loess belt to the northwest, the silt loess belt covering the central region, and the clay loess belt found in the southern CLP. Liu (1966) found that the average median grain size of the L1 loess tended to decrease from NW to SE and the bulk density in turn tended to increase. However, in spite of the general trend, the range of regional BD measurements are overlapping and this makes the assignment of average BD by geographic region somewhat arbitrary. Unfortunately, actual bulk density measurements are only reported at two sites (Heimugou and Zhangjiayuan). For these two sites we used the measured values. At every other location we use an average BD of 1.48 g/cm^3 to estimate MAR. Using a constant BD, as we have been forced to do, will undoubtedly create a slight bias in our estimates of MAR, leading to underestimates of MAR in the southern CLP and overestimates of MAR in the northwestern CLP. The MAR estimates can be revised, or course, as additional BD measurements become available.

3.2.2 Depth and Thickness Estimates

The thickness of each unit is required to estimate the accumulation rates for each time period. In sections where depths and thicknesses were not provided, they were estimated from the diagrams in the publication.

Table 1. Site Information.

Site	Latitude (ºN)	Longitude (ºE)	Elevation (m)	Land-form	Sources of data	Basis for chronology	Stages for MAR	Page
Ancun	35.57	106.87	1400	yuan	pedostratigraphy, pollen	pedostratigraphy	2, 3, 4, 5	19
Baicaoyuan	36.2.7	105.10	2100	yuan	MS, GS, $CaCO_3$, $\delta^{13}C$, chemical parameters, pedostratigraphy	MS, pedostratigraphy	1, 2, 3, 4, 5	21
Baige	34.80	112.62	90	loess terrace	pedostratigraphy, mammal fossils	pedostratigraphy	5	24
Baimapo	34.17	109.32	650	yuan	pedostratigraphy, MS, TL	MS, pedostratigraphy	2, 3, 4, 5	26
Baishui	35.20	109.59	880	yuan	MS	MS	2, 3, 4, 5	31
Banshan	34.68	105.70	1400	yuan	pedostratigraphy	pedostratigraphy	1, 2, 3, 4, 5	33
Baoji (Lingyuan)	34.33	107.00	970	yuan	pedostratigraphy, GS, MS, $\delta^{18}O$, $CaCO_3$, magnetic polarity, micromorphology	MS, pedostratigraphy	1, 2, 3, 4, 5	35
Baxie (Dongxiang)	35.58	103.57	2000	loess terrace	pedostratigraphy, MS, GS, $\delta^{13}C$, TOC, ^{14}C, TL	^{14}C, TL	1, 2	38
Beiyuan	35.62	103.20	2100	loess terrace	pedostratigraphy, MS, GS, ^{14}C, TL, chemical parameters, $CaCO_3$, micromorphology, mammal fossils, pollen	TL, MS, pedostratigraphy	1, 2, 3, 4, 5	42
Beiyuantou	36.05	107.50	1250	yuan	MS	MS	1, 2, 3, 4, 5	47
Beizhuangcun (Weinan)	34.50	109.50	950	river terrace	pedostratigraphy, ^{14}C, MS	^{14}C	1	49
Caijiagou	38.12	109.83	1250	loess terrace	pedostratigraphy, MS, GS, TL, CBD-Fe	TL, pedostratigraphy	3, 5	55
Caocun	34.63	111.15	760	loess terrace	pedostratigraphy, MS	pedostratigraphy	1, 5	61
Caoxian	36.37	104.62	2115	yuan	pedostratigraphy, magnetic polarity, MS, GS	pedostratigraphy	5	63
Chagelebulu_1 (Cagelebulu)	39.88	103.30	1800	marginal desert site	pedostratigraphy, pollen, $CaCO_3$, ^{14}C, SiO_2/Al_2O_3	^{14}C	1	65
Chagelebulu_2 (Cagelebulu)	39.88	103.30	1800	marginal desert site	pedostratigraphy, ^{14}C	^{14}C	1	68
Changqugou	37.45	108.70	1700	liang	pedostratigraphy, MS	pedostratigraphy	5	71
Changwu	35.20	107.82	1200	yuan	pedostratigraphy, MS, chemical parameters	pedostratigraphy	1, 2, 3, 4, 5	74
Chenjiawo (Lantian_1)	34.18	109.48	700	yuan	pedostratigraphy, TL, mammal fossils, magnetic polarity	TL, pedostratigraphy	1, 2, 3, 4, 5	76
Chifeng	42.17	119.02	750	liang	MS	MS	1, 2, 3, 4, 5	80
Chunhua	34.80	108.55	1100	yuan	MS	MS	1, 2, 3, 4, 5	82
Dadiwan	35.00	105.92	1400	loess terrace	pedostratigraphy, MS, ^{14}C	^{14}C, pedostratigraphy	1, 2	84
Dengkou	40.35	106.95	1100	marginal desert site	pedostratigraphy, ^{14}C	^{14}C	none	89
Duanjiapo (Lantian_2)	34.20	109.20	700	yuan	pedostratigraphy, MS, ^{13}C(organic), ^{13}C(carbonate) ^{18}O(carbonate), magnetic polarity	pedostratigraphy; MS	1, 2, 3, 4, 5	92
Dunwashan	35.85	103.25	n/a	loess terrace	pedostratigraphy	pedostratigraphy	4, 5	95
Duobutang	29.36	88.50	3900	loess terrace	pedostratigraphy, TL	none	none	98
Fujiazhuang	36.60	118.50	160	loess terrace	pedostratigraphy, TL	pedostratigraphy	5	99
Ganzi	31.63	99.98	3480	loess terrace	pedostratigraphy, magnetic polarity	pedostratigraphy	1, 2, 3, 4, 5	102

Site	Latitude (ºN)	Longitude (ºE)	Elevation (m)	Land-form	Sources of data	Basis for chronology	Stages for MAR	Page
Gaolanshan	36.00	103.83	2135	loess terrace	pedostratigraphy, MS, GS, ^{14}C, organic carbon, $CaCO_3$, micromorphology	^{14}C, pedostratigraphy, MS	1, 2, 3, 4, 5	104
Guojialiang	37.50	108.88	1730	liang	pedostratigraphy, MS	pedostratigraphy	5	109
Halali	36.67	99.88	3220	loess terrace	pedostratigraphy, ^{14}C, pollen, GS	pedostratigraphy, ^{14}C	1	112
Heimugou_1 (Luochuan)	35.75	109.42	1100	yuan	pedostratigraphy, MS, GS, ^{10}Be, phytoliths, ^{13}C(organic), ^{13}C(carbonate) ^{18}O(carbonate), magnetic polarity, DBD, $CaCO_3$, chemical parameters, TL	MS (2), pedostratigraphy	2, 3, 4, 5	115
Heimugou_2	35.75	109.42	1100	yuan	pedostratigraphy, TL, chemical parameters, MS	pedostratigraphy	1, 5	120
Heishan	n/a	n/a	n/a	n/a	^{10}Be, pollen	none	none	124
Heshui	35.82	108.03	1250	yuan	pedostratigraphy	pedostratigraphy	5	125
Huangling	35.60	109.37	1100	yuan	pedostratigraphy	pedostratigraphy	5	127
Huanglong	35.62	109.78	1120	yuan	MS, GS	MS	1, 2, 3, 4, 5	129
Huanxian	36.58	107.35	1270	yuan	MS	MS	1, 2, 3, 4, 5	131
Jiezicun (Jiezhichun)	34.33	109.57	650	yuan	pedostratigraphy, MS, ^{14}C, TL	^{14}C, TL, MS, pedostratigraphy	1, 2, 3, 4, 5	133
Jinjiyuan (Shangzhou)	33.90	109.92	950	loess terrace	pedostratigraphy, GS, magnetic polarity	pedostratigraphy	5	138
Jiuzhoutai (Lanzhou)	36.07	103.75	2067	loess terrace	pedostratigraphy, MS, ^{14}C, TL, magnetic polarity, micromorphology, mollusc fauna, GS, clay mineralogy	^{14}C, TL, MS, pedostratigraphy	1, 2, 3, 4, 5	140
Jiyuan	37.15	107.38	1900	yuan	MS, GS	MS	2, 3, 4, 5	146
Kansu	39.75	75.05	1490	loess terrace	pedostratigraphy, TL	pedostratigraphy, TL	5	148
Landa	36.05	103.84	1510	loess terrace	pedostratigraphy, ^{14}C, MS	^{14}C	1	151
Lijiagang	32.17	118.84	70	loess terrace	MS	none	none	155
Lijiayuan	36.12	104.85	1700	yuan	MS, GS	MS	1, 2, 3, 4, 5	156
Lintaigou	42.03	119.00	1100	liang	MS	none	none	158
Liujiapo_1	34.20	109.20	600	yuan	pedostratigraphy, MS, GS, TL, micromorphology	TL, pedostratigraphy	2, 3, 4, 5	159
Liujiapo_2 (Xian)	34.23	109.12	600	yuan	pedostratigraphy, magnetic polarity	pedostratigraphy	2, 3, 4, 5	164
Lujiaowan	44.33	85.63	1960	loess terrace	pedostratigraphy, ^{14}C, TL	pedostratigraphy	1, 5	166
Majiayuan	36.27	107.50	1250	yuan	MS	MS	1, 2, 3, 4, 5	169
Mangshan_1	34.93	113.53	228	loess terrace	pedostratigraphy	pedostratigraphy	5	171
Mangshan_2	34.97	113.37	228	loess terrace	pedostratigraphy, OSL, TL, MS, magnetic polarity	OSL, pedostratigraphy	1, 2, 3, 4, 5	173
Mengdashan	35.77	102.00	3200	loess terrace	pedostratigraphy	pedostratigraphy	1, 5	177
Mizhi	37.83	110.08	1100	mao	pedostratigraphy, MS	pedostratigraphy	5	179
Mujiayuan (Wupu)	37.57	110.72	1020	yuan	MS	MS	1, 2, 3, 4, 5	182
Ningxian	35.48	107.97	1200	yuan	MS	MS	1, 2, 3, 4, 5	184
Niuquanzi	44.18	85.10	1400	loess terrace	pedostratigraphy, ^{14}C, TL	pedostratigraphy	3	186
Pucheng	34.97	109.60	500	yuan	MS	MS	2, 3, 4, 5	189
Qijidong	29.32	89.20	3900	loess terrace	pedostratigraphy, TL	none	none	191

Site	Latitude (°N)	Longitude (°E)	Elevation (m)	Land-form	Sources of data	Basis for chronology	Stages for MAR	Page
Qinjiazhai	35.74	109.43	1100	yuan	pedostratigraphy, ^{18}O of quartz, clay mineralogy	pedostratigraphy	5	192
Qishan	34.45	107.63	720	yuan	pedostratigraphy, MS, $\delta^{13}C$, $\delta^{18}O$, chemical parameters	MS, pedostratigraphy	2, 3, 4, 5	194
Renjiahutong	35.75	109.42	1100	yuan	pedostratigraphy, MS, ^{14}C	^{14}C	1, 2	197
Renjiapo	35.02	107.37	1200	yuan	GS	none	none	201
Salawusu	37.83	108.67	1400	river terrace	pedostratigraphy, ^{14}C	none	none	none
Shangjiapo	34.32	108.12	530	yuan	pedostratigraphy, micromorphology	pedostratigraphy	2, 3, 4, 5	202
Shenjiazhuang	36.72	104.13	1900	loess terrace	pedostratigraphy, ^{14}C	^{14}C	1, 2	204
Shimao	37.92	110.00	1180	mao	pedostratigraphy, TL. MS, GS, CBD-Fe, magnetic polarity	TL, pedostratigraphy	5	207
Taishanxincun	32.17	118.60	70	loess terrace	pedostratigraphy	none	none	211
Tuxiangdao	36.58	101.73	2600	loess terrace	pedostratigraphy, MS, GS, $CaCO_3$, TL	TL, pedostratigraphy	1, 5	212
Wangning	37.02	112.95	1100	loess terrace	pedostratigraphy, magnetic polarity, MS	none	none	215
Weinan (Yangguo)	34.35	109.52	650	yuan	pedostratigraphy, MS, ^{14}C, TL, chemical parameters, micromorphology, magnetic polarity	^{14}C, TL, MS, pedostratigraphy	1, 2, 3, 4, 5	216
Wudangzhao	40.83	110.25	1200	n/a	pedostratigraphy, ^{14}C	none	none	none
Wuyishan	35.80	103.22	n/a	loess terrace	pedostratigraphy	pedostratigraphy	3, 4, 5	221
Xiadongcun (Jixian)	36.10	110.67	1300	yuan	pedostratigraphy, MS, GS, magnetic remanence	MS (2), pedostratigraphy	1, 2, 3, 4, 5	223
Xiangyang (Chenshan)	30.87	118.87	150	loess terrace	pedostratigraphy, MS, GS	none	none	227
Xiazhupan	37.77	120.66	50	loess terrace	pedostratigraphy	none	none	229
Xietongmen	29.43	88.36	3900	loess terrace	pedostratigraphy, TL, magnetic polarity	none	none	230
Xifeng	35.70	107.70	1330	yuan	pedostratigraphy, MS, GS, micromorphology, magnetic polarity, chemical parameters	MS, pedostratigraphy	1, 2, 3, 4, 5	231
Xigaze	29.27	88.85	3920	loess terrace	pedostratigraphy, TL	none	none	235
Xining (Dadunling)	36.63	101.80	2755	loess terrace	pedostratigraphy, MS, GS, magnetic polarity	pedostratigraphy, MS	1, 2, 3, 4, 5	236
Xinzhuangyuan	36.20	104.73	1700	yuan	MS, GS	MS	1, 2, 3, 4, 5	239
Xuancheng	30.90	118.85	150	loess terrace	pedostratigraphy, MS, $\delta^{13}C$, chemical parameters	none	none	241
Xueyuan	36.92	106.97	1650	yuan	MS	MS	1, 2, 3, 4, 5	243
Xunyi	35.13	108.33	1200	yuan	MS	MS	1, 2, 3, 4, 5	245
Yanchang	36.60	110.02	1102	yuan	MS, GS	MS	1, 2, 3, 4, 5	247
Yangjiashan (Fenzhou)	34.00	106.65	1600	loess terrace	pedostratigraphy, GS, magnetic polarity	pedostratigraphy	2, 3, 4, 5	249
Yangmeitang	32.17	118.84	n/a	n/a	MS	none	none	251
Yangtaomao	38.80	110.45	1400	sand dune	pedostratigraphy, MS, GS, ^{14}C	none	none	252
Yanziji	32.15	118.82	70	loess terrace	pedostratigraphy, TL	none	none	254
Yichuan	36.13	110.15	1100	yuan	MS, pedostratigraphy, chemical parameters, GS	MS	1, 2, 3, 4, 5	256

Site	Latitude (ºN)	Longitude (ºE)	Elevation (m)	Land-form	Sources of data	Basis for chronology	Stages for MAR	Page
Yinwan	34.93	104.17	2100	loess terrace	pedostratigraphy, MS, GS, organic matter, $CaCO_3$, ^{14}C, TL, mineralogy, pollen, magnetic polarity	^{14}C	1	258
Yuanpu (Yuanbo)	35.63	103.17	2100	yuan	pedostratigraphy, pollen, MS, ^{14}C, GS, $CaCO_3$	^{14}C, MS, pedostratigraphy	1, 2, 3, 4, 5	263
Yulin	38.35	109.70	1200	marginal desert	pedostratigraphy, ^{14}C	^{14}C	1	267
Zhaitang	39.98	115.68	150	loess terrace	pedostratigraphy, ^{14}C , TL, GS	pedostratigraphy	1, 2, 3, 4, 5	271
Zhangjiayuan	34.27	107.83	550	yuan	pedostratigraphy, GS, DBD, mechanical parameters	pedostratigraphy	1, 2, 3, 4, 5	274
Zihedian	36.78	118.37	120	loess terrace	pedostratigraphy, TL	none	none	276
117 km milestone site	44.28	86.25	1965	loess terrace	pedostratigraphy, ^{14}C	none	none	278

MS = magnetic susceptibility; GS = grain size; TL = thermoluminescence; OSL = optically stimulated luminescence; ^{14}C = radiocarbon dating, ^{10}Be = Beryllium-10 dating; TOC = total organic carbon; DBD = dry bulk density; CBD-Fe = "citrate-bicarbonate-dithionite" extracted Fe; mechanical parameters = void ratio, porosity, liquid limit, plastic limit, plastic index

3.3 Chronology

Calculations of the accumulation rates (AR) are dependent on the age model developed for each section. We have applied four standard methods to develop age models for sections on the CLP: two based on independent dating methods (radiocarbon and thermoluminescence) and two based on correlation with the marine isotope stratigraphy (pedostratigraphy and magnetic susceptibility). We used the standard marine isotope stratigraphy of Martinson et al. (1987) to derive ages for the last two methods (Table 2). For sections that are not on the CLP and where pedostratigraphic correlation cannot therefore be used, the age models were based on ^{14}C or TL dating or magnetic susceptibility.

Table 2. Definition of Marine Isotope Stages (Martinson et al., 1987).

Marine Isotope Stage (MIS)	Age Boundaries (kyr BP)
1	0-12
2	12-24
3	24-59
4	59-74
5	74-130

3.3.1 Radiocarbon Dating

The basic assumption of using radiocarbon (^{14}C) to date loess sections is that the radiocarbon age of organic matter in a buried soil is expected to reflect the radiocarbon age of the soil during formation plus the time since burial. However, the measured age of a buried soil can be biased by (a) the post-depositional incorporation of younger material (e.g. roots growing on younger soils penetrating into the palaeosols below), (b) the post-depositional incorporation of old carbon (e.g. through the decomposition of carbonates in loess), or (c) the erosion of younger surface layers of the soil before burial.

The measured age of a soil can also be affected by the type of material dated. Martin and Johnson (1995), for example, have demonstrated that differences exist between the radiocarbon ages generated on humic acid (soluble), residue (insoluble), and bulk organic matter found in buried soils in the loess from the mid-continental USA. Although they found no consistent age offset between the different fractions, the average differences were between 700 and 910 years (and exceeded 2000 years in two of the 14 samples they considered).

The materials used for dating the samples from the CLP include bulk organic matter, soluble or insoluble organic fractions, humin, and humic acid. At the one site on the CLP where both the humin and humic acid fractions were analysed (Yanggou (Weinan): Liu, 1994), no consistent age offset is found between the humin and humic acid fractions. For the two ages from this site <20,265 ^{14}C years (and therefore used in our age models), the humin fraction is older than the humic acid fraction by 700 and 3800 years respectively. In this instance we followed the decision of the authors to use the insoluble (humin) fraction. Dates determined on humic acid are not used to determine

age models or MAR at any site on the CLP. Only one date on the soluble organic fraction is used, and one date in which the author averaged the soluble and insoluble fraction ages to get an age estimate (Renjiahutong section: Zhou et al., 1994). We acknowledge that a future standardisation of techniques for samples on the CLP would minimise errors associated with dating different soil fractions.

Additional factors must be considered when using radiocarbon dates. Specifically, the radiocarbon inventory of the atmosphere has varied by a few percent over time, causing the measured ^{14}C age of a sample to be significantly but not consistently different from the true calendar age of that sample. Furthermore, the true half-life of radiocarbon is 5730 years and not 5568 years as originally measured. Calibration programs have been developed to convert ^{14}C years to calendar years (see e.g. Stuiver and Kra, 1986; Stuiver and Reimer, 1993; Bronk Ramsey, 1998; Stuiver et al., 1998a; 1998b), to account for these fluctuations in the atmosphere's radiocarbon content and the differences in ^{14}C half-life, and therefore provide a means of calibrating ^{14}C dates as old as 20,265 years BP (Stuiver and Reimer, 1993; Stuiver et al., 1998b).

Radiocarbon dates were only used to erect a site chronology if they met the following criteria:

(1) The date was < 20,265 years B.P., and thus could be converted to calendar ages;

(2) The standard deviation (SD) was < 2000 years;

(3) If two neighbouring dates overlapped (with the standard deviations considered) the age with smaller error bar was used;

(4) If an age reversal occurred within the section, the decision of the author about which date was acceptable was followed; if no decision was made by the author, the age with the smaller error bar was used;

(5) Dates indicated by the authors as contaminated were not used.

Reported information on these dates (e.g. depth, dating laboratory, laboratory number, material dated and standard deviations) was not always complete. When not complete an attempt was made to obtain this information from the original author. Otherwise, we state that the information is not available (n/a). When depth information was not provided it was estimated from the diagrams in the original publication.

3.3.1.1 Conversion from ^{14}C to Calendar Years

Radiocarbon dates younger than 20,265 yr. BP were converted to calendar ages using the INTCAL98.14C calibration data set included as part of the CALIB 4.1 software (Stuiver and Reimer, 1993). In the absence of documentation by the authors, we assumed that all radiocarbon dates were conventional. Thus we assume that the Libby half-life of 5568 years was used and the radiocarbon age has been corrected for isotope fractionation by normalisation to –25 ‰ ($\delta^{13}C_{PDB,}$ relative to Pee Dee Belemnite). Using the CALIB 4.1 software, the relative probability distributions and 1-sigma (68.3%) confidence intervals of all possible calendar ages were determined for each radiocarbon age. The midpoint of the range of the calendar ages with the highest relative probability was assumed to be the calendar age when subsequently erecting site chronologies.

3.3.1.2 Rules for Estimation of MAR Based on ^{14}C dating

The MAR for marine isotope stages (MIS) 1 and/or 2 were calculated using the converted ^{14}C dates that met the established criteria. The duration of each MIS is given in Table 2. The following methods were used for calculating MAR on radiocarbon-dated sections:

(1) When sedimentation was known to be continuous and there were radiocarbon dates closely bracketing both the upper and the lower MIS boundaries, we used linear interpolation between the two dates that bracketed each boundary to establish the depth of that boundary. We then used these interpolated depths to calculate the length of the stage in meters, and hence to calculate the MAR for that stage.

(2) When sedimentation was known to be continuous, and there were at least two radiocarbon dates from within the stratigraphic unit corresponding to a specific stage but there were no radiocarbon dates closely bracketing one or both of the stratigraphic stage boundaries, we calculated the within-unit sedimentation rate between the two dates closest to the stage boundaries.

(3) When sedimentation was known to be discontinuous, we estimated the MAR between every pair of dates on those parts of the section that were continuous. If there was only one such estimate from within a stage, we assumed that this MAR was representative of the whole stage. If there were more than one such estimate from within a stage, we recorded the number and range of the estimates but used the MAR calculated using the top and bottom radiocarbon ages to represent the MAR for that stage.

3.3.2 Luminescence Dating

Luminescence dating has also been used to date loess sediments (see summaries in e.g. Bradley, 1985; Wintle, 1990; Wintle et al., 1993; Prescott and Robertson, 1997; Aitken, 1998). Luminescence dating is based on the principle that the ionising radiation from the naturally radioactive elements in the sediment contributes to the build-up of trapped elections within the mineral crystals of buried sediments. When exposed to the photons in sunlight, these electrons are released and the mineral crystals are optically reset. Upon burial the number of trapped electrons builds up with time. During the dating procedure, these trapped electrons are released by heating or optical stimulation, and the resulting luminescence can be quantified and converted to age since burial. The radioactive dose rate of the surrounding sediments depends both on the concentration of naturally radioactive materials (e.g. uranium, thorium, and potassium) as well as the water content (which acts to attenuate the radiation).

The reliability of thermoluminescence (TL) dates depends on a large number of factors, including the post-depositional history of the deposit, the mineralogy and grain size of the materials analysed, and the laboratory method used. There are many unresolved questions about the technique (see e.g. discussions in Wintle, 1997; Aitken, 1998; Murray and Wintle, 2000; Zhou and Shackleton, in press) and no generally accepted standard for TL dating. Furthermore, much of the information that would be required to evaluate the reliability of a given date (e.g. material analysed, size fraction analysed, natural radioactive content and water content of the sediments, optical filter used, added dose) is not routinely given in the literature. The laboratory number of a sample is also

not routinely given, so that information about the techniques employed could not be obtained directly from the measurement laboratory. Given this, it is currently impractical to attempt to determine the inherent reliability of the available TL dates from China and hence to screen the dates used to erect an age model on this basis. The only exception that we have made is to exclude dates that have yielded ages >130,000 years. The maximum limit for TL dating is still the subject of debate, with estimates ranging from as little as 80,000 to as much as 800,000 years (Berger, 1988; Berger et al., 1992; Wintle, 1997; Aitken, 1998). The consensus opinion appears to be that dates on bulk samples of heterogeneous mineral mixtures at the older of this range (i.e. >130,000 years) are unreliable.

Thus, acceptable TL dates were selected using the following criteria:

(1) The date was < 130,000 years BP;

(2) Only samples with standard deviation (S.D.) < 10% were used;

(3) If two neighbouring dates overlapped (with the standard deviations considered) the age with smaller error bar was used;

(4) If an age reversal occurred within the section, the decision of the author about which date was acceptable was followed; if no decision was made by the author, the age with the smaller error bar was used.

The methods used for estimating MAR using TL dates are the same as those applied to the radiocarbon dates.

3.3.3 Age Models Based on Pedostratigraphy

The pedostratigraphy of the CLP has been established by Liu et al. (1985) and Kukla (1987a). The Holocene soil (S0), assumed to correlate with the MIS 1 (0-12 kyr), is characterised by a diagnostic A horizon, with an A(AC)/C profile (Liu, 1985). The underlying loess (L1), which is assumed to correlate with MIS 2, 3, and 4, is interrupted by one (central CLP), two (southern CLP) or three (northwestern CLP) weakly developed soils. At sites in the southern CLP, for example, the soils within the L1 loess are characterised by AC/Ck or Ah/Ck horizons (Rutter and Ding, 1993; Liu et al., 1995). The last glacial loess in the northern CLP does not contain soils. Interstadial soils in L1 are assumed to have developed during Stage 3 (24-59 kyr). The last interglacial soil (S1) is better developed than S0 or the weakly developed soils of MIS 3 (Liu, 1985). It is generally characterised by either a diagnostic illuvial horizon (Bt, in the central and southern CLP) or a weathered B horizon (Bw, in the northern CLP), with or without an underlying carbonate illuvial horizon (Bk). The S1 soil is correlated with MIS 5 (74-130 kyr) (Liu, 1985).

The use of pedostratigraphic correlation for erecting an age model is based on the assumptions that (1) soils develop only under interglacial and interstadial conditions, (2) soils begin to develop immediately as soon as interglacial or interstadial conditions are established and soil boundaries can therefore be directly assigned the dates attributed to the beginning/end of individual interglacial or interstadial periods according to the marine oxygen isotope stratigraphy of e.g. Martinson et al. (1987), and (3) dust accumulation ceases during soil formation periods.

The assumption that soils on the CLP were formed during interglacial and interstadial conditions seems inherently reasonable and is supported by e.g. pollen evidence

showing that the vegetation during times of soil formation was characterised by species adapted to warmer and/or wetter conditions (Sun et al., 1997). However, the remaining assumptions are more problematic.

The assumption that soil formation began and ended synchronously across the whole of the CLP and at times coherent with the beginning and end of interglacial and interstadial periods as determined by the marine isotope record, is clearly an oversimplification. Soils can be formed extremely rapidly under favourable conditions, but in general the creation of a distinct soil profile is thought to take anything from several hundred to several thousand years (Duchaufour, 1982). Unfortunately, although there is a good qualitative understanding that pedological characteristics develop as a function of the existence and persistence of favourable climatic conditions, we are unable to quantify these relationships in such a way as to determine the age of the soil from its internal (pedological or morphological) characteristics alone. Even if it were possible to derive an independent and detailed estimate of climatic conditions at the time of soil formation, it would still be difficult to estimate how long a given soil took to form because there is little quantitative information on the climatic threshold at which certain pedological processes begin to operate. Finally, palynological evidence from many regions (including China) indicates that the development, duration, and maximum expression of climatic conditions during successive interglacials (and interstadials) were very different (Watts, 1988; Sun et al., 1997). Thus the timing of the onset of soil formation and the duration of favourable soil-forming conditions at the regional scale represented by China is unlikely to be correlated in a consistent and unchanging way with the global and composite signal of climate change represented by the marine isotope record. In those cases where there is independent radiometric dating of the soil material itself, we can use these dates to evaluate the reliability of pedostratigraphic correlation as a dating tool for individual sites from China. Such an evaluation may help determine the magnitude of the dating uncertainties inherent in using pedostratigraphic correlation and hence whether it is reasonable to use pedostratigraphic correlation as a dating tool for Chinese sites which lack radiometric dates. However, given that the assumption that soil formation is synchronous with interglacials or interstadials as defined by the marine isotope record is a simplification, the results of our assessment cannot be applied to other loess regions without a similar and independent evaluation.

The assumption that dust accumulation ceases during soil formation periods is clearly untenable, since dust accumulation is occurring on the CLP today. There are geochemical and micromorphological techniques that could be used to quantify how much of the material within a soil is being deposited during the soil-forming interval and how much consists of altered aeolian parent material (see e.g. Guo et al., 1993; Derbyshire et al., 1995; Kemp et al., 1995). Unfortunately, such techniques are time-consuming and have not been widely applied to individual sections. It is therefore necessary to adopt an *a priori* pedostratigraphic model to determine how much of the soil consists of altered parent material and how much is the result of continued aeolian deposition during the soil-forming interval. There are three such *a priori* models that have been used in China. We have evaluated how large the impact of adopting one rather than another of these models on the calculation of MAR during interglacial or interstadial intervals at specific sites, as follows:

In **Model I** we assume that soils are directly correlative with interglacial or interstadial periods in the marine isotope stratigraphy (Figure 2). Soil formation during these periods occurs through modification of dust that is accumulating continuously though at sufficiently low rates for pedogenesis to occur, and the whole part of the soil represents

Figure 2. Pedostratigraphic Models

Schematic figure demonstrating how stage boundaries (and associated aeolian mass accumulation rates) were determined for each pedostratigraphic model, for different cases observed in the data.

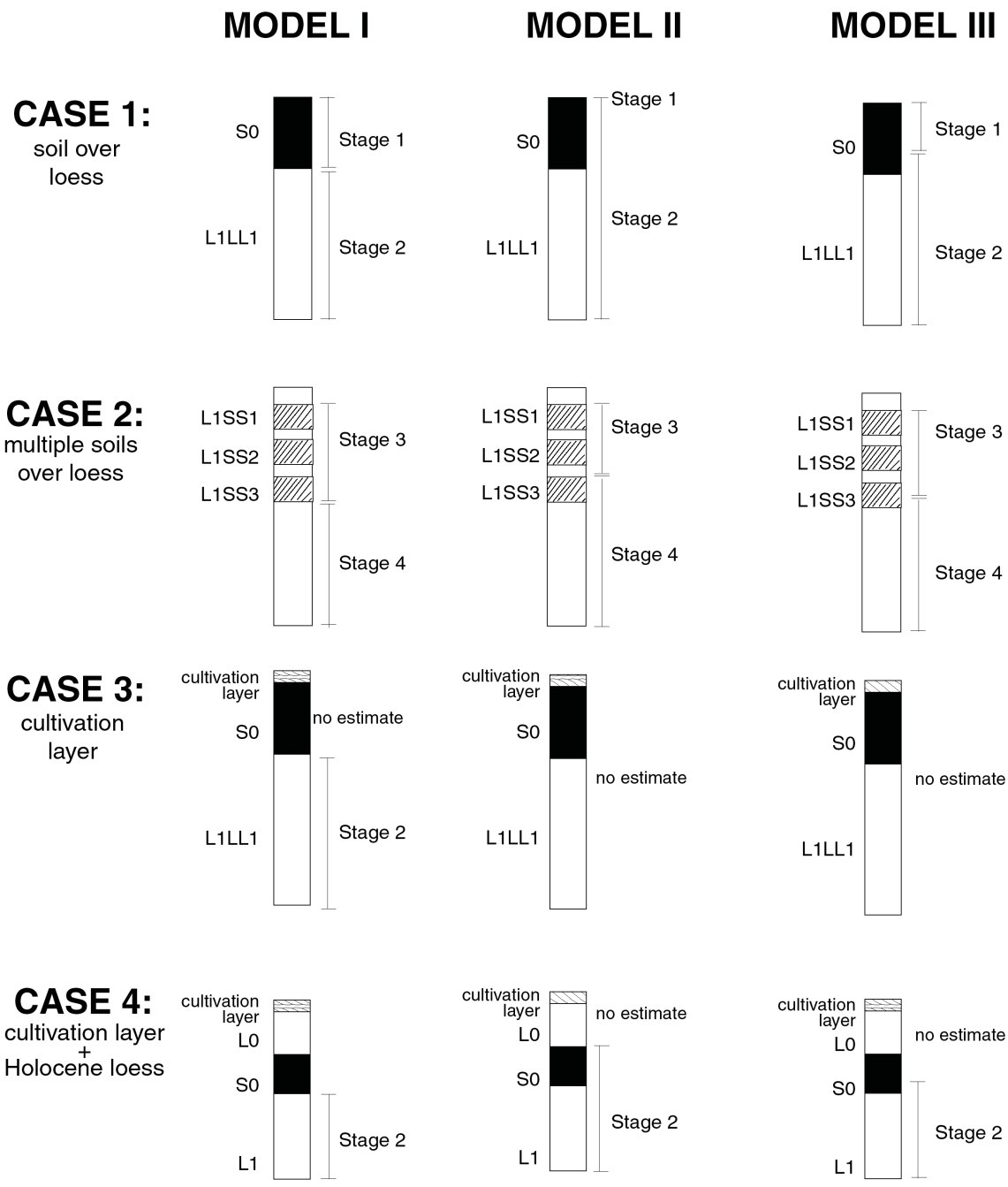

aeolian deposition. This model yields a maximum estimate of dust accumulation rates during interglacial and interstadial stages (thereby yielding minimum estimates of glacial accumulation).

Model II assumes that while soils are directly correlative with the interglacial or interstadial periods in the marine isotope stratigraphy, there is no dust deposition during these periods. Instead, the soils are formed entirely by modification of the loess. This model provides minimum estimates of interglacial/interstadial dust accumulation (and thereby maximum estimates of glacial dust accumulation). In cases where multiple soils are present within a soil complex attributed to an interglacial or interstadial period (e.g. Guojialiang section), the lowermost soil is assumed to have formed in the underlying glacial loess, and the remaining loess/soil complexes represent the accumulation within the interglacial/interstadial period.

Models I and II present end-member models of aeolian accumulation, and it seems likely that neither is realistic. Analyses of the iron oxides and hydroxides in loesses and paleosols have been used to estimate that approximately one-third of each soil unit is derived from underlying loess material (Guo et al., 1993). Two-thirds of the material comprising a soil is thus assumed to be derived from aeolian deposition during the interglacial/interstadial period. Thus **Model III** assumes that the upper two thirds of each soil unit can be correlated with interglacial/interstadial periods in the marine oxygen isotope stratigraphy and therefore represents aeolian deposition during interglacial/interstadial periods.

We use these three models to calculate MAR separately in order to compare the range of MAR estimates for each stage. Implicit in our estimate of MAR is the assumption that sedimentation across each stage is continuous. Hiatuses and cultivation layers both present cases where this assumption is violated. Thus, we apply the following constraints to our calculations:

(1) No MAR was estimated from the part of a section containing a documented sedimentary hiatus;
(2) In sections with a cultivation layer overlying the Holocene soil (e.g. Ancun Section), it is unclear exactly how much of the S0 has been anthropogenically modified. In these instances, no Stage 1 MAR was estimated (for all models), and Stage 2 MAR was only estimated for Model I;
(3) In sections containing a Holocene loess layer between the cultivation layer and the underlying Holocene soil (e.g. Jiezicun Section), Stage 2 MAR could be estimated for all three models. No Stage 1 MAR was estimated;
(4) We realise that cultivation is undoubtedly extensive on the CLP, but in the absence of explicit documentation of a cultivation layer by the authors, we include a Stage 1 MAR estimate for the site.

3.3.4 Magnetic Susceptibility Chronology

The bulk concentration of magnetic minerals (i.e. bulk magnetic susceptibility) is generally higher in soils than in unweathered loess on the CLP (An et al., 1977; Heller and Liu, 1982). Certain magnetic susceptibility records from the CLP reveal a distinctive pattern that has similar structure to that seen in the global ice volume record, as interpreted from marine oxygen isotope records (Kukla et al., 1988). Periods of low magnetic susceptibility (and high dust accumulation rates) appear to correspond with periods of maximum global ice volume. Thus, correlation of the magnetic susceptibility

records with the marine oxygen isotope stratigraphy has been used extensively as a chronostratigraphic tool on the CLP (e.g. Heller and Liu, 1982; Kukla et al., 1988).

The use of magnetic susceptibility correlation as a dating tool is dependent on two major assumptions. First, enhancement of the susceptibility signal is associated with the strength of pedogenesis (Zhou et al., 1990; Han et al., 1991; Liu et al., 1991; Maher and Thompson, 1991; Zheng et al., 1991; Liu et al., 1992; Verosub et al., 1993), which is coincident with warm, moist interstadial periods. Second, there is no time lag between the acquisition of the susceptibility signal and soil development.

Several complications are associated with using magnetic susceptibility estimates as a dating tool. First, the hypothesised covariance between magnetic susceptibility and climate records is at best a regional CLP signal. Magnetic susceptibility records in other regions are negatively correlated with the marine oxygen isotope record (e.g. in central Europe: Chlachula et al., 1998) or show no enhancement in magnetic susceptibility during soil-forming periods (e.g. in Alaska: Begét, 1990; Vlag et al., 1999). Second, the mechanisms which control the enhancement of magnetic minerals in soils, their links to climate, and the possible time-lags between these processes are as yet poorly understood (see e.g. Zhou et al., 1990; Maher and Thompson, 1991; Heller and Evans, 1995).

In order to test the hypothesis that magnetic susceptibility can be used for chronology, we have estimated the correlation coefficients between individual magnetic susceptibility records and the oxygen isotope stratigraphy. Magnetic susceptibility measurements were available for 20 sites. In the absence of published data, magnetic susceptibility curves were scanned and digitized. At two sites (Heimugou_1 (Luochuan) and Xiadongcun), two magnetic susceptibility curves were available and both are included in the report.

The data for each section were first normalized using a standard normalisation procedure:

$$Z = \frac{(x' - \overline{x})}{s.d.} \tag{3}$$

Where Z is the normalized value, x' is the measured value, $\overline{x}$ is the mean, and s.d. is the standard deviation. The normalized magnetic susceptibility data were visually tied to the stacked marine oxygen record from Martinson et al., 1987) using AnalySeries 1.1 software (Paillard et al., 1996). Several tie points were chosen, primarily from the troughs and peaks of the two curves, in order to maximise the correlation coefficient R^2 between the two records. The R^2 values and age-depth relationship for the section based on this tuning procedure are recorded. Simple linear interpolation between each tie point was then used to estimate the age for each MS value. Stage MARs were then estimated based on the depths determined for each stage boundary.

Sections containing sedimentary hiatuses were not used to establish a magnetic susceptibility chronology. The presence of hiatuses violates the assumptions of continuous deposition that are required for stratigraphic correlation. Of the sections with magnetic susceptibility data, eight contain hiatuses. Stage 1 MAR was not estimated in sections containing a documented cultivation layer (see Section 3.3.3).

3.4 Comparison of Chronologies and MAR Using Average Estimates

Instead of creating a "composite chronology" based on the combined age information for each site (which would be the normal approach taken with respect to a single site) we treat all dating techniques independently. We do this in order to be able to compare the age models derived using each technique with one another. This also enables us to assess the impact of using different dating techniques and age models on calculated MAR. To compare the age models based on the individual dating techniques, ages were estimated at regular depth intervals across the portions of each section from which acceptable dates and ages for each dating method were available. Only estimates based on Model III were used as the basis for the pedostratigraphic age models. The age estimates for each depth were then averaged together in order to calculate the average chronology. However, the range of age estimates for each depth interval is also given in the documentation tables. The same approach is used to derive an average MAR. That is, the MAR based on each method were averaged together.

4. Site Documentation

This section provides documentation of the individual sites in the database. The description of each site is organised in the same way, except when particular kinds of data are not available for a particular site. The organisational structure is as follows:

(1) Metadata (name, latitude, longitude and special notes about the section including information about e.g. the stratigraphy and the geographic setting) are given first;

(2) A stratigraphic diagram, with an indication of the pedostratigraphic subdivision of the section, is given next. MARs calculated using the three different pedostratigraphic models are shown on the diagram. A table giving the stratigraphic data is included below the diagram;

(3) A stratigraphic diagram, showing the location of all radiometric dates is given next. The diagram also shows calibrated ages of acceptable dates and the age versus depth plot used to calculate MAR. The MAR is also given in the diagram. A table giving the radiometric data (including information about the radiocarbon calibration if applicable) is included below the diagram;

(4) A diagram showing measured magnetic susceptibility versus depth through the section, and the same data normalized and replotted against time are included next. The Martinson et al. (1987) stacked curve is also shown in the diagram for comparison. The stratigraphic points used to tie the magnetic susceptibility record and the Martinson et al. (1987) curve (tie points) are shown. The diagram also includes the MAR calculated using the magnetic susceptibility method. The table below the diagram gives the depth and assumed age for each tie point.

Following these diagrams, there are a number of summary tables giving (a) age model data, (b) MAR estimates according to each of the different methods and models, (c) the sources for all of the data included in this report and used to calculate MAR. This last table also lists references in addition to these primary sources which contain information about the site (i.e. references duplicating information in the primary sources or comparing sites with one another, as well as references documenting other kinds of palaeoenvironmental records from the loess).

Ancun section: MAR (g/m^2/yr) based on pedostratigraphy

(Model I: min. glacial, max. interglacial; Model II: max. glacial, min. interglacial; Model III: 2/3 of interglacial soil is aeolian deposit)

Site location: 35.57° N, 106.87° E

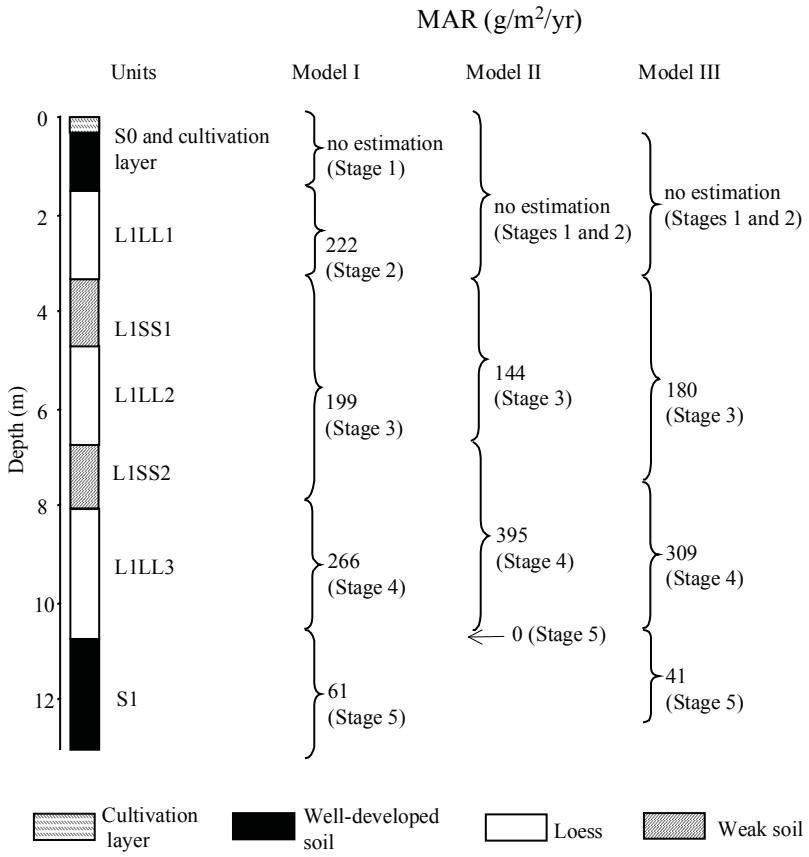

Stratigraphic data: Ancun (depth and thickness estimated from diagram, to nearest 10 cm)				
Top depth (m)	Bottom depth (m)	Thickness (m)	Stratigraphic units	DBD (g/cm³)
0.0	1.5	1.5	S0 and cultivation layer	n/a
1.5	3.3	1.8	L1LL1	n/a
3.3	4.7	1.4	L1SS1	n/a
4.7	6.7	2.0	L1LL2	n/a
6.7	8.0	1.3	L1SS2	n/a
8.0	10.7	2.7	L1LL3	n/a
10.7	13.0	2.3	S1	n/a

Age model (kyr): Ancun						
Depth (m)	^{14}C	TL	Magnetic susceptibility	Pedostratigraphy (Model III)	Average chronology	Range
0						
2						
4				29.9	29.9	
6				46.1	46.1	
8				61.1	61.1	
10				70.6	70.6	
12				122.0	122.0	

MAR ($g/m^2/yr$): Ancun								
Stage (range in kyr)	Assumed DBD (g/cm^3)	^{14}C	TL	MS	Pedostratigraphy			Average MAR
					Model I	Model II	Model III	
Stage 1 (12-0)	1.48							
Stage 2 (24-12)	1.48				222			
Stage 3 (59-24)	1.48				199	144	**180**	180
Stage 4 (74-59)	1.48				266	395	**309**	309
Stage 5 (130-74)	1.48				61	0	**41**	41

References used to generate data report: Ancun	
Data used	**Source**
Pedostratigraphy	Liu and Su (1994)
Magnetic susceptibility	-
^{14}C dating	-
TL dating	-
Additional References:	
Data available	**Source**
Pollen	Liu and Su (1994)

Baicaoyuan section: MAR (g/m^2/yr) based on pedostratigraphy

Note: Last glacial loess (L1) is not subdivided.

(Model I: min. glacial, max. interglacial; Model II: max. glacial, min. interglacial; Model III: 2/3 of interglacial soil is aeolian deposit)

Site location: 36.27° N, 105.10° E

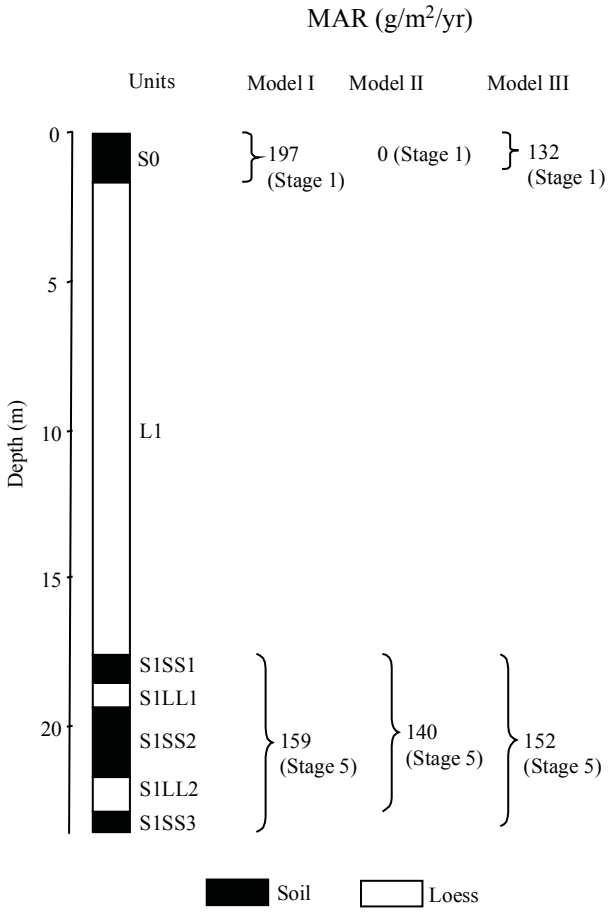

Stratigraphic data: Baicaoyuan (depth and thickness estimated from diagram, to nearest 10 cm)				
Top depth (m)	Bottom depth (m)	Thickness (m)	Stratigraphic units	DBD (g/cm^3)
0.0	1.6	1.6	S0	n/a
1.6	17.5	15.9	L1	n/a
17.5	18.5	1.0	S1SS1	n/a
18.5	19.3	0.8	S1LL1	n/a
19.3	21.6	2.3	S1SS2	n/a
21.6	22.8	1.2	S1LL2	n/a
22.8	23.5	0.7	S1SS3	n/a

Baicaoyuan section: MAR (g/m^2/yr) based on magnetic susceptibility

Note: Digitized MS data. Last glacial loess (L1) is not subdivided.

Site location: 36.27° N, 105.10° E

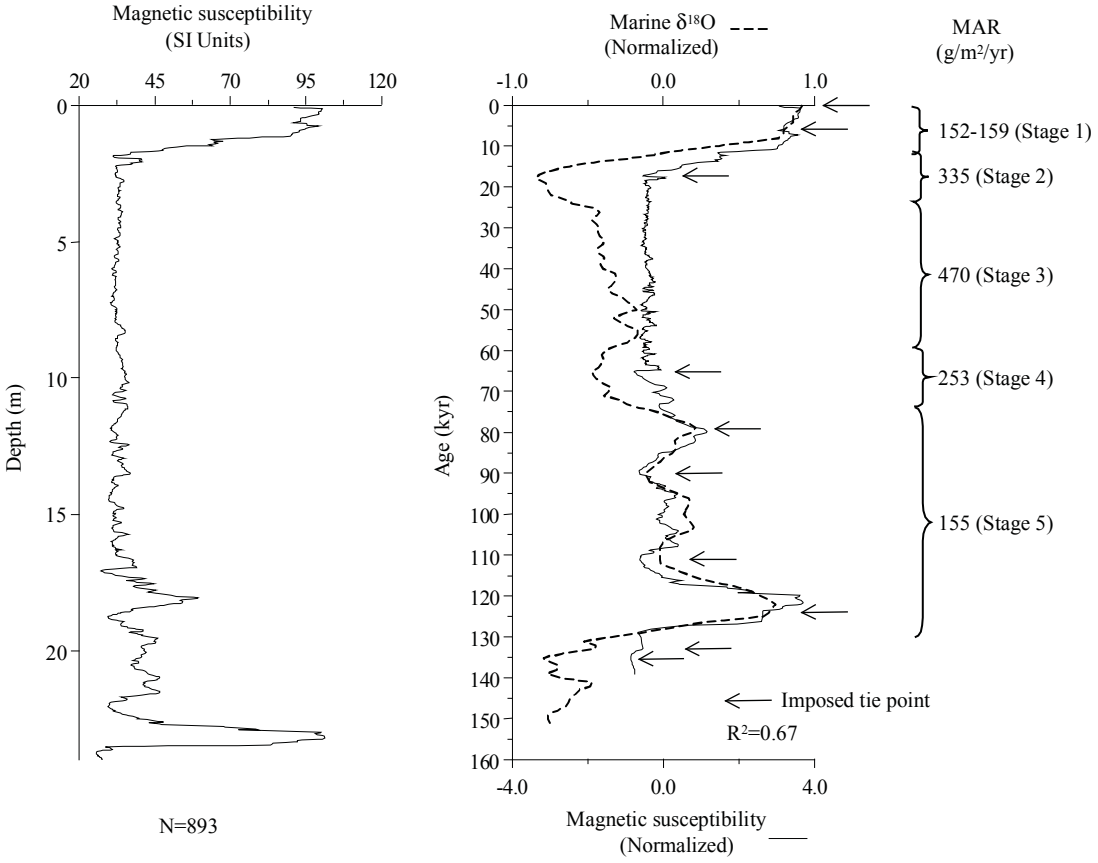

MS age model: Baicaoyuan		
Tie-Point	Depth (m)	Age (ka)
1	0.08	0.21
2	0.65	6.27
3	1.88	17.31
4	17.10	65.22
5	18.04	79.25
6	18.80	90.10
7	22.00	110.79
8	23.41	123.79
9	23.62	132.81
10	23.77	135.34

Age model (kyr): Baicaoyuan						
Depth (m)	^{14}C	TL	Magnetic susceptibility	Pedostratigraphy (Model III)	Average chronology	Range
0			0	0.0	0.0	
3			20.8		20.8	
6			30.3		30.3	
9			39.7		39.7	
12			49.2		49.2	
15			58.6		58.6	
18			78.8	78.9	78.8	78.8-78.9
21			104.2	107.8	106	104.2-107.8

MAR (g/m²/yr): Baicaoyuan								
Stage (range in kyr)	Assumed DBD (g/cm^3)	^{14}C	TL	MS	Pedostratigraphy			
					Model I	Model II	Model III	Average MAR
Stage 1 (12-0)	1.48			**156**	197	0	**132**	144
Stage 2 (24-12)	1.48			**335**				335
Stage 3 (59-24)	1.48			**470**				470
Stage 4 (74-59)	1.48			**253**				253
Stage 5 (130-74)	1.48			**155**	159	140	**152**	153.5

References used to generate data report: Baicaoyuan	
Data used	**Source**
Pedostratigraphy	Chu (1998)
Magnetic susceptibility	Chu (1998)
^{14}C dating	-
TL dating	-
Additional References:	
Data available	**Source**
Grain size, $CaCO_3$, $\delta^{13}C$, chemical parameters	Chu (1998)
Pedostratigraphy	Ding et al. (1990)
Pedostratigraphy	Ding et al. (1991)
Pedostratigraphy	Liu et al. (1991)
Pedostratigraphy	Rutter et al. (1991)

Baige section: MAR (g/m^2/yr) based on pedostratigraphy

Note: No Stage 1. The last glacial loess (L1) is not subdivided.

(Model I: min. glacial, max. interglacial; Model II: max. glacial, min. interglacial; Model III: 2/3 of interglacial soil is aeolian deposit)

Site location: 34.80° N, 112.62° E

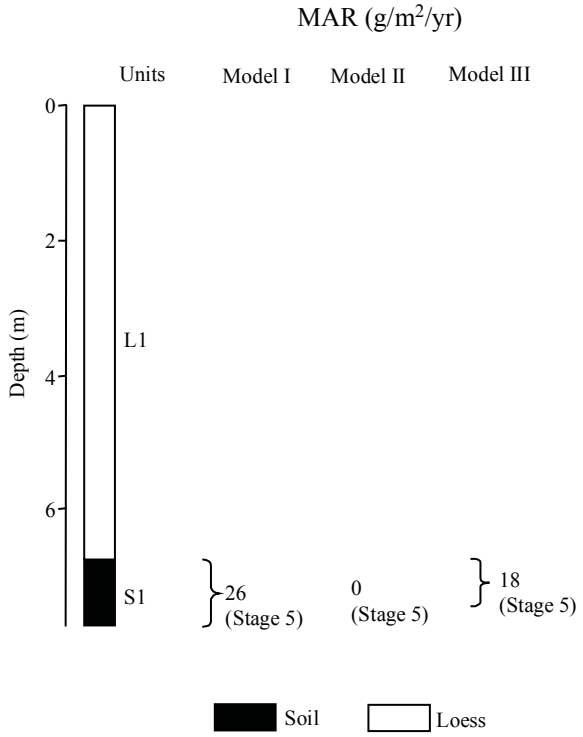

Stratigraphic data: Baige (thickness given by author, depth calculated from thickness)				
Top depth (m)	Bottom depth (m)	Thickness (m)	Stratigraphic units	DBD (g/cm^3)
0.0	6.7	6.7	L1	n/a
6.7	7.7	1.0	S1	n/a

Age model (kyr): Baige						
Depth (m)	^{14}C	TL	Magnetic susceptibility	Pedostratigraphy (Model III)	Average chronology	Range
0						
1						
2						
3						
4						
5						
6						
7				100.2	100.2	

MAR (g/m²/yr): Baige								
Stage (range in kyr)	Assumed DBD (g/cm^3)	^{14}C	TL	MS	Pedostratigraphy			Average MAR
					Model I	Model II	Model III	
Stage 1 (12-0)	1.48							
Stage 2 (24-12)	1.48							
Stage 3 (59-24)	1.48							
Stage 4 (74-59)	1.48							
Stage 5 (130-74)	1.48				26	0	**18**	18

References used to generate data report: Baige	
Data used	**Source**
Pedostratigraphy	Teng (1998)
Magnetic susceptibility	-
^{14}C dating	-
TL dating	-
Additional References:	
Data available	**Source**
Mammal fossils	Teng (1998)

Baimapo section: MAR (g/m^2/yr) based on pedostratigraphy

Note: Guo et al. (1996c) refer to this site as Beimapo (Lantian), and the site location is the same as for our site Baimapo. Guo et al. (1996c) claim to take data from Lu et al. (1988) but, in fact, they neither use the stratigraphy nor the dates from the Lu et al. (1988) paper. The Lu et al. (1988) section appears to refer to an entirely different site, here included as Chenjiawo (Lantian). Stage 1 affected by cultivation layer.

(Model I: min. glacial, max. interglacial; Model II: max. glacial, min. interglacial; Model III: 2/3 of interglacial soil is aeolian deposit)

Site location: 34.17° N, 109.32° E

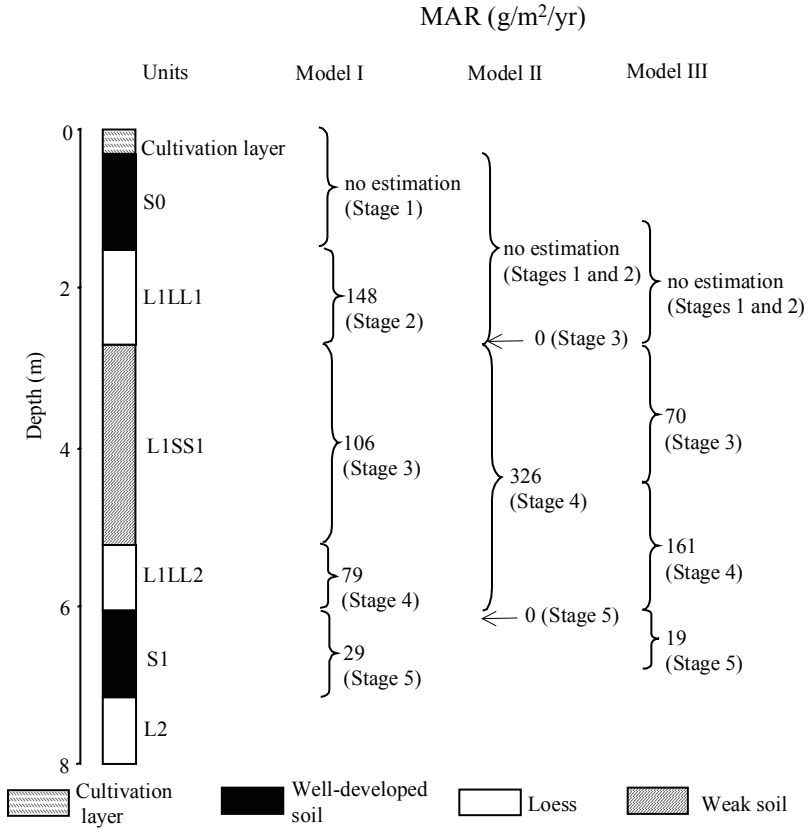

Stratigraphic data: Baimapo (depth and thickness estimated from diagram, to nearest 10 cm)				
Top depth (m)	Bottom depth (m)	Thickness (m)	Stratigraphic units	DBD (g/cm^3)
0.0	0.3	0.3	cultivation layer	n/a
0.3	1.5	1.2	S0	n/a
1.5	2.7	1.2	L1LL1	n/a
2.7	5.2	2.5	L1SS1	n/a
5.2	6.0	0.8	L1LL2	n/a
6.0	7.1	1.1	S1	n/a
7.1			L2	n/a

Baimapo section: TL dating

Note: Guo et al. (1996c) refer to this site as Beimapo (Lantian), and the site location is the same as for our site Baimapo. Guo et al. (1996c) claim to take data from Lu et al. (1988) but, in fact, they neither use the stratigraphy nor the dates from the Lu et al. (1988) paper. The Lu et al. (1988) section appears to refer to an entirely different site, here included as Chenjiawo (Lantian). In addition to taking the magnetic susceptibility and stratigraphic boundaries from An et al. (1991a) (as stated), Guo et al. (1996) take the TL dates from An et al. (1991a). One of the dates in An et al. (1991a) (88.5 ± 8) is misquoted as (88 ± 8) in Guo et al. (1996c). Stage 1 affected by cultivation layer; no MAR calculated because only one TL date is used.

Site location: 34.17° N, 109.32° E

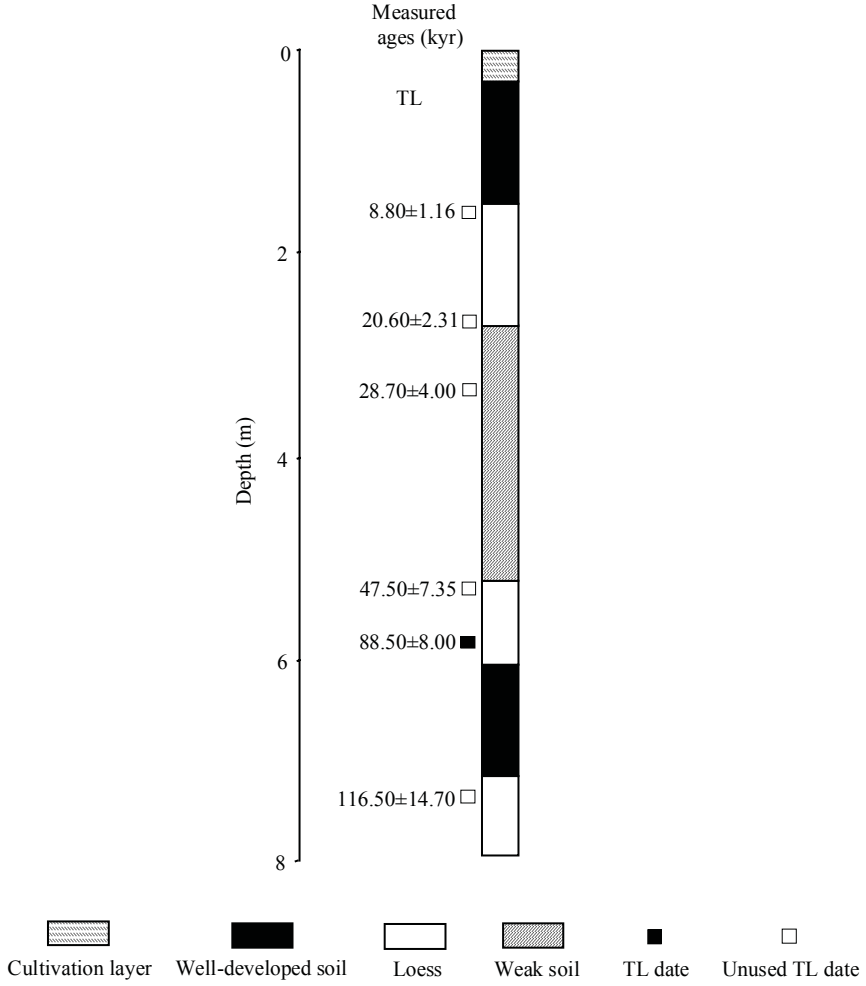

TL dating: Baimapo
(depth for TL dates estimated from diagram, to nearest 1 cm)

Depth (m)	Dating laboratory	Lab. No.	Dating material	TL-method	Age (kyr)	s.d. (kyr)	Reference	Comments
1.6	Xi'an Loess Lab.	n/a	n/a	Fine-grain (4-11 μm) technique	8.8	1.16	An et al. (1991a)	uncertainties larger than 10 %
2.67	Xi'an Loess Lab.	n/a	n/a	Fine-grain (4-11 μm) technique	20.6	2.31	An et al. (1991a)	uncertainties larger than 10 %
3.33	Xi'an Loess Lab.	n/a	n/a	Fine-grain (4-11 μm) technique	28.7	4.0	An et al. (1991a)	uncertainties larger than 10 %
5.28	Xi'an Loess Lab.	n/a	n/a	Fine-grain (4-11 μm) technique	47.5	7.35	An et al. (1991a)	uncertainties larger than 10 %
5.81	Xi'an Loess Lab.	n/a	n/a	Fine-grain (4-11 μm) technique	88.5	8.0	An et al. (1991a)	
7.33	Xi'an Loess Lab.	n/a	n/a	Fine-grain (4-11 μm) technique	116.5	14.7	An et al. (1991a)	uncertainties larger than 10 %

Baimapo section: Magnetic susceptibility

Note: Digitized MS data. Stage 1 affected by cultivation layer. Guo et al. (1996c) refer to this site as Beimapo (Lantian) and the site location is the same as for our site Baimapo. Guo et al. (1996c) claim to take data from Lu et al. (1988) but, in fact, they neither use the stratigraphy nor the dates from the Lu et al. (1988) paper. The Lu et al. (1988) section appears to refer to an entirely different site, here included as Chenjiawo (Lantian).

Site location: 34.17° N, 109.32° E

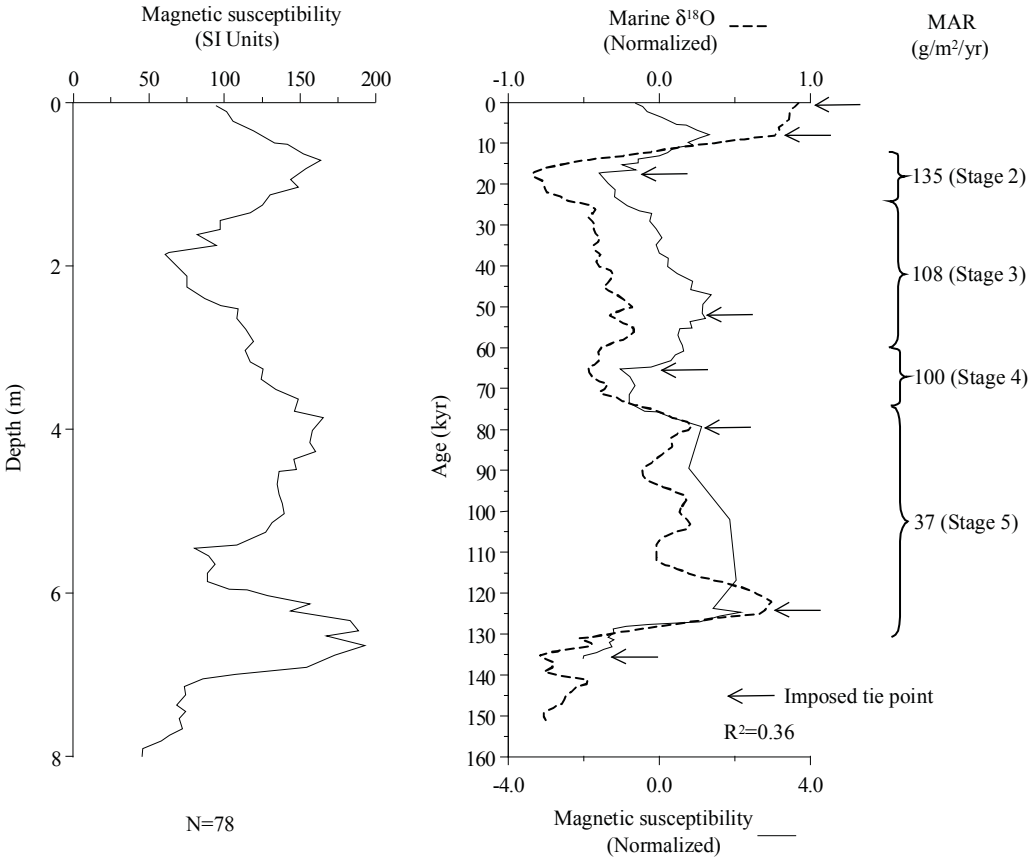

MS age model: Baimapo		
Tie-Point	Depth (m)	Age (kyr)
1	0.04	0.21
2	0.71	7.81
3	1.86	17.31
4	4.16	51.57
5	5.46	65.22
6	6.14	79.25
7	6.53	123.82
8	7.92	135.34

Age model (kyr): Baimapo						
Depth (m)	^{14}C	TL	Magnetic susceptibility	Pedostratigraphy (Model III)	Average chronology	Range
0						
1			10		10.0	
2			19		19.0	
3			34	30.2	32.1	30.2-34.0
4			49	51.0	50.0	49.0-51.0
5			60	64.6	62.3	60.0-64.6
6			76	74.0	75.0	74.0-76.0
7			128		128	

MAR (g/m²/yr): Baimapo								
Stage (range in kyr)	Assumed DBD (g/cm^3)	^{14}C	TL	MS	Pedostratigraphy			Average MAR
					Model I	Model II	Model III	
Stage 1 (12-0)	1.48							
Stage 2 (24-12)	1.48			**153**	148			153.0
Stage 3 (59-24)	1.48			**108**	106	0	**70**	89.0
Stage 4 (74-59)	1.48			**100**	79	326	**161**	130.5
Stage 5 (130-74)	1.48			**37**	29	0	**19**	28.0

References used to generate data report: Baimapo	
Data used	**Source**
Pedostratigraphy	An et al. (1991a)
Magnetic susceptibility	An et al. (1991a)
^{14}C dating	-
TL dating	An et al. (1991a)
Additional References:	
Data available	**Source**
Magnetic susceptibility	An et al. (1991c)
Pedostratigraphy, TL	Guo et al. (1996c)

Baishui section: MAR (g/m^2/yr) based on magnetic susceptibility

Note: Stage 1 affected by cultivation layer.

Site location: 35.20° N, 109.59° E

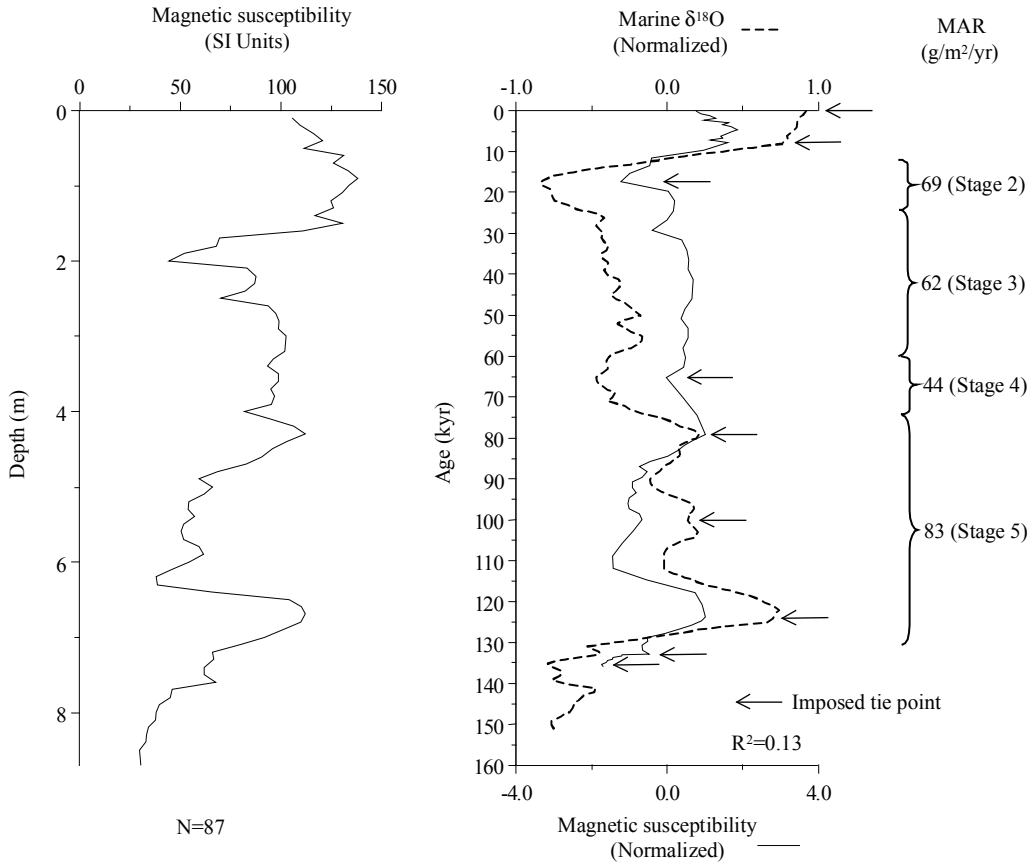

MS age model: Baishui		
Tie-Point	Depth (m)	Age (kyr)
1	0.10	0.21
2	1.50	7.81
3	2.00	17.31
4	4.00	65.22
5	4.30	79.25
6	5.90	99.96
7	6.70	123.79
8	7.60	132.81
9	8.50	135.34

Age model (kyr): Baishui						
Depth (m)	^{14}C	TL	Magnetic susceptibility	Pedostratigraphy (Model III)	Average chronology	Range
0						
1			5.1		5.1	
2			17.3		17.3	
3			41.3		41.3	
4			65.2		65.2	
5			88.3		88.3	
6			102.9		102.9	
7			126.8		126.8	
8			133.9		133.9	

MAR (g/m²/yr): Baishui								
Stage (range in kyr)	Assumed DBD (g/cm^3)	^{14}C	TL	MS	Pedostratigraphy			Average MAR
					Model I	Model II	Model III	
Stage 1 (12-0)	1.48							
Stage 2 (24-12)	1.48			**69**				69
Stage 3 (59-24)	1.48			**62**				62
Stage 4 (74-59)	1.48			**44**				44
Stage 5 (130-74)	1.48			**83**				83

References used to generate data report: Baishui	
Data used	**Source**
Pedostratigraphy	-
Magnetic susceptibility	Ding et al. (1999b)
^{14}C dating	-
TL dating	-
Additional References:	
Data available	**Source**
-	-

Banshan section: MAR (g/m^2/yr) based on pedostratigraphy

(Model I: min. glacial, max. interglacial; Model II: max. glacial, min. interglacial; Model III: 2/3 of interglacial soil is aeolian deposit)

Site location: 34.68° N, 105.70° E

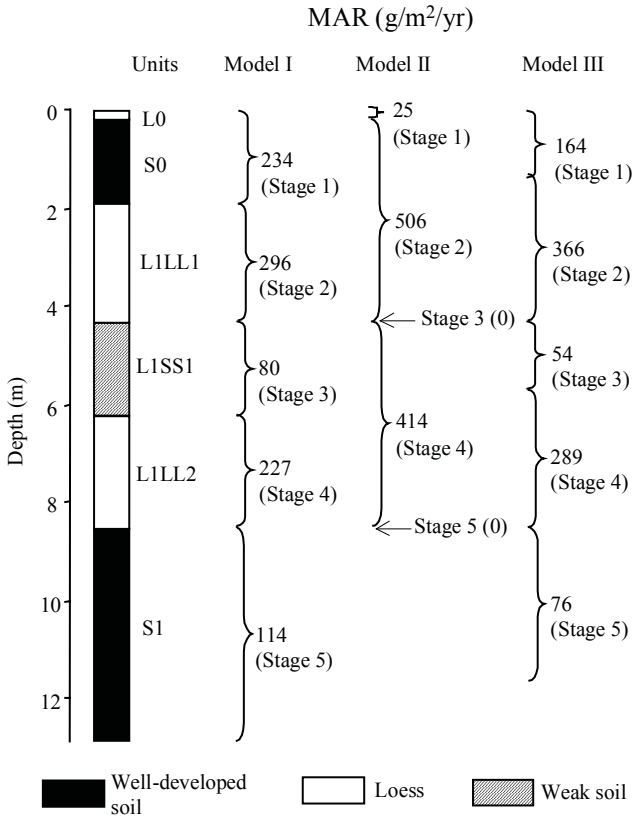

Stratigraphic data: Banshan (depth given by the authors, thickness calculated from depths)				
Top depth (m)	Bottom depth (m)	Thickness (m)	Stratigraphic units	DBD (g/cm^3)
0.0	0.2	0.2	L0	n/a
0.2	1.9	1.7	S0	n/a
1.9	4.3	2.4	L1LL1	n/a
4.3	6.2	1.9	L1SS1	n/a
6.2	8.5	2.3	L1LL2	n/a
8.5	12.8	4.3	S1	n/a

Age model (kyr): Banshan						
Depth (m)	^{14}C	TL	Magnetic susceptibility	Pedostratigraphy (Model III)	Average chronology	Range
0				0.0	0.0	
2				14.7	14.7	
4				22.7	22.7	
6				61.0	61.0	
8				71.4	71.4	
10				102.9	102.9	
12						

MAR (g/m²/yr): Banshan								
Stage (range in kyr)	Assumed DBD (g/cm^3)	^{14}C	TL	MS	Pedostratigraphy			Average MAR
					Model I	Model II	Model III	
Stage 1 (12-0)	1.48				234	25	**164**	164
Stage 2 (24-12)	1.48				296	506	**366**	366
Stage 3 (59-24)	1.48				80	0	**54**	54
Stage 4 (74-59)	1.48				227	414	**289**	289
Stage 5 (130-74)	1.48				114	0	**76**	76

References used to generate data report:	
Data used	**Source**
Pedostratigraphy	Derbyshire et al. (1995a)
Magnetic susceptibility	-
^{14}C dating	-
TL dating	-
Additional References:	
Data available	**Source**
Pedostratigraphy	Kemp et al. (1995)

Baoji (Lingyuan) section: MAR (g/m^2/yr) based on pedostratigraphy

Note: Rutter et al. (1991) called this section Baoji after the name of the nearest city (Baoji City of Shaaxi Province). Lingyuan is the name of the village where the section is located (surburb of Baoji City).

(Model I: min. glacial, max. interglacial; Model II: max. glacial, min. interglacial; Model III: 2/3 of interglacial soil is aeolian deposit)

Site location: 34.33° N, 107.00° E

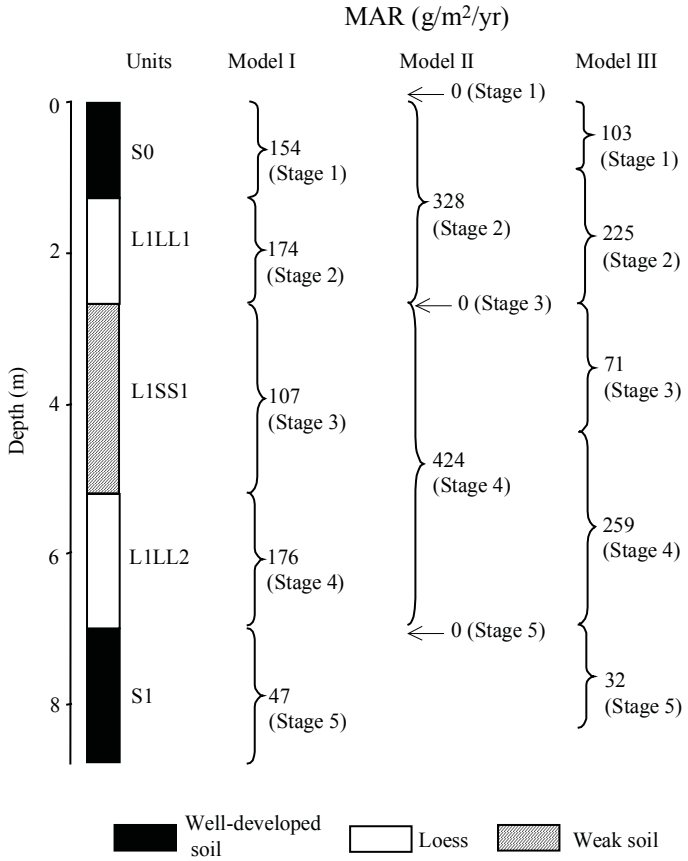

Stratigraphic data: Baoji (Lingyuan) (depth and thickness estimated from diagram, to nearest 1 cm)				
Top depth (m)	Bottom depth (m)	Thickness (m)	Stratigraphic units	DBD (g/cm^3)
0.00	1.25	1.25	S0	n/a
1.25	2.66	1.41	L1LL1	n/a
2.66	5.18	2.52	L1SS1	n/a
5.18	6.96	1.78	L1LL2	n/a
6.96	8.75	1.79	S1	n/a

Baoji (Lingyuan) section: MAR (g/m^2/yr) based on magnetic susceptibility

Note: Rutter et al. (1991) called this section Baoji after the name of the nearest city (Baoji City of Shaaxi Province). Lingyuan is the name of the village where the section is located (surburb of Baoji City). Unpublished data measured by Dr. Ding Zhongli.

Site location: 34.33° N, 107.00° E

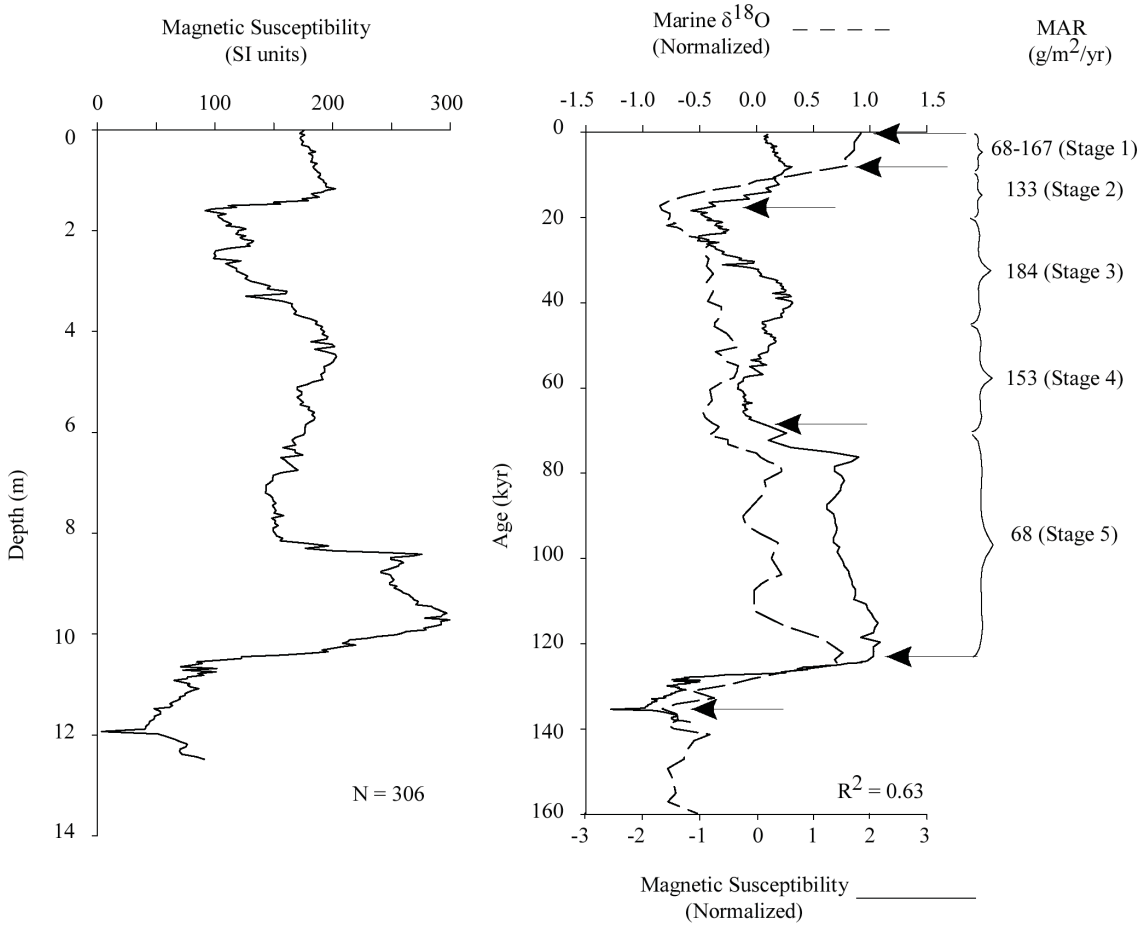

MS age model: Baoji (Lingyuan)		
Tie-Point	Depth (m)	Age (kyr)
1	0.00	0.21
2	1.17	7.81
3	1.57	17.85
4	8.15	66.97
5	9.85	123.79
6	11.93	135.10

Age model (kyr): Baoji (Lingyuan)						
Depth (m)	^{14}C	TL	Magnetic susceptibility	Pedostratigraphy (Model III)	Average chronology	Range
0			0.2	0.0	0.1	0.0-0.2
2			21.1	19.5	20.3	19.5-21.1
4			36.0	51.8	43.9	36.0-51.8
6			50.9	68.5	59.7	50.9-68.5
8			65.9	122.6	94.3	65.9-122.6
10			124.6		124.6	

MAR (g/m²/yr): Baoji (Lingyuan)								
Stage (range in kyr)	Assumed DBD (g/cm^3)	^{14}C	TL	MS	Pedostratigraphy			Average MAR
					Model I	Model II	Model III	
Stage 1 (12-0)	1.48			**118**	154	0	**103**	**111**
Stage 2 (24-12)	1.48			**133**	174	328	**225**	**179**
Stage 3 (59-24)	1.48			**184**	107	0	**71**	**128**
Stage 4 (74-59)	1.48			**153**	176	424	**259**	**206**
Stage 5 (130-74)	1.48			**68**	47	0	**32**	**50**

References used to generate data report: Baoji (Lingyuan)	
Data used	**Source**
Pedostratigraphy	Liu and Ding (1993)
Magnetic susceptibility	Z. Ding (unpublished data)
^{14}C dating	-
TL dating	-
Additional References:	
Data available	**Source**
Pedostratigraphy, magnetic polarity	Ding et al. (1990)
Pedostratigraphy, magnetic susceptibility, magnetic polarity, micromorphology	Ding et al. (1991)
Pedostratigraphy, magnetic susceptibility, grain size, magnetic polarity	Ding et al. (1992)
Pedostratigraphy, grain size, magnetic polarity	Ding et al. (1994)
Grain size	Ding et al. (1995)
Pedostratigraphy, magnetic susceptibility, $\delta^{18}O$, $CaCO_3$	Gu et al. (1991)
Pedostratigraphy, micromorphology, magnetic polarity	Rutter et al. (1991)
Pedostratigraphy, magnetic polarity	Liu et al. (1991)
Pedostratigraphy	Wei et al. (1991)
Pedostratigraphy, magnetic polarity	Yu et al. (1991)
Pedostratigraphy, grain size, magnetic susceptibility, magnetic polarity	Rutter (1992)
Grain size, $\delta^{18}O$, $CaCO_3$	Liu and Ding (1993)
Pedostratigraphy, micromorphology, magnetic polarity	Rutter and Ding (1993)

Baxie (Dongxiang) section: Pedostratigraphy

Note: This site is generally called Baxie, which is the name of the village where the section is located. It is also called Dongxiang (e.g. Zhou and An, 1991) which is the name of the County in which Baxie lies. Section with potential local river sources. Stage 1 affected by reworked loess.

(Model I: min. glacial, max. interglacial; Model II: max. glacial, min. interglacial; Model III: 2/3 of interglacial soil is aeolian deposit)

Site location: 35.58° N, 103.57° E

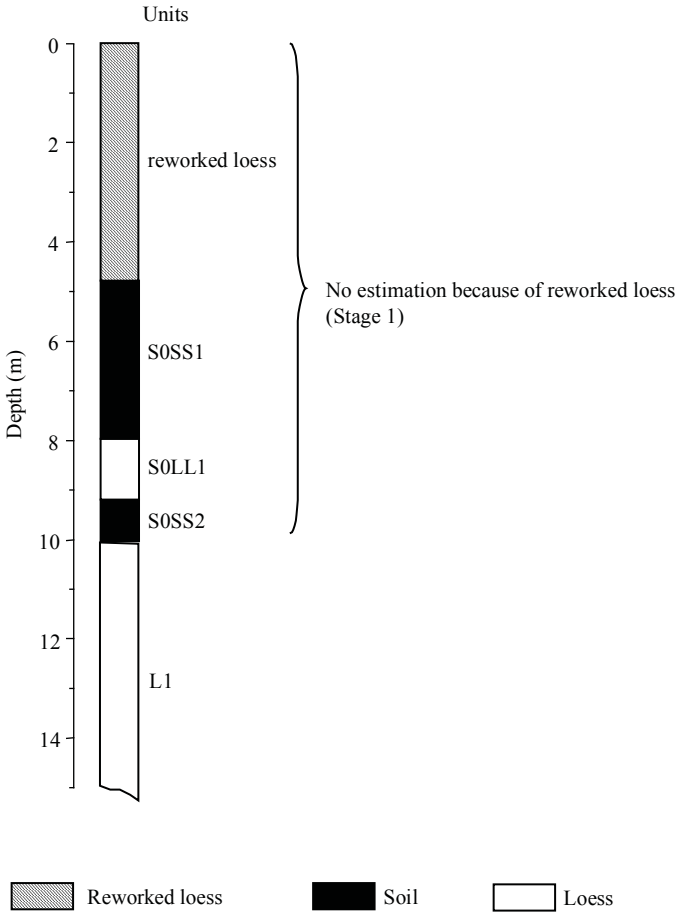

Stratigraphic data: Baxie (Dongxiang) (depth given by the authors, thickness calculated from depths)				
Top depth (m)	Bottom depth (m)	Thickness (m)	Stratigraphic units	DBD (g/cm^3)
0.00	4.90	4.90	reworked loess	n/a
4.90	8.00	3.10	S0SS1	n/a
8.00	9.25	1.25	S0LL1	n/a
9.25	10.00	0.75	S0SS2	n/a
10.00	15.00	5.00	L1	n/a

Baxie (Dongxiang) section: MAR (g/m^2/yr) based on ^{14}C and TL dating

Note: This site is generally called Baxie, which is the name of the village where the section is located. It is also called Dongxiang (e.g. Zhou and An, 1991) which is the name of the County in which Baxie lies. Section with potential local river sources. Stages 1 and 2 MAR calculated excluding reworked loess based on available dates.

Site location: 35.58° N, 103.57° E

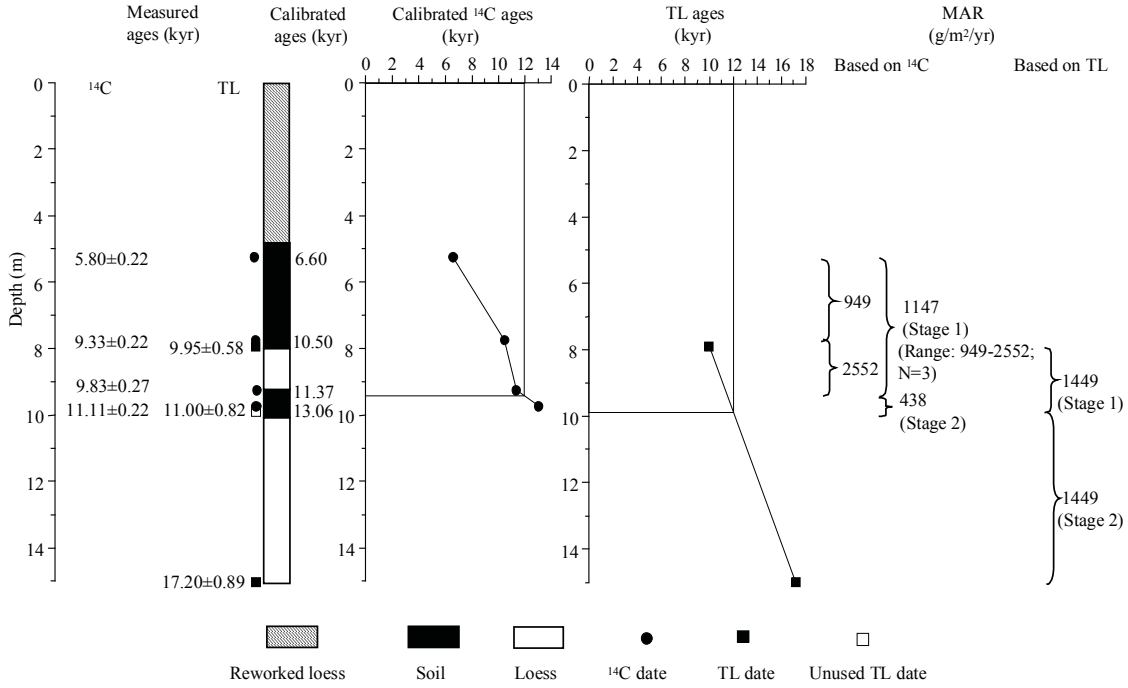

^{14}C dating: Baxie (Dongxiang) (depth given by the authors)										
Depth (m)	Dating laboratory	Lab. No.	Dating material	Age (kyr)	s.d. (kyr)	(1σ) Calendar age ranges (kyr)	Relative probability	Assumed calendar age (kyr)	Reference	Comments
5.25	Xi'an Loess Lab.	XLLQ442	humin	5.8	0.2	6.40-6.81	0.859	6.6	Zhou et al. (1992)	
						6.82-6.89	0.112			
						6.35-6.37	0.029			
7.75	Xi'an Loess Lab.	XLLQ416	humin	9.33	0.22	10.24-10.76	0.893	10.5	Zhou et al. (1992)	
						10.96-11.00	0.054			
						11.02-11.06	0.054			
9.25	Xi'an Loess Lab.	XLLQ415	humin	9.83	0.27	11.04-11.71	0.735	11.37	Zhou et al. (1992)	
						11.86-11.90	0.031			
						11.71-11.75	0.023			
9.75	Xi'an Loess Lab.	XLLQ441	humin	11.1	0.22	12.90-13.21	0.76	13.06	Zhou et al. (1992)	

TL dating: Baxie (Dongxiang) (depth given by the authors)							
Depth (m)	Dating laboratory	Lab. No.	Dating material	TL-method	Age (kyr)	s.d. (kyr)	Reference	Comments
7.9	n/a	n/a	n/a	n/a	9.95	0.58	Zhou et al. (1992)	
9.8	n/a	n/a	n/a	n/a	11.0	0.82	Zhou et al. (1992)	not used, overlapping
15.0	n/a	n/a	n/a	n/a	17.2	0.89	Zhou et al. (1992)	

Baxie (Dongxiang) section: Magnetic susceptibility

Note: This site is generally called Baxie, which is the name of the village where the section is located. It is also called Dongxiang (e.g. Zhou and An, 1991) which is the name of the County in which Baxie lies. Section with potential local river sources. Section with potential local river sources. Digitized MS data.

Site location: 35.58° N, 103.57° E

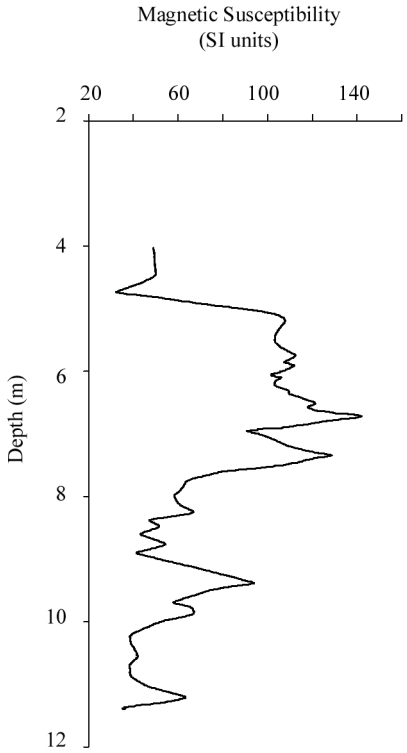

Age model (kyr): Baxie (Dongxiang)						
Depth (m)	^{14}C	TL	Magnetic susceptibility	Pedostratigraphy (Model III)	Average chronology	Range
0						
3						
6	7.7				7.7	
9	11.2	11.1			11.2	11.1-11.2
12		14.2			14.2	
15		17.2			17.2	

MAR (g/m²/yr): Baxie (Dongxiang)								
Stage (range in kyr)	Assumed DBD (g/cm^3)	^{14}C	TL	MS	Pedostratigraphy			Average MAR
					Model I	Model II	Model III	
Stage 1 (12-0)	1.48	**1147**	**1449**					1298
Stage 2 (24-12)	1.48	**438**	**1449**					943.5
Stage 3 (59-24)	1.48							
Stage 4 (74-59)	1.48							
Stage 5 (130-74)	1.48							

References used to generate data report: Baxie (Dongxiang)	
Data used	**Source**
Pedostratigraphy	Zhou et al. (1992)
Magnetic susceptibility	Zhou et al. (1992)
^{14}C dating	Zhou et al. (1992)
TL dating	Zhou et al. (1992)
Additional References:	
Data available	**Source**
^{14}C, TL, pedostratigraphy	Zhou and An (1991)
Magnetic susceptibility, $\delta^{13}C$, total organic carbon	Zhou et al. (1992)
Magnetic susceptibility, grain size, $\delta^{13}C$, total organic carbon, ^{14}C, TL, pedostratigraphy	An et al. (1993)
Magnetic susceptibility, ^{14}C, pedostratigraphy	An et al. (2000)
Pedostratigraphy	Zhang (1989)

Beiyuan section: MAR (g/m^2/yr) based on pedostratigraphy

Note: Guo et al. (1996c) refer to this site as Beiyuan (Linxia).

(Model I: min. glacial, max. interglacial; Model II: max. glacial, min. interglacial; Model III: 2/3 of interglacial soil is aeolian deposit)

Site location: 35.62° N, 103.20° E

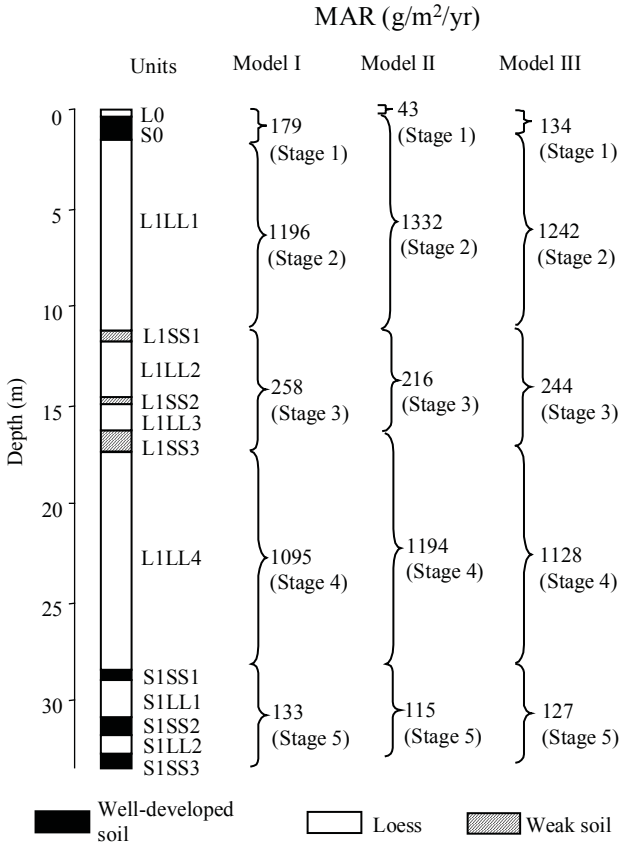

Stratigraphic data: Beiyuan (depth and thickness from L0 to L1LL4 given by the authors, the other depths and thickness estimated from diagram, to nearest 1 cm)				
Top depth (m)	Bottom depth (m)	Thickness (m)	Stratigraphic units	DBD (g/cm^3)
0.00	0.35	0.35	L0	n/a
0.35	1.45	1.10	S0	n/a
1.45	11.15	9.70	L1LL1	n/a
11.15	11.65	0.50	L1SS1	n/a
11.65	14.50	2.85	L1LL2	n/a
14.50	14.95	0.45	L1SS2	n/a
14.95	16.25	1.30	L1LL3	n/a
16.25	17.25	1.00	L1SS3	n/a
17.25	28.35	11.10	L1LL4	n/a
28.35	29.00	0.65	S1SS1	n/a
29.00	30.70	1.70	S1LL1	n/a
30.70	31.70	1.00	S1SS2	n/a
31.70	32.70	1.00	S1LL2	n/a
32.70	33.40	0.70	S1SS3	n/a

Beiyuan section: MAR (g/m^2/yr) based on ^{14}C and TL dating

Note: Guo et al. (1996) refer to this site as Beiyuan (Linxia). Only one calibrated ^{14}C date is used, so no MAR calculated based on ^{14}C dating.

Site location: 35.62° N, 103.20° E

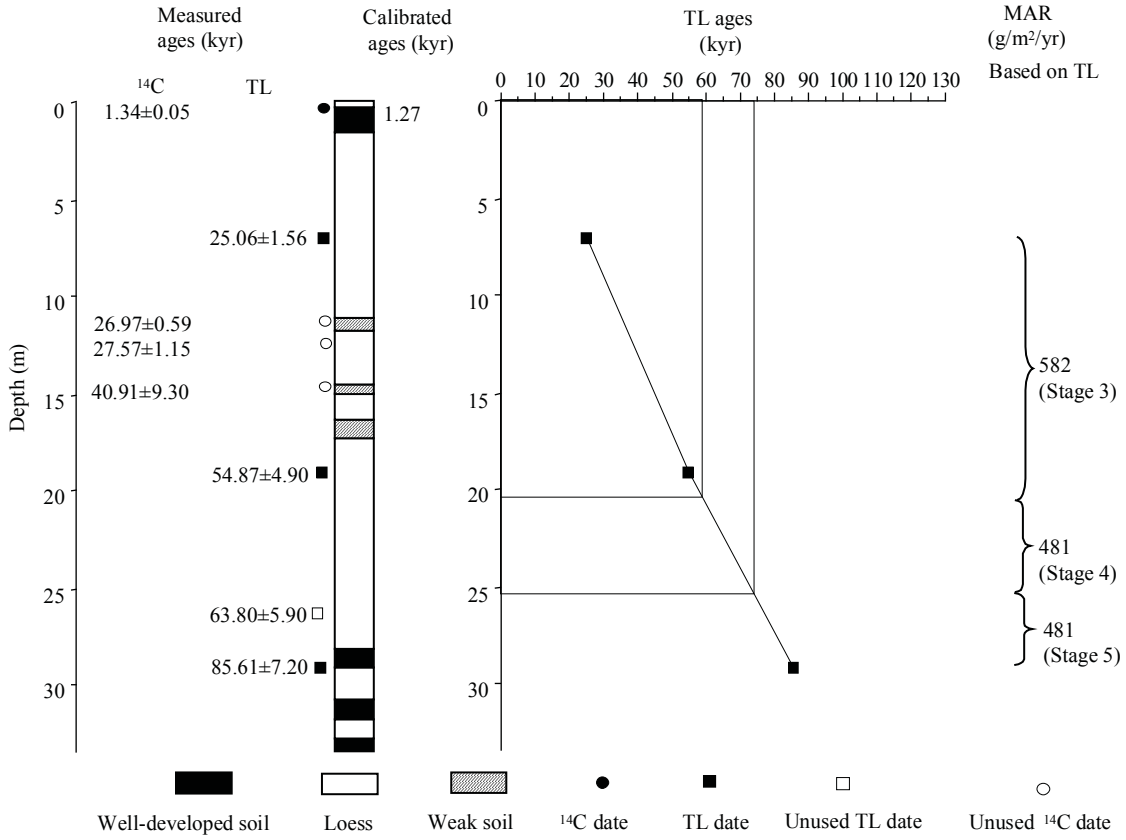

^{14}C dating: Beiyuan
(depth for the upper two and the lowest dates given by Li et al. (1990); depth of other date estimated from diagram of Kang and Li (1993) at the same section, to nearest 1 cm)

Depth (m)	Dating laboratory	Lab. No.	Dating material	Age (kyr)	s.d. (kyr)	(1σ) Calendar age ranges (kyr)	Relative probability	Assumed calendar age (kyr)	Reference	Comments
0.35	n/a	n/a	n/a	1.34	0.05	1.24-1.30	0.82	1.27	Li et al. (1990)	
						1.19-1.20	0.18			
11.15	n/a	n/a	n/a	26.97	0.59				Li et al. (1990)	beyond calibration range
12.30	n/a	n/a	n/a	27.57	1.15				Kang and Li (1993)	not used, overlapping
14.50	n/a	n/a	n/a	40.91	9.30				Li et al. (1990)	not used, error bar >2 kyr

TL dating: Beiyuan
(depth estimated from diagrams of Li et al. (1990), An et al. (1991a) and Fang et al. (1994))

Depth (m)	Dating laboratory	Lab. No.	Dating material	TL-method	Age (kyr)	s.d. (kyr)	Reference	Comments
7.0	Xi'an Loess Lab.	n/a	n/a	n/a	25.06	1.56	An et al. (1991a)	
19.0	Xi'an Loess Lab.	n/a	n/a	n/a	54.87	4.9	An et al. (1991a)	
26.0	Xi'an Loess Lab.	n/a	n/a	n/a	63.8	5.9	An et al. (1991a)	not used, overlapping
29.0	n/a	n/a	n/a	n/a	85.61	7.2	Li et al. (1990)	
32.8	n/a	n/a	n/a	n/a	94.0	10.0	Fang et al. (1994)	estimated to nearest 10 cm from graph; uncertainties >10%
34.4	n/a	n/a	n/a	n/a	125.0	13.0	Fang et al. (1994)	estimated to nearest 10 cm from graph; uncertainties >10%
35.0	n/a	n/a	n/a	n/a	138.0	14.0	Fang et al. (1994)	estimated to nearest 10 cm from graph; uncertainties >10%
35.5	n/a	n/a	n/a	n/a	141.4	14.1	Li et al. (1990)	not used, age >130kyr

Beiyuan section: MAR (g/m^2/yr) based on magnetic susceptibility

Note: Guo et al. (1996c) refer to this site as Beiyuan (Linxia). Digitized MS data.

Site location: 35.62° N, 103.20° E

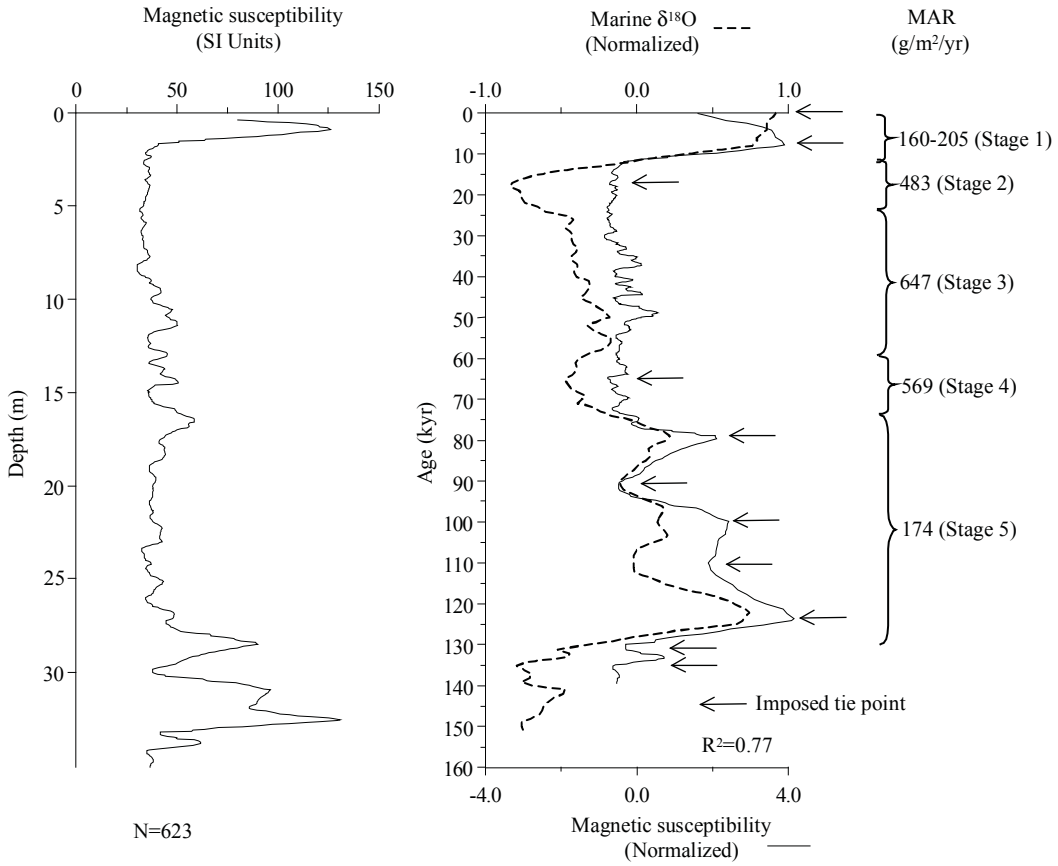

MS age model: Beiyuan		
Tie-Point	Depth (m)	Age (kyr)
1	0.39	0.21
2	0.88	7.81
3	2.65	17.31
4	23.61	65.22
5	28.48	79.25
6	29.91	90.95
7	30.96	99.96
8	31.96	110.79
9	32.57	123.79
10	33.34	131.09
11	34.23	135.34

Age model (kyr): Beiyuan						
Depth (m)	^{14}C	TL	Magnetic susceptibility	Pedostratigraphy (Model III)	Average chronology	Range
0			0	0.0	0.0	
4			20.4	15.5	17.9	15.5-20.4
8		27.8	29.5	20.2	25.8	20.2-29.5
12		37.7	38.7	29.0	35.1	29.0-38.7
16		47.8	47.8	53.5	49.7	47.8-53.5
20		58.3	57	63.0	59.4	57.0-63.0
24		70.5	66.3	68.3	68.4	66.3-70.5
28		82.5	77.9	73.5	78	73.5-82.5
32			110.8	116.8	113.8	110.8-116.8

MAR (g/m²/yr): Beiyuan								
Stage (range in kyr)	Assumed DBD (g/cm^3)	^{14}C	TL	MS	Pedostratigraphy			Average MAR
					Model I	Model II	Model III	
Stage 1 (12-0)	1.48			**183**	179	43	**134**	158
Stage 2 (24-12)	1.48			**483**	1196	1332	**1242**	862.5
Stage 3 (59-24)	1.48		**582**	**647**	258	216	**244**	491
Stage 4 (74-59)	1.48		**481**	**569**	1095	1194	**1128**	726
Stage 5 (130-74)	1.48		**481**	**174**	133	115	**127**	261

References used to generate data report: Beiyuan	
Data used	**Source**
Pedostratigraphy	Li et al. (1990)
Magnetic susceptibility	Li et al. (1990)
^{14}C dating	Li et al. (1990), Kang and Li (1993)
TL dating	Li et al. (1990), An et al. (1991a), Fang et al. (1994)
Additional References:	
Data available	**Source**
Grain size, chemical parameters	Li et al. (1990)
Pedostratigraphy, magnetic susceptibility, TL, grain size, micromorphology, carbonate content	Fang et al. (1994)
Magnetic susceptibility, pedostratigraphy	An et al. (1991a)
Magnetic susceptibility, pedostratigraphy	An et al. (1991c)
Magnetic susceptibility, ^{14}C, TL, pedostratigraphy	Chen et al. (1991b)
Magnetic susceptibility, pedostratigraphy	Kang and Li (1993)
Chemical parameters, pedostratigraphy, magnetic susceptibility, carbonate content, grain size, mammal fossils, pollen	Li et al. (1992a)
Pedostratigraphy, TL	Guo et al. (1996c)

Beiyuantou section: MAR (g/m^2/yr) based on magnetic susceptibility

Note: Digitized MS data.

Site location: 36.05° N, 107.50° E

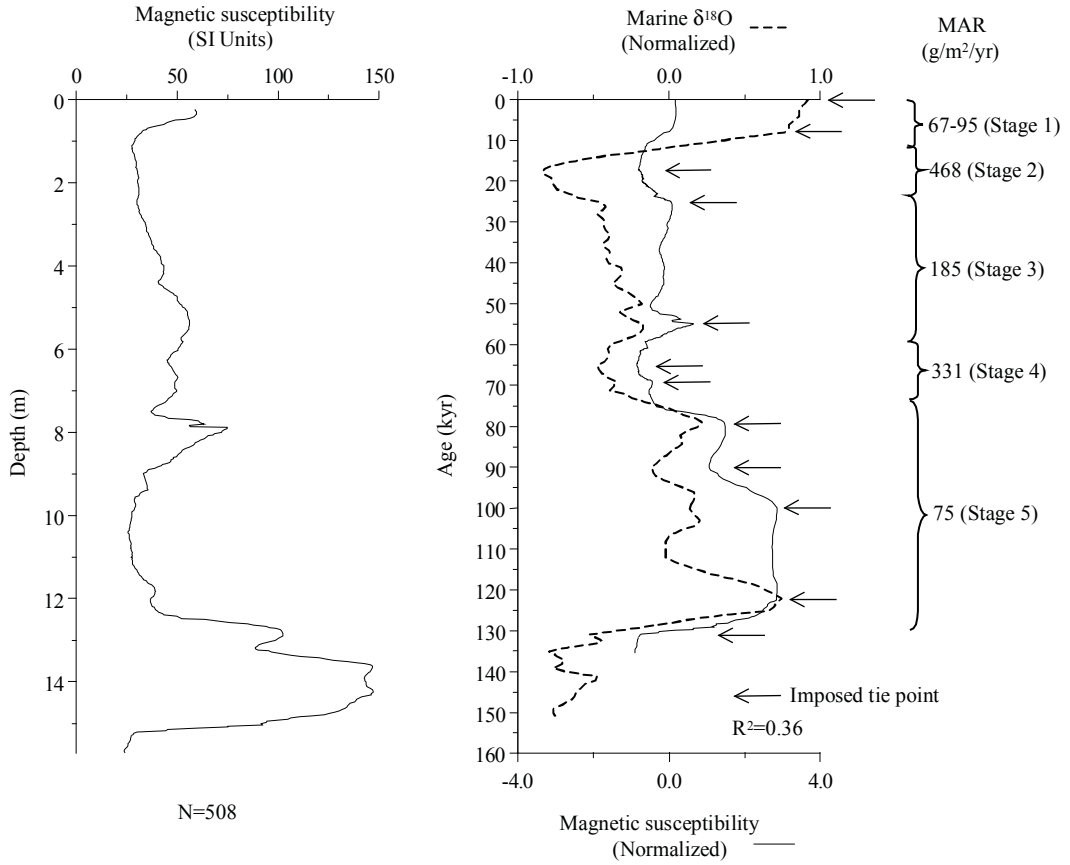

MS age model: Beiyuantou		
Tie-Point	Depth (m)	Age (kyr)
1	0.24	0.21
2	0.48	7.81
3	1.14	17.31
4	5.29	25.42
5	7.89	54.84
6	10.49	65.22
7	11.83	69.19
8	12.79	79.25
9	13.21	90.10
10	13.63	99.96
11	14.31	122.56
12	15.24	131.09

Age model (kyr): Beiyuantou						
Depth (m)	^{14}C	TL	Magnetic susceptibility	Pedostratigraphy (Model III)	Average chronology	Range
0			0.0		0.0	
3			20.9		20.9	
6			33.3		33.3	
9			59.2		59.2	
12			71.0		71.0	
15			128.9		128.9	

MAR (g/m²/yr): Beiyuantou								
Stage (range in kyr)	Assumed DBD (g/cm^3)	^{14}C	TL	MS	Pedostratigraphy			Average MAR
					Model I	Model II	Model III	
Stage 1 (12-0)	1.48			**81**				81
Stage 2 (24-12)	1.48			**468**				468
Stage 3 (59-24)	1.48			**185**				185
Stage 4 (74-59)	1.48			**331**				331
Stage 5 (130-74)	1.48			**75**				75

References used to generate data report: Beiyuantou	
Data used	**Source**
Pedostratigraphy	-
Magnetic susceptibility	Sun et al. (1995)
^{14}C dating	-
TL dating	-
Additional References:	
Data available	**Source**
-	-

Beizhuangcun (Weinan) section: Pedostratigraphy

Note: The soils are not the zonal soils of this region, and they cannot be totally aeolian in origin. Zhou and An (1991) used the name Weinan for this section. However, Weinan is usually used as the name of the typical loess section near Yangguo. The authors mention that the section studied is actually near the village of Beizhuangcun so, in order to avoid confusion, we use the village name. Mainly fluvial deposits (modern river terrace of Weihe River).

Site location: 34.50° N, 109.50° E

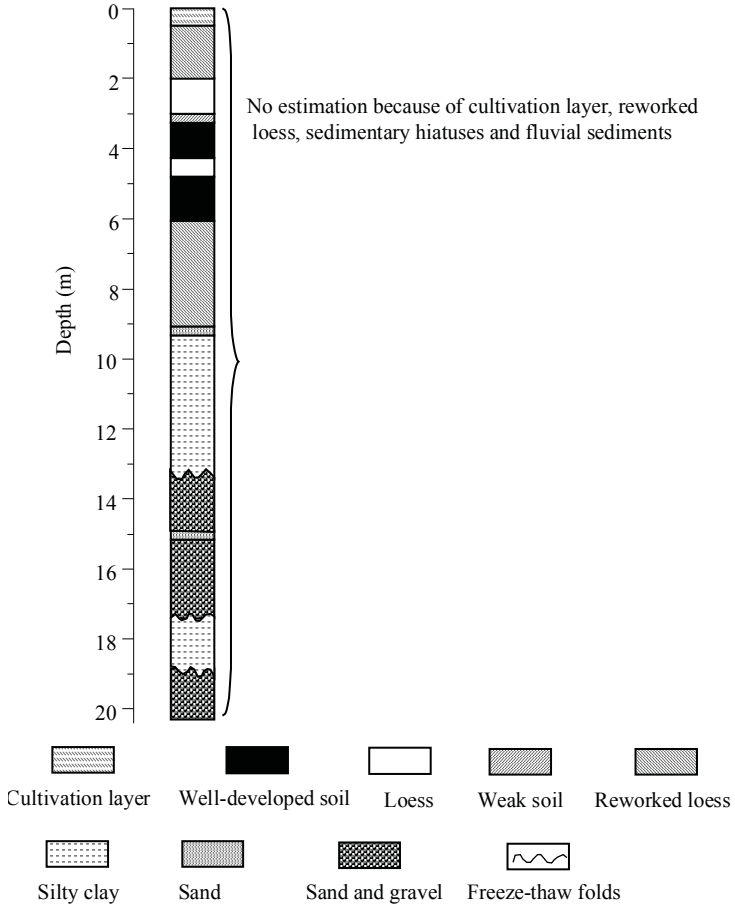

Stratigraphic data: Beizhuangcun (Weinan) (depth and thickness estimated from diagram, to nearest 10 cm)				
Top depth (m)	Bottom depth (m)	Thickness (m)	Stratigraphic units	DBD (g/cm^3)
0	0.58	0.58	cultivated soil	n/a
0.58	2.04	1.46	reworked loess	n/a
2.04	3.05	1.01	loess	n/a
3.05	3.43	0.38	weakly developed soil	n/a
3.43	4.31	0.88	palaeosol	n/a
4.31	4.89	0.58	loess	n/a
4.89	6.11	1.22	palaeosol	n/a
6.11	9.02	2.91	reworked loess	n/a
9.02	9.31	0.29	sand	n/a
9.31	13.38	4.07	silty clay	n/a
13.38	14.98	1.6	sand and gravel	n/a
14.98	15.27	0.29	sand	n/a
15.27	17.45	2.18	sand and gravel	n/a
17.45	18.91	1.46	silty clay	n/a
18.91	20.22	1.31	sand and gravel	n/a

Beizhuangcun (Weinan) section: MAR (g/m^2/yr) based on ^{14}C dating

Note: Zhou and An (1991) used the name Weinan for this section. However, Weinan is usually used as the name of the typical loess section near Yangguo. The authors mention that the section studied is actually near the village of Beizhuangcun so, in order to avoid confusion, we use the village name. Mainly fluvial deposits (modern river terrace of Weihe River).

Site location: 34.50° N, 109.50° E

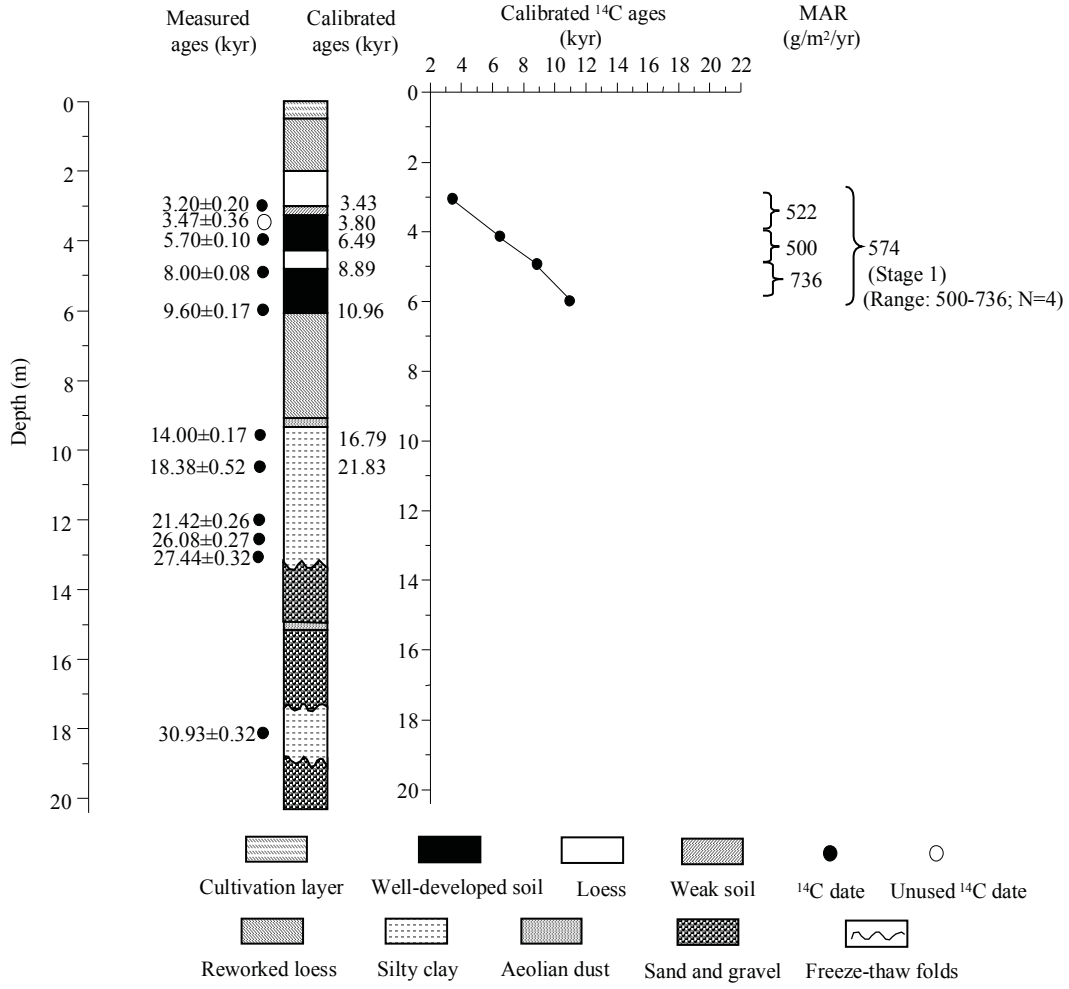

^{14}C dating: Beizhuangcun (Weinan) (depth estimated from diagram, to nearest 1 cm)										
Depth (m)	Dating laboratory	Lab. No.	Dating material	Age (kyr)	s.d. (kyr)	(1σ) Calendar age ranges (kyr)	Relative probability	Assumed calendar age (kyr)	Reference	Comments
3.05	n/a	n/a	humin	3.20	0.20	3.64-3.21	0.898	3.43	Zhou and An (1991)	
						3.19-3.16	0.044			
						3.68-3.66	0.043			
						3.08-3.08	0.014			
3.46	n/a	n/a	humin	3.47	0.36	4.25-3.34	0.992	3.80	Zhou and An (1991)	not used, overlapping
						3.28-3.27	0.008			
4.13	n/a	n/a	humin	5.70	0.10	6.57-6.40	0.772	6.49	Zhou and An (1991)	
						6.63-6.58	0.193			
						6.36-6.36	0.035			
4.94	n/a	n/a	humin	8.00	0.08	9.01-8.76	0.968	8.89	Zhou and An (1991)	
						8.74-8.72	0.032			
5.97	n/a	n/a	humin	9.60	0.17	11.17-10.74	0.980	10.96	Zhou and An (1991)	
						10.71-10.70	0.020			
9.89	n/a	n/a	humus	14.00	0.17	17.09-16.49	1.000	16.79	Zhou and An (1991)	
10.73	n/a	n/a	humus	18.38	0.52	22.52-21.14	1.000	21.83	Zhou and An (1991)	
12.01	n/a	n/a	humus	21.42	0.26				Zhou and An (1991)	beyond calibration range
12.57	n/a	n/a	humus	26.08	0.27				Zhou and An (1991)	beyond calibration range
13.06	n/a	n/a	humus	27.44	0.32				Zhou and An (1991)	beyond calibration range
18.03	n/a	n/a	humus	30.93	0.32				Zhou and An (1991)	beyond calibration range

Beizhuangcun (Weinan) section: Magnetic susceptibility

Note: Zhou and An (1991) used the name Weinan for this section. However, Weinan is usually used as the name of the typical loess section near Yangguo. The authors mention that the section studied is actually near the village of Beizhuangcun so, in order to avoid confusion, we use the village name. Mainly fluvial deposits (modern river terrace of Weihe River). Digitized MS data.

Site location: 34.50° N, 109.50° E

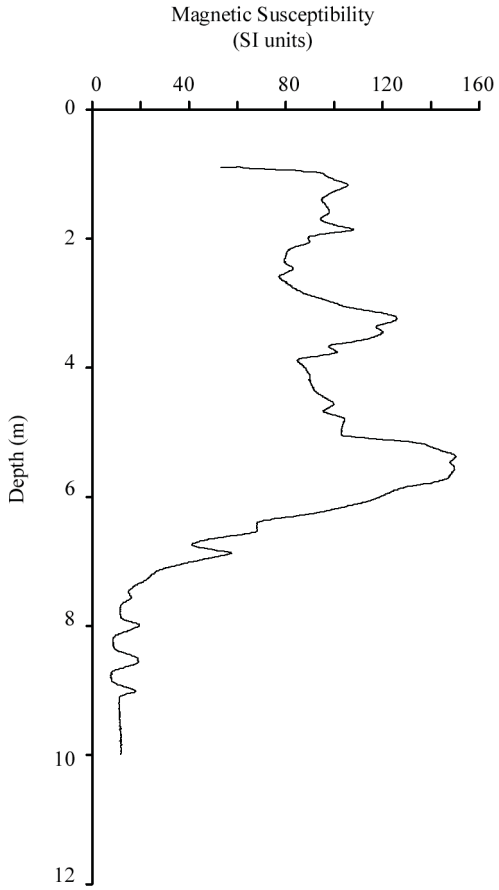

Age model (kyr): Beizhuangcun (Weinan)						
Depth (m)	^{14}C	TL	Magnetic susceptibility	Pedostratigraphy (Model III)	Average chronology	Range
0	0.00				0.00	
4	6.12				6.12	
8	11.05				11.05	
12						
16						
20						

MAR ($g/m^2/yr$): Beizhuangcun (Weinan)								
Stage (range in kyr)	Assumed DBD (g/cm^3)	^{14}C	TL	MS	Pedostratigraphy			Average MAR
					Model I	Model II	Model III	
Stage 1 (12-0)	1.48	**574**						574
Stage 2 (24-12)	1.48							
Stage 3 (59-24)	1.48							
Stage 4 (74-59)	1.48							
Stage 5 (130-74)	1.48							

References used to generate data report: Beizhuangcun (Weinan)	
Data used	**Source**
Pedostratigraphy	Zhou and An (1991)
Magnetic susceptibility	Zhou and An (1991)
^{14}C dating	Zhou and An (1991)
TL dating	-
Additional References:	
Data available	**Source**
-	-

Caijiagou section: MAR (g/m^2/yr) based on pedostratigraphy

Note: Site location for Caijiagou (Yulin) in Guo et al. (1996c) is slightly different from the one used here. This section is not the same section as the Yulin (Yuling) section. Deposits from Stages 1 2, 3 and 4 contain sedimentary hiatuses.

(Model I: min. glacial, max. interglacial; Model II: max. glacial, min. interglacial; Model III: 2/3 of interglacial soil is aeolian deposit)

Site location: 38.12° N, 109.83° E

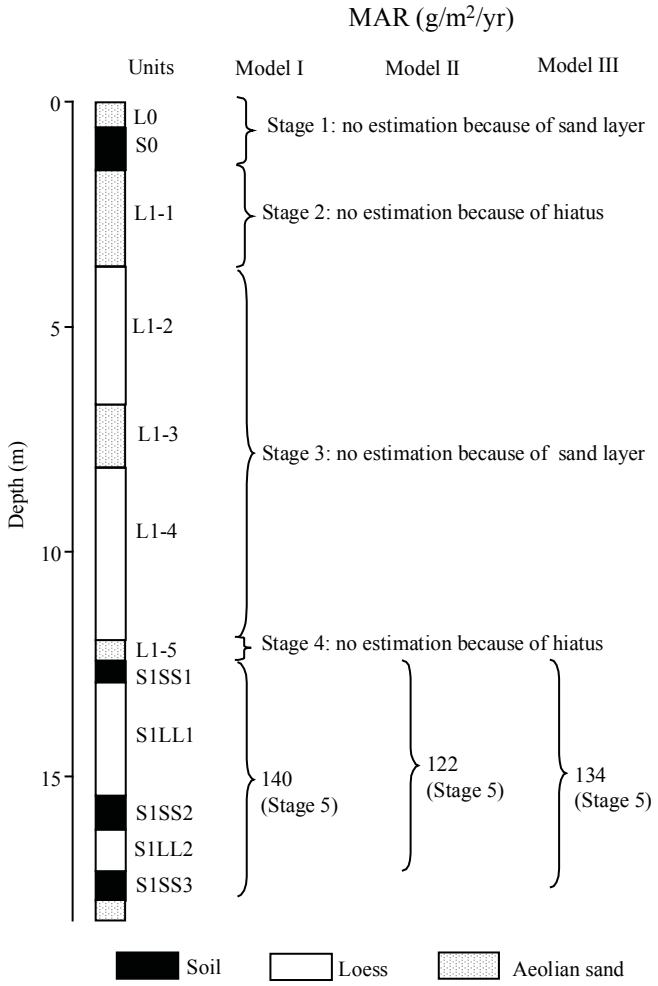

Stratigraphic data: Caijiagou (depth and thickness estimated from diagram, to nearest 10 cm)				
Top depth (m)	Bottom depth (m)	Thickness (m)	Stratigraphic units	DBD (g/cm³)
0.0	0.6	0.6	L0-sand	n/a
0.6	1.5	0.9	S0	n/a
1.5	3.7	2.2	L1-1-sand	n/a
3.7	6.8	3.1	L1-2	n/a
6.8	8.2	1.4	L1-3-sand	n/a
8.2	12.0	3.8	L1-4	n/a
12.0	12.5	0.5	L1-5-sand	n/a
12.5	12.9	0.4	S1SS1	n/a
12.9	15.5	2.6	S1LL1	n/a
15.5	16.2	0.7	S1SS2	n/a
16.2	17.1	0.9	S1LL2	n/a
17.1	17.8	0.7	S1SS3	n/a

Caijiagou section: MAR (g/m^2/yr) based on TL dating

Note: Site location for Caijiagou (Yulin) in Guo et al. (1996c) is slightly different from the one used here. This section is not the same section as the Yulin (Yuling) section. Guo et al. (1996c) have a set of TL dates which they derived from Sun et al. (1995). We have used TL dates from a later article by Sun et al. (1998). The dates given in Guo et al. (1996c) are provided in the table below for completeness, but are not used to generate MAR values. Deposits from Stages 1 2, 3 and 4 contain sedimentary hiatuses. Stages 3 and 5 MAR calculated excluding aeolian sand, based on available dates.

Site location: 38.12° N, 109.83° E

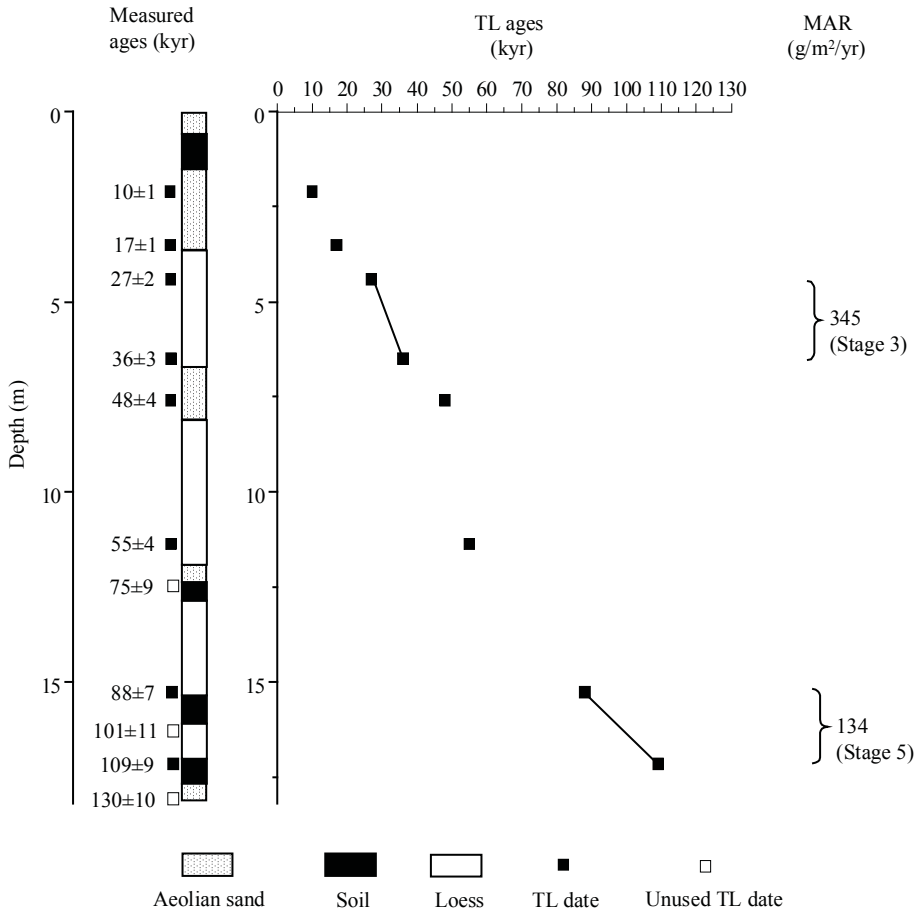

TL dating: Caijiagou
(depth estimated from diagram, to nearest 10 cm)

Depth (m)	Dating laboratory	Lab. No.	Dating material	TL-method	Age (kyr)	s.d. (kyr)	Reference	Comments
2.1	TL Lab. in Geology Institute, SSB	TL-4	n/a	fine-grain (4-11 μm) technique	10	1	Sun et al. (1998)	
3.5	TL Lab. in Geology Institute, SSB	TL-5	n/a	fine-grain (4-11 μm) technique	17	1	Sun et al. (1998)	
4.4	TL Lab. in Geology Institute, SSB	TL-6	n/a	fine-grain (4-11 μm) technique	27	2	Sun et al. (1998)	
6.5	TL Lab. in Geology Institute, SSB	TL-19	n/a	fine-grain (4-11 μm) technique	36	3	Sun et al. (1998)	
7.6	TL Lab. in Geology Institute, SSB	TL-7	n/a	fine-grain (4-11 μm) technique	48	4	Sun et al. (1998)	
11.4	TL Lab. in Geology Institute, SSB	TL-14	n/a	fine-grain (4-11 μm) technique	55	4	Sun et al. (1998)	
12.6	TL Lab. in Geology Institute, SSB	TL-15	n/a	fine-grain (4-11 μm) technique	75	9	Sun et al. (1998)	uncertainties larger than 10 %
15.3	TL Lab. in Geology Institute, SSB	TL-10	n/a	fine-grain (4-11 μm) technique	88	7	Sun et al. (1998)	
16.4	TL Lab. in Geology Institute, SSB	TL-11	n/a	fine-grain (4-11 μm) technique	101	11	Sun et al. (1998)	uncertainties larger than 10 %
17.2	TL Lab. in Geology Institute, SSB	TL-12	n/a	fine-grain (4-11 μm) technique	109	9	Sun et al. (1998)	
18.2	TL Lab. in Geology Institute, SSB	TL-13	n/a	fine-grain (4-11 μm) technique	130	10	Sun et al. (1998)	

TL dating 2: Caijiagou
(dates from Guo et al. (1996c), as taken from Sun et al. (1995); depth estimated from diagram, to nearest 10 cm)

Depth (m)	Dating laboratory	Lab. No.	Dating material	TL-method	Age (kyr)	s.d. (kyr)	Reference	Comments
4.2	n/a	n/a	n/a	n/a	30.10	2.17	Guo et al. (1996c)	
8.7	n/a	n/a	n/a	n/a	43.89	3.25	Guo et al. (1996c)	
11.7	n/a	n/a	n/a	n/a	50.24	2.17	Guo et al. (1996c)	
13.0	n/a	n/a	n/a	n/a	69.80	6.70	Guo et al. (1996c)	
15.0	n/a	n/a	n/a	n/a	85.43	8.50	Guo et al. (1996c)	
18.1	n/a	n/a	n/a	n/a	125.85	14.20	Guo et al. (1996c)	uncertainties >10 %

Caijiagou section: Magnetic susceptibility

Note: Site location for Caijiagou (Yulin) in Guo et al. (1996c) is slightly different from the one used here. This section is not the same section as the Yulin (Yuling) section. Deposits from Stages 1, 2, 3 and 4 deposits contain sedimentary hiatuses. MS MAR unused because of hiatuses.

Site location: 38.12° N, 109.83° E

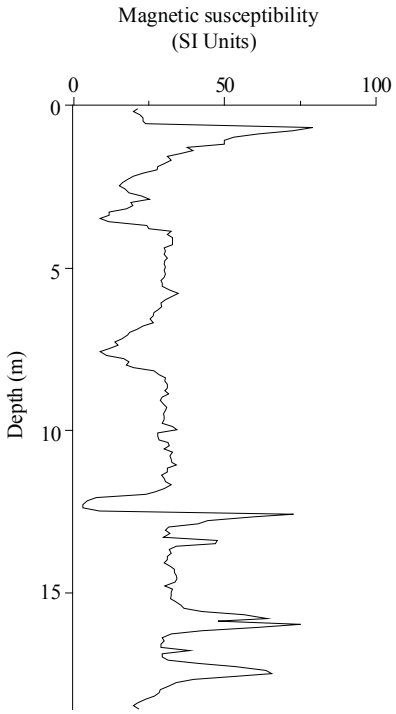

Age model (kyr): Caijiagou						
Depth (m)	^{14}C	TL	Magnetic susceptibility	Pedostratigraphy (Model III)	Average chronology	Range
0						
3						
6						
9						
12						
15		85.7		101.3	93.5	85.7-101.3

MAR (g/m^2/yr): Caijiagou								
Stage (range in kyr)	Assumed DBD (g/cm^3)	^{14}C	TL	MS	Pedostratigraphy			Average MAR
					Model I	Model II	Model III	
Stage 1 (12-0)	1.48							
Stage 2 (24-12)	1.48							
Stage 3 (59-24)	1.48		**345**					345
Stage 4 (74-59)	1.48							
Stage 5 (130-74)	1.48		**134**		140	122	**134**	134

References used to generate data report: Caijiagou	
Data used	**Source**
Pedostratigraphy	Sun and Ding (1998)
Magnetic susceptibility	Sun and Ding (1998)
^{14}C dating	-
TL dating	Sun et al. (1998), Guo et al. (1996c)
Additional References:	
Data available	**Source**
Grain size , CBD-Fe, TL	Sun and Ding (1998)
Grain size, TL, CBD-Fe, magnetic susceptibility, pedostratigraphy	Sun et al. (1998)
Pedostratigraphy	Guo et al. (1996c)

Caocun section: MAR (g/m^2/yr) based on pedostratigraphy

Note: Site with local dust sources. Last glacial loess (L1) is not subdivided.

(Model I: min. glacial, max. interglacial; Model II: max. glacial, min. interglacial; Model III: 2/3 of interglacial soil is aeolian deposit)

Site location: 34.63° N, 111.15° E

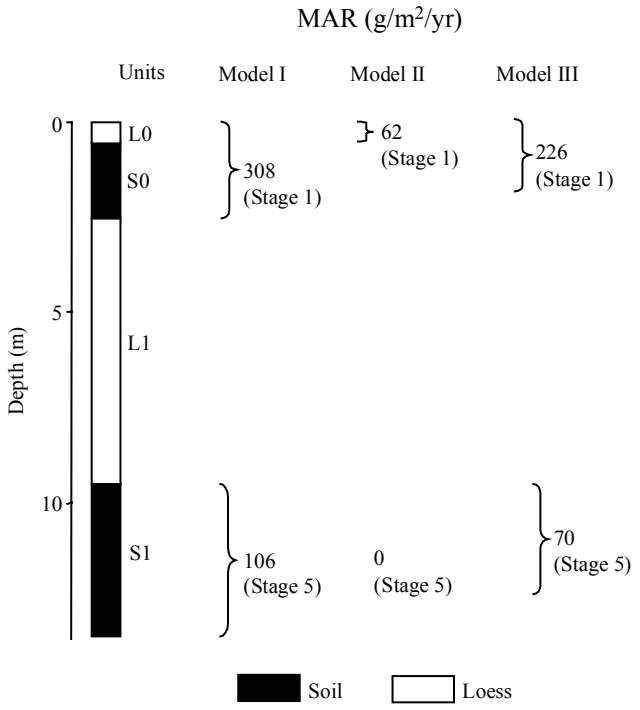

Stratigraphic data: Caocun (thickness given by authors, depth calculated from thickness)				
Top depth (m)	Bottom depth (m)	Thickness (m)	Stratigraphic units	DBD (g/cm^3)
0.0	0.5	0.5	L0	n/a
0.5	2.5	2.0	S0	n/a
2.5	9.5	7.0	L1	n/a
9.5	13.5	4.0	S1	n/a

Age model (kyr): Caocun						
Depth (m)	^{14}C	TL	Magnetic susceptibility	Pedostratigraphy (Model III)	Average chronology	Range
0				0.0	0.0	
2				13.3	13.3	
4						
6						
8						
10				84.4	84.4	
12				125.9	125.9	

MAR ($g/m^2/yr$): Caocun								
Stage (range in kyr)	Assumed DBD (g/cm^3)	^{14}C	TL	MS	Pedostratigraphy			Average MAR
					Model I	Model II	Model III	
Stage 1 (12-0)	1.48				308	62	**262**	262
Stage 2 (24-12)	1.48							
Stage 3 (59-24)	1.48							
Stage 4 (74-59)	1.48							
Stage 5 (130-74)	1.48				106	0	**70**	70

References used to generate data report: Caocun	
Data used	**Source**
Pedostratigraphy	Xiao et al. (1998)
Magnetic susceptibility	-
^{14}C dating	-
TL dating	-
Additional References:	
Data available	**Source**
Magnetic susceptibility	Xiao et al. (1998)

Caoxian section: MAR (g/m^2/yr) based on pedostratigraphy

Note: Only data from Stage 5 is available.

(Model I: min. glacial, max. interglacial; Model II: max. glacial, min. interglacial; Model III: 2/3 of interglacial soil is aeolian deposit)

Site location: 36.37° N, 104.62° E

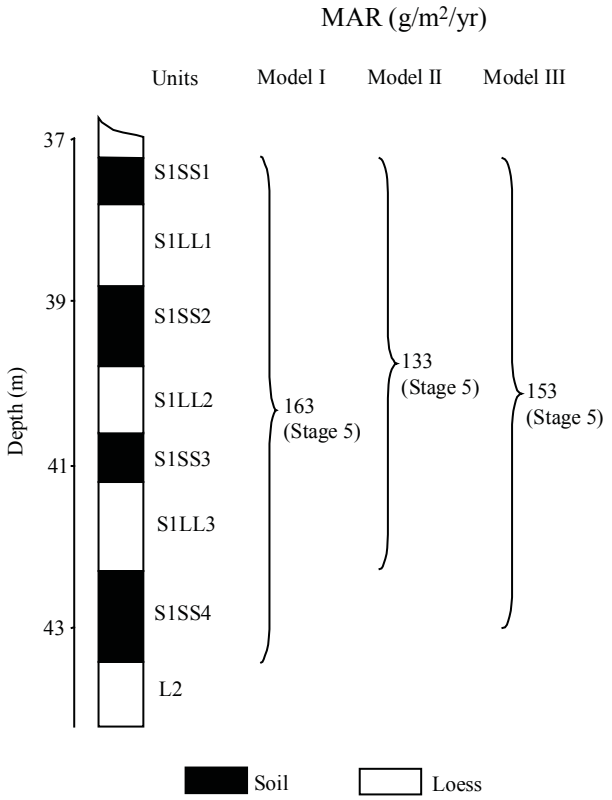

Stratigraphic data: Caoxian (depth and thickness estimated from diagram, to nearest 1 cm)				
Top depth (m)	Bottom depth (m)	Thickness (m)	Stratigraphic units	DBD (g/cm³)
37.25	37.82	0.57	S1SS1	n/a
37.82	38.80	0.98	S1LL1	n/a
38.80	39.80	1.00	S1SS2	n/a
39.80	40.60	0.80	S1LL2	n/a
40.60	41.20	0.60	S1SS3	n/a
41.20	42.30	1.10	S1LL3	n/a
42.30	43.40	1.10	S1SS4	n/a
43.40	-	-	L2	n/a

Age model (kyr): Caoxian						
Depth (m)	^{14}C	TL	Magnetic susceptibility	Pedostratigraphy (Model III)	Average chronology	Range
38				81.4	81.4	
39				90.9	90.9	
40				100.4	100.4	
41				109.8	109.8	
42				120.1	120.1	
43				130.0	130.0	

MAR ($g/m^2/yr$): Caoxian								
Stage (range in kyr)	Assumed DBD (g/cm^3)	^{14}C	TL	MS	Pedostratigraphy			Average MAR
					Model I	Model II	Model III	
Stage 1 (12-0)	1.48							
Stage 2 (24-12)	1.48							
Stage 3 (59-24)	1.48							
Stage 4 (74-59)	1.48							
Stage 5 (130-74)	1.48				163	133	**153**	153

References used to generate data report: Caoxian	
Data used	**Source**
Pedostratigraphy	Chen et al. (1999)
Magnetic susceptibility	Chen et al. (1999)
^{14}C dating	-
TL dating	-
Additional References:	
Data available	**Source**
Magnetic polarity, grain size	Chen et al. (1999)

Chagelebulu_1 (Cagelebulu) : MAR (g/m^2/yr) based on ^{14}C dating

Note: Chaglebulu_1 and Chagelebulu_2 are the same section, but there are two alternative stratigraphies given with different ^{14}C dates. The site is referred to as Cagelebulu by Zhou et al. (1998) and the longitude is given as 108.30° E. Section with potential local sources. Stage 1 MAR calculated excluding aeolian sands, based on available dates.

Site location: 39.88° N, 103.30° E

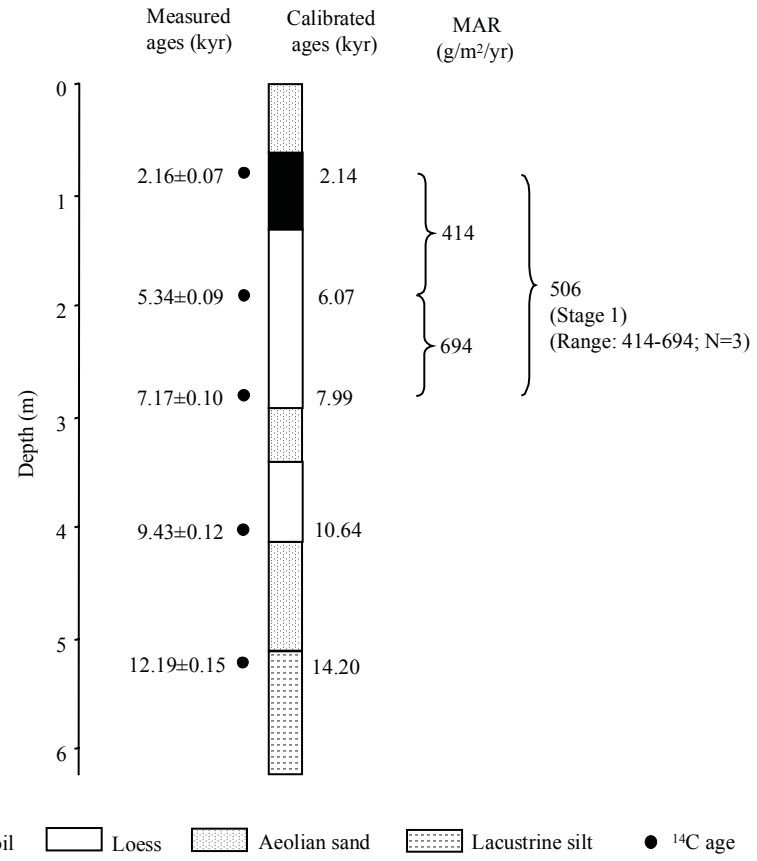

^{14}C dating: Chagelebulu_1 (Cagelebulu)
(depth estimated from diagram, to nearest 10 cm)

Depth (m)	Dating laboratory	Lab. No.	Dating material	Age (kyr)	s.d. (kyr)	(1σ) Calendar age ranges (kyr)	Relative probability	Assumed calendar age (kyr)	Reference	Comments
0.8	n/a	n/a	organic matter	2.16	0.07	2.06-2.18	0.603	2.14	Dong et al. (1995a)	
						2.24-2.30	0.356			
						2.20-2.20	0.041			
1.9	n/a	n/a	organic matter	5.34	0.09	6.00-6.15	0.767	6.07	Dong et al. (1995a)	
						6.16-6.20	0.189			
						6.25-6.27	0.045			
2.8	n/a	n/a	organic matter	7.17	0.1	7.92-8.05	0.708	7.99	Dong et al. (1995a)	
						7.86-7.90	0.171			
						8.08-8.11	0.091			
						8.14-8.14	0.03			
4.0	n/a	n/a	organic matter	9.43	0.12	10.50-10.78	0.74	10.64	Dong et al. (1995a)	
						10.95-11.06	0.242			
						10.83-10.84	0.018			
5.2	n/a	n/a	organic matter	12.19	0.15	14.03-14.37	0.585	14.20	Dong et al. (1995a)	
						14.70-15.06	0.303			
						13.84-13.95	0.112			

Age model (kyr): Chagelebulu_1 (Cagelebulu)

Depth (m)	^{14}C	TL	Magnetic susceptibility	Pedostratigraphy (Model III)	Average chronology	Range
0						
1	2.8				2.8	
2	6.3				6.3	
3	8.5				8.5	
4	10.6				10.6	
5	13.6				13.6	

MAR (g/m^2/yr): Chagelebulu_1 (Cagelebulu)

Stage (range in kyr)	Assumed DBD (g/cm^3)	^{14}C	TL	MS	Pedostratigraphy			Average MAR
					Model I	Model II	Model III	
Stage 1 (12-0)	1.48	**506**						506
Stage 2 (24-12)	1.48							
Stage 3 (59-24)	1.48							
Stage 4 (74-59)	1.48							
Stage 5 (130-74)	1.48							

References used to generate data report: Chagelebulu_1 (Cagelebulu)	
Data used	**Source**
Pedostratigraphy	Dong et al. (1995a)
Magnetic susceptibility	-
^{14}C dating	Dong et al. (1995a)
TL dating	-
Additional References:	
Data available	**Source**
Pollen, $CaCO_3$, ^{14}C, SiO_2/Al_2O_3	Dong et al. (1995a)

Chagelebulu_2 (Cagelebulu): MAR (g/m^2/yr) based on ^{14}C dating

Note: Chaglebulu_1 and Chagelebulu_2 are the same section, but there are two alternative stratigraphies given with different ^{14}C dates. The site is referred to as Cagelebulu by Zhou et al. (1998) and the longitude is given as 108.3 °E. Section with potential local sources. Stage 1 MAR calculated excluding aeolian sands, based on available dates.

Site location: 39.88° N, 103.30° E

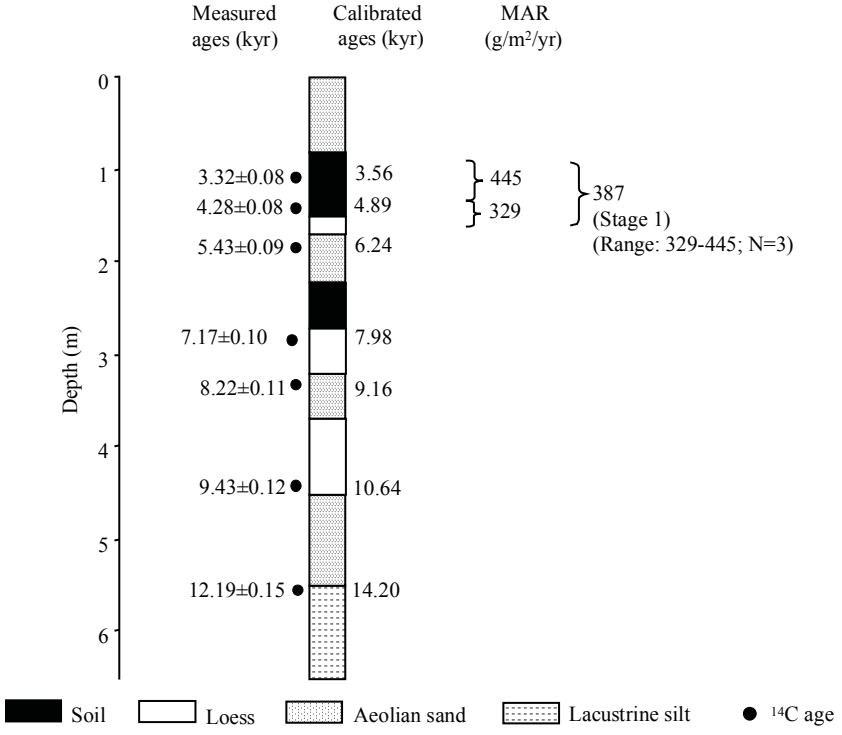

^{14}C dating: Chagelebulu_2 (Cagelebulu)
(depth estimated from diagram, to nearest 10 cm)

Depth (m)	Dating laboratory	Laboratory No.	Dating material	Age (kyr)	s.d. (kyr)	(1σ) Calendar age ranges (kyr)	Relative probability	Assumed cal. age (kyr)	Reference	Comments
1.15-1.25	Lanzhou Institute	LZ102696 202	organic matter	3.32	0.08	3.47-3.64	1	3.56	Dong et al. (1995b)	
1.55-1.65	Lanzhou Institute	LZ102696 203	organic matter	4.28	0.08	4.81-4.97 4.69-4.76 4.65-4.67 5.02-5.02	0.695 0.215 0.067 0.023	4.89	Dong et al. (1995b)	
1.80-2.00	Lanzhou Institute	LZ102696 204	organic matter	5.43	0.09	6.17-6.31 6.11-6.14 6.03-6.04 6.06-6.07	0.763 0.148 0.058 0.031	6.24	Dong et al. (1995b)	
2.85-3.00	Lanzhou Institute	LZ102696 205	organic matter	7.17	0.10	7.92-8.05 7.86-7.90 8.08-8.11 8.15-8.15	0.679 0.171 0.12 0.03	7.98	Dong et al. (1995b)	
3.00-3.50	Lanzhou Institute	LZ102696 206	organic matter	8.22	0.11	9.03-9.29 9.39-9.39 9.36-9.36	0.936 0.032 0.031	9.16	Dong et al. (1995b)	
4.30-4.45	Lanzhou Institute	LZ102696 207	organic matter	9.43	0.12	10.50-10.78 10.95-11.06 10.83-10.84 10.43-10.44	0.738 0.226 0.018 0.017	10.64	Dong et al. (1995b)	
5.45-5.55	Lanzhou Institute	LZ102696 208	organic matter	12.19	0.15	14.03-14.37 14.70-15.05 13.84-13.94	0.585 0.303 0.112	14.2	Dong et al. (1995b)	

Age model (kyr): Chagelebulu_2 (Cagelebulu)

Depth (m)	^{14}C	TL	Magnetic susceptibility	Pedostratigraphy (Model III)	Average chronology	Range
0						
1	2.9				2.9	
2	6.4				6.4	
3	8.3				8.3	
4	10.1				10.1	
5	12.6				12.6	

MAR (g/m^2/yr): Chagelebulu_2 (Cagelebulu)

Stage (range in kyr)	Assumed DBD (g/cm^3)	^{14}C	TL	MS	Pedostratigraphy			Average MAR
					Model I	Model II	Model III	
Stage 1 (12-0)	1.48	387						387
Stage 2 (24-12)	1.48							
Stage 3 (59-24)	1.48							
Stage 4 (74-59)	1.48							
Stage 5 (130-74)	1.48							

References used to generate data report: Chagelebulu_2 (Cagelebulu)	
Data used	**Source**
Pedostratigraphy	Dong et al. (1995b); Zhou et al. (1998)
Magnetic susceptibility	-
^{14}C dating	Dong et al. (1995b)
TL dating	-
Additional References:	
Data available	**Source**
^{14}C	Zhou et al. (1998)

Changqugou section: MAR (g/m^2/yr) based on pedostratigraphy

Note: Stage 1 affected by cultivation layer. Last glacial loess (L1) contains sedimentary hiatus.

(Model I: min. glacial, max. interglacial; Model II: max. glacial, min. interglacial; Model III: 2/3 of interglacial soil is aeolian deposit)

Site location: 37.45° N, 108.70° E

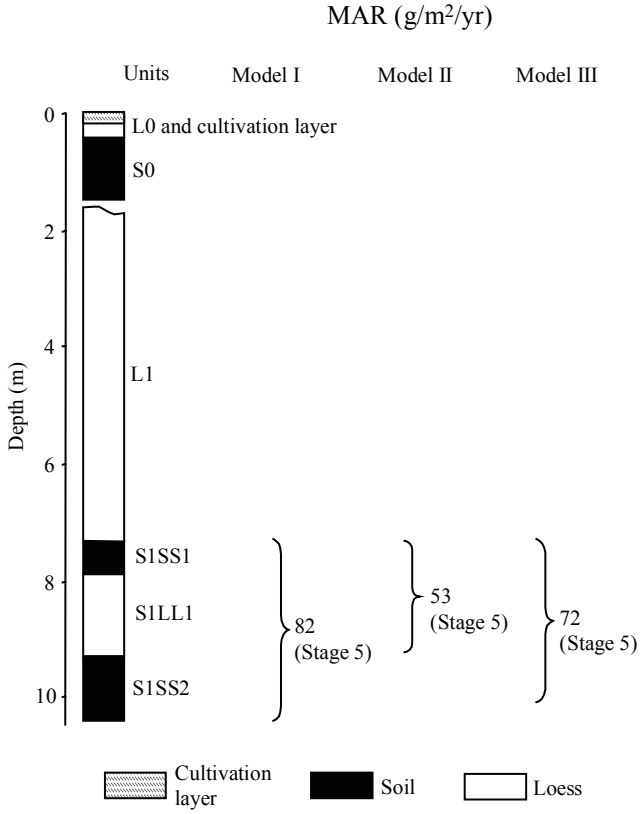

Stratigraphic data: Changqugou (depth and thickness estimated from diagram, to nearest 10 cm)				
Top depth (m)	Bottom depth (m)	Thickness (m)	Stratigraphic units	DBD (g/cm^3)
0.0	0.4	0.4	L0 and cultivation layer	n/a
0.4	1.5	1.1	S0	n/a
1.5	7.3	5.8	L1 with hiatus	n/a
7.3	7.9	0.6	S1SS1	n/a
7.9	9.3	1.4	S1LL1	n/a
9.3	10.4	1.1	S1SS2	n/a

Changqugou section: MAR (g/m^2/yr) based on magnetic susceptibility

Note: Stage 1 affected by cultivation layer. Last glacial loess (L1) contains sedimentary hiatus. MS data unused.

Site location: 37.45° N, 108.70° E

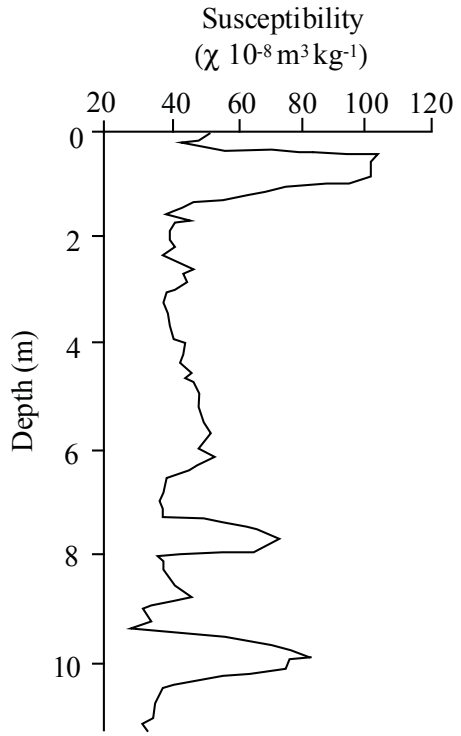

Age model (kyr): Changqugou						
Depth (m)	^{14}C	TL	Magnetic susceptibility	Pedostratigraphy (Model III)	Average chronology	Range
0						
2						
4						
6						
8				88.0	88.0	
10				130.0	130.0	

MAR ($g/m^2/yr$): Changqugou								
Stage (range in kyr)	Assumed DBD (g/cm^3)	^{14}C	TL	MS	Pedostratigraphy			Average MAR
					Model I	Model II	Model III	
Stage 1 (12-0)	1.48							
Stage 2 (24-12)	1.48							
Stage 3 (59-24)	1.48							
Stage 4 (74-59)	1.48							
Stage 5 (130-74)	1.48				82	53	**72**	72

References used to generate data report: Changqugou	
Data used	**Source**
Pedostratigraphy	Sun (unpublished data)
Magnetic susceptibility	Sun (unpublished data)
^{14}C dating	-
TL dating	-
Additional References:	
Data available	**Source**
-	-

Changwu section: MAR (g/m^2/yr) based on pedostratigraphy

Note: Site location given by Zhao (1994) is 34.58° N, 106.87° E and is wrong.

(Model I: min. glacial, max. interglacial; Model II: max. glacial, min. interglacial; Model III: 2/3 of interglacial soil is aeolian deposit)

Site location: 35.20° N, 107.82° E

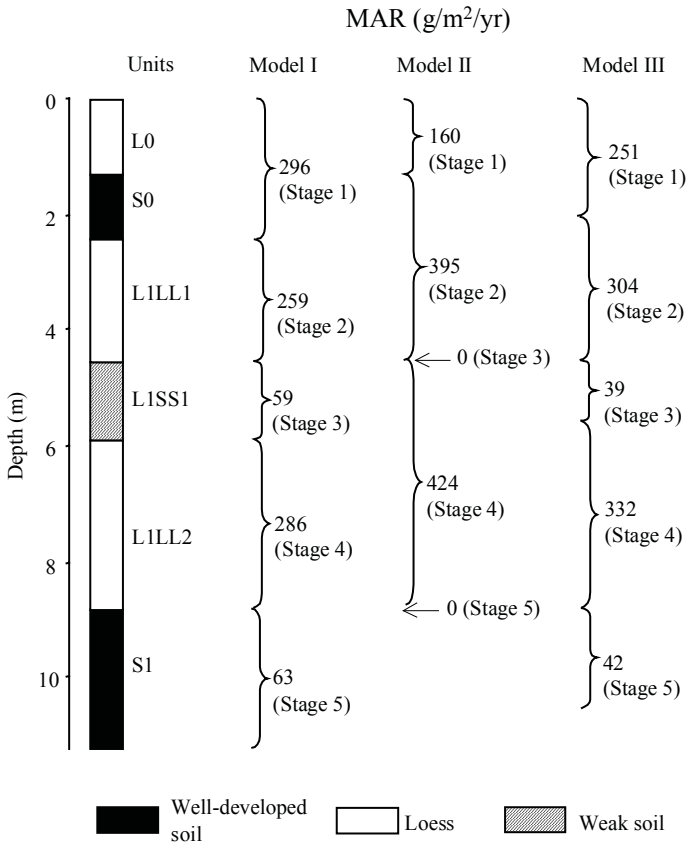

Stratigraphic data: Changwu (thickness given by author, depth calculated from thicknesses)				
Top depth (m)	Bottom depth (m)	Thickness (m)	Stratigraphic units	DBD (g/cm³)
0.0	1.3	1.3	L0	n/a
1.3	2.4	1.1	S0	n/a
2.4	4.5	2.1	L1LL1	n/a
4.5	5.9	1.4	L1SS1	n/a
5.9	8.8	2.9	L1LL2	n/a
8.8	11.2	2.4	S1	n/a

Age model (kyr): Changwu						
Depth (m)	^{14}C	TL	Magnetic susceptibility	Pedostratigraphy (Model III)	Average chronology	Range
0				0.0	0.0	
2				12.0	12.0	
4				21.5	21.5	
6				61.5	61.5	
8				70.4	70.4	
10				116.1	116.1	

MAR ($g/m^2/yr$): Changwu								
Stage (range in kyr)	Assumed DBD (g/cm^3)	^{14}C	TL	MS	Pedostratigraphy			Average MAR
					Model I	Model II	Model III	
Stage 1 (12-0)	1.48				296	160	**251**	251
Stage 2 (24-12)	1.48				259	395	**304**	304
Stage 3 (59-24)	1.48				59	0	**39**	39
Stage 4 (74-59)	1.48				286	424	**332**	332
Stage 5 (130-74)	1.48				63	0	**42**	42

References used to generate data report: Changwu	
Data used	**Source**
Pedostratigraphy	Zhao (1994)
Magnetic susceptibility	-
^{14}C dating	-
TL dating	-
Additional References:	
Data available	**Source**
Magnetic susceptibility, chemical parameters	Guo et al. (1998)

Chenjiawo (Lantian_1) section: MAR (g/m^2/yr) based on pedostratigraphy

Note: Lantian is the name of the County of Shaaxi Province in which this site is located. Chenjiawo is the name of the village where the section is located (Lu et al., 1987a). Only uppermost 6.7 m of section shown here, although the full stratigraphy is shown on next page.

(Model I: min. glacial, max. interglacial; Model II: max. glacial, min. interglacial; Model III: 2/3 of interglacial soil is aeolian deposit)

Site location: 34.18° N, 109.48° E

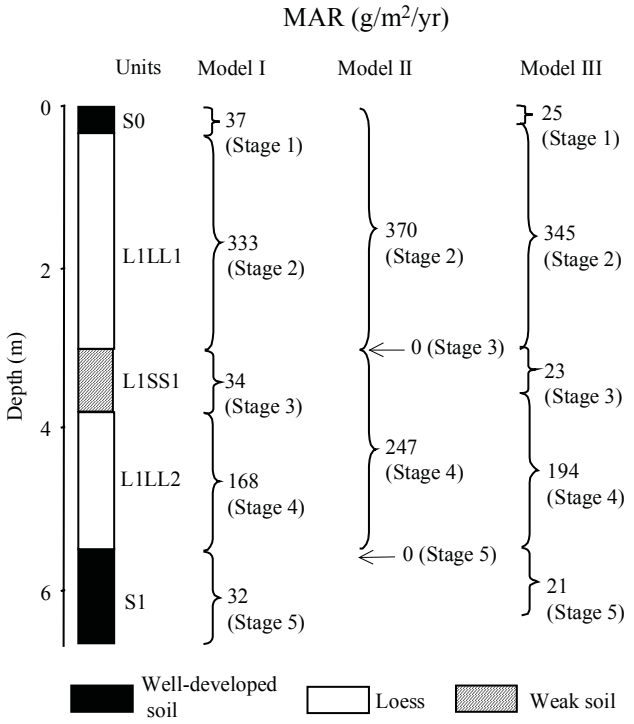

Stratigraphic data: Chenjiawo (Lantian_1) (depth and thickness estimated from diagram, to nearest 10 cm)				
Top depth (m)	Bottom depth (m)	Thickness (m)	Stratigraphic units	DBD (g/cm^3)
0.0	0.3	0.3	S0	n/a
0.3	3.0	2.7	L1LL1	n/a
3.0	3.8	0.8	L1SS1	n/a
3.8	5.5	1.7	L1LL2	n/a
5.5	6.7	1.2	S1	n/a
6.7	10.8	4.1	L2LL1	n/a
10.8	11.4	0.6	L2SS1	n/a
11.4	12.3	0.9	L2LL2	n/a

Chenjiawo (Lantian_1) section: MAR (g/m^2/yr) based on TL dating

Note: Lantian is the name of the County of Shaaxi Province in which this site is located. Chenjiawo is the name of the village where the section is located (Lu et al., 1987a).

Site location: 34.18° N, 109.48° E

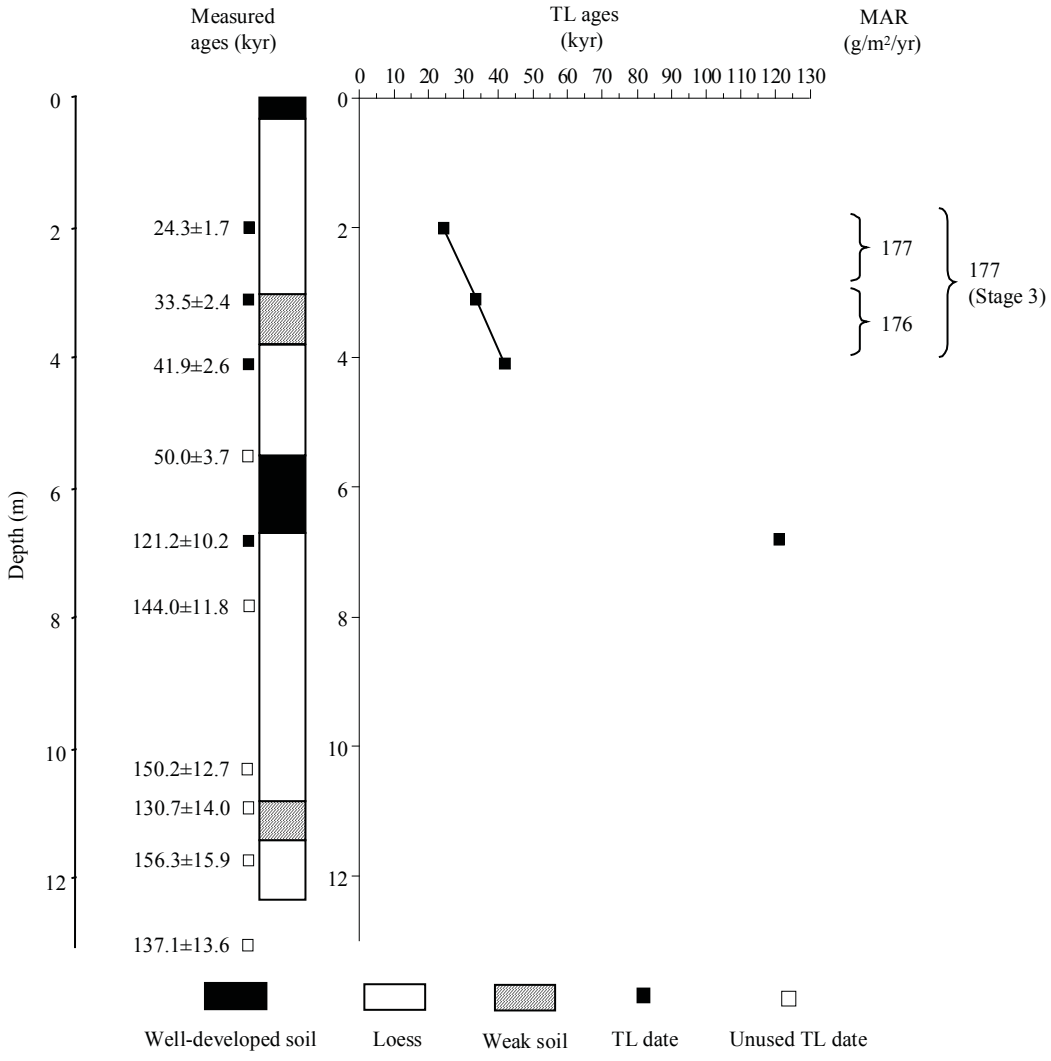

TL dating: Chenjiawo (Lantian_1)
(depth given by authors)

Depth (m)	Dating laboratory	Lab. No.	Dating material	TL-method	Age (kyr)	s.d. (kyr)	Reference	Comments
2	Xi'an Loess Lab.	1	n/a	fine-grain (4-11 μm) technique	24.3	1.7	Lu et al. (1988)	
3.1	Xi'an Loess Lab.	2	n/a	fine-grain (4-11 μm) technique	33.5	2.4	Lu et al. (1988)	
4.1	Xi'an Loess Lab.	3	n/a	fine-grain (4-11 μm) technique	41.9	2.6	Lu et al. (1988)	
5.5	Xi'an Loess Lab.	4	n/a	fine-grain (4-11 μm) technique	50.0	3.7	Lu et al. (1988)	authors think age is too young
6.8	Xi'an Loess Lab.	5	n/a	fine-grain (4-11 μm) technique	121.0	10.2	Lu et al. (1988)	
7.8	Xi'an Loess Lab.	6	n/a	fine-grain (4-11 μm) technique	144.0	11.8	Lu et al. (1988)	age > 130 kyr
10.3	Xi'an Loess Lab.	7	n/a	fine-grain (4-11 μm) technique	150.0	12.7	Lu et al. (1988)	age > 130 kyr
10.9	Xi'an Loess Lab.	8	n/a	fine-grain (4-11 μm) technique	131.0	14.0	Lu et al. (1988)	age > 130 kyr; questioned by authors
11.7	Xi'an Loess Lab.	9	n/a	fine-grain (4-11 μm) technique	156.0	15.9	Lu et al. (1988)	age > 130 kyr; questioned by authors
13.0	Xi'an Loess Lab.	10	n/a	fine-grain (4-11 μm) technique	137.0	13.6	Lu et al. (1988)	age > 130 kyr; questioned by authors

Age model (kyr): Chenjiawo (Lantian_1)

Depth (m)	^{14}C	TL	Magnetic susceptibility	Pedostratigraphy (Model III)	Average chronology	Range
0				0.0	0.0	
1				15.5	15.5	
2		24.3		19.7	22.0	19.7-24.3
3		32.8		24.0	28.4	24.0-32.8
4		41.1		62.4	51.7	41.1-62.4
5				70.1	70.1	
6				108.8	108.8	

MAR ($g/m^2/yr$): Chenjiawo (Lantian_1)

Stage (range in kyr)	Assumed DBD (g/cm^3)	^{14}C	TL	MS	Pedostratigraphy			Average MAR
					Model I	Model II	Model III	
Stage 1 (12-0)	1.48				37		**25**	25
Stage 2 (24-12)	1.48				333	370	**345**	345
Stage 3 (59-24)	1.48		**177**		34	0	**23**	100
Stage 4 (74-59)	1.48				168	247	**194**	194
Stage 5 (130-74)	1.48				32	0	**21**	21

References used to generate data report: Chenjiawo (Lantian_1)	
Data used	**Source**
Pedostratigraphy	Lu et al. (1988)
Magnetic susceptibility	-
^{14}C dating	-
TL dating	Lu et al. (1988)
Additional References:	
Data available	**Source**
Mammal fossils	Woo (1964)
Mammal fossils	Woo (1966)
Pedostratigraphy, mammal fossils	Chang et al. (1964)
Pedostratigraphy, mammal fossils	Jia (1965)
Pedostratigraphy, mammal fossils	Jia (1966)
Pedostratigraphy, magnetic polarity	Ma et al. (1978)
Pedostratigraphy, magnetic polarity	Cheng et al. (1978)
Pedostratigraphy, mammal fossils	Liu and Ding (1984)
Pedostratigraphy, magnetic polarity	An et al. (1987)

Chifeng section: MAR (g/m^2/yr) based on magnetic susceptibility

Site location: 42.17° N, 119.02° E

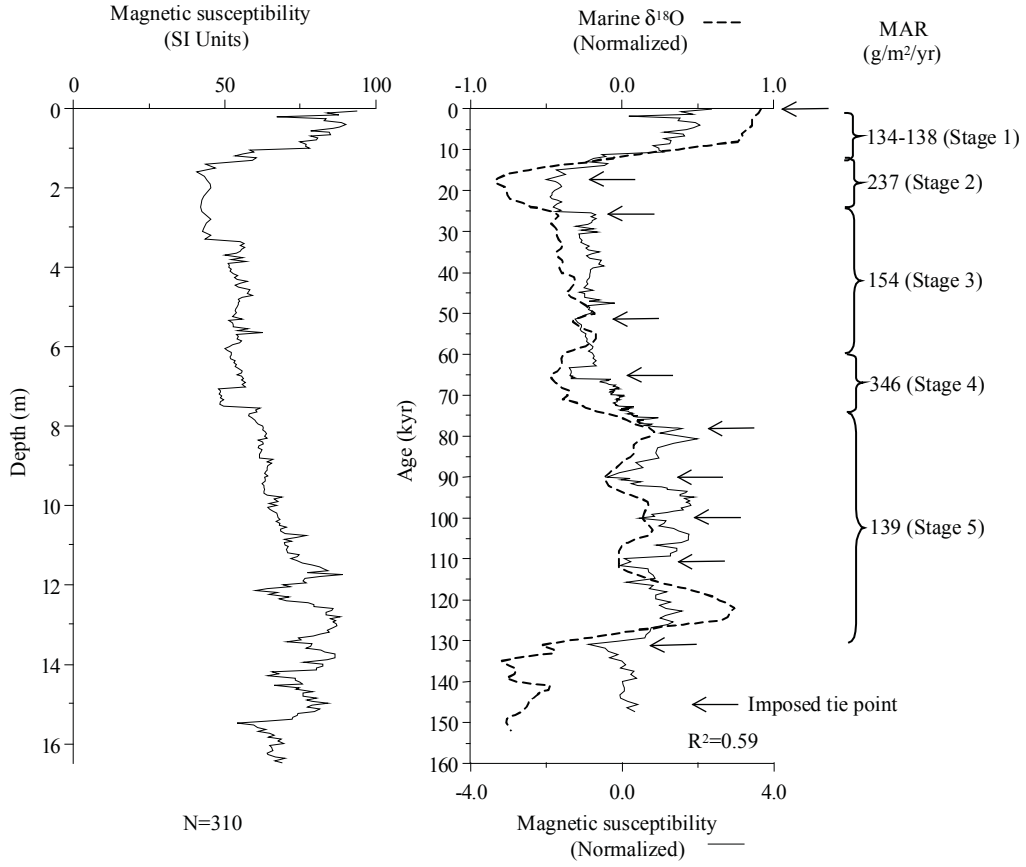

MS age model: Chifeng		
Tie-Point	Depth (m)	Age (kyr)
1	0.05	0.21
2	1.60	17.31
3	3.35	25.42
4	6.05	51.57
5	7.20	65.22
6	11.65	78.30
7	12.15	90.10
8	13.45	99.96
9	14.25	110.79
10	15.50	131.09

Age model (kyr): Chifeng						
Depth (m)	^{14}C	TL	Magnetic susceptibility	Pedostratigraphy (Model III)	Average chronology	Range
0			0		0.0	
3			23.8		23.8	
6			51.1		51.1	
9			70.5		70.5	
12			86.6		86.6	
15			123		123.0	

MAR ($g/m^2/yr$): Chifeng								
Stage (range in kyr)	Assumed DBD (g/cm^3)	^{14}C	TL	MS	Pedostratigraphy			Average MAR
					Model I	Model II	Model III	
Stage 1 (12-0)	1.48			**136**				136
Stage 2 (24-12)	1.48			**237**				237
Stage 3 (59-24)	1.48			**154**				154
Stage 4 (74-59)	1.48			**346**				346
Stage 5 (130-74)	1.48			**139**				139

References used to generate data report: Chifeng	
Data used	**Source**
Pedostratigraphy	-
Magnetic susceptibility	Sun (unpublished data)
^{14}C dating	-
TL dating	-
Additional References:	
Data available	**Source**
-	-

Chunhua section: MAR (g/m^2/yr) based on magnetic susceptibility

Note: Digitized MS data.

Site location: 34.80° N, 108.55° E

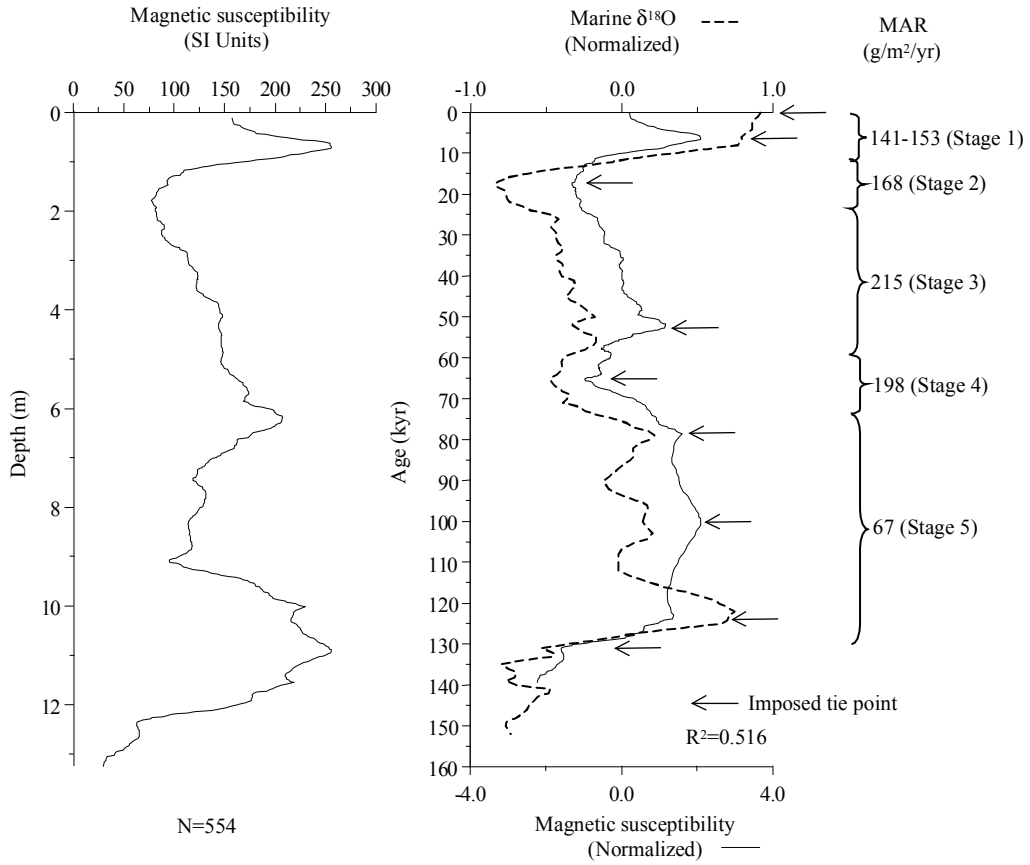

MS age model: Chunhua		
Tie-Point	Depth (m)	Age (kyr)
1	0.12	0.21
2	0.69	6.27
3	1.75	17.31
4	6.26	52.67
5	9.10	65.22
6	10.00	78.30
7	10.92	99.96
8	11.58	123.79
9	12.36	131.09

Age model (kyr): Chunhua						
Depth (m)	^{14}C	TL	Magnetic susceptibility	Pedostratigraphy (Model III)	Average chronology	Range
0			0		0.0	
2			19.2		19.2	
4			34.9		34.9	
6			50.6		50.6	
8			60.4		60.4	
10			78.3		78.3	
12			127.7		127.7	

MAR ($g/m^2/yr$): Chunhua								
Stage (range in kyr)	Assumed DBD (g/cm^3)	^{14}C	TL	MS	Pedostratigraphy			Average MAR
					Model I	Model II	Model III	
Stage 1 (12-0)	1.48			**147**				147
Stage 2 (24-12)	1.48			**168**				168
Stage 3 (59-24)	1.48			**215**				215
Stage 4 (74-59)	1.48			**198**				198
Stage 5 (130-74)	1.48			**67**				67

References used to generate data report: Chunhua	
Data used	**Source**
Pedostratigraphy	-
Magnetic susceptibility	Sun et al. (1995)
^{14}C dating	-
TL dating	-
Additional References:	
Data available	**Source**
-	-

Dadiwan section: MAR (g/m^2/yr) based on pedostratigraphy

Note: Section with potential local river sources. Stage 1 affected by cultivation layer.

(Model I: min. glacial, max. interglacial; Model II: max. glacial, min. interglacial; Model III: 2/3 of interglacial soil is aeolian deposit)

Site location: 35.00° N, 105.92° E

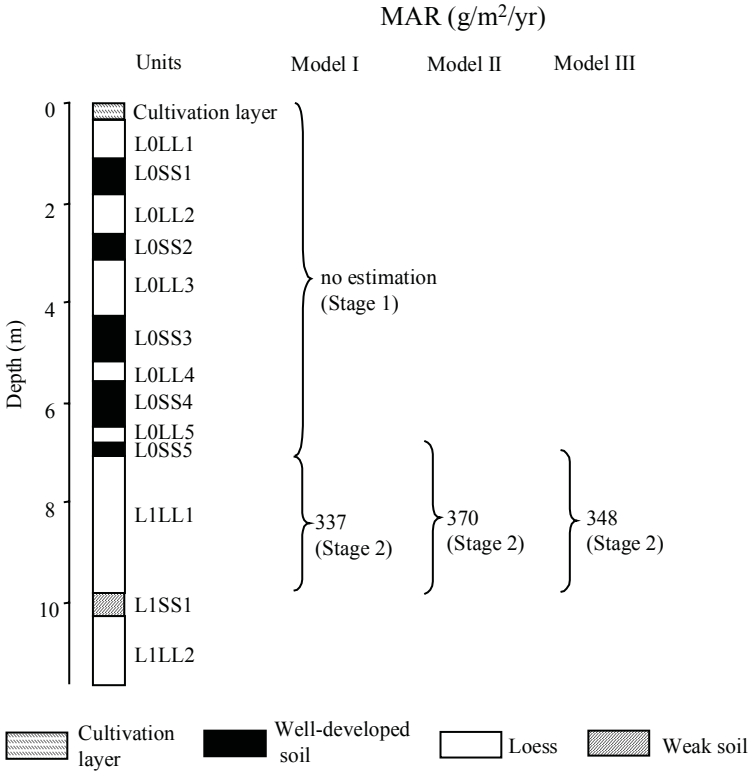

Note: The depths provided in the text are inconsistent with the depths shown in the figure. The authors did not provide all of the information about the stratigraphy in the text, and in some cases only provided thickness ranges for a given stratigraphic unit. We therefore could not use these data to calculate MAR, and were forced to rely on the information derived from the diagram.

Stratigraphic data: Dadiwan
(depth and thickness estimated from diagram, to nearest 1 cm)

Top depth (m)	Bottom depth (m)	Thickness (m)	Stratigraphic units	DBD (g/cm³)
0.00	0.35	0.35	cultivation layer	n/a
0.35	1.12	0.77	L0LL1	n/a
1.12	1.81	0.69	L0SS1	n/a
1.81	2.59	0.78	L0LL2	n/a
2.59	3.12	0.53	L0SS2	n/a
3.12	4.23	1.11	L0LL3	n/a
4.23	5.15	0.92	L0SS3	n/a
5.15	5.59	0.44	L0LL4	n/a
5.59	6.47	0.88	L0SS4	n/a
6.47	6.82	0.35	L0LL5	n/a
6.82	7.09	0.27	L0SS5	n/a
7.09	9.82	2.73	L1LL1	n/a
9.82	10.26	0.44	L1SS1	n/a
10.26	11.65	1.39	L1LL2	n/a

Stratigraphic data: Dadiwan
(depth and thickness information given in the text)

Top depth (m)	Bottom depth (m)	Thickness (m)	Stratigraphic units	DBD (g/cm³)
n/a	n/a	n/a	cultivation layer	n/a
n/a	n/a	n/a	L0LL1	n/a
1.3	1.7	0.4	L0SS1	n/a
1.7	2.5	0.8	L0LL2	n/a
2.5	3.4	0.9	L0SS2	n/a
3.4	4	0.6	L0LL3	n/a
4	5.1	1.1	L0SS3	n/a
5.1	5.5	0.4	L0LL4	n/a
5.5	6.4	0.9	L0SS4	n/a
n/a	n/a	n/a	L0LL5	n/a
n/a	n/a	0.4-0.5	L0SS5	n/a
n/a	n/a	n/a	L1LL2	n/a
n/a	n/a	n/a	L1SS1	n/a
n/a	n/a	n/a	L1LL2	n/a

Dadiwan section: MAR (g/m^2/yr) based on ^{14}C dating

Note: Section with potential local river sources. Stage 1 affected by cultivation layer.

Site location: 35.00° N, 105.92° E

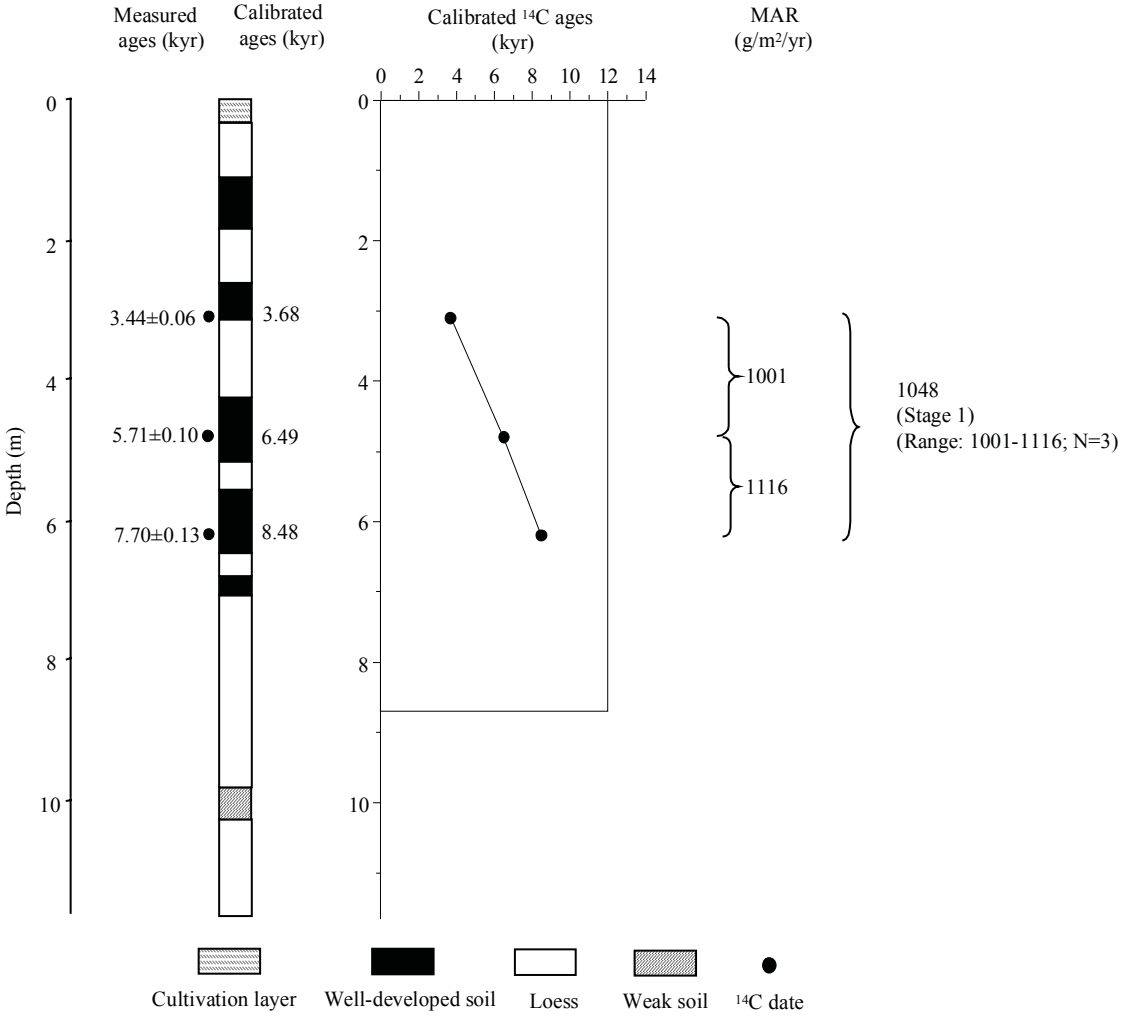

^{14}C dating: Dadiwan (depth of the middle date given by the authors, depth of the other two dates estimated from diagram, to nearest 10 cm)										
Depth (m)	Dating laboratory	Lab. No.	Dating material	Age (kyr)	s.d. (kyr)	(1σ) Calendar age ranges (kyr)	Relative probability	Assumed calendar age (kyr)	Reference	Comments
2.9	n/a	n/a	organic matter	3.44	0.06	3.63-3.73	0.639	3.68	Chen and Zhang (1994)	
						3.79-3.82	0.247			
						3.74-3.77	0.114			
4.8	n/a	n/a	organic matter	5.71	0.1	6.41-6.57	0.761	6.49	Chen and Zhang (1994)	
						6.58-6.63	0.239			
6.3	n/a	n/a	organic matter	7.7	0.13	8.36-8.61	0.958	8.48	Chen and Zhang (1994)	
						8.61-8.63	0.042			

Dadiwan section: Magnetic susceptibility

Note: Section with potential local river sources. Stage 1 affected by cultivation layer. Digitized MS data.

Site location: 35.00° N, 105.92° E

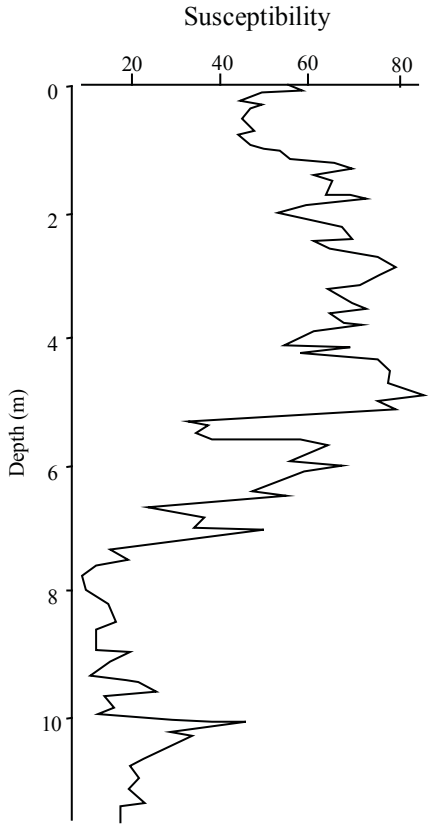

Age model (kyr): Dadiwan						
Depth (m)	^{14}C	TL	Magnetic susceptibility	Pedostratigraphy (Model III)	Average chronology	Range
0						
2						
4	5.2				5.2	
6	8.2				8.2	
8	11			16.3	16.3	

MAR ($g/m^2/yr$): Dadiwan								
Stage (range in kyr)	Assumed DBD (g/cm^3)	^{14}C	TL	MS	Pedostratigraphy			Average MAR
					Model I	Model II	Model III	
Stage 1 (12-0)	1.48	**1048**						1048
Stage 2 (24-12)	1.48				337	370	**348**	348
Stage 3 (59-24)	1.48							
Stage 4 (74-59)	1.48							
Stage 5 (130-74)	1.48							

References used to generate data report: Dadiwan	
Data used	**Source**
Pedostratigraphy	Chen and Zhang (1994)
Magnetic susceptibility	Chen and Zhang (1994)
^{14}C dating	Chen and Zhang (1994)
TL dating	-
Additional References:	
Data available	**Source**
-	-

Dengkou section: Pedostratigraphy

Note: Section with potential local sources. Not possible to calculate MAR because of sand layers.

(Model I: min. glacial, max. interglacial; Model II: max. glacial, min. interglacial; Model III: 2/3 of interglacial soil is aeolian deposit)

Site location: 40.35° N, 106.95° E

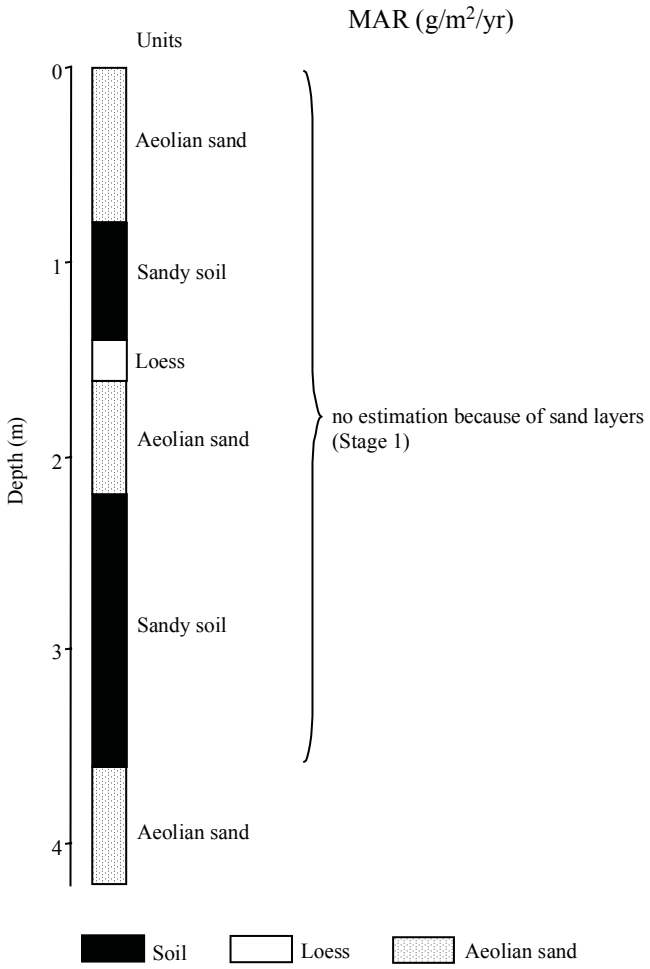

Stratigraphic data: Dengkou (depth given by authors, thickness calculated from depths)				
Top depth (m)	Bottom depth (m)	Thickness (m)	Stratigraphic units	DBD (g/cm³)
0.0	0.8	0.8	aeolian sand	n/a
0.8	1.4	0.6	sandy soil	n/a
1.4	1.6	0.2	loess	n/a
1.6	2.2	0.6	aeolian sand	n/a
2.2	3.6	1.4	sandy soil	n/a
3.6	4.2	0.6	sand	n/a

Dengkou section: ^{14}C dating information

Note: Section with potential local sources. Not possible to calculate MAR because of sand layers.

Site location: 40.35° N, 106.95° E

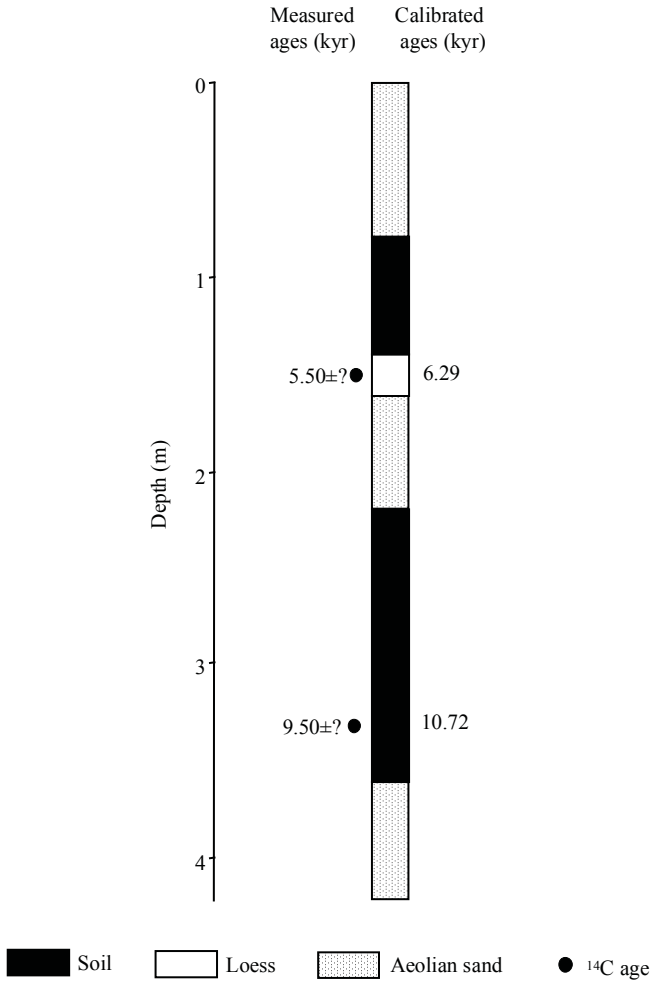

^{14}C dating: Dengkou (depth estimated from diagram, to nearest 10 cm)										
Depth (m)	Dating laboratory	Lab. No.	Dating material	Age (kyr)	s.d. (kyr)	(1σ) Calendar age ranges (kyr)	Relative probability	Assumed calendar age (kyr)	Reference	Comments
1.5	n/a	n/a	n/a	5.5	n/a	6.29-6.30	1	6.29	Zhou et al. (1998)	
3.3	n/a	n/a	n/a	9.5	n/a	10.69-10.75	0.678	10.72	Zhou et al. (1998)	
						11.02-11.04	0.224			
						10.97-10.98	0.098			

Age model (kyr): Dengkou						
Depth (m)	^{14}C	TL	Magnetic susceptibility	Pedostratigraphy (Model III)	Average chronology	Range
0						
1	4.2				4.2	
2	7.5				7.5	
3	10.0				10.0	

MAR ($g/m^2/yr$): Dengkou								
Stage (range in kyr)	Assumed DBD (g/cm^3)	^{14}C	TL	MS	Pedostratigraphy			Average MAR
					Model I	Model II	Model III	
Stage 1 (12-0)	1.48							
Stage 2 (24-12)	1.48							
Stage 3 (59-24)	1.48							
Stage 4 (74-59)	1.48							
Stage 5 (130-74)	1.48							

References used to generate data report: Dengkou	
Data used	**Source**
Pedostratigraphy	Zhou et al. (1998)
Magnetic susceptibility	-
^{14}C dating	Zhou et al. (1998)
TL dating	-
Additional References:	
Data available	**Source**
-	-

Duanjiapo (Lantian_2) section: MAR (g/m^2/yr) based on pedostratigraphy

Note: The name Lantian has been given to multiple sites in is the name of Lantian County of Shaaxi Province. Duanjiapo is the name of the village in Lantian County where this section is located, and we use it here to minimise confusion.

(Model I: min. glacial, max. interglacial; Model II: max. glacial, min. interglacial; Model III: 2/3 of interglacial soil is aeolian deposit)

Site location: 34.20° N, 109.20° E

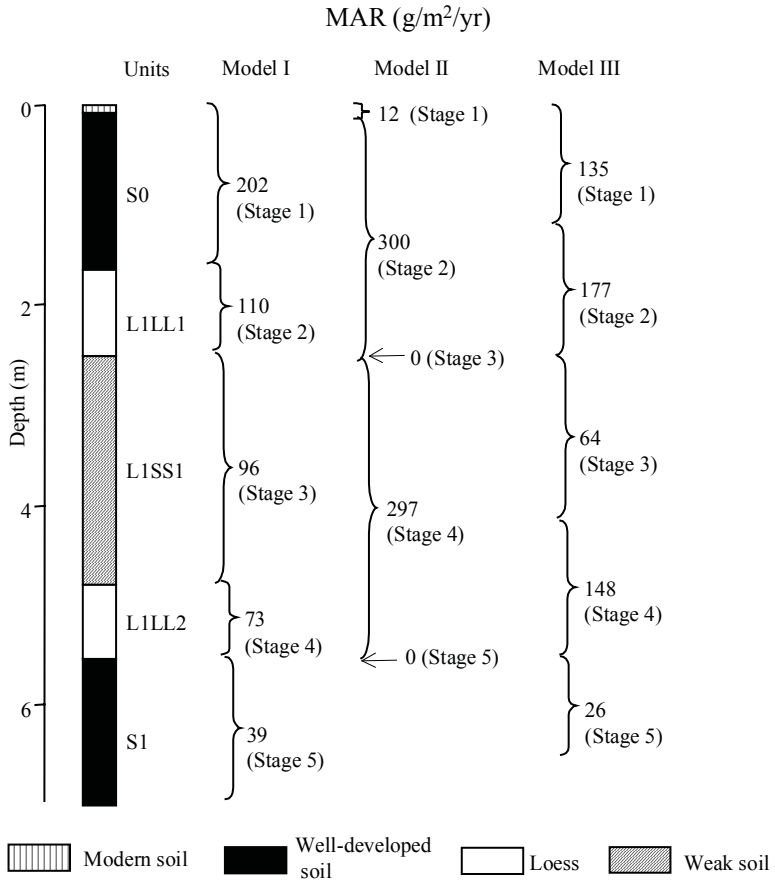

Stratigraphic data: Duanjiapo (Lantian_2) (depth and thickness estimated from diagram, to nearest 1 cm)				
Top depth (m)	Bottom depth (m)	Thickness (m)	Stratigraphic units	DBD (g/cm^3)
0.00	0.10	0.10	modern soil	n/a
0.10	1.64	1.54	S0	n/a
1.64	2.53	0.89	L1LL1	n/a
2.53	4.80	2.27	L1SS1	n/a
4.80	5.54	0.74	L1LL2	n/a
5.54	7.00	1.46	S1	n/a

Duanjiapo (Lantian_2) section: MAR (g/m^2/yr) based on magnetic susceptibility

Note: The name Lantian has been given to multiple sites in is the name of Lantian County of Shaaxi Province. Duanjiapo is the name of the village in Lantian County where this section is located, and we use it here to minimise confusion. Digitized MS data.

Site location: 34.20° N, 109.20° E

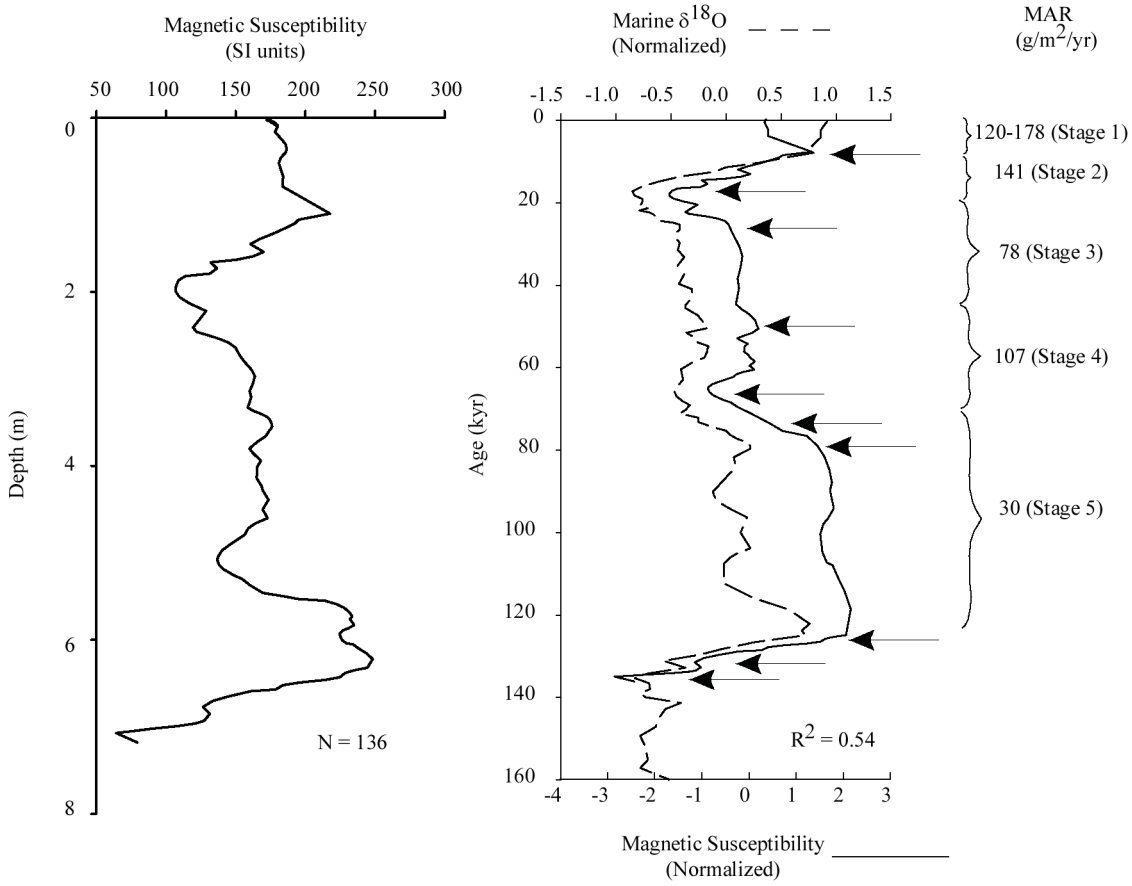

MS age model: Duanjiapo (Lantian_2)		
Tie-Point	Depth (m)	Age (kyr)
1	1.1	7.81
2	1.87	17.31
3	2.73	25.42
4	3.5	50.21
5	5.08	65.22
6	5.46	71.12
7	5.59	79.25
8	6.32	125
9	6.85	132.81
10	7.07	135.1

Age model (kyr): Duanjiapo (Lantian_2)						
Depth (m)	^{14}C	TL	Magnetic susceptibility	Pedostratigraphy (Model III)	Average chronology	Range
1			7.1	11.0	9.1	7.1-9.1
2			18.5	19.6	19.1	18.5-19.6
3			34.1	34.9	34.5	34.1-34.9
4			55.0	58.1	56.6	55.0-58.1
5			64.5	68.6	66.6	64.5-68.6
6			104.9	100.6	102.8	100.6-104.9

MAR ($g/m^2/yr$): Duanjiapo (Lantian_2)								
Stage (range in kyr)	Assumed DBD (g/cm^3)	^{14}C	TL	MS	Pedostratigraphy			Average MAR
					Model I	Model II	Model III	
Stage 1 (12-0)	1.48			**149**	202	12	**135**	142
Stage 2 (24-12)	1.48			**141**	110	300	**177**	159
Stage 3 (59-24)	1.48			**78**	96	0	**64**	71
Stage 4 (74-59)	1.48			**107**	73	297	**148**	128
Stage 5 (130-74)	1.48			**30**	39	0	**26**	28

References used to generate data report: Duanjiapo (Lantian_2)	
Data used	**Source**
Pedostratigraphy	Lin et al. (1991)
Magnetic susceptibility	Lin et al. (1991)
^{14}C dating	-
TL dating	-
Additional References:	
Data available	**Source**
Pedostratigraphy, magnetic polarity	Yue (1989)
Magnetic susceptibility, $\delta^{13}C$ (organic), $\delta^{18}O$ (carbonate), $\delta^{13}C$ (carbonate)	Lin et al. (1991)
Pedostratigraphy, magnetic polarity	Zheng et al. (1991a)

Dunwashan section: MAR (g/m^2/yr) based on pedostratigraphy

Note: The stratigraphy for Dunwashan was included in a summary paper (Chen et al., 1991b). From the documentation it is not clear whether the top two soils (here labeled L1SS1 and L1SS2) occur in Stage 2 or Stage 3. We have therefore chosen to estimate MAR only for Stages 4 and 5.

(Model I: min. glacial, max. interglacial; Model II: max. glacial, min. interglacial; Model III: 2/3 of interglacial soil is aeolian deposit)

Site location: 35.85° N, 103.25° E

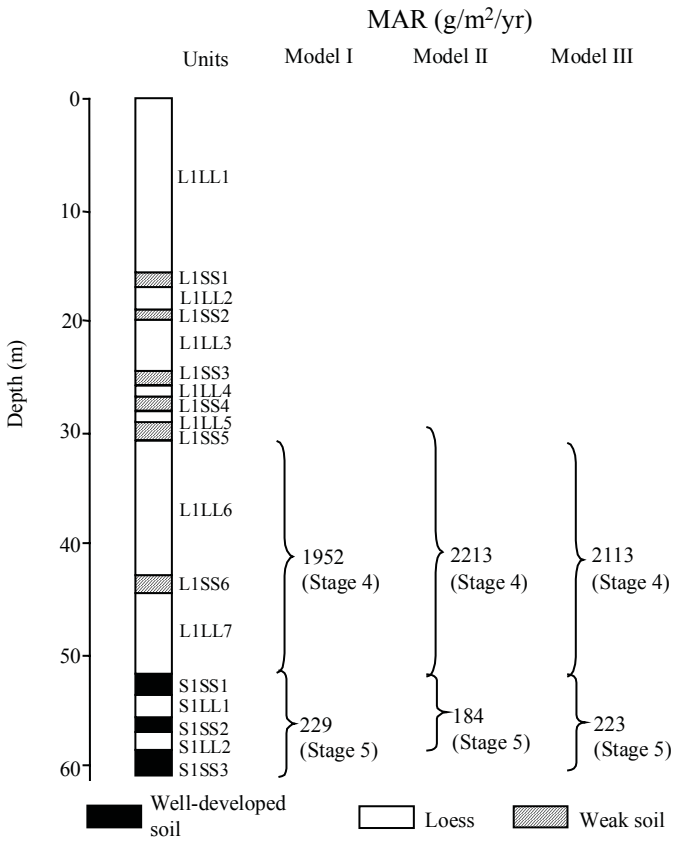

Stratigraphic data: Dunwashan
(depth and thickness estimated from diagram, to nearest 1 cm)

Top depth (m)	Bottom depth (m)	Thickness (m)	Stratigraphic units	DBD (g/cm³)
0.00	15.90	15.90	L1LL1	n/a
15.90	17.21	1.31	L1SS1	n/a
17.21	19.04	1.83	L1LL2	n/a
19.04	20.00	0.96	L1SS2	n/a
20.00	24.81	4.81	L1LL3	n/a
24.81	25.97	1.16	L1SS3	n/a
25.97	26.94	0.97	L1LL4	n/a
26.94	28.35	1.41	L1SS4	n/a
28.35	29.37	1.02	L1LL5	n/a
29.37	30.89	1.52	L1SS5	n/a
30.89	43.04	12.15	L1LL6	n/a
43.04	44.56	1.52	L1SS6	n/a
44.56	51.80	7.24	L1LL7	n/a
51.80	53.92	2.12	S1SS1	n/a
53.92	55.65	1.73	S1LL1	n/a
55.65	57.11	1.46	S1SS2	n/a
57.11	58.78	1.67	S1LL2	n/a
58.78	60.96	2.18	S1SS3	n/a

Age model (kyr): Dunwashan

Depth (m)	^{14}C	TL	Magnetic susceptibility	Pedostratigraphy (Model III)	Average chronology	Range
0						
10						
20						
30						
40				65.7	65.7	
50				72.7	72.7	
60				128.5	128.5	

MAR (g/m²/yr): Dunwashan

Stage (range in kyr)	Assumed DBD (g/cm³)	^{14}C	TL	MS	Pedostratigraphy			Average MAR
					Model I	Model II	Model III	
Stage 1 (12-0)	1.48							
Stage 2 (24-12)	1.48							
Stage 3 (59-24)	1.48							
Stage 4 (74-59)	1.48				1952	2213	**2113**	2113
Stage 5 (130-74)	1.48				229	184	**223**	223

References used to generate data report: Dunwashan	
Data used	**Source**
Pedostratigraphy	Chen et al. (1991b)
Magnetic susceptibility	-
^{14}C dating	-
TL dating	-
Additional References:	
Data available	**Source**
-	-

Duobutang section: Pedostratigraphy

Note: Section not used to estimate MAR, because the stratigraphy cannot be correlated with the CLP stratigraphy, and the section contains sand layers. These four sections (Duobutang, Qijidong, Xietongmen, and Xigaze) are all from the Tibetan Plateau, and were scanned as a unit. The top age on the Xietongmen section is ^{14}C date, all the other ages are TL dates.

Site location: 29.36º N, 88.50º E

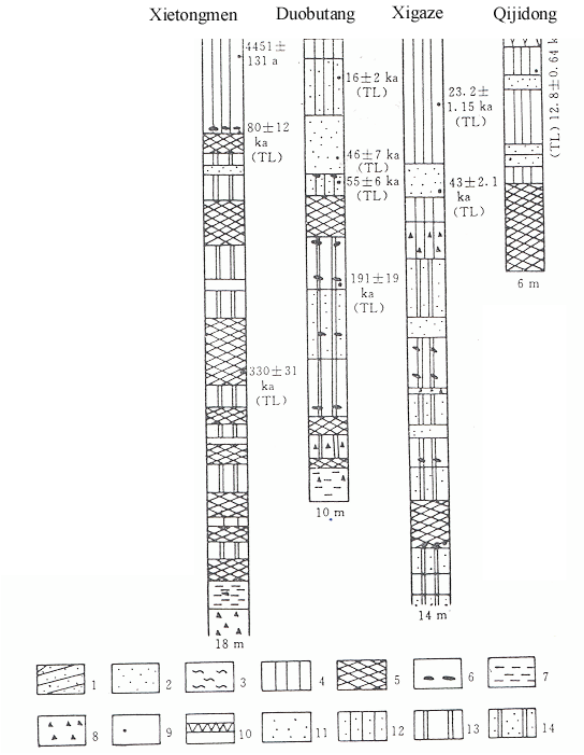

Legend: 1. Bedded sand; 2. Aeolian fine sand, 3. Fluvial layer, 4. Loess, 5. Palaeosol, 6. Nodule
7. Fluvial clay, 8. Gravel layer, 9. Sampling position, 10. Grass layer, 11. Medium sand

Stratigraphic data: Duobutang (depth and thickness estimated from diagram, to nearest 10 cm)				
Top depth (m)	Bottom depth (m)	Thickness (m)	Stratigraphic units	DBD (g/cm³)
0	0.18	0.18	grass layer	n/a
0.18	0.61	0.43	loess	n/a
0.61	1.79	1.18	sandy loess	n/a
1.79	3.05	1.26	aeolian sand	n/a
3.05	3.52	0.47	sandy loess	n/a
3.52	4.35	0.83	soil	n/a
4.35	5.49	1.14	loess	n/a

References used to generate data report: Duobutang	
Data used	**Source**
Pedostratigraphy	Jin et al. (1998)
Magnetic susceptibility	-
^{14}C dating	-
TL dating	Jin et al. (1998)
Additional References:	
Data available	**Source**
-	-

Fujiazhuang section: MAR (g/m^2/yr) based on pedostratigraphy

Note: Stage 1 affected by colluvium. Last glacial loess (L1) contains sedimentary hiatus.

(Model I: min. glacial, max. interglacial; Model II: max. glacial, min. interglacial; Model III: 2/3 of interglacial soil is aeolian deposit)

Site location: 36.60° N, 118.50° E

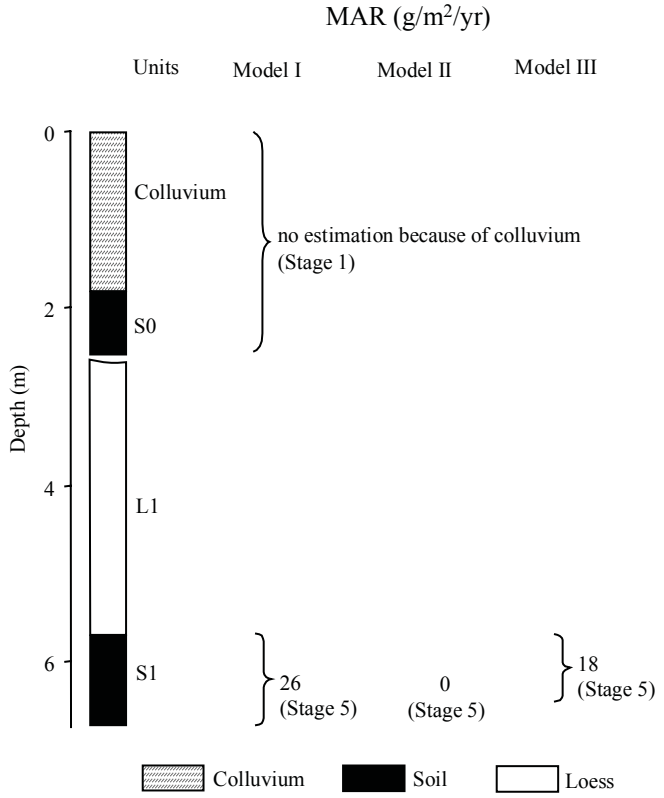

Stratigraphic data: Fujiazhuang (thickness given by authors, depth calculated from thickness)				
Top depth (m)	Bottom depth (m)	Thickness (m)	Stratigraphic units	DBD (g/cm³)
0.0	1.8	1.8	colluvium	n/a
1.8	2.5	0.7	S0	n/a
2.5	5.7	3.2	L1 with hiatus	n/a
5.7	6.7	1.0	S1	n/a

Fujiazhuang section: TL dating

Note: Stage 1 affected by colluvium. Last glacial loess (L1) contains sedimentary hiatus. No MAR calculated because only one TL date within 130 kyr.

Site location: 36.60° N, 118.50° E

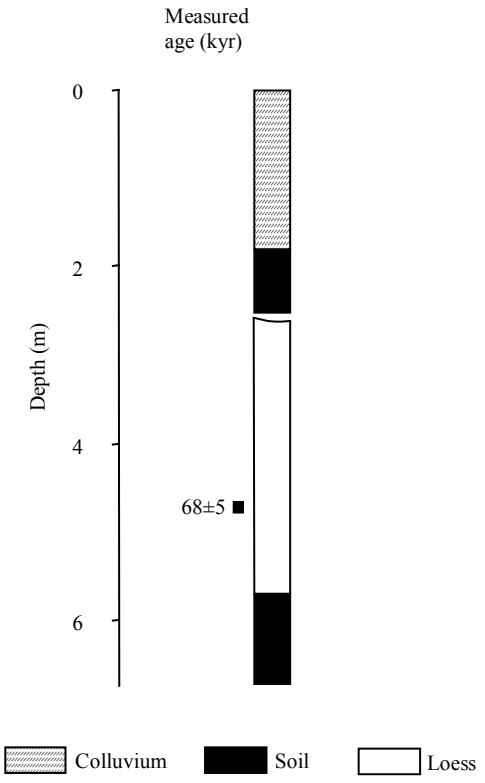

TL dating: Fujiazhuang (depth for TL dates estimated from diagram, to nearest 10 cm)								
Depth (m)	Dating laboratory	Lab. No.	Dating material	TL-method	Age (kyr)	s.d. (kyr)	Reference	Comments
4.7	n/a	n/a	n/a	n/a	68	5	Zheng et al. (1994)	

Age model (kyr): Fujiazhuang						
Depth (m)	^{14}C	TL	Magnetic susceptibility	Pedostratigraphy (Model III)	Average chronology	Range
0						
1						
2						
3						
4						
5						
6				99.0	99.0	

MAR ($g/m^2/yr$): Fujiazhuang								
Stage (range in kyr)	Assumed DBD (g/cm^3)	^{14}C	TL	MS	Pedostratigraphy			Average MAR
					Model I	Model II	Model III	
Stage 1 (12-0)	1.48							
Stage 2 (24-12)	1.48							
Stage 3 (59-24)	1.48							
Stage 4 (74-59)	1.48							
Stage 5 (130-74)	1.48				26	0	**18**	18

References used to generate data report: Fujiazhuang	
Data used	**Source**
Pedostratigraphy	Zheng et al. (1994)
Magnetic susceptibility	-
^{14}C dating	-
TL dating	Zheng et al. (1994)
Additional References:	
Data available	**Source**
-	-

Ganzi section: MAR (g/m^2/yr) based on pedostratigraphy

(Model I: min. glacial, max. interglacial; Model II: max. glacial, min. interglacial; Model III: 2/3 of interglacial soil is aeolian deposit)

Site location: 31.63° N, 99.98° E

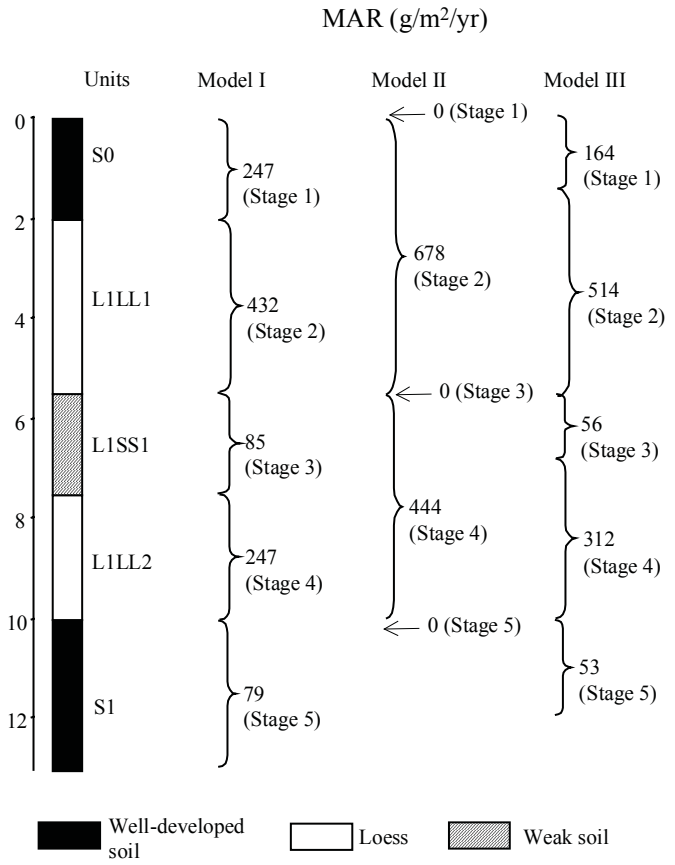

Stratigraphic data: Ganzi (depth and thickness estimated from diagram, to nearest 10 cm)				
Top depth (m)	Bottom depth (m)	Thickness (m)	Stratigraphic units	DBD (g/cm^3)
0.0	2.0	2.0	S0	n/a
2.0	5.5	3.5	L1LL1	n/a
5.5	7.5	2.0	L1SS1	n/a
7.5	10.0	2.5	L1LL2	n/a
10.0	13.0	3.0	S1	n/a

Age model (kyr): Ganzi						
Depth (m)	^{14}C	TL	Magnetic susceptibility	Pedostratigraphy (Model III)	Average chronology	Range
0				0.0	0.0	
2				14.0	14.0	
4				19.8	19.8	
6				37.2	37.2	
8				64.5	64.5	
10				74.0	74.0	
12				130.0	130.0	

MAR ($g/m^2/yr$): Ganzi								
Stage (range in kyr)	Assumed DBD (g/cm^3)	^{14}C	TL	MS	Pedostratigraphy			Average MAR
					Model I	Model II	Model III	
Stage 1 (12-0)	1.48				247	0	**164**	164
Stage 2 (24-12)	1.48				432	678	**514**	514
Stage 3 (59-24)	1.48				85	0	**56**	56
Stage 4 (74-59)	1.48				247	444	**312**	312
Stage 5 (130-74)	1.48				79	0	**53**	53

References used to generate data report: Ganzi	
Data used	**Source**
Pedostratigraphy	Fang et al. (1996)
Magnetic susceptibility	-
^{14}C dating	-
TL dating	-
Additional References:	
Data available	**Source**
Magnetic polarity	Fang et al. (1996)

Gaolanshan section: MAR (g/m^2/yr) based on pedostratigraphy

(Model I: min. glacial, max. interglacial; Model II: max. glacial, min. interglacial; Model III: 2/3 of interglacial soil is aeolian deposit)

Site location: 36.00° N, 103.83° E

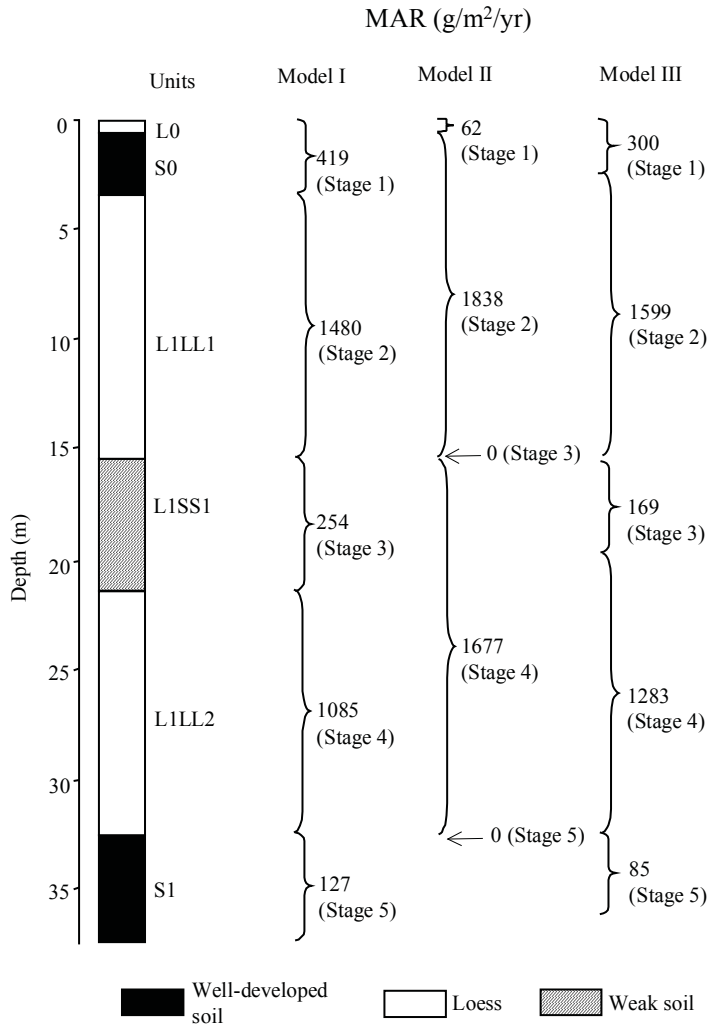

Note: The depths provided in the text are inconsistent with the depths shown in the figure. We used information derived from the diagram to calculate MAR,because the information in the text appears to have been rounded to the nearest meter.

Stratigraphic data: Gaolanshan
(thickness given in text by authors different from their diagram, the used depth and thickness estimated from diagram, to nearest 10 cm)

Top depth (m)	Bottom depth (m)	Thickness (m)	Stratigraphic units	DBD (g/cm³)
0.0	0.5	0.5	L0	n/a
0.5	3.4	2.9	S0	n/a
3.4	15.4	12.0	L1LL1	n/a
15.4	21.4	6.0	L1SS1	n/a
21.4	32.4	11.0	L1LL2	n/a
32.4	37.2	4.8	S1	n/a

Stratigraphic data: Gaolanshan
(depth and thickness information given in text)

Top depth (m)	Bottom depth (m)	Thickness (m)	Stratigraphic units	DBD (g/cm³)
0	0.5	0.5	L0	n/a
0.5	4	3.5	S0	n/a
4	15	11	L1LL1	n/a
15	21	6	L1SS1	n/a
21	28.5	7.5	L1LL2	n/a
n/a	n/a	n/a	S1	n/a

Gaolanshan section: MAR (g/m^2/yr) based on ^{14}C dating

Site location: 36.00° N, 103.83° E

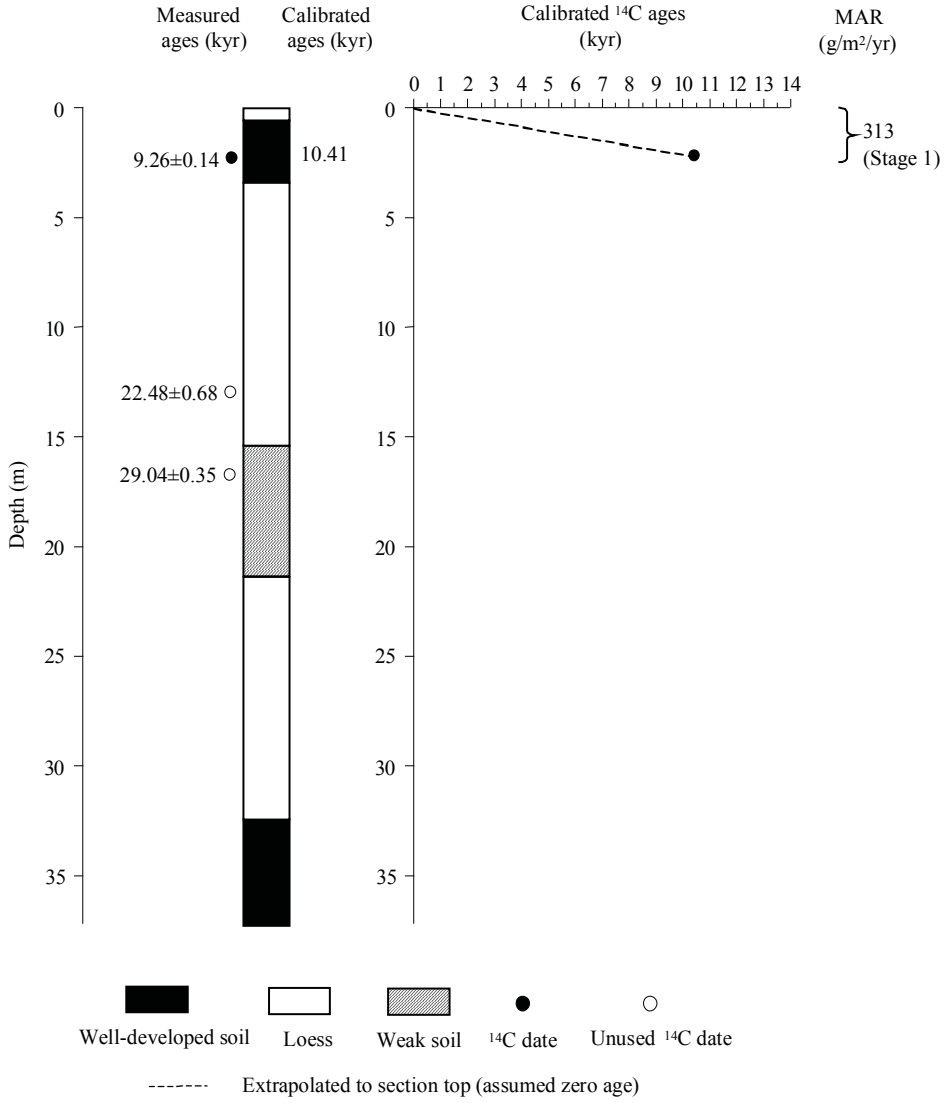

^{14}C dating: Gaolanshan (depth of the uppermost date estimated from diagram, to nearest 1 cm; depth of the other two dates given by authors)										
Depth (m)	Dating laboratory	Lab. No.	Dating material	Age (kyr)	s.d. (kyr)	(1σ) Calendar age ranges (kyr)	Relative probability	Assumed calendar age (kyr)	Reference	Comments
2.2	n/a	n/a	organic matter	9.26	0.14	10.24-10.58	0.977	10.41	Chen et al. (1996a)	
						10.63-10.63	0.023			
12.9	n/a	n/a	organic matter	22.5	0.68				Chen et al. (1996a)	beyond calibration range
16.65	n/a	n/a	organic matter	29	0.35				Chen et al. (1996a)	beyond calibration range

Gaolanshan section: MAR (g/m^2/yr) based on magnetic susceptibility

Note: Digitized MS data.

Site location: 36.00° N, 103.83° E

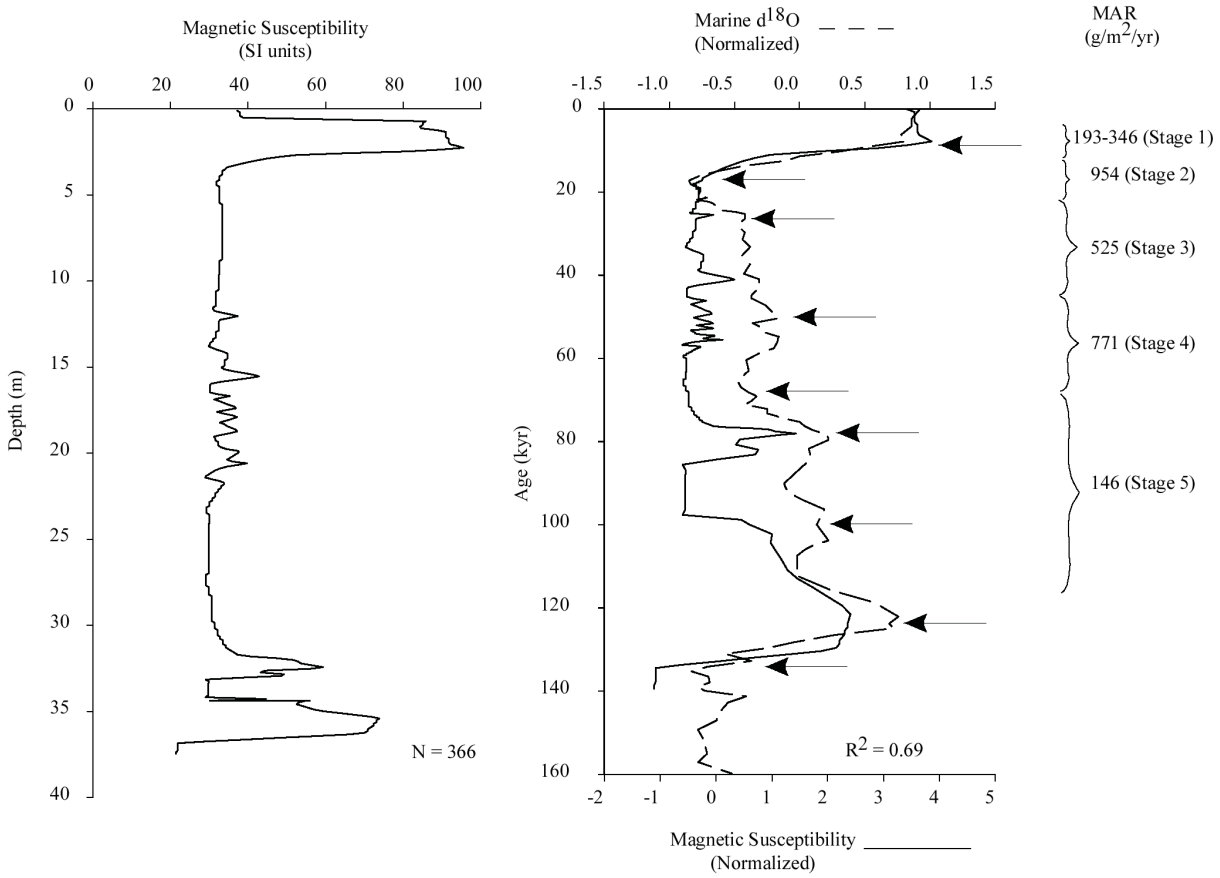

MS age model: Gaolanshan		
Tie-Point	Depth (m)	Age (kyr)
1	2.26	7.81
2	3.5	17.31
3	12.04	25.42
4	17.91	51.57
5	27.18	65.22
6	32.53	78.3
7	34.38	99.96
8	35.52	123.82
9	36.96	135.34

Age model (kyr): Gaolanshan						
Depth (m)	^{14}C	TL	Magnetic susceptibility	Pedostratigraphy (Model III)	Average chronology	Range
0	0			0.0	0.0	
5			18.7	14.3	16.5	14.3-18.7
10			23.5	18.9	21.2	18.9-23.5
15			38.6	23.6	31.1	23.6-38.6
20			54.6	59.7	57.2	54.6-59.7
25			62.0	65.4	63.7	62.0-65.4
30			72.1	71.2	71.7	71.2-72.1
35			112.9	119.6	116.3	112.9-119.6

MAR ($g/m^2/yr$): Gaolanshan								
Stage (range in kyr)	Assumed DBD (g/cm^3)	^{14}C	TL	MS	Pedostratigraphy			Average MAR
					Model I	Model II	Model III	
Stage 1 (12-0)	1.48	**313**		**270**	419	62	**300**	294
Stage 2 (24-12)	1.48			**954**	1480	1838	**1599**	1277
Stage 3 (59-24)	1.48			**525**	254	0	**169**	347
Stage 4 (74-59)	1.48			**771**	1085	1677	**1283**	1027
Stage 5 (130-74)	1.48			**146**	127	0	**85**	116

References used to generate data report: Gaolanshan	
Data used	**Source**
Pedostratigraphy	Derbyshire et al. (1995a)
Magnetic susceptibility	Derbyshire et al. (1995a)
^{14}C dating	Chen et al. (1996a)
TL dating	-
Additional References:	
Data available	**Source**
Grain size, micromorphology	Derbyshire et al. (1995a)
Magnetic susceptibility, grain size, micromorphology, pedostratigraphy	Derbyshire et al. (1995b)
Magnetic susceptibility, grain size, micromorphology, pedostratigraphy	Derbyshire et al. (1997)
Magnetic susceptibility, grain size, organic carbon, $CaCO_3$ micromorphology, pedostratigraphy	Kemp et al. (1995)
Magnetic susceptibility, pedostratigraphy	Chen et al. (1996a)
Magnetic susceptibility, ^{14}C, pedostratigraphy	Chen et al. (1997)

Guojialiang section: MAR (g/m^2/yr) based on pedostratigraphy

Note: Stage 1 affected by sand layer. Last glacial loess (L1) contains sedimentary hiatus.

(Model I: min. glacial, max. interglacial; Model II: max. glacial, min. interglacial; Model III: 2/3 of interglacial soil is aeolian deposit)

Site location: 37.50° N, 108.88° E

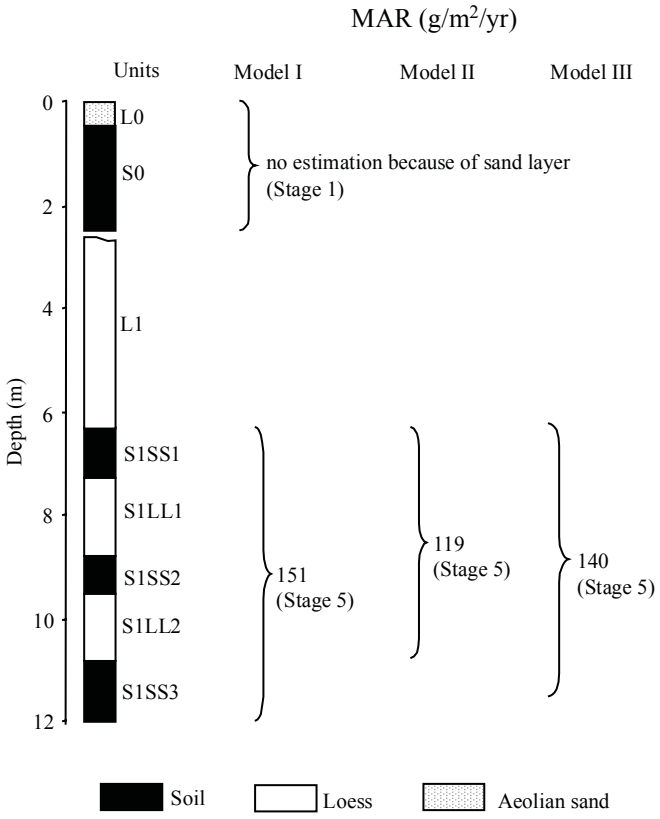

Stratigraphic data: Guojialiang (depth and thickness estimated from diagram, to nearest 10 cm)				
Top depth (m)	Bottom depth (m)	Thickness (m)	Stratigraphic units	DBD (g/cm³)
0.0	0.5	0.5	L0 (aeolian sand)	n/a
0.5	2.5	2.0	S0	n/a
2.5	6.3	3.8	L1 with hiatus	n/a
6.3	7.3	1.0	S1SS1	n/a
7.3	8.8	1.5	S1LL1	n/a
8.8	9.5	0.7	S1SS2	n/a
9.5	10.8	1.3	S1LL2	n/a
10.8	12.0	1.2	S1SS3	n/a

Guojialiang section: Magnetic susceptibility

Note: Stage 1 affected by sand layer. Last glacial loess (L1) contains sedimentary hiatus. MS MAR unused because of sand layer and hiatuses.

Site location: 37.50° N, 108.88° E

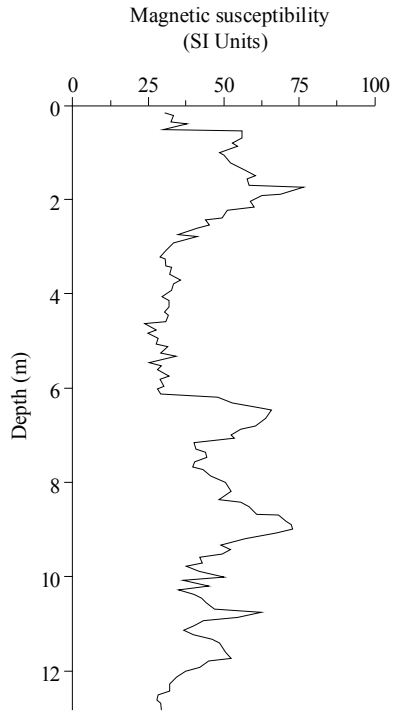

Age model (kyr): Guojialiang						
Depth (m)	^{14}C	TL	Magnetic susceptibility	Pedostratigraphy (Model III)	Average chronology	Range
0						
2						
4						
6						
8				91.9	91.9	
10				113.0	113.0	
12						

MAR ($g/m^2/yr$): Guojialiang								
Stage (range in kyr)	Assumed DBD (g/cm^3)	^{14}C	TL	MS	Pedostratigraphy			Average MAR
					Model I	Model II	Model III	
Stage 1 (12-0)	1.48							
Stage 2 (24-12)	1.48							
Stage 3 (59-24)	1.48							
Stage 4 (74-59)	1.48							
Stage 5 (130-74)	1.48				151	119	**140**	140

References used to generate data report: Guojialiang	
Data used	**Source**
Pedostratigraphy	Sun (1994)
Magnetic susceptibility	Sun (1994)
^{14}C dating	-
TL dating	-
Additional References:	
Data available	**Source**
-	-

Halali section: MAR (g/m^2/yr) based on pedostratigraphy

Note: Section with potential local sources from the lacustrine sediments of Qinghai Lake. Stratigraphic units of S0SS1 and S0SS3 have variable thicknesses. MAR estimated, based on the assumption that the age of the top of the modern soil is zero and the soil has not been disturbed.

(Model I: min. glacial, max. interglacial; Model II: max. glacial, min. interglacial; Model III: 2/3 of interglacial soil is aeolian deposit)

Site location: 36.67° N, 99.88° E

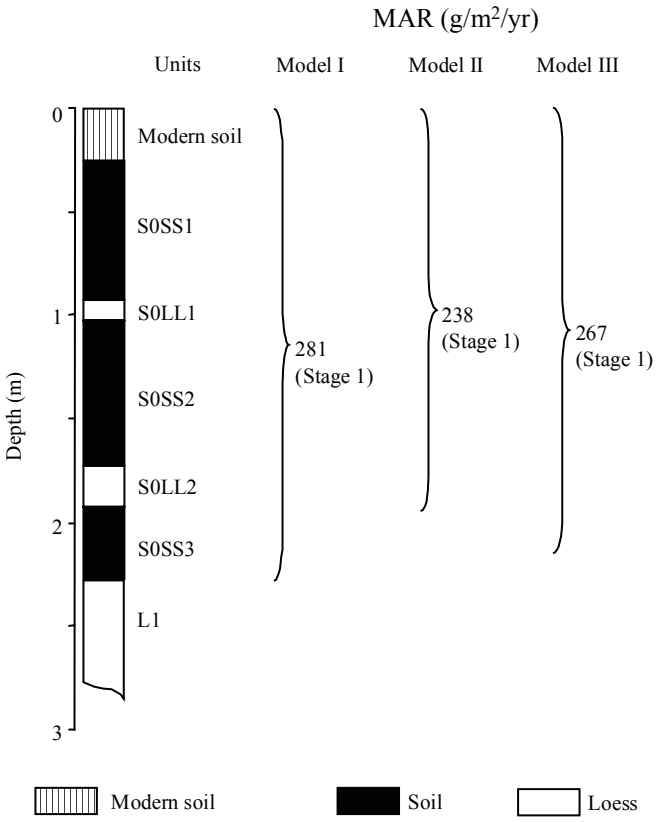

Stratigraphic data: Halali (depths given by the authors, thickness calculated from depths)				
Top depth (m)	Bottom depth (m)	Thickness (m)	Stratigraphic units	DBD (g/cm³)
0.00	0.25	0.25	modern soil	n/a
0.25	0.93	0.68	S0SS1	n/a
0.93	1.03	0.10	S0LL1	n/a
1.03	1.73	0.70	S0SS2	n/a
1.73	1.93	0.20	S0LL2	n/a
1.93	2.28	0.35	S0SS3	n/a
2.28	-	-	L1	n/a

Halali section: MAR (g/m^2/yr) based on ^{14}C dating

Note: Section with potential local sources from the lacustrine sediments of Qinghai Lake.

Site location: 36.67° N, 99.88° E

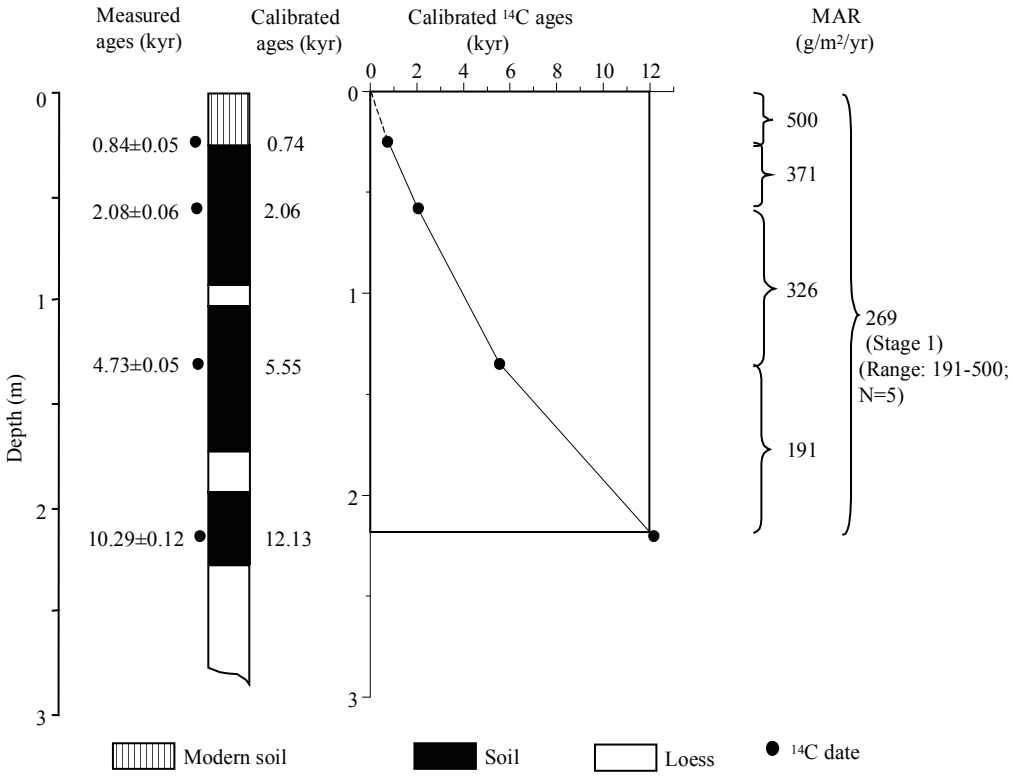

^{14}C dating: Halali (depth given by the authors)										
Depth (m)	Dating laboratory	Lab. No.	Dating material	Age (kyr)	s.d. (kyr)	(1σ) Calendar age ranges (kyr)	Relative probability	Assumed calendar age (kyr)	Reference	Comments
0.25	^{14}C Lab. Lanzhou Univ.	n/a	organic matter	0.84	0.05	0.69-0.79	1	0.74	Chen et al. (1991a)	
0.58	^{14}C Lab. Lanzhou Univ.	n/a	organic matter	2.08	0.06	1.99-2.12	0.903	2.06	Chen et al. (1991a)	
						1.97	0.047			
						1.95	0.05			
1.35	^{14}C Lab. Lanzhou Univ.	n/a	organic matter	4.73	0.05	5.52-5.58	0.498	5.55	Chen et al. (1991a)	
						5.46-5.48	0.216			
						5.33-5.38	0.286			
2.2	^{14}C Lab. Lanzhou Univ	n/a	organic matter	10.3	0.12	11.90-12.35	0.744	12.13	Chen et al. (1991a)	
						11.75-11.86	0.162			
						12.52-12.59	0.094			

Age model (kyr): Halali						
Depth (m)	^{14}C	TL	Magnetic susceptibility	Pedostratigraphy (Model III)	Average chronology	Range
0.0	0			0	0	
0.5	1.7			2.8	2.3	1.7-2.8
1.0	4.0			5.6	4.8	4.0-5.6
1.5	6.7			8.3	7.5	6.7-8.3
2.0	10.6			11.1	10.9	10.6-11.1

MAR ($g/m^2/yr$): Halali								
Stage (range in kyr)	Assumed DBD (g/cm^3)	^{14}C	TL	MS	Pedostratigraphy			Average MAR
					Model I	Model II	Model III	
Stage 1 (12-0)	1.48	**269**			281	238	**267**	268
Stage 2 (24-12)	1.48							
Stage 3 (59-24)	1.48							
Stage 4 (74-59)	1.48							
Stage 5 (130-74)	1.48							

References used to generate data report: Halali	
Data used	**Source**
Pedostratigraphy	Chen et al. (1991a)
Magnetic susceptibility	-
^{14}C dating	Chen et al. (1991a)
TL dating	-
Additional References:	
Data available	**Source**
Grain size, pollen	Chen et al. (1991a))
Pedostratigraphy, ^{14}C	An et al. (2000)

Heimugou_1 (Luochuan) section: MAR (g/m^2/yr) based on pedostratigraphy

Note: Stage 1 affected by cultivation layer. Heimugou is the name of a loess gulley near the suburb of Luochuan in Shaaxi Province. The most commonly used section is referred to here as Heimugou_1 (Luochuan), the pedostratigraphy for which is taken from An et al. (1991a). Heimugou_2 (Louchuan) is used to identify the section (and different stratigraphy) published by Forman (1991). Guo et al., (1996c) and Forman (1991) refer to the sites at Luochuan as Upper and Lower Heimugou (Luochuan). Forman (1991) additionally provides TL dates from a site called the Heimugou brickyard. The pedostratigrahy of Upper Heimugou (used by Forman, 1991) is presented here as Heimugou_2 (Luochuan). Although site locations are the same, the pedostratigraphies of Guo et al. (1996c) are different from both of the ones shown here.

(Model I: min. glacial, max. interglacial; Model II: max. glacial, min. interglacial; Model III: 2/3 of interglacial soil is aeolian deposit)

Site location: 35.75° N, 109.42° E

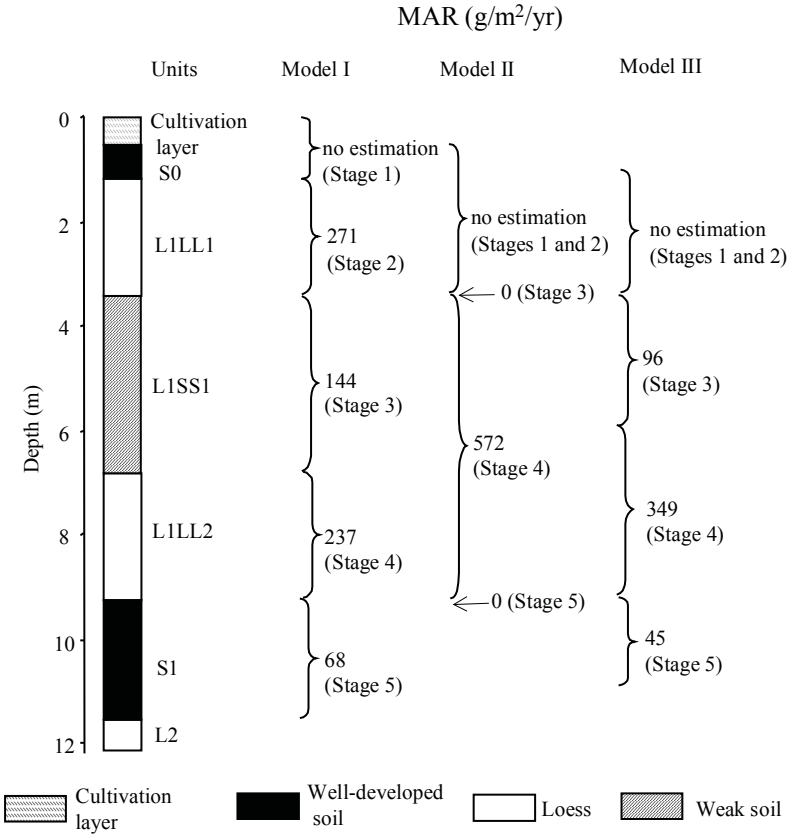

Stratigraphic data: Heimugou_1 (Luochuan) (depth and thickness estimated from diagram, to nearest 10 cm)				
Top depth (m)	Bottom depth (m)	Thickness (m)	Stratigraphic units	DBD (g/cm^3)
0.0	0.5	0.5	cultivation layer	1.4
0.5	1.2	0.7	S0	1.4
1.2	3.4	2.2	L1LL1	1.48
3.4	6.8	3.4	L1SS1	1.48
6.8	9.2	2.4	L1LL2	1.48
9.2	11.5	2.3	S1	1.65
11.5			L2	n/a

Heimugou_1 (Luochuan) section: MAR (g/m^2/yr) based on magnetic susceptibility

Note: Heimugou is the name of a loess gulley near the suburb of Luochuan in Shaaxi Province. The most commonly used section is referred to here as Heimugou_1 (Luochuan), the pedostratigraphy for which is taken from An et al. (1991a). Heimugou_2 (Louchuan) is used to identify the section (and different stratigraphy) published by Forman (1991). Guo et al., (1996c) and Forman (1991) refer to the sites at Luochuan as Upper and Lower Heimugou (Luochuan). Forman (1991) additionally provides TL dates from a site called the Heimugou brickyard. The pedostratigrahy of Upper Heimugou (used by Forman, 1991) is presented here as Heimugou_2 (Luochuan). Although site locations are the same, the pedostratigraphies of Guo et al. (1996c) are different from both of the ones shown here. There are two versions of the MS data. One was digitized from An et al. (1991a). The other was made available from Dr. Sun Jimin (see next page). Stage 1 affected by cultivation layer.

Site location: 35.75° N, 109.42° E

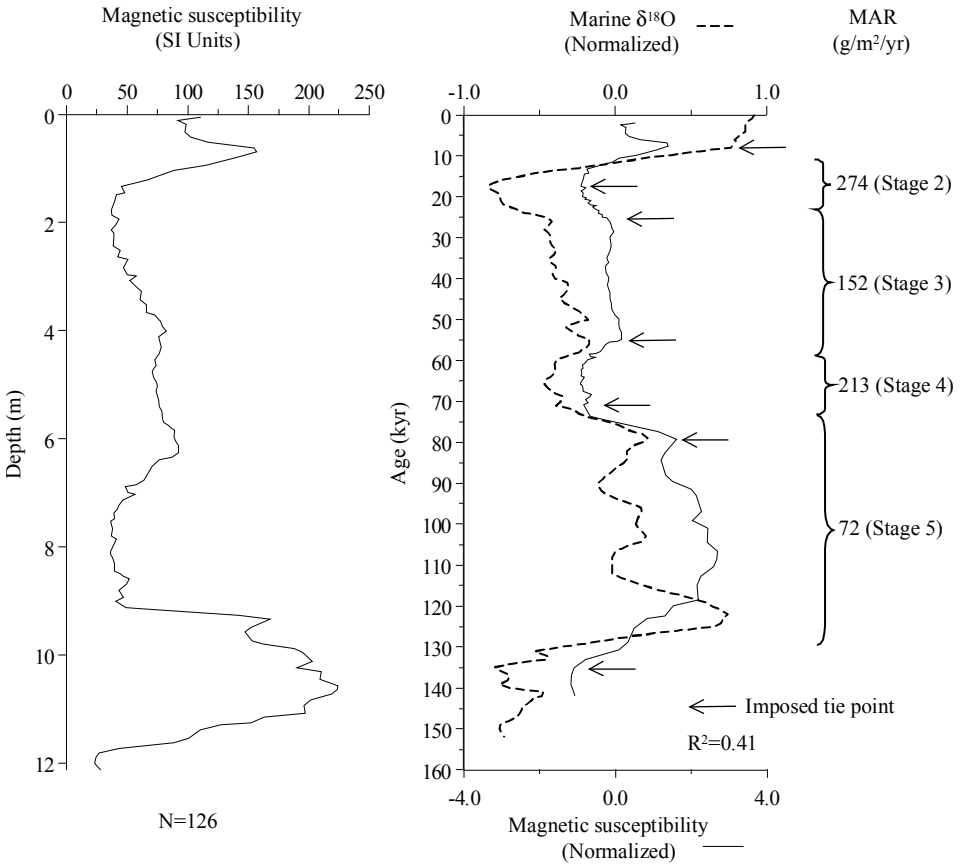

MS age model: Heimugou_1 (Luochuan)		
Tie-Point	Depth (m)	Age (kyr)
1	0.69	7.81
2	1.77	17.31
3	3.72	25.35
4	6.26	54.84
5	9.02	70.82
6	9.35	79.25
7	11.82	135.10

Heimugou_1 (Luochuan) section: MAR (g/m^2/yr) based on magnetic susceptibility

Note: Heimugou is the name of a loess gulley near the suburb of Luochuan in Shaaxi Province. The most commonly used section is referred to here as Heimugou_1 (Luochuan), the pedostratigraphy for which is taken from An et al. (1991a). Heimugou_2 (Louchuan) is used to identify the section (and different stratigraphy) published by Forman (1991). Guo et al., (1996c) and Forman (1991) refer to the sites at Luochuan as Upper and Lower Heimugou (Luochuan). Forman (1991) additionally provides TL dates from a site called the Heimugou brickyard. The pedostratigrahy of Upper Heimugou (used by Forman, 1991) is presented here as Heimugou_2 (Luochuan). Although site locations are the same, the pedostratigraphies of Guo et al. (1996c) are different from both of the ones shown here. . There are two versions of the MS data. One (previous page) was digitized from An et al. (1991a). The other is unpuclished data made available from Dr. Sun Jimin and taken from the data archive at the Institute of Geology, Chinese Aademy of Science, P. O. Box 9825, Beijing 100029; China.

Site location: 35.75° N, 109.42° E

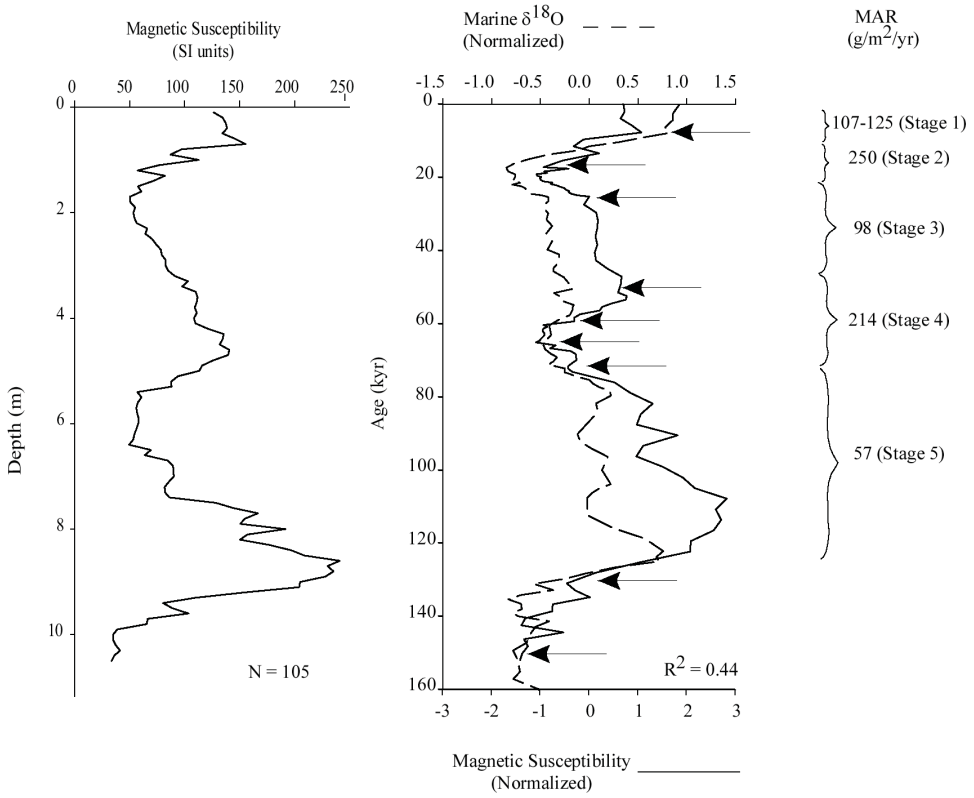

MS age model: Heimugou_1 (Luochuan)		
Tie-Point	Depth (m)	Age (kyr)
1	0.7	7.81
2	1.2	17.31
3	3.3	25.35
4	4.5	51.57
5	5.4	60.44
6	6.4	65.22
7	7.4	73.25
8	9.4	131.09
9	10.5	152.14

Age model (kyr): Heimugou_1 (Luochuan)							
Depth (m)	^{14}C	TL	Magnetic susceptibility	Magnetic susceptibility (2)	Pedostratigraphy (Model III)	Average chronology	Range
0				0.0		0	
2			18.4	20.4		19.4	18.4-20.4
4			28.7	40.6	33.1	34.1	28.7-40.6
6			52.3	63.3	60.2	58.6	52.3-63.3
8			65	90.6	68.9	74.8	65.0-90.6
10			93	142.6	103.0	112.9	93.0-142.6

MAR (g/m²/yr): Heimugou_1 (Luochuan)									
Stage (range in kyr)	DBD (g/cm^3)	^{14}C	TL	MS	**MS (2)**	Pedostratigraphy			Average MAR
						Model I	Model II	Model III	
Stage 1 (12-0)	1.40				**116**				116
Stage 2 (24-12)	1.48			**274**	**250**	271			262
Stage 3 (59-24)	1.48			**152**	**98**	144	0	**96**	115
Stage 4 (74-59)	1.48			**213**	**214**	237	572	**349**	259
Stage 5 (130-74)	1.65			**72**	**57**	68	0	**45**	58

References used to generate data report: Heimugou_1 (Luochuan)	
Data used	**Source**
Pedostratigraphy	An et al. (1991a)
Magnetic susceptibility	An et al. (1991a)
^{14}C dating	-
TL dating	-
Additional References:	
Data available	**Source**
$CaCO_3$, pedostratigraphy	Lu (1981)
Magnetic susceptibility, magnetic polarity, pedostratigraphy	Heller and Liu (1982)
Magnetic susceptibility, magnetic polarity, pedostratigraphy	Heller and Liu (1984)
Grain size, magnetic polarity, DBD, pedostratigraphy	Liu et al. (1985)
Magnetic susceptibility, magnetic polarity, pedostratigraphy	Heller et al. (1987)
Magnetic susceptibility, grain size, magnetic polarity, chemical parameters, pedostratigraphy	Liu and Yuan (1987)
Magnetic susceptibility, magnetic polarity, $CaCO_3$, pedostratigraphy	Kukla (1987a)
Magnetic susceptibility, grain size, magnetic polarity, chemical parameters, pedostratigraphy	Yuan et al. (1987)
Magnetic susceptibility, magnetic polarity, pedostratigraphy	Kukla and An (1989)
Magnetic susceptibility, grain size, pedostratigraphy	An and Xiao (1990)
Magnetic susceptibility, grain size	Zheng et al. (1991b)
TL	An et al. (1991a)
Magnetic susceptibility, pedostratigraphy	An et al. (1991b)
Magnetic susceptibility, pedostratigraphy	An et al. (1991c)
Magnetic polarity, pedostratigraphy	Ding et al. (1991)
Magnetic susceptibility, pedostratigraphy	Han et al. (1991a)
Magnetic susceptibility, pedostratigraphy	Han et al. (1991b)
Magnetic susceptibility, pedostratigraphy, TL, chemical parameters	Guo et al. (1996c)
Micromorphology, chemical parameters	Guo et al. (1996b)
Magnetic susceptibility, $\delta^{13}C$ (organic), $\delta^{18}O$ (carbonate), $\delta^{13}C$ (carbonate), pedostratigraphy	Lin et al. (1991)
Magnetic susceptibility, phytoliths, pedostratigraphy	Lu et al. (1991)
Magnetic susceptibility, pedostratigraphy	Maher and Thompson (1991)
Magnetic polarity, pedostratigraphy	Rutter et al. (1991)
Grain size, ^{10}Be, $CaCO_3$, magnetic polarity, pedostratigraphy	Shen et al. (1987)
Grain size, ^{10}Be, $CaCO_3$, magnetic polarity, pedostratigraphy	Shen et al. (1991)
Magnetic polarity, pedostratigraphy	Wei et al. (1991)
Magnetic susceptibility, pedostratigraphy	Xu et al. (1991)
Magnetic polarity, pedostratigraphy	Rutter (1992)
Magnetic susceptibility, grain size, TL, pedostratigraphy	Porter and An (1995)
$CaCO_3$, magnetic polarity, chemical parameters, pedostratigraphy	Gallet et al. (1996)
Magnetic susceptibility, pedostratigraphy	Han and Jiang (1999)
Magnetic susceptibility, magnetic polarity, pedostratigraphy	Zhou and Shackleton (1999)
Pedostratigraphy	Wen and Zheng (1987)

Heimugou_2 (Luochuan) section : MAR (g/m^2/yr) based on pedostratigraphy

Note: Last glacial loess (L1) is not subdivided. Heimugou is the name of a loess gulley near the suburb of Luochuan in Shaaxi Province. The most commonly used section is referred to here as Heimugou_1 (Luochuan), the pedostratigraphy for which is taken from An et al. (1991a). Heimugou_2 (Louchuan) is used to identify the section (and different stratigraphy) published by Forman (1991). Guo et al., (1996c) and Forman (1991) refer to the sites at Luochuan as Upper and Lower Heimugou (Luochuan). Forman (1991) additionally provides TL dates from a site called the Heimugou brickyard. The pedostratigraphy of Upper Heimugou (used by Forman, 1991) is presented here as Heimugou_2 (Luochuan). Although site locations are the same, the pedostratigraphies of Guo et al. (1996c) are different from both of the ones shown here.

(Model I: min. glacial, max. interglacial; Model II: max. glacial, min. interglacial; Model III: 2/3 of interglacial soil is aeolian deposit)

Site location: 35.75° N, 109.42° E

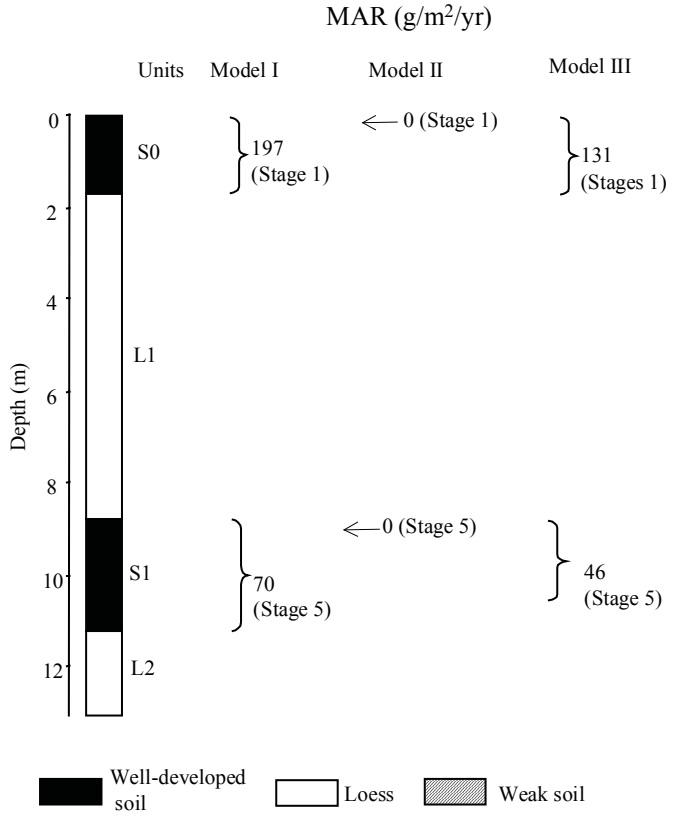

Stratigraphic data: Heimugou_2 (Luochuan) (depth and thickness estimated from diagram, to nearest 1 cm)				
Top depth (m)	Bottom depth (m)	Thickness (m)	Stratigraphic units	DBD (g/cm^3)
0.00	1.69	1.69	S0	1.40
1.69	8.79	7.10	L1	1.48
8.79	11.15	2.36	S1	1.65
11.15			L2	n/a

Heimugou_2 (Luochuan) section : TL dating

Note: Last glacial loess (L1) is not subdivided. Heimugou is the name of a loess gulley near the suburb of Luochuan in Shaaxi Province. The most commonly used section is referred to here as Heimugou_1 (Luochuan), the pedostratigraphy for which is taken from An et al. (1991a). Heimugou_2 (Louchuan) is used to identify the section (and different stratigraphy) published by Forman (1991). No MAR calculated because only one TL date used. The TL dates used for this section are from Forman's Upper Heimuguo section (Forman, 1991). The dates from the Heimugou Brickyard and Lower Heimugou (estimated to the nearest 10 cm) are included in the table of TL dates, but are not used for estimating MAR.

Site location: 35.75° N, 109.42° E

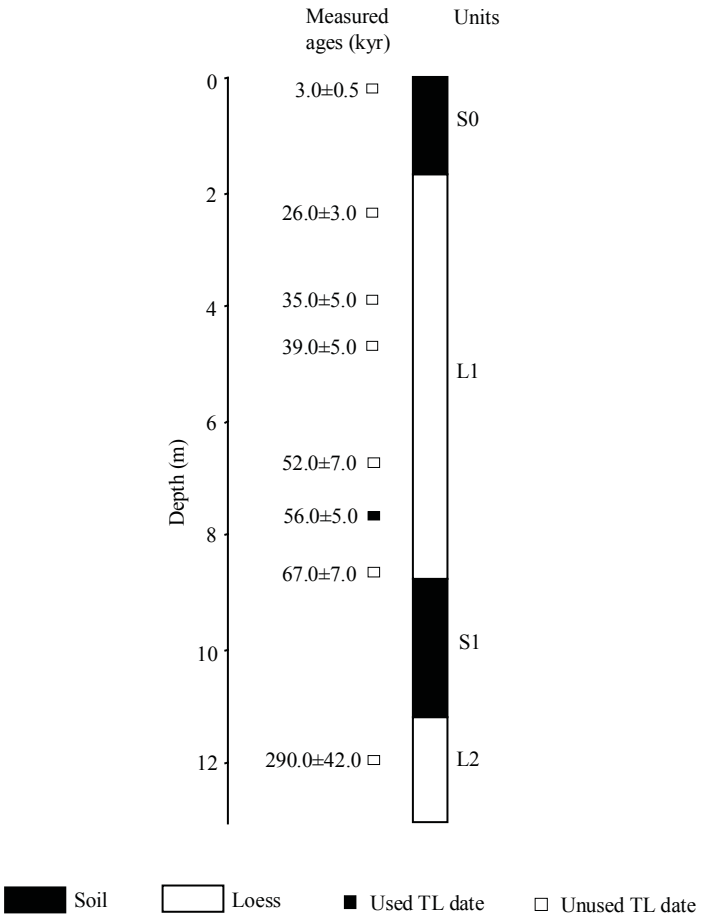

TL dating: Heimugou_2 (Luochuan)
(depth for TL dates estimated from diagram, to nearest 1 cm)

Depth (m)	Dating laboratory	Lab. No.	Dating material	TL-method	Age (kyr)	s.d. (kyr)	Reference	Comments
0.20	n/a	ITL-73	bulk fine-silt fraction	fine-grain (4-11 mm) technique	3	0.5	Forman (1991)	Upper Heimugou, uncertainties > 10 %
2.37	n/a	ITL-81	bulk fine-silt fraction	fine-grain (4-11 mm) technique	26	3	Forman (1991)	Upper Heimugou, uncertainties > 10 %
3.89	n/a	ITL-53	bulk fine-silt fraction	fine-grain (4-11 mm) technique	35	5	Forman (1991)	Upper Heimugou, uncertainties > 10 %
4.73	n/a	ITL-93	bulk fine-silt fraction	fine-grain (4-11 mm) technique	39	5	Forman (1991)	Upper Heimugou, uncertainties > 10 %
6.76	n/a	ITL-92	bulk fine-silt fraction	fine-grain (4-11 mm) technique	52	7	Forman (1991)	Upper Heimugou, uncertainties > 10 %
7.69	n/a	ITL-94	bulk fine-silt fraction	fine-grain (4-11 mm) technique	56	5	Forman (1991)	Upper Heimugou
8.62	n/a	ITL-52	bulk fine-silt fraction	fine-grain (4-11 mm) technique	67	7	Forman (1991)	Upper Heimugou, uncertainties > 10 %
11.93	n/a	ITL-95	bulk fine-silt fraction	fine-grain (4-11 mm) technique	290	42	Forman (1991)	Upper Heimugou, uncertainties > 10 %

TL dating: Heimugou_2 (Luochuan)
Additional dates from Heimugou Brickyard and Lower Heimugou (depth estimated from diagram, to nearest 10 cm)

Depth (m)	Dating laboratory	Lab. No.	Dating material	TL-method	Age (kyr)	s.d. (kyr)	Reference	Comments
2.20	n/a	ITL-96	bulk fine-silt fraction	fine-grain (4-11 mm) technique	22	3	Forman (1991)	Heimugou Brickyard, uncertainties >10%
2.80	n/a	ITL-148	bulk fine-silt fraction	fine-grain (4-11 mm) technique	29	3	Forman (1991)	Heimugou Brickyard
5.00	n/a	ITL-147	bulk fine-silt fraction	fine-grain (4-11 mm) technique	46	6	Forman (1991)	Lower Heimugou, uncertainties >10%
8.40	n/a	ITL-146	bulk fine-silt fraction	fine-grain (4-11 mm) technique	52	7	Forman (1991)	Lower Heimugou, uncertainties >10%
8.80	n/a	ITL-140	bulk fine-silt fraction	fine-grain (4-11 mm) technique	69	8	Forman (1991)	Lower Heimugou, uncertainties >10%
11.70	n/a	ITL-142	bulk fine-silt fraction	fine-grain (4-11 mm) technique	170	25	Forman (1991)	Lower Heimugou, Age >130 kyr

Age model (kyr): Heimugou_2 (Luochuan)						
Depth (m)	^{14}C	TL	Magnetic susceptibility	Pedostratigraphy (Model III)	Average chronology	Range
0				0.0	0.0	
2						
4						
6						
8						
10				117.0	117.0	

MAR (g/m^2/yr): Heimugou_2 (Luochuan)								
Stage (range in kyr)	DBD (g/cm^3)	^{14}C	TL	MS	Pedostratigraphy			Average MAR
					Model I	Model II	Model III	
Stage 1 (12-0)	1.40				197	0	**131**	131
Stage 2 (24-12)	1.48							
Stage 3 (59-24)	1.48							
Stage 4 (74-59)	1.48							
Stage 5 (130-74)	1.65				70	0	**46**	46

References used to generate data report: Heimugou_2 (Luochuan)	
Data used	**Source**
Pedostratigraphy	Forman (1991)
Magnetic susceptibility	-
^{14}C dating	-
TL dating	Forman (1991)
Additional References:	
Data available	**Source**
Magnetic susceptibility, pedostratigraphy, TL, chemical parameters	Guo et al. (1996c)

Heishan section: Pedostratigraphy

Note: Section not used for analysis, because there is no location information and the stratigraphy cannot be correlated to the CLP.

Site location: Datong Basin, details not available

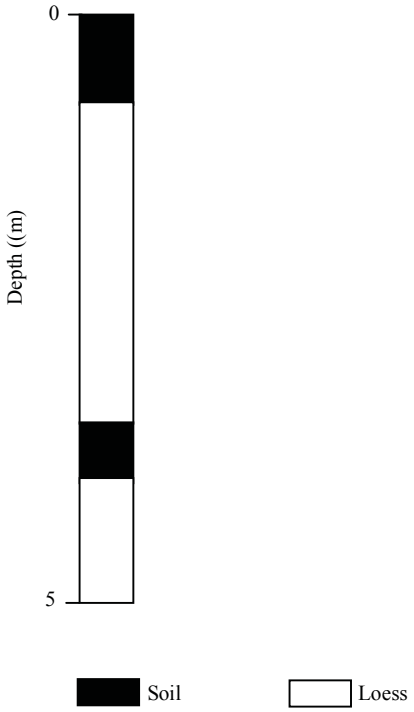

References used to generate data report: Heishan	
Data used	**Source**
Pedostratigraphy	-
Magnetic susceptibility	-
^{14}C dating	-
TL dating	-
Additional References:	
Data available	**Source**
^{10}Be, pollen	Fan et al. (1998)

Heshui section: MAR (g/m^2/yr) based on pedostratigraphy

Note: No Stage 1. The last glacial loess (L1) is not subdivided.

(Model I: min. glacial, max. interglacial; Model II: max. glacial, min. interglacial; Model III: 2/3 of interglacial soil is aeolian deposit)

Site location: 35.82° N, 108.03° E

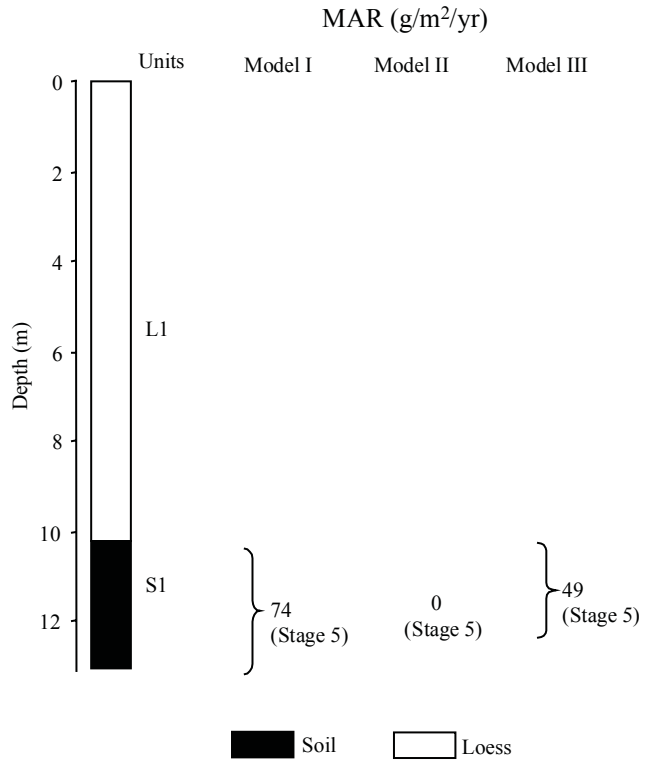

Stratigraphic data: Heshui (thickness given by author, depth calculated from thickness)				
Top depth (m)	Bottom depth (m)	Thickness (m)	Stratigraphic units	DBD (g/cm³)
0.0	10.2	10.2	L1	n/a
10.2	13.0	2.8	S1	n/a

Age model (kyr): Heshui						
Depth (m)	^{14}C	TL	Magnetic susceptibility	Pedostratigraphy (Model III)	Average chronology	Range
0						
2						
4						
6						
8						
11				97.5	97.5	
12				127.3	127.3	

MAR ($g/m^2/yr$): Heshui								
Stage (range in kyr)	Assumed DBD (g/cm^3)	^{14}C	TL	MS	Pedostratigraphy			Average MAR
					Model I	Model II	Model III	
Stage 1 (12-0)	1.48							
Stage 2 (24-12)	1.48							
Stage 3 (59-24)	1.48							
Stage 4 (74-59)	1.48							
Stage 5 (130-74)	1.48				74	0	**49**	49

References used to generate data report: Heshui	
Data used	**Source**
Pedostratigraphy	Liu (1964)
Magnetic susceptibility	-
^{14}C dating	-
TL dating	-
Additional References:	
Data available	**Source**
-	-

Huangling section: MAR (g/m^2/yr) based on pedostratigraphy

Note: No Stage 1. The last glacial loess (L1) is not subdivided.

(Model I: min. glacial, max. interglacial; Model II: max. glacial, min. interglacial; Model III: 2/3 of interglacial soil is aeolian deposit)

Site location: 35.60° N, 109.37° E

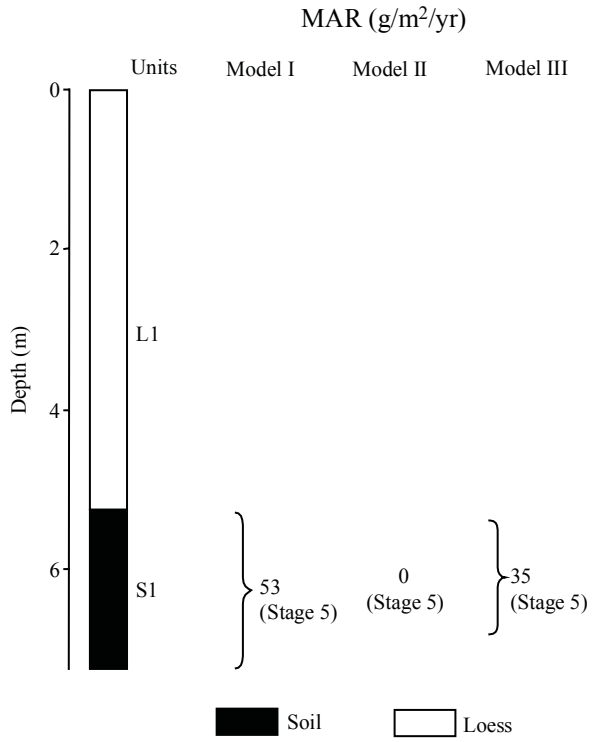

Stratigraphic data: Huangling (thickness given by author, depth calculated from thickness)				
Top depth (m)	Bottom depth (m)	Thickness (m)	Stratigraphic units	DBD (g/cm³)
0.0	5.2	5.2	L1	n/a
5.2	7.2	2.0	S1	n/a

Age model (kyr): Huangling						
Depth (m)	^{14}C	TL	Magnetic susceptibility	Pedostratigraphy (Model III)	Average chronology	Range
0						
1						
2						
3						
4						
5						
6				107.7	107.7	
7						

MAR ($g/m^2/yr$): Huangling								
Stage (range in kyr)	Assumed DBD (g/cm^3)	^{14}C	TL	MS	Pedostratigraphy			Average MAR
					Model I	Model II	Model III	
Stage 1 (12-0)	1.48							
Stage 2 (24-12)	1.48							
Stage 3 (59-24)	1.48							
Stage 4 (74-59)	1.48							
Stage 5 (130-74)	1.48				53	0	**35**	35

References used to generate data report: Huangling	
Data used	**Source**
Pedostratigraphy	Liu (1964)
Magnetic susceptibility	-
^{14}C dating	-
TL dating	-
Additional References:	
Data available	**Source**
-	-

Huanglong section: MAR (g/m^2/yr) based on magnetic susceptibility

Site location: 35.62° N, 109.78° E

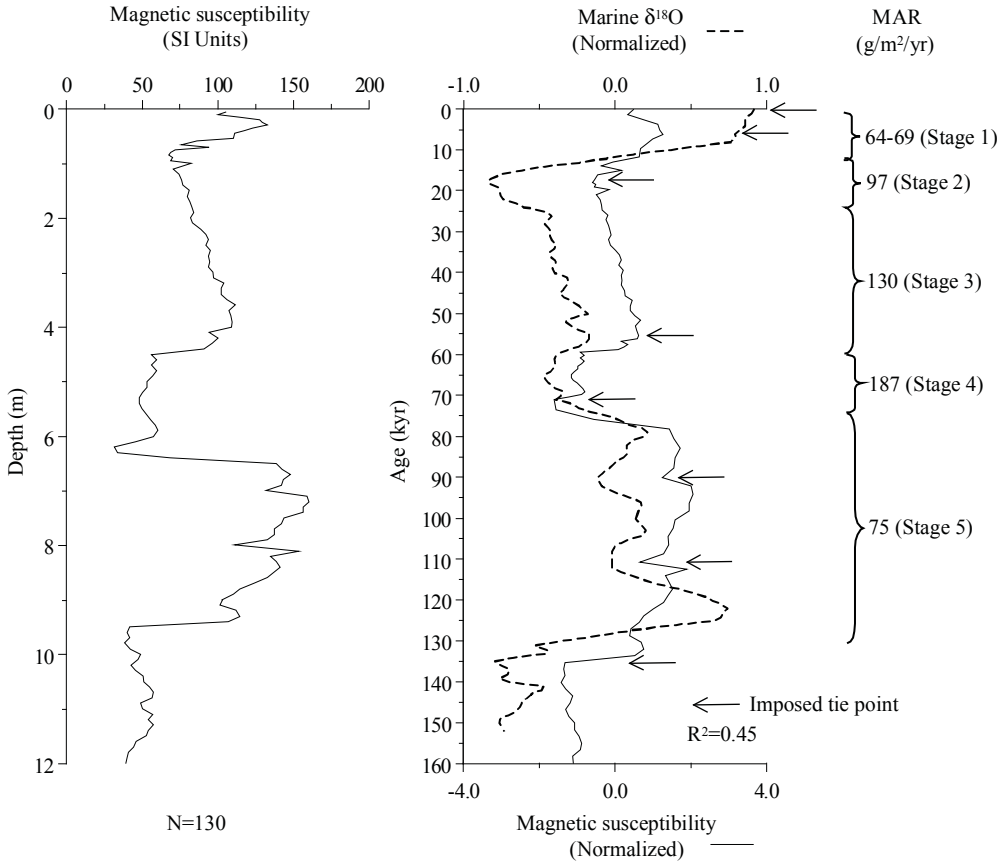

MS age model: Huanglong		
Tie-Point	Depth (m)	Age (kyr)
1	0.05	0.21
2	0.30	6.27
3	0.80	17.31
4	3.90	55.45
5	6.20	71.12
6	7.00	90.10
7	8.00	110.79
8	9.50	135.34

Age model (kyr): Huanglong						
Depth (m)	^{14}C	TL	Magnetic susceptibility	Pedostratigraphy (Model III)	Average chronology	Range
0			0.0		0.0	
2			32.1		32.1	
4			56.1		56.1	
6			69.8		69.8	
8			110.8		110.8	
10			143.5		143.5	
12			176.3		176.3	

MAR ($g/m^2/yr$): Huanglong								
Stage (range in kyr)	Assumed DBD (g/cm^3)	^{14}C	TL	MS	Pedostratigraphy			Average MAR
					Model I	Model II	Model III	
Stage 1 (12-0)	1.48			**67**				67
Stage 2 (24-12)	1.48			**97**				97
Stage 3 (59-24)	1.48			**130**				130
Stage 4 (74-59)	1.48			**187**				187
Stage 5 (130-74)	1.48			**75**				75

References used to generate data report: Huanglong	
Data used	**Source**
Pedostratigraphy	-
Magnetic susceptibility	Ding et al. (1999b)
^{14}C dating	-
TL dating	-
Additional References:	
Data available	**Source**
Grain size	Ding et al. (1999b)
Magnetic susceptibility	Sun and Ding (1997)

Huanxian section: MAR (g/m^2/yr) based on magnetic susceptibility

Note: Digitized MS data.

Site location: 36.58° N, 107.35° E

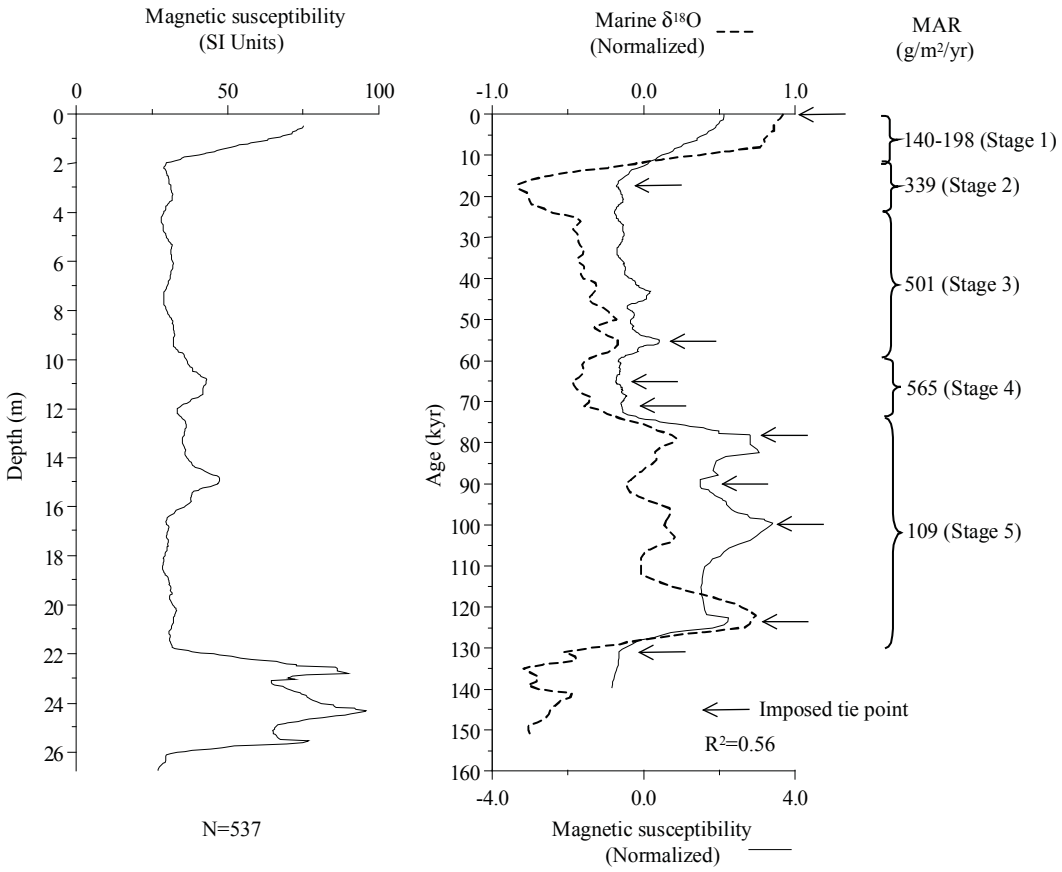

MS age model: Huanxian		
Tie-Point	Depth (m)	Age (kyr)
1	0.49	0.21
2	2.11	17.31
3	14.90	55.45
4	18.48	65.22
5	21.47	71.12
6	22.60	78.30
7	23.14	90.10
8	24.36	99.96
9	25.59	123.82
10	26.13	131.09

Age model (kyr): Huanxian						
Depth (m)	^{14}C	TL	Magnetic susceptibility	Pedostratigraphy (Model III)	Average chronology	Range
0			0		0.0	
5			25.9		25.9	
10			40.8		40.8	
15			55.7		55.7	
20			68.2		68.2	
25			112.4		112.4	

MAR ($g/m^2/yr$): Huanxian								
Stage (range in kyr)	Assumed DBD (g/cm^3)	^{14}C	TL	MS	Pedostratigraphy			Average MAR
					Model I	Model II	Model III	
Stage 1 (12-0)	1.48			**169**				169
Stage 2 (24-12)	1.48			**339**				339
Stage 3 (59-24)	1.48			**501**				501
Stage 4 (74-59)	1.48			**565**				565
Stage 5 (130-74)	1.48			**109**				109

References used to generate data report: Huanxian	
Data used	**Source**
Pedostratigraphy	-
Magnetic susceptibility	Sun et al. (1995)
^{14}C dating	-
TL dating	-
Additional References:	
Data available	**Source**
-	-

Jiezicun (Jiezhichun) section: MAR (g/m^2/yr) based on pedostratigraphy

Note: Lu and Zhao (1991) translate the site name as Jiezhichun. Stage 1 affected by cultivation layer.

(Model I: min. glacial, max. interglacial; Model II: max. glacial, min. interglacial; Model III: 2/3 of interglacial soil is aeolian deposit)

Site location: 34.33° N, 109.57° E

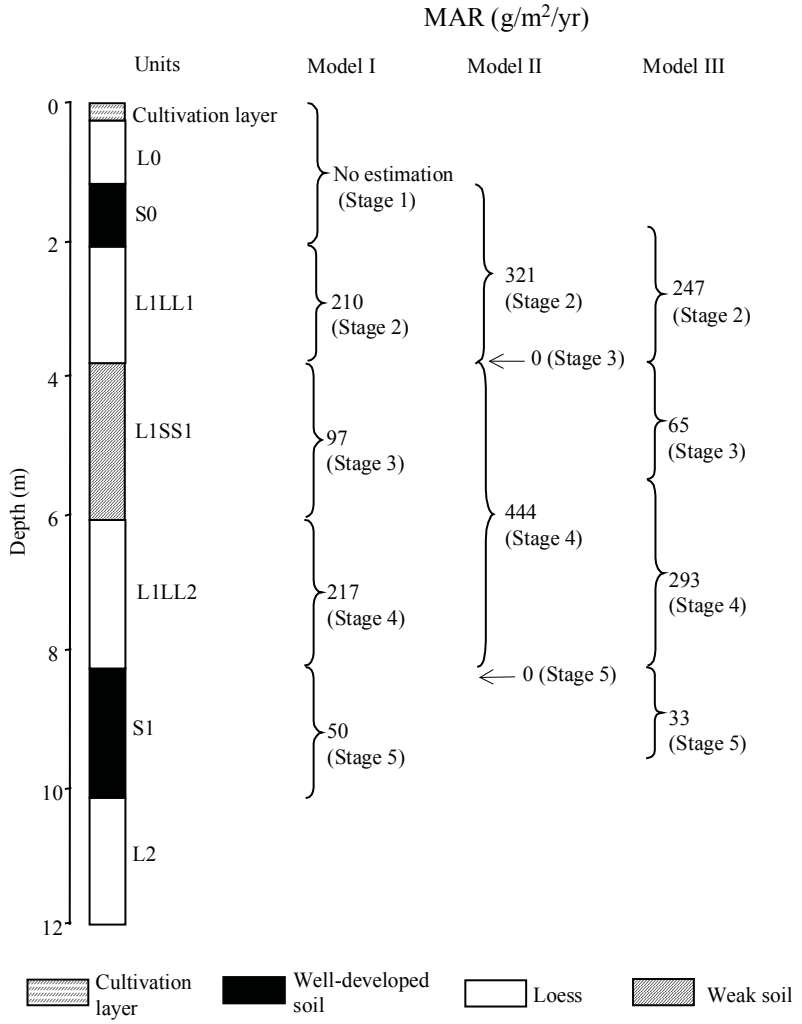

Stratigraphic data: Jiezicun (Jiezhichun) (depth and thickness estimated from diagram, to nearest 10 cm)				
Top depth (m)	Bottom depth (m)	Thickness (m)	Stratigraphic units	DBD (g/cm^3)
0.0	0.3	0.3	cultivation layer	n/a
0.3	1.2	0.9	L0	n/a
1.2	2.1	0.9	S0	n/a
2.1	3.8	1.7	L1LL1	n/a
3.8	6.1	2.3	L1SS1	n/a
6.1	8.3	2.2	L1LL2	n/a
8.3	10.2	1.9	S1	n/a
10.2	12.0	1.8	L2	n/a

Jiezicun (Jiezhichun) section: MAR (g/m^2/yr) based on ^{14}C and TL dating

Note: Lu and Zhao (1991) translate the site name as Jiezhichun. Stage 1 affected by cultivation layer.

Site location: 34.33° N, 109.57° E

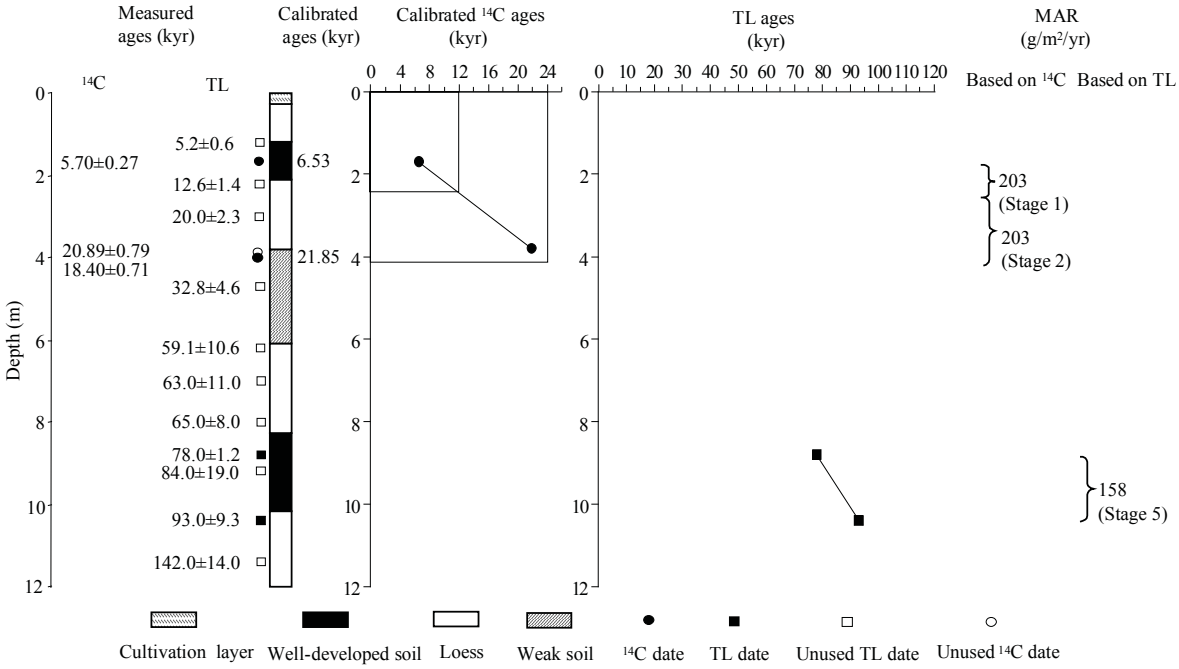

^{14}C dating: Jiezicun (Jiezhichun) (depth given by the authors)										
Depth (m)	Dating laboratory	Lab. No.	Dating material	Age (kyr)	s.d. (kyr)	(1σ) Calendar age ranges (kyr)	Relative probability	Assumed calendar age (kyr)	Reference	Comments
1.7	Xi'an Loess Lab.	JC-01	bulk organic matter	5.7	0.27	6.26-6.80	0.929	6.53	Lu and Zhao (1991)	
						6.20-6.25	0.049			
						6.84-6.85	0.022			
3.8	Xi'an Loess Lab.	JC-02	soluble organic matter	20.9	0.79				Lu and Zhao (1991)	beyond calibration range
3.8	Xi'an Loess Lab.	JC-02	insoluble organic matter	18.4	0.71	20.97-22.74	1	21.85	Lu and Zhao (1991)	

TL dating: Jiezicun (Jiezhichun)
(depth given by authors)

Depth (m)	Dating laboratory	Lab. No.	Dating material	TL-method	Age (kyr)	s.d. (kyr)	Reference	Comments
1.2	Xi'an Loess Lab.	ZH-11	n/a	fine-grain (4-11 µm) technique	5.2	0.6	Lu and Zhao (1991)	uncertainties larger than 10 %
2.2	Xi'an Loess Lab.	ZH-10	n/a	fine-grain (4-11 µm) technique	12.6	1.4	Lu and Zhao (1991)	uncertainties larger than 10 %
3.0	Xi'an Loess Lab.	ZH-12	n/a	fine-grain (4-11 µm) technique	20	2.3	Lu and Zhao (1991)	uncertainties larger than 10 %
4.7	Xi'an Loess Lab.	ZH-09	n/a	fine-grain (4-11 µm) technique	32.8	4.6	Lu and Zhao (1991)	uncertainties larger than 10 %
6.2	Xi'an Loess Lab.	ZH-08	n/a	fine-grain (4-11 µm) technique	59.1	10.6	Lu and Zhao (1991)	uncertainties larger than 10 %
7.0	Xi'an Loess Lab.	ZH-07	n/a	fine-grain (4-11 µm) technique	63	11	Lu and Zhao (1991)	uncertainties larger than 10 %
8.0	Xi'an Loess Lab.	ZH-06	n/a	fine-grain (4-11 µm) technique	65	8	Lu and Zhao (1991)	uncertainties larger than 10 %
8.8	Xi'an Loess Lab.	ZH-05	n/a	fine-grain (4-11 µm) technique	78	1.2	Lu and Zhao (1991)	
9.2	Xi'an Loess Lab.	ZH-04	n/a	fine-grain (4-11 µm) technique	84	19	Lu and Zhao (1991)	uncertainties larger than 10 %
10.4	Xi'an Loess Lab.	ZH-03	n/a	fine-grain (4-11 µm) technique	93	9.3	Lu and Zhao (1991)	
11.4	Xi'an Loess Lab.	ZH-02	n/a	fine-grain (4-11 µm) technique	142	14	Lu and Zhao (1991)	not used, age >130 kyr

Jiezicun (Jiezhichun) section: MAR (g/m^2/yr) based on magnetic susceptibility

Note: Lu and Zhao (1991) translate the site name as Jiezhichun. Digitized MS data. Stage 1 affected by cultivation layer.

Site location: 34.33° N, 109.57° E

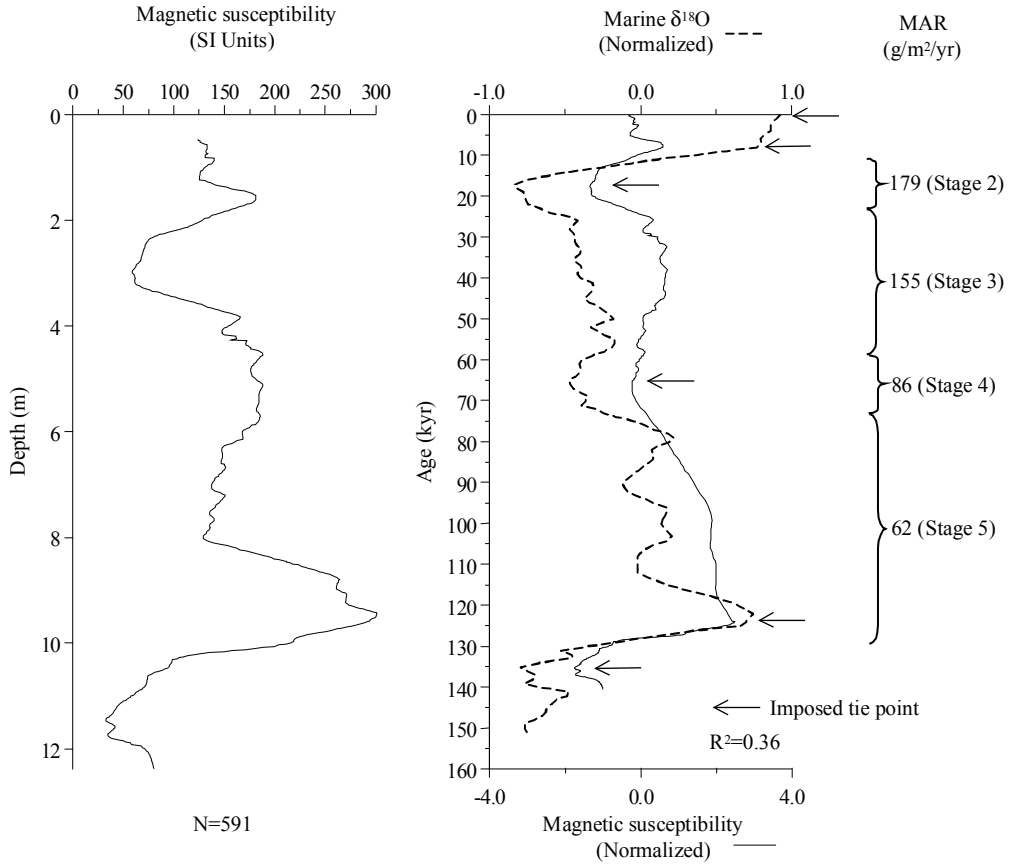

MS age model: Jiezicun (Jiezhichun)		
Tie-Points	Depth (m)	Age (kyr)
1	0.48	0.21
2	1.62	7.81
3	2.96	17.31
4	7.97	65.22
5	9.42	123.79
6	11.46	135.34

Age model (kyr): Jiezicun (Jiezhichun)						
Depth (m)	^{14}C	TL	Magnetic susceptibility	Pedostratigraphy (Model III)	Average chronology	Range
0						
2	8.6		10.5	13.2	10.8	8.6-13.2
4	23.3		27.3	28.1	26.2	23.3-28.1
6			46.4	62.2	54.3	46.4-62.2
8			66.5	72.4	69.4	66.5-72.4
10		89.5	127.1		108.3	89.5-127.1

MAR ($g/m^2/yr$): Jiezicun (Jiezhichun)								
Stage (range in kyr)	Assumed DBD (g/cm^3)	^{14}C	TL	MS	Pedostratigraphy			Average MAR
					Model I	Model II	Model III	
Stage 1 (12-0)	1.48	**203**						203
Stage 2 (24-12)	1.48	**203**		**179**	210	321	**247**	210
Stage 3 (59-24)	1.48			**155**	97	0	**65**	110
Stage 4 (74-59)	1.48			**86**	217	444	**293**	190
Stage 5 (130-74)	1.48		**158**	**62**	50	0	**33**	84

References used to generate data report: Jiezicun (Jiezhichun)	
Data used	**Source**
Pedostratigraphy	Lu and Zhao (1991)
Magnetic susceptibility	Lu and Zhao (1991)
^{14}C dating	Lu and Zhao (1991)
TL dating	Lu and Zhao (1991)
Additional References:	
Data available	**Source**
-	-

Jinjiyuan (Shangzhou) section: MAR (g/m^2/yr) based on pedostratigraphy

Note: Stage 1 affected by cultivation layer. Last glacial loess (L1) is not subdivided.

(Model I: min. glacial, max. interglacial; Model II: max. glacial, min. interglacial; Model III: 2/3 of interglacial soil is aeolian deposit)

Site location: 33.90° N, 109.92° E

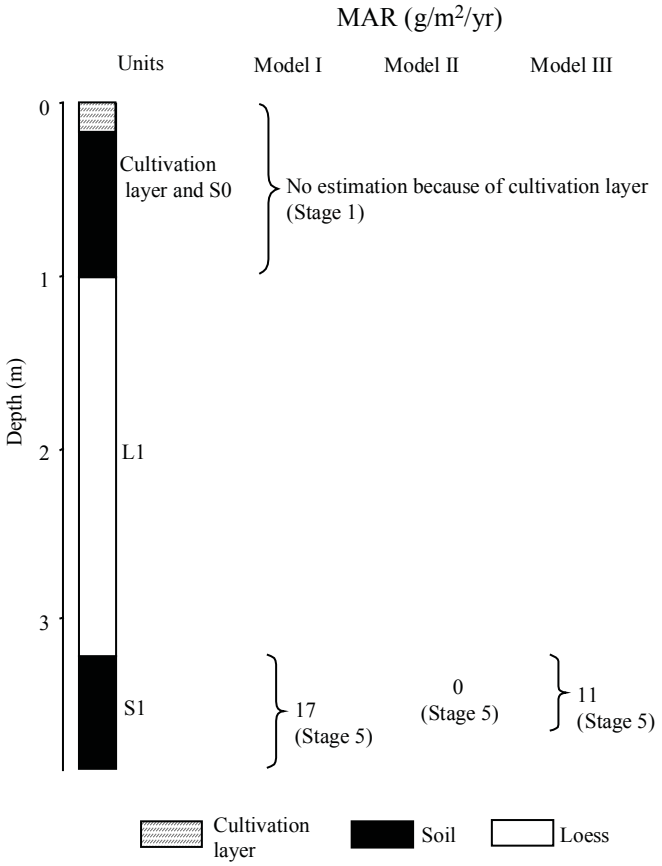

Stratigraphic data: Jinjiyuan (Shangzhou) (depth and thickness estimated from diagram, to nearest 1 cm)				
Top depth (m)	Bottom depth (m)	Thickness (m)	Stratigraphic units	DBD (g/cm^3)
0.00	1.00	1.00	cultivation layer and S0	n/a
1.00	3.20	2.20	L1	n/a
3.20	3.85	0.65	S1	n/a

Age model (kyr): Jinjiyuan (Shangzhou)						
Depth (m)	^{14}C	TL	Magnetic susceptibility	Pedostratigraphy (Model III)	Average chronology	Range
0.0						
0.5						
1.0						
1.5						
2.0						
2.5						
3.0						
3.5				112.5	112.5	

MAR ($g/m^2/yr$): Jinjiyuan (Shangzhou)								
Stage (range in kyr)	Assumed DBD (g/cm^3)	^{14}C	TL	MS	Pedostratigraphy			Average MAR
					Model I	Model II	Model III	
Stage 1 (12-0)	1.48							
Stage 2 (24-12)	1.48							
Stage 3 (59-24)	1.48							
Stage 4 (74-59)	1.48							
Stage 5 (130-74)	1.48				17	0	**11**	11

References used to generate data report: Jinjiyuan (Shangzhou)	
Data used	**Source**
Pedostratigraphy	Lei (1998)
Magnetic susceptibility	-
^{14}C dating	-
TL dating	-
Additional References:	
Data available	**Source**
Grain size, magnetic polarity	Lei (1998)

Jiuzhoutai (Lanzhou) section: MAR (g/m^2/yr) based on pedostratigraphy

Note: This section is generally called Jiuzhoutai, the name of a high mountain near the suburb of Lanzhou where the section is located (Chen et al., 1991b). Ding et al. (1990) used the name Lanzhou for this section. Stage 1 affected by cultivation layer

(Model I: min. glacial, max. interglacial; Model II: max. glacial, min. interglacial; Model III: 2/3 of interglacial soil is aeolian deposit)

Site location: 36.07° N, 103.75° E

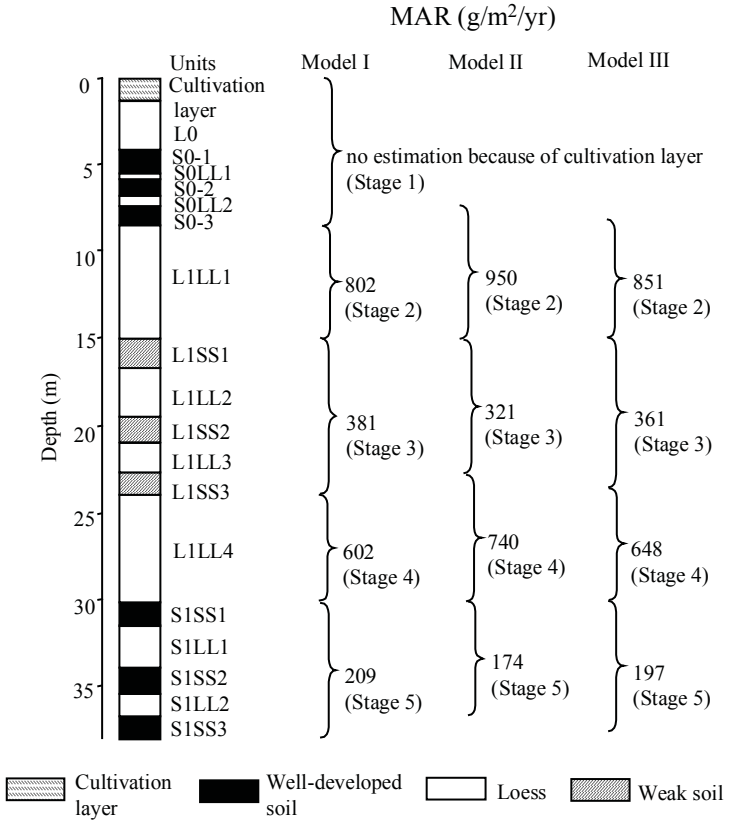

Stratigraphic data: Jiuzhoutai (Lanzhou)
(depth and thickness estimated from diagram, to nearest 10 cm)

Top depth (m)	Bottom depth (m)	Thickness (m)	Stratigraphic units	DBD (g/cm³)
0.0	1.4	1.4	cultivation layer	n/a
1.4	4.1	2.7	L0	n/a
4.1	5.4	1.3	S0-1	n/a
5.4	5.8	0.4	S0LL1	n/a
5.8	6.7	0.9	S0-2	n/a
6.7	7.3	0.6	S0LL2	n/a
7.3	8.5	1.2	S0-3	n/a
8.5	15.0	6.5	L1LL1	n/a
15.0	16.6	1.6	L1SS1	n/a
16.6	19.5	2.9	L1LL2	n/a
19.5	20.9	1.4	L1SS2	n/a
20.9	22.6	1.7	L1LL3	n/a
22.6	24.0	1.4	L1SS3	n/a
24.0	30.1	6.1	L1LL4	n/a
30.1	31.5	1.4	S1SS1	n/a
31.5	33.8	2.3	S1LL1	n/a
33.8	35.3	1.5	S1SS2	n/a
35.3	36.7	1.4	S1LL2	n/a
36.7	38.0	1.3	S1SS3	n/a

Jiuzhoutai (Lanzhou) section: MAR (g/m^2/yr) based on ^{14}C and TL dating

Note: This section is generally called Jiuzhoutai, the name of a high mountain near the suburb of Lanzhou where the section is located (Chen et al., 1991b). Ding et al. (1990) used the name Lanzhou for this section. Stage 1 affected by cultivation layer. Stage 1 MAR calculated excluding cultivation layer based on available dates.

Site location: 36.07° N, 103.75° E

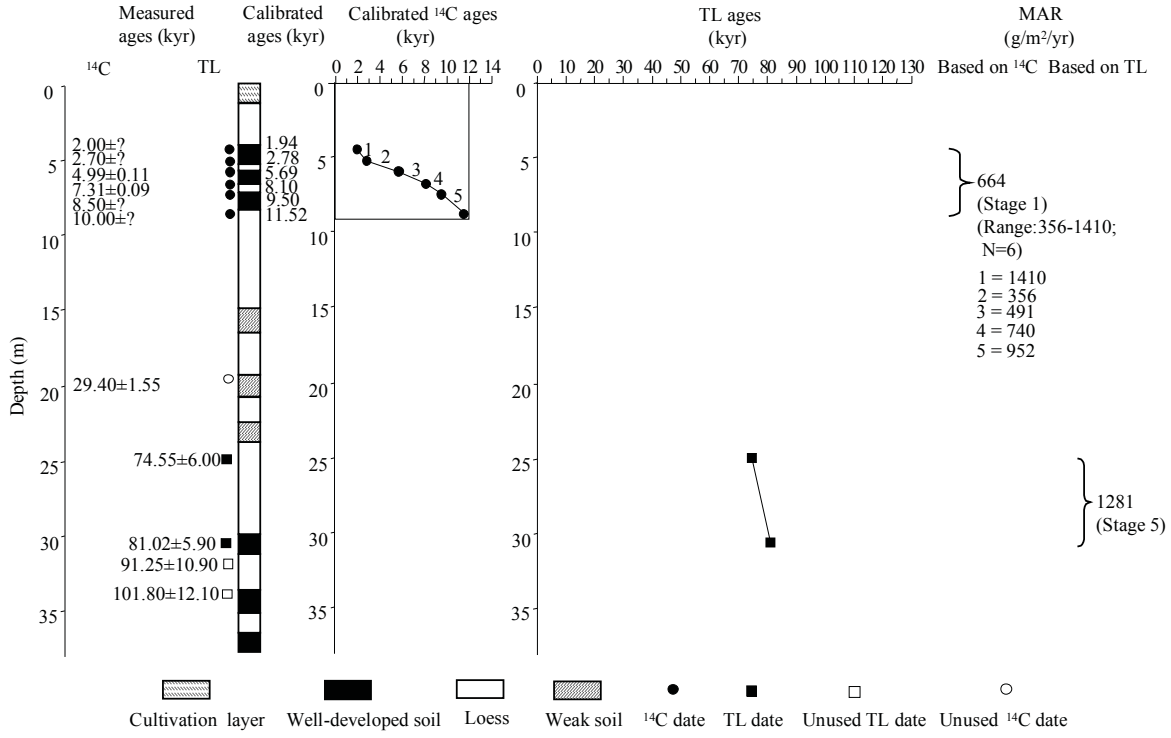

^{14}C dating: Jiuzhoutai (Lanzhou)
(depth estimated from diagram, to nearest 10 cm)

Depth (m)	Dating laboratory	Lab. No.	Dating material	Age (kyr)	s.d. (kyr)	(1σ) Calendar age ranges (kyr)	Relative probability	Assumed calendar age (kyr)	Reference	Comments
4.4	n/a	n/a	n/a	2	n/a	1.93-1.94	0.734	1.94	Fang et al. (1998)	
						1.96-1.96	0.266			
5.2	n/a	n/a	n/a	2.7	n/a	2.77-2.78	0.544	2.78	Fang et al. (1998)	
						2.83-2.83	0.456			
5.9	n/a	n/a	n/a	4.99	0.11	5.61-5.76	0.659	5.69	Fang et al. (1998)	
						5.81-5.88	0.341			
6.7	n/a	n/a	n/a	7.31	0.09	8.01-8.18	0.963	8.1	Fang et al. (1998)	
						7.99-7.99	0.037			
7.4	n/a	n/a	n/a	8.5	n/a	9.50-9.51	1	9.5	Fang et al. (1998)	
8.7	n/a	n/a	n/a	10	n/a	11.50-11.55	0.403	11.52	Fang et al. (1998)	
						11.39-11.42	0.269			
						11.30-11.32	0.179			
						11.34-11.35	0.077			
						11.47-11.48	0.073			
18.7	n/a	n/a	n/a	29.4	1.55				Fang et al. (1998)	beyond calibration range

TL dating: Jiuzhoutai (Lanzhou)
(depth estimated from diagram, to nearest 10 cm)

Depth (m)	Dating laboratory	Lab. No.	Dating material	TL-method	Age (kyr)	s.d. (kyr)	Reference	Comments
25.0	n/a	n/a	n/a	n/a	74.6	6.0	Fang et al. (1998)	
30.6	n/a	n/a	n/a	n/a	81.0	5.9	Fang et al. (1998)	
32.0	n/a	n/a	n/a	n/a	91.3	10.9	Fang et al. (1998)	uncertainties larger than 10 %
34.0	n/a	n/a	n/a	n/a	102.0	12.1	Fang et al. (1998)	uncertainties larger than 10 %

Jiuzhoutai (Lanzhou) section: MAR (g/m^2/yr) based on magnetic susceptibility

Note: This section is generally called Jiuzhoutai, the name of a high mountain near the suburb of Lanzhou where the section is located (Chen et al., 1991b). Ding et al. (1990) used the name Lanzhou for this section. Digitized MS data. Stage 1 affected by cultivation layer.

Site location: 36.07° N, 103.75° E

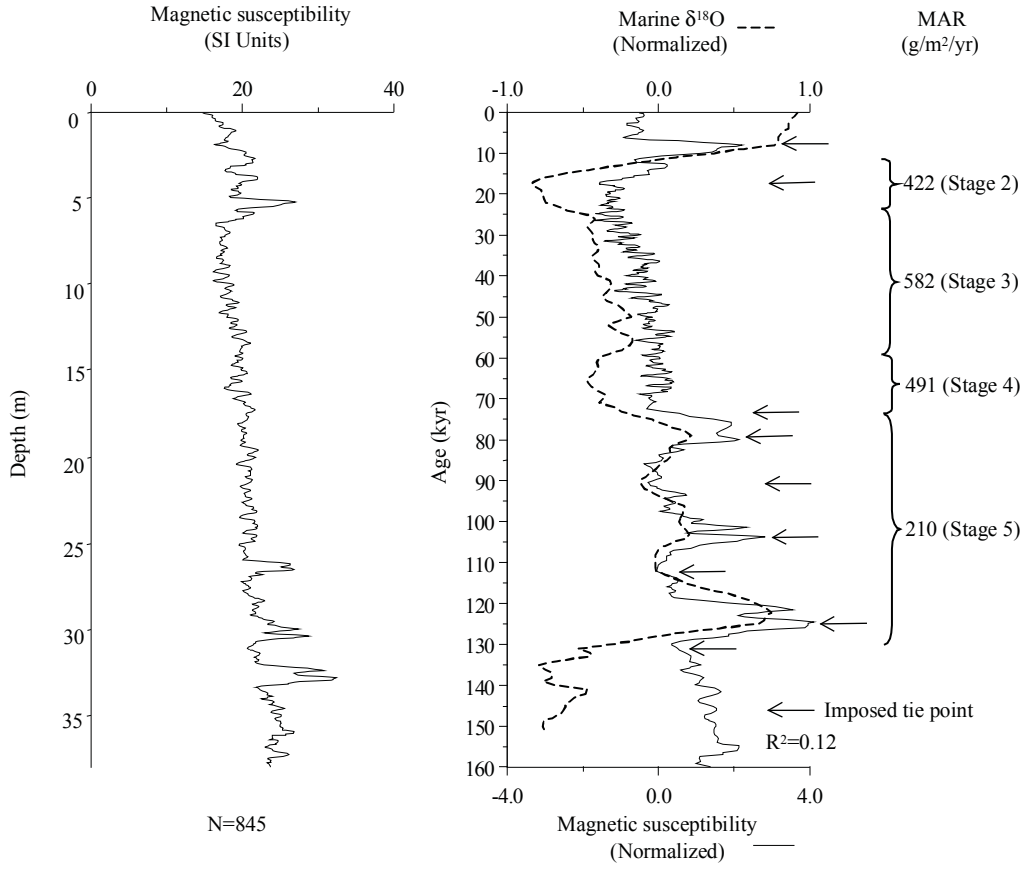

MS age model: Jiuzhoutai (Lanzhou)		
Tie-Point	Depth (m)	Age (kyr)
1	7.64	7.81
2	9.06	17.31
3	30.21	71.12
4	30.80	79.25
5	32.31	90.95
6	35.15	103.80
7	35.94	112.28
8	37.80	125.00
9	38.48	131.09

Age model (kyr): Jiuzhoutai (Lanzhou)						
Depth (m)	^{14}C	TL	Magnetic susceptibility	Pedostratigraphy (Model III)	Average chronology	Range
0						
6	6				6.0	
12			24.8	18.8	21.8	18.8-24.8
18			40	36.2	38.1	36.2-40.0
24			55.3	60.0	57.6	55.3-60.0
30		80	70.6	73.8	74.8	70.6-80.0
36			112.7	118.0	115.3	112.7-118.0

MAR ($g/m^2/yr$): Jiuzhoutai (Lanzhou)								
Stage (range in kyr)	Assumed DBD (g/cm^3)	^{14}C	TL	MS	Pedostratigraphy			Average MAR
					Model I	Model II	Model III	
Stage 1 (12-0)	1.48	**664**						664.0
Stage 2 (24-12)	1.48			**422**	802	950	**851**	636.5
Stage 3 (59-24)	1.48			**582**	381	321	**361**	471.5
Stage 4 (74-59)	1.48			**491**	602	740	**648**	569.5
Stage 5 (130-74)	1.48		**1281**	**210**	209	174	**197**	562.7

References used to generate data report: Jiuzhoutai (Lanzhou)	
Data used	**Source**
Pedostratigraphy	Fang et al. (1998)
Magnetic susceptibility	Fang et al. (1998)
^{14}C dating	Fang et al. (1998)
TL dating	Fang et al. (1998)
Additional References:	
Data available	**Source**
Pedostratigraphy, magnetic polarity	Wang et al. (1966)
Pedostratigraphy, magnetic polarity	Wang et al. (1978)
Pedostratigraphy, magnetic polarity	Wang (1982)
Pedostratigraphy, magnetic polarity	Burbank and Li (1985)
Pedostratigraphy, magnetic polarity, micromorphology	Derbyshire et al. (1987)
Pedostratigraphy, magnetic susceptibility, magnetic polarity	Cao (1988)
Pedostratigraphy, magnetic polarity	Ding et al. (1990)
Pedostratigraphy, magnetic polarity	Ding et al. (1991)
Pedostratigraphy, magnetic polarity	Liu et al. (1991)
Pedostratigraphy, magnetic susceptibility, ^{14}C	Chen et al. (1991b)
Pedostratigraphy, magnetic polarity	Rutter et al. (1991)
Pedostratigraphy, magnetic polarity	Rutter (1992)
Pedostratigraphy, magnetic susceptibility, ^{14}C , TL, magnetic polarity	Chen and Zhang (1994)
Pedostratigraphy, magnetic susceptibility, grain size, clay mineralogy	Derbyshire et al. (1995a)
Pedostratigraphy, magnetic susceptibility, molluscs	Derbyshire et al. (1995b)
Pedostratigraphy, ^{14}C	An et al. (2000)

Jiyuan section: MAR (g/m^2/yr) based on magnetic susceptibility

Note: Stage 1 affected by cultivation layer.

Site location: 37.15° N, 107.38° E

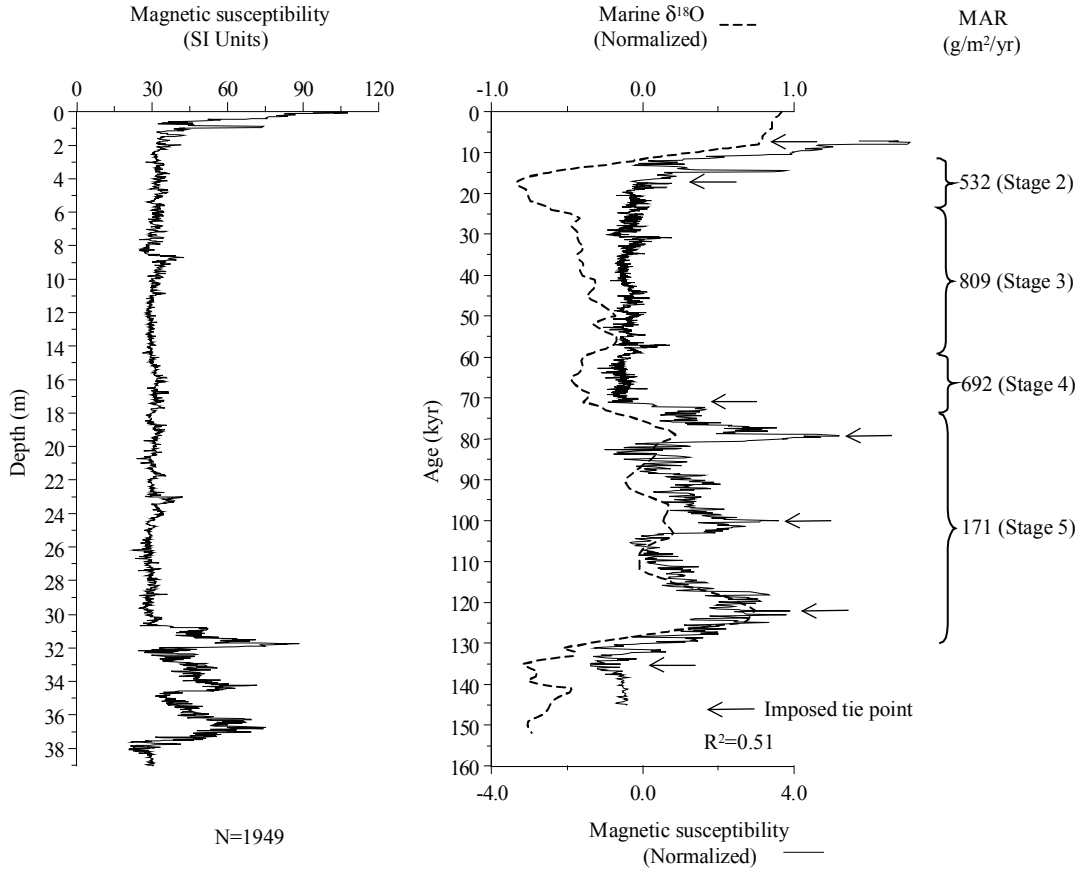

MS age model: Jiyuan		
Tie-Point	Depth (m)	Age (kyr)
1	0.08	7.81
2	1.26	17.31
3	30.68	71.12
4	31.78	79.25
5	34.26	99.96
6	36.74	122.19
7	38.06	135.34

Age model (kyr): Jiyuan						
Depth (m)	^{14}C	TL	Magnetic susceptibility	Pedostratigraphy (Model III)	Average chronology	Range
0						
6			26.0		26.0	
12			36.9		36.9	
18			47.9		47.9	
24			58.9		58.9	
30			69.9		69.9	
36			115.6		115.6	

MAR ($g/m^2/yr$): Jiyuan								
Stage (range in kyr)	Assumed DBD (g/cm^3)	^{14}C	TL	MS	Pedostratigraphy			Average MAR
					Model I	Model II	Model III	
Stage 1 (12-0)	1.48							
Stage 2 (24-12)	1.48			**532**				532
Stage 3 (59-24)	1.48			**809**				809
Stage 4 (74-59)	1.48			**692**				692
Stage 5 (130-74)	1.48			**171**				171

References used to generate data report:	
Data used	**Source**
Pedostratigraphy	-
Magnetic susceptibility	Ding et al. (1998)
^{14}C dating	-
TL dating	-
Additional References:	
Data available	**Source**
Magnetic susceptibility	Sun and Ding (1997)
Grain size	Ding et al. (1998)

Kansu section: MAR (g/m^2/yr) based on pedostratigraphy

Note: Missing Stage 1 deposit.

(Model I: min. glacial, max. interglacial; Model II: max. glacial, min. interglacial; Model III: 2/3 of interglacial soil is aeolian deposit)

Site location: 39.75° N, 75.05° E

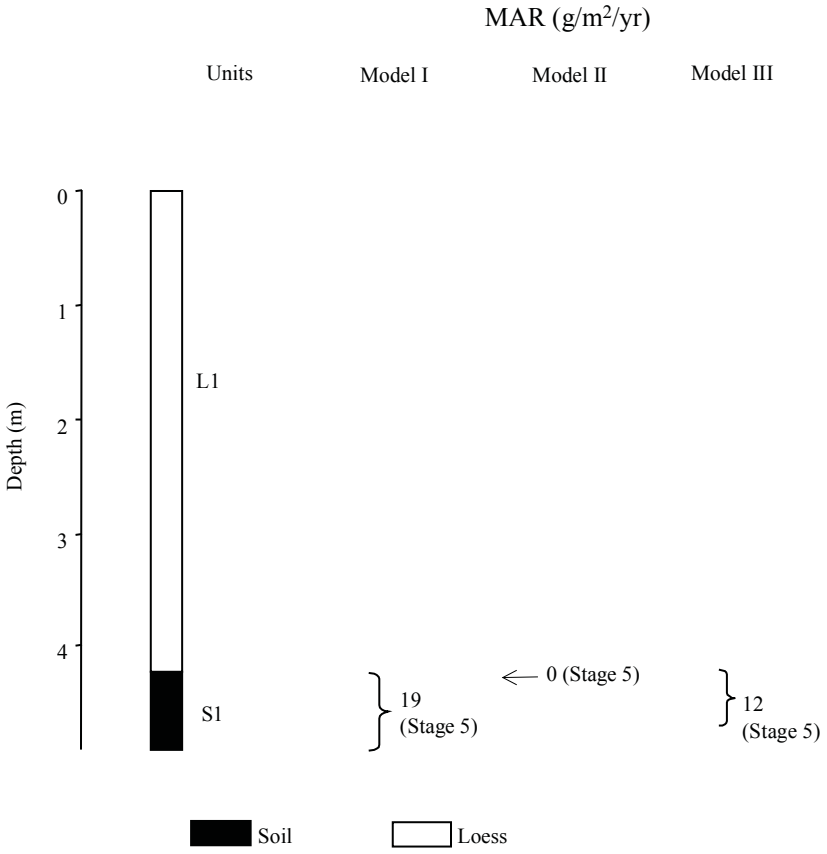

Stratigraphic data: Kansu (depth and thickness estimated from diagram, to nearest 10 cm)				
Top depth (m)	Bottom depth (m)	Thickness (m)	Stratigraphic units	DBD (g/cm^3)
0.0	4.2	4.2	L1	n/a
4.2	4.9	0.7	S1	n/a

Kansu section: MAR (g/m^2/yr) based on TL dating

Note: Missing Stage 1 deposit.

(Model I: min. glacial, max. interglacial; Model II: max. glacial, min. interglacial; Model III: 2/3 of interglacial soil is aeolian deposit)

Site location: 39.75° N, 75.05° E

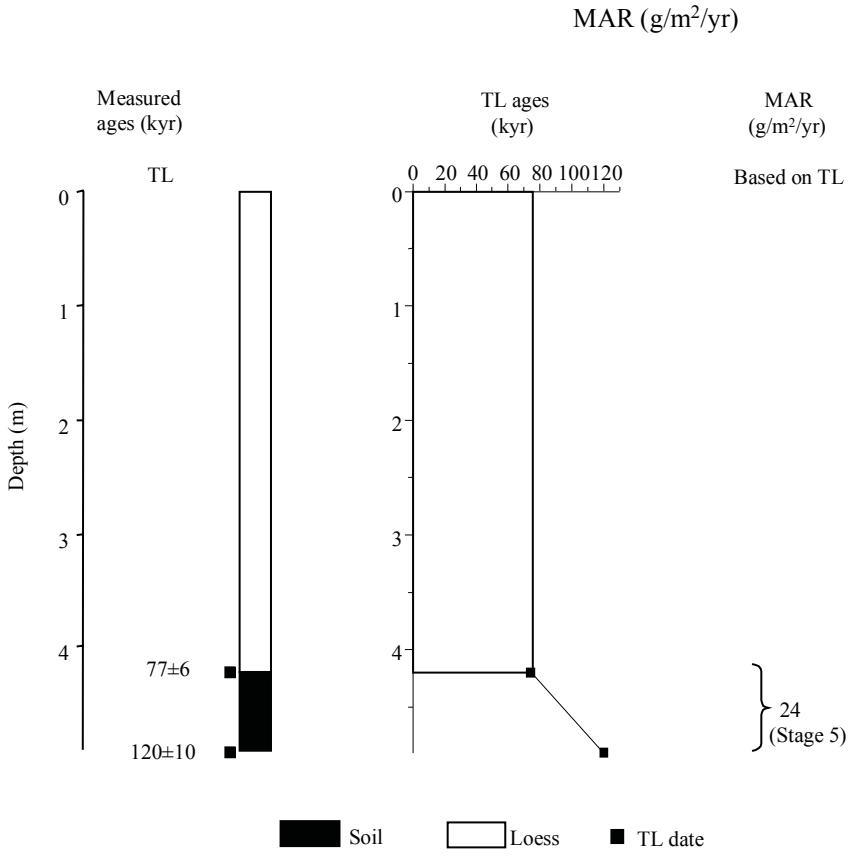

TL dating: Kansu (depth estimated from diagram, to nearest 10 cm)								
Depth (m)	Dating laboratory	Lab. No.	Dating material	TL-method	Age (kyr)	s.d. (kyr)	Reference	Comments
4.2	n/a	n/a	n/a	n/a	77	6	Wen and Zheng (1987)	
4.9	n/a	n/a	n/a	n/a	120	10	Wen and Zheng (1987)	

Age model (kyr): Kansu						
Depth (m)	^{14}C	TL	Magnetic susceptibility	Pedostratigraphy (Model III)	Average chronology	Range
0.0						
0.6						
1.2						
1.8						
2.4						
3.0						
3.6						
4.2		77.0		74.0	75.5	74.0-77.0
4.8		113.9		145.5	129.7	113.9-145.5

MAR ($g/m^2/yr$): Kansu								
Stage (range in kyr)	Assumed DBD (g/cm^3)	^{14}C	TL	MS	Pedostratigraphy			Average MAR
					Model I	Model II	Model II)	
Stage 1 (12-0)	1.48							
Stage 2 (24-12)	1.48							
Stage 3 (59-24)	1.48							
Stage 4 (74-59)	1.48							
Stage 5 (130-74)	1.48		**24**		19	0	**12**	18

References used to generate data report: Kansu	
Data used	**Source**
Pedostratigraphy	Wen and Zheng (1987)
Magnetic susceptibility	-
^{14}C dating	-
TL dating	Wen and Zheng (1987)
Additional References:	
Data available	**Source**
-	-

Landa section: Pedostratigraphy

Note: Thickness of top loess bed uncertain. No estimation for pedostratigraphy based MAR.

Site location: 36.05° N, 103.84° E

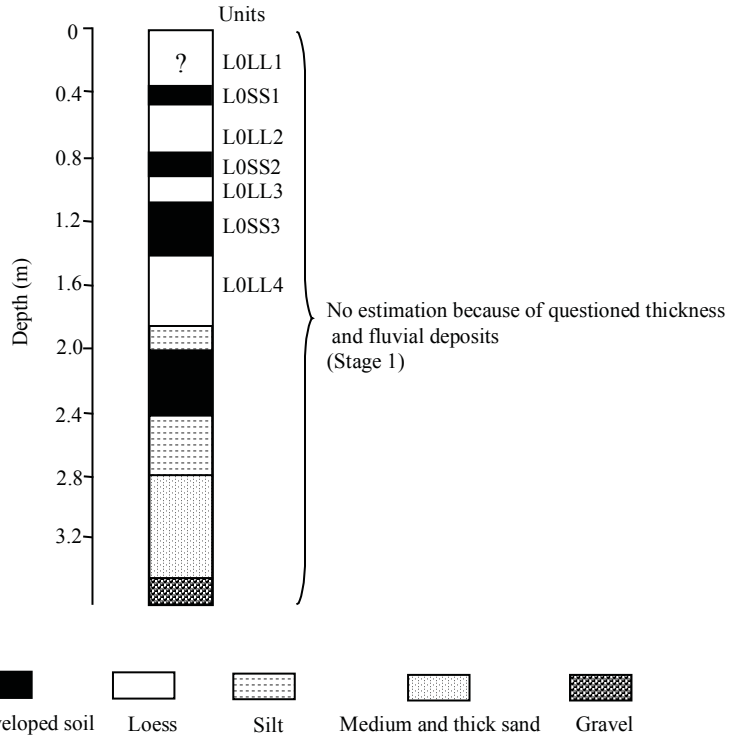

Stratigraphic data: Landa (depth and thickness estimated from diagram, to nearest 1cm)				
Top depth (m)	Bottom depth (m)	Thickness (m)	Stratigraphic units	DBD (g/cm³)
0.00	0.33	0.33	L0LL1	n/a
0.33	0.45	0.12	L0SS1	n/a
0.45	0.76	0.31	L0LL1	n/a
0.76	0.91	0.15	L0SS2	n/a
0.91	1.07	0.16	L0LL3	n/a
1.07	1.40	0.33	L0SS3	n/a
1.40	1.85	0.45	L0LL4	n/a
1.85	2.02	0.17	alluvial loess	n/a
2.02	2.43	0.41	palaeosol	n/a
2.43	2.82	0.39	silt	n/a
2.82	3.45	0.63	medium/thick sand	n/a
3.45	3.63	0.18	gravel	n/a

Landa section: MAR (g/m^2/yr) based on ^{14}C dating

Note: Thickness of top loess bed uncertain.

Site location: 36.05° N, 103.84° E

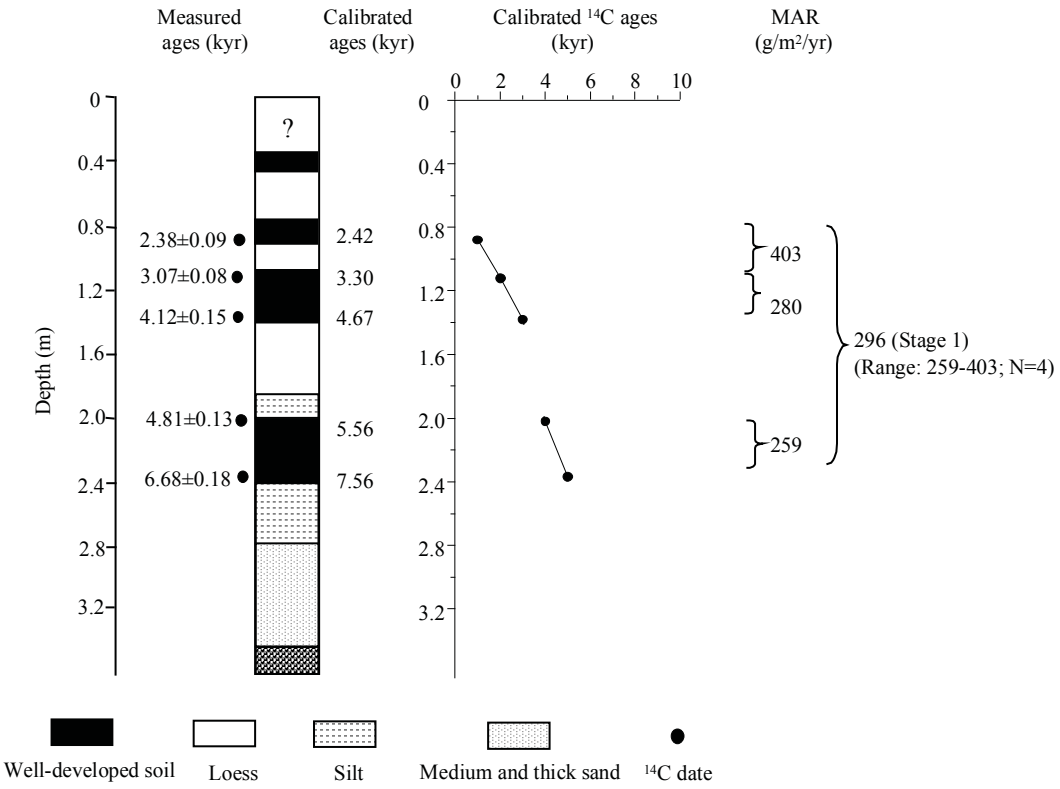

^{14}C dating: Landa (depth given by the authors)										
Depth (m)	Dating laboratory	Lab. No.	Dating material	Age (kyr)	s.d. (kyr)	(1σ) Calendar age ranges (kyr)	Relative probability	Assumed calendar age (kyr)	Reference	Comments
0.88	n/a	n/a	n/a	2.38	0.09	2.50-2.33	0.681	2.42	Chen et al. (1991b)	
						2.71-2.63	0.237			
						2.61-2.59	0.082			
1.12	n/a	n/a	n/a	3.07	0.08	3.38-3.21	0.887	3.30	Chen et al. (1991b)	
						3.19-3.16	0.113			
1.38	n/a	n/a	n/a	4.12	0.15	4.83-4.51	0.904	4.67	Chen et al. (1991b)	
						4.48-4.44	0.096			
2.02	n/a	n/a	n/a	4.81	0.13	5.66-5.45	0.764	5.56	Chen et al. (1991b)	
						5.41-5.33	0.236			
2.37	n/a	n/a	n/a	6.68	0.18	7.69-7.42	0.961	7.56	Chen et al. (1991b)	
						7.38-7.38	0.02			
						7.34-7.34	0.02			

Landa section: Magnetic susceptibility

Note: Thickness of top loess bed uncertain. Digitized MS data.

Site location: 36.05° N, 103.84° E

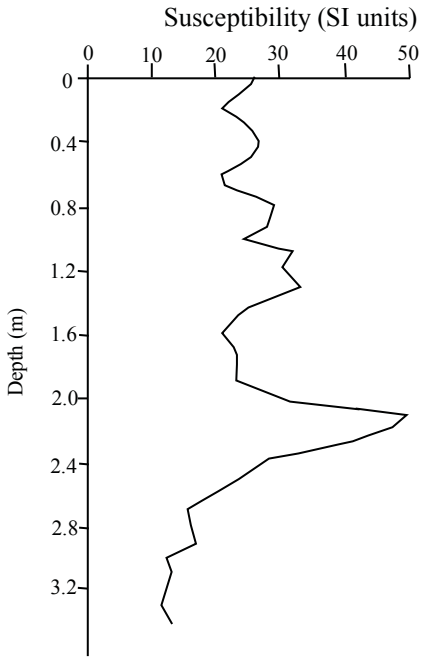

Age model (kyr): Landa						
Depth (m)	^{14}C	TL	Magnetic susceptibility	Pedostratigraphy (Model III)	Average chronology	Range
0.0						
0.4						
0.8						
1.2	3.5				3.5	
1.6	5.0				5.0	
2.0	5.6				5.6	
2.4						

MAR (g/m^2/yr): Landa								
Stage (range in kyr)	Assumed DBD (g/cm^3)	^{14}C	TL	MS	Pedostratigraphy			Average MAR
					Model I	Model II	Model III	
Stage 1 (12-0)	1.48	**296**						296
Stage 2 (24-12)	1.48							
Stage 3 (59-24)	1.48							
Stage 4 (74-59)	1.48							
Stage 5 (130-74)	1.48							

References used to generate data report: Landa	
Data used	**Source**
Pedostratigraphy	Chen et al. (1991b)
Magnetic susceptibility	Chen et al. (1991b)
^{14}C dating	Chen et al. (1991b)
TL dating	-
Additional References:	
Data available	**Source**
-	-

Lijiagang section: Magnetic susceptibility

Note: Located in southern China, about 0.5 km SE of Xinshengyu Harbor. Digitized MS data. Section not used to estimate MAR because top missing.

Site location: 32.17º N, 118.84º E

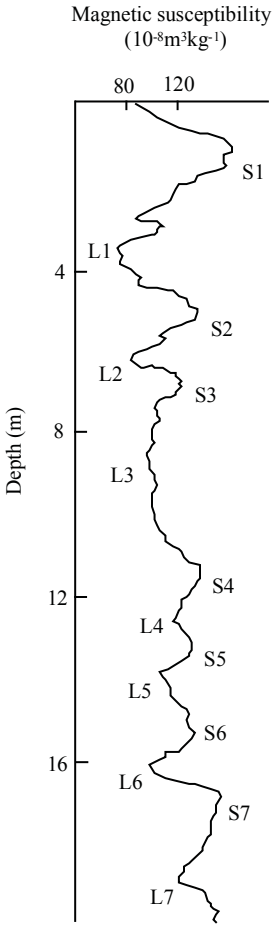

References used to generate data report: Lijiagang	
Data used	**Source**
Pedostratigraphy	-
Magnetic susceptibility	Zhang et al. (1994)
^{14}C dating	-
TL dating	-
Additional References:	
Data available	**Source**
-	-

Lijiayuan section: MAR (g/m^2/yr) based on magnetic susceptibility

Site location: 36.12° N, 104.85° E

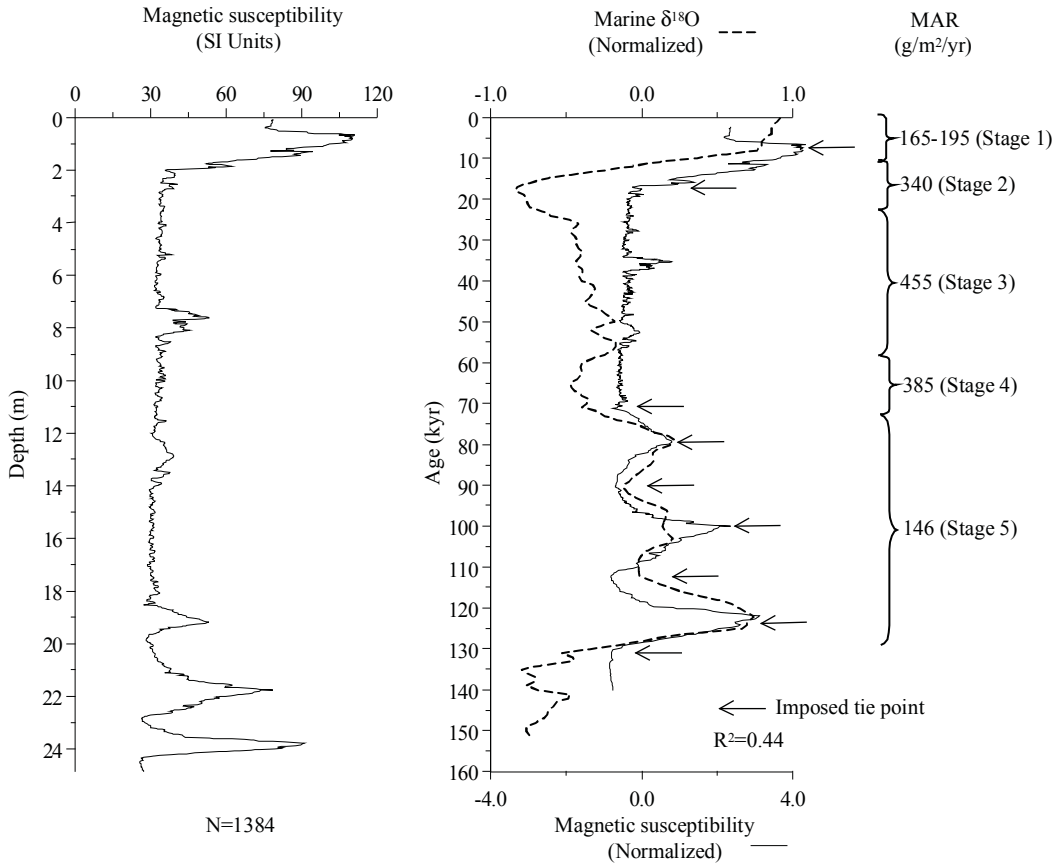

MS age model: Lijiayuan		
Tie-Point	Depth (m)	Age (kyr)
1	0.79	7.81
2	2.04	17.31
3	18.50	70.82
4	19.21	79.25
5	19.84	90.10
6	21.77	99.96
7	22.84	112.28
8	23.96	123.79
9	24.36	131.09

Age model (kyr): Lijiayuan						
Depth (m)	^{14}C	TL	Magnetic susceptibility	Pedostratigraphy (Model III)	Average chronology	Range
0			0		0.0	
4			23.7		23.7	
8			36.7		36.7	
12			49.7		49.7	
16			62.7		62.7	
20			90.9		90.9	
24			124.5		124.5	

MAR (g/m²/yr): Lijiayuan								
Stage (range in kyr)	Assumed DBD (g/cm^3)	^{14}C	TL	MS	Pedostratigraphy			Average MAR
					Model I	Model II	Model III	
Stage 1 (12-0)	1.48			**180**				180
Stage 2 (24-12)	1.48			**340**				340
Stage 3 (59-24)	1.48			**455**				455
Stage 4 (74-59)	1.48			**385**				385
Stage 5 (130-74)	1.48			**146**				146

References used to generate data report: Lijiayuan	
Data used	**Source**
Pedostratigraphy	-
Magnetic susceptibility	Ren (1996)
^{14}C dating	-
TL dating	-
Additional References:	
Data available	**Source**
Grain size	Ren (1996)
Magnetic susceptibility, grain size	Ding et al. (1996)
Magnetic susceptibility, grain size	Ding et al. (1998)
Magnetic susceptibility, grain size	Ding et al. (1999a)

Lintaigou section: Magnetic susceptibility

Note: Missing top of section. MS MAR not calculated because of hiatuses.

Site location: 42.03° N, 119.00° E

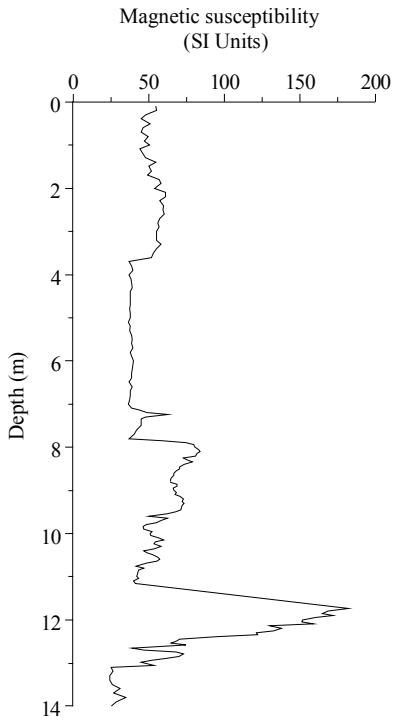

References used to generate data report: Lintaigou	
Data used	**Source**
Pedostratigraphy	-
Magnetic susceptibility	Sun (unpublished data)
^{14}C dating	-
TL dating	-
Additional References:	
Data available	**Source**
-	-

Liujiapo_1 section: MAR (g/m^2/yr) based on pedostratigraphy

Note: Liujiapo_1 and Liujiapo_2 (Xian) are used to differentiate two versions of the same section with different pedostratigraphies. The section is located in the suburb of Xian City (capital city of Shaaxi Province), so Ding et al. (1990) used the name Xian for the site. Stage 1 and part of Stage 2 missing

(Model I: min. glacial, max. interglacial; Model II: max. glacial, min. interglacial; Model III: 2/3 of interglacial soil is aeolian deposit)

Site location: 34.20° N, 109.20° E

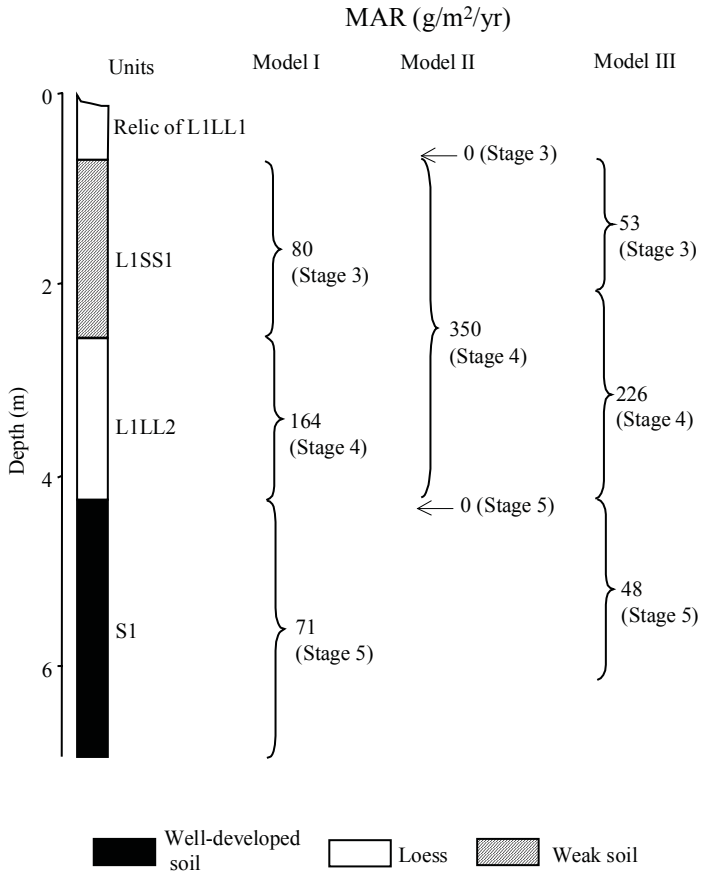

Note: The depths provided in the text are inconsistent with the depths shown in the figure. We used estimates derived from the diagram.

Stratigraphic data: Liujiapo_1
(depth and thickness estimated from diagram, to nearest 1 cm)

Top depth (m)	Bottom depth (m)	Thickness (m)	Stratigraphic units	DBD (g/cm³)
0.00	0.65	0.65	relic of L1LL1	n/a
0.65	2.54	1.89	L1SS1	n/a
2.54	4.20	1.66	L1LL2	n/a
4.20	6.90	2.70	S1	n/a

Stratigraphic data: Liujiapo_1
(depth and thickness information given in the text)

Top depth (m)	Bottom depth (m)	Thickness (m)	Stratigraphic units	DBD
0	0.8	0.8	relic of L1LL1	n/a
0.8	2.5	1.7	L1SS1	n/a
2.5	4.1	1.6	L1LL2	n/a
4.1	7	2.9	S1	n/a

Liujiapo_1 section: MAR (g/m^2/yr) based on TL dating

Note: Liujiapo_1 and Liujiapo_2 (Xian) are used to differentiate two versions of the same section with different pedostratigraphies. The section is located in the suburb of Xian City (capital city of Shaaxi Province), so Ding et al. (1990) used the name Xian for the site. Stage 1 and part of Stage 2 missing.

Site location: 34.20° N, 109.20°E

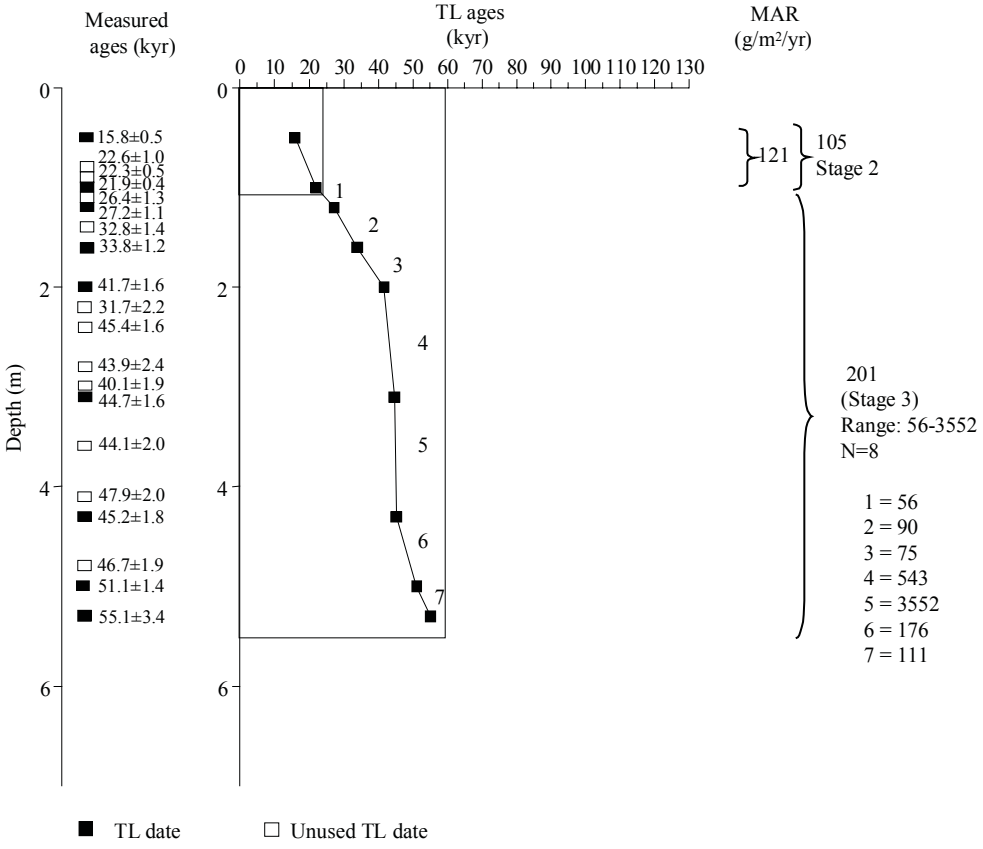

TL dating: Liujiapo_1
(depth given by authors)

Depth (m)	Dating laboratory	Lab. No.	Dating material	TL-method	Age (kyr)	s.d. (kyr)	Reference	Comments
0.5	Univ. of Wales	0.5	non-carb, non-org	fine-grain (4-11 mm) technique	15.8	0.5	Musson et al. (1994)	
0.8	Univ. of Wales	0.8	non-carb, non-org	fine-grain (4-11 mm) technique	22.6	1	Musson et al. (1994)	overlapping, not used
0.9	Univ. of Wales	0.9	non-carb, non-org	fine-grain (4-11 mm) technique	22.3	0.5	Musson et al. (1994)	overlapping, not used
1.0	Univ. of Wales	1.0	non-carb, non-org	fine-grain (4-11 mm) technique	21.9	0.4	Musson et al. (1994)	
1.1	Univ. of Wales	1.1	non-carb, non-org	fine-grain (4-11 mm) technique	26.4	1.3	Musson et al. (1994)	overlapping, not used
1.2	Univ. of Wales	1.2	non-carb, non-org	fine-grain (4-11 mm) technique	27.2	1.1	Musson et al. (1994)	
1.4	Univ. of Wales	1.4	non-carb, non-org	fine-grain (4-11 mm) technique	32.8	1.4	Musson et al. (1994)	overlapping, not used
1.6	Univ. of Wales	1.6	non-carb, non-org	fine-grain (4-11 mm) technique	33.8	1.2	Musson et al. (1994)	
2.0	Univ. of Wales	2.0	non-carb, non-org	fine-grain (4-11 mm) technique	41.7	1.6	Musson et al. (1994)	
2.2	Univ. of Wales	2.2	non-carb, non-org	fine-grain (4-11 mm) technique	31.7	2.2	Musson et al. (1994)	reversal?
2.4	Univ. of Wales	2.4	non-carb, non-org	fine-grain (4-11 mm) technique	45.4	1.6	Musson et al. (1994)	reversal?
2.8	Univ. of Wales	2.8	non-carb, non-org	fine-grain (4-11 mm) technique	43.9	2.4	Musson et al. (1994)	overlapping, not used
3.0	Univ. of Wales	3.0	non-carb, non-org	fine-grain (4-11 mm) technique	40.1	1.9	Musson et al. (1994)	reversal?
3.1	Univ. of Wales	3.1	non-carb, non-org	fine-grain (4-11 mm) technique	44.7	1.6	Musson et al. (1994)	
3.6	Univ. of Wales	3.6	non-carb, non-org	fine-grain (4-11 mm) technique	44.1	2	Musson et al. (1994)	overlapping, not used
4.1	Univ. of Wales	4.1	non-carb, non-org	fine-grain (4-11 mm) technique	47.9	2	Musson et al. (1994)	overlapping, not used
4.3	Univ. of Wales	4.3	non-carb, non-org	fine-grain (4-11 mm) technique	45.2	1.8	Musson et al. (1994)	
4.8	Univ. of Wales	4.8	non-carb, non-org	fine-grain (4-11 mm) technique	46.7	1.9	Musson et al. (1994)	overlapping, not used
5.0	Univ. of Wales	5.0	non-carb, non-org	fine-grain (4-11 mm) technique	51.1	1.4	Musson et al. (1994)	
5.3	Univ. of Wales	5.3	non-carb, non-org	fine-grain (4-11 mm) technique	55.1	3.4	Musson et al. (1994)	

Age model (kyr): Liujiapo_1

Depth (m)	^{14}C	TL	Magnetic susceptibility	Pedostratigraphy (Model III)	Average chronology	Range
0						
1		22.3		33.6	27.9	22.3-33.6
2		41.7		59.5	50.6	41.7-59.5
3		44.6		66.0	55.3	44.6-66.0
4		45.0		72.6	58.8	45.0-72.6
5		51.5		98.6	75.0	51.5-98.6
6		-		130.0	130.0	

MAR (g/m²/yr): Liujiapo_1								
Stage (range in kyr)	Assumed DBD (g/cm^3)	^{14}C	TL	MS	Pedostratigraphy			Average MAR
					Model I	Model II	Model III	
Stage 1 (12-0)	1.48							
Stage 2 (24-12)	1.48		**105**					105
Stage 3 (59-24)	1.48		**201**		80	0	**53**	127
Stage 4 (74-59)	1.48				164	350	**226**	226
Stage 5 (130-74)	1.48				71	0	**48**	48

References used to generate data report: Liujiapo_1	
Data used	**Source**
Pedostratigraphy	Derbyshire et al. (1995a)
Magnetic susceptibility	-
^{14}C dating	-
TL dating	Musson et al. (1994)
Additional References:	
Data available	**Source**
Magnetic susceptibility, grain size, micromorphology	Derbyshire et al. (1995a)
Pedostratigraphy, magnetic susceptibility, micromorphology	Derbyshire et al. (1995b)
Pedostratigraphy, magnetic susceptibility, micromorphology	Kemp et al. (1997)

Liujiapo_2 (Xian) section: MAR (g/m^2/yr) based on pedostratigraphy

Note: Liujiapo_1 and Liujiapo_2 (Xian) are used to differentiate two versions of the same section with different pedostratigraphies. The section is located in the suburb of Xian City (capital city of Shaaxi Province), so Ding et al. (1990) used the name Xian for the site. Stage 1 affected by cultivation layer.

(Model I: min. glacial, max. interglacial; Model II: max. glacial, min. interglacial; Model III: 2/3 of interglacial soil is aeolian deposit)

Site location: 34.23° N, 109.12° E

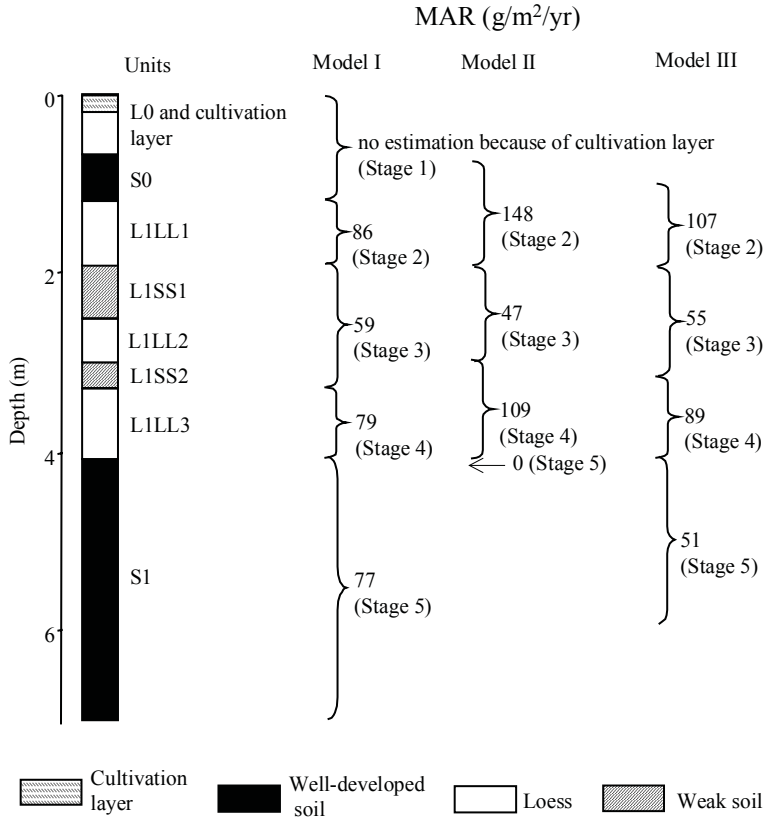

Stratigraphic data: Liujiapo_2 (Xian) (thickness given by author, depth calculated from thickness)				
Top depth (m)	Bottom depth (m)	Thickness (m)	Stratigraphic units	DBD (g/cm^3)
0.0	0.7	0.7	L0 and cultivation layer	n/a
0.7	1.2	0.5	S0	n/a
1.2	1.9	0.7	L1LL1	n/a
1.9	2.5	0.6	L1SS1	n/a
2.5	3.0	0.5	L1LL2	n/a
3.0	3.3	0.3	L1SS2	n/a
3.3	4.1	0.8	L1LL3	n/a
4.1	7.0	2.9	S1	n/a

Age model (kyr): Liujiapo_2 (Xian)						
Depth (m)	^{14}C	TL	Magnetic susceptibility	Pedostratigraphy (Model III)	Average chronology	Range
0						
1						
2				26.7	26.7	
3				53.4	53.4	
4				72.2	72.2	
5				100.0	100.0	
6				129.2	129.2	

MAR (g/m²/yr): Liujiapo_2 (Xian)								
Stage (range in kyr)	Assumed DBD (g/cm^3)	^{14}C	TL	MS	Pedostratigraphy			Average MAR
					Model I	Model II	Model III	
Stage 1 (12-0)	1.48							
Stage 2 (24-12)	1.48				86	148	**107**	107
Stage 3 (59-24)	1.48				59	47	**55**	55
Stage 4 (74-59)	1.48				79	109	**89**	89
Stage 5 (130-74)	1.48				77	0	**51**	51

References used to generate data report: Liujiapo_2 (Xian)	
Data used	**Source**
Pedostratigraphy	Zhao (1994)
Magnetic susceptibility	-
^{14}C dating	-
TL dating	-
Additional References:	
Data available	**Source**
Pedostratigraphy	Kukla (1987a)
Pedostratigraphy, magnetic polarity	Ding et al. (1990)
Pedostratigraphy, magnetic polarity	Ding et al. (1991)
Pedostratigraphy, magnetic polarity	Liu et al. (1991)
Pedostratigraphy, magnetic polarity	Rutter et al. (1991)

Lujiaowan section: MAR (g/m^2/yr) based on pedostratigraphy

(Model I: min. glacial, max. interglacial; Model II: max. glacial, min. interglacial; Model III: 2/3 of interglacial soil is aeolian deposit)

Site location: 44.33° N, 85.63° E

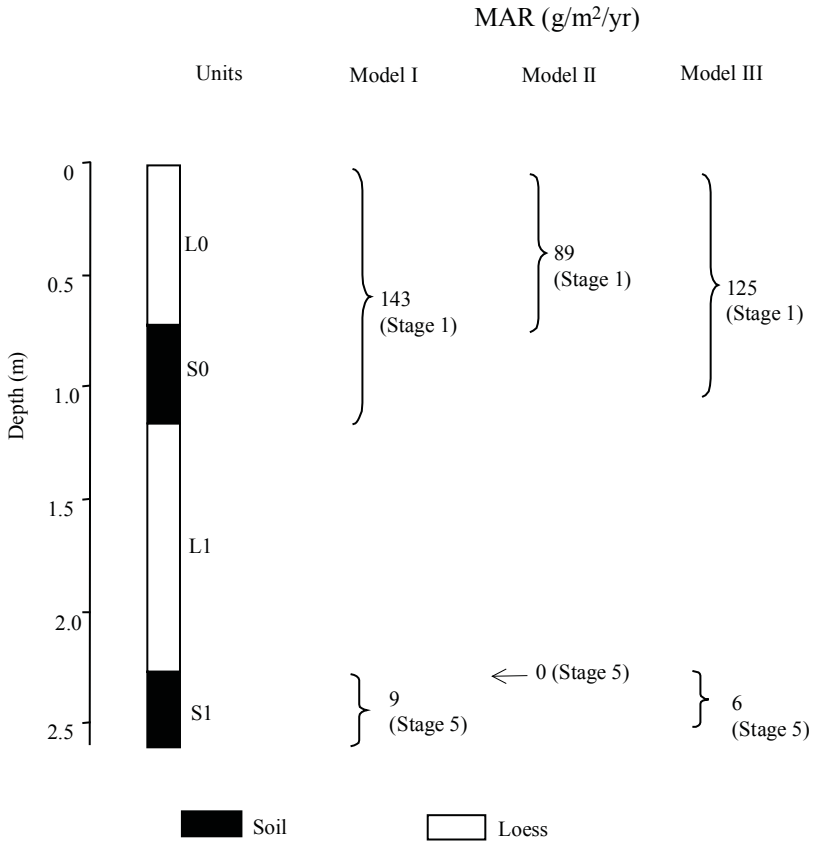

Stratigraphic data: Lujiaowan (depth and thickness estimated from diagram, to nearest 10 cm)				
Top depth (m)	Bottom depth (m)	Thickness (m)	Stratigraphic units	DBD (g/cm³)
0.00	0.72	0.72	L0	n/a
0.72	1.16	0.44	S0	n/a
1.16	2.26	1.10	L1	n/a
2.26	2.60	0.34	S1	n/a

Lujiaowan section: ^{14}C and TL dating

Note: Position of ^{14}C sample not indicated (authors say it is from S0).

(Model I: min. glacial, max. interglacial; Model II: max. glacial, min. interglacial; Model III: 2/3 of interglacial soil is aeolian deposit)

Site location: 44.33° N, 85.63° E

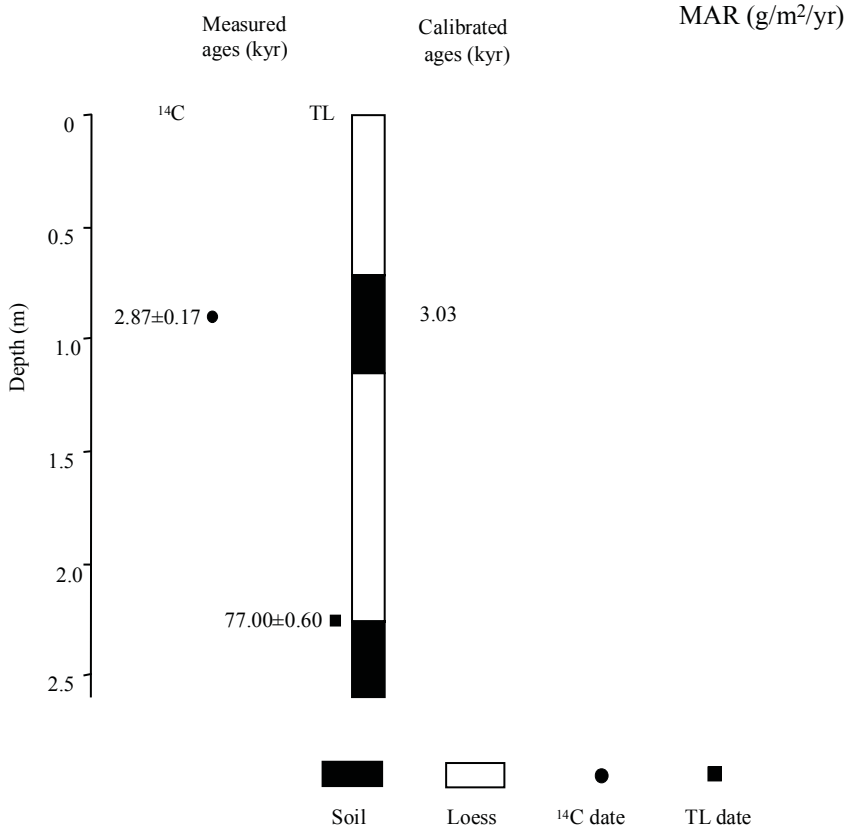

^{14}C dating: Lujiaowan (position of sample not indicated)										
Depth (m)	Dating laboratory	Lab. No.	Dating material	Age (kyr)	s.d. (kyr)	(1σ) Calendar age ranges (kyr)	Relative probability	Assumed calendar age (kyr)	Reference	Comments
-	n/a	n/a	n/a	2.87	0.17	3.21-2.84	0.938	3.03	Wen and Zheng (1987)	
						2.82-2.80	0.062			

TL dating: Lujiaowan (depth estimated from diagram, to nearest 1 cm)								
Depth (m)	Dating laboratory	Lab. No.	Dating material	TL-method	Age (kyr)	s.d. (kyr)	Reference	Comments
2.26	n/a	n/a	n/a	n/a	77	0.6	Wen and Zheng (1987)	

Age model (kyr): Lujiaowan						
Depth (m)	^{14}C	TL	Magnetic susceptibility	Pedostratigraphy (Model III)	Average chronology	Range
0.0				0.0	0.0	
0.5				5.9	5.9	
1.0				11.9	11.9	
1.5						
2.0						

MAR (g/m²/yr): Lujiaowan								
Stage (range in kyr)	Assumed DBD (g/cm^3)	^{14}C	TL	MS	Pedostratigraphy			Average MAR
					Model I	Model II	Model III	
Stage 1 (12-0)	1.48				143	89	**125**	125
Stage 2 (24-12)	1.48							
Stage 3 (59-24)	1.48							
Stage 4 (74-59)	1.48							
Stage 5 (130-74)	1.48				9	0	**6**	6

References used to generate data report: Lujiaowan	
Data used	**Source**
Pedostratigraphy	Wen and Zheng (1987)
Magnetic susceptibility	-
^{14}C dating	Wen and Zheng (1987)
TL dating	Wen and Zheng (1987)
Additional References:	
Data available	**Source**
-	-

Majiayuan: MAR (g/m^2/yr) based on magnetic susceptibility

Note: Digitized MS data.

Site location: 36.27° N, 107.50° E

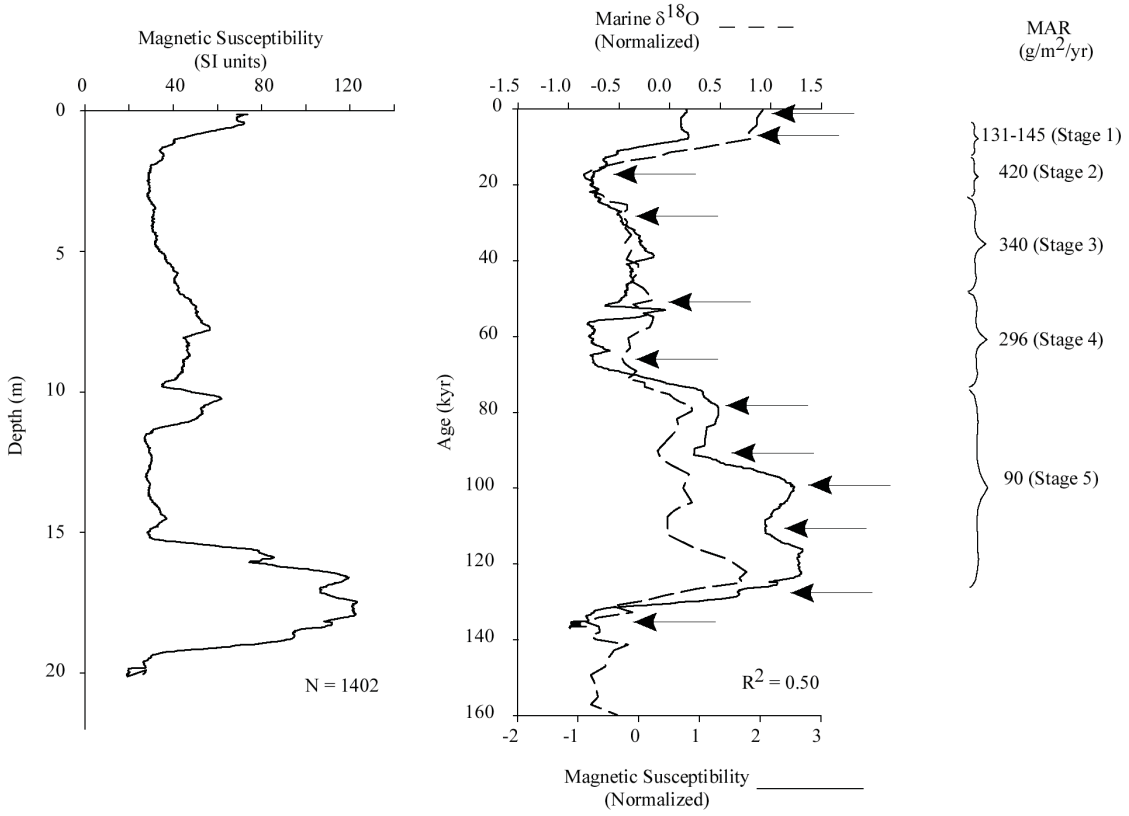

MS age model: Majiayuan		
Tie-Point	Depth (m)	Age (kyr)
1	0.13	0.21
2	0.47	7.81
3	2.16	17.85
4	6.13	27.95
5	9.66	51.57
6	15.09	65.22
7	15.87	78.3
8	16.05	90.95
9	16.62	99.96
10	17.07	110.79
11	18.02	123.79
12	19.86	135.34

Age model (kyr): Majiayuan						
Depth (m)	^{14}C	TL	Magnetic susceptibility	Pedostratigraphy (Model III)	Average chronology	Range
0			0.0		0.0	
4			22.5		22.5	
8			40.5		40.5	
12			57.5		57.5	
16			87.4		87.4	

MAR (g/m²/yr): Majiayuan								
Stage (range in kyr)	DBD (g/cm^3)	^{14}C	TL	MS	Pedostratigraphy			Average MAR
					Model I	Model II	Model III	
Stage 1 (12-0)	1.48			**138**				138
Stage 2 (24-12)	1.48			**420**				420
Stage 3 (59-24)	1.48			**340**				340
Stage 4 (74-59)	1.48			**296**				296
Stage 5 (130-74)	1.48			**90**				90

References used to generate data report: Majiayuan	
Data used	**Source**
Pedostratigraphy	-
Magnetic susceptibility	Sun et al. (1995)
^{14}C dating	-
TL dating	-
Additional References:	
Data available	**Source**
-	-

Mangshan_1 section: MAR (g/m^2/yr) based on pedostratigraphy

Note: Mangshan_1 and Mangshan_2 are used to distinguish two different versions of the pedostratigraphy of the section. Section with potential local Yellow River sources. Stage 1 affected by cultivation layer. Last glacial loess (L1) is not subdivided.

(Model I: min. glacial, max. interglacial; Model II: max. glacial, min. interglacial; Model III: 2/3 of interglacial soil is aeolian deposit)

Site location: 34.93° N, 113.53° E

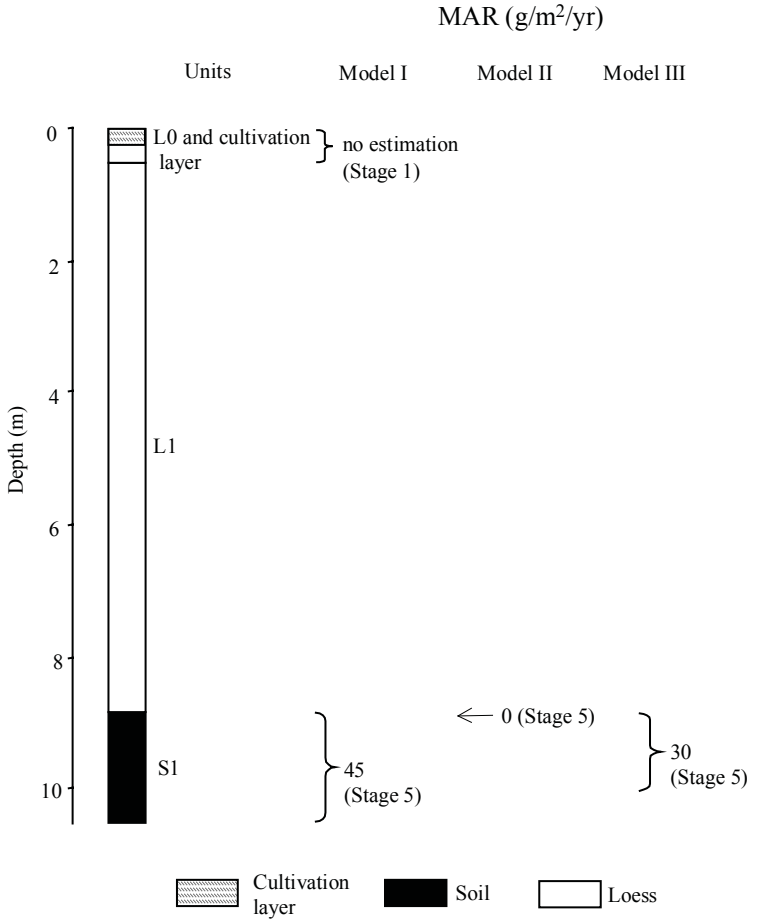

Stratigraphic data: Mangshan_1 (thicknesses of L0 + cultivation layer and L1+S1 given by author, depth and thickness of L1 and S1 estimated from diagram based on the stated thickness, to nearest 10 cm)				
Top depth (m)	Bottom depth (m)	Thickness (m)	Stratigraphic units	DBD (g/cm^3)
0.0	0.5	0.5	L0 and cultivation layer	n/a
0.5	8.8	8.3	L1	n/a
8.8	10.5	1.7	S1	n/a

Age model (kyr): Mangshan_1						
Depth (m)	^{14}C	TL	Magnetic susceptibility	Pedostratigraphy (Model III)	Average chronology	Range
0						
1.5						
3.0						
4.5						
6.0						
7.5						
9				83.9	83.9	

MAR (g/m²/yr): Mangshan_1								
Stage (range in kyr)	Assumed DBD (g/cm^3)	^{14}C	TL	MS	Pedostratigraphy			Average MAR
					Model I	Model II	Model III	
Stage 1 (12-0)	1.48							
Stage 2 (24-12)	1.48							
Stage 3 (59-24)	1.48							
Stage 4 (74-59)	1.48							
Stage 5 (130-74)	1.48				45	0	**30**	30

References used to generate data report:	
Data used	**Source**
Pedostratigraphy	Teng (1998)
Magnetic susceptibility	-
^{14}C dating	-
TL dating	-
Additional References:	
Data available	**Source**
-	-

Mangshan_2 section: MAR (g/m^2/yr) based on pedostratigraphy

Note: Mangshan_1 and Mangshan_2 are used to distinguish two different versions of the pedostratigraphy of the section. Section with potential local Yellow River sources.

(Model I: min. glacial, max. interglacial; Model II: max. glacial, min. interglacial; Model III: 2/3 of interglacial soil is aeolian deposit)

Site location: 34.97° N, 113.37° E

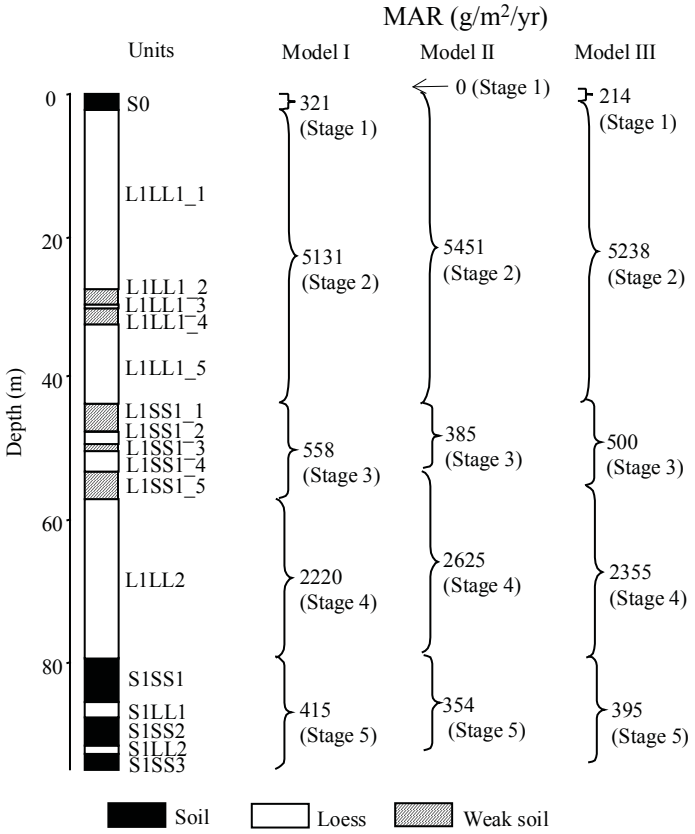

Stratigraphic data: Mangshan_2
(depth and thickness of S1SS1, S1LL1, S1SS2, S1LL2, S1SS3 estimated from diagram, to nearest 10 cm; the other depths and thicknesses given by authors)

Top depth (m)	Bottom depth (m)	Thickness (m)	Stratigraphic units	DBD (g/cm³)
0.0	2.6	2.6	S0	n/a
2.6	27.9	25.3	L1LL1_1	n/a
27.9	29.9	2.0	L1LL1_2	n/a
29.9	30.4	0.5	L1LL1_3	n/a
30.4	32.8	2.4	L1LL1_4	n/a
32.8	44.2	11.4	L1LL1_5	n/a
44.2	48.2	4.0	L1SS1_1	n/a
48.2	49.8	1.6	L1SS1_2	n/a
49.8	51.0	1.2	L1SS1_3	n/a
51.0	53.3	2.3	L1SS1_4	n/a
53.3	57.4	4.1	L1SS1_5	n/a
57.4	79.9	22.5	L1LL2	n/a
79.9	86.1	6.2	S1SS1	n/a
86.1	88.5	2.4	S1LL1	n/a
88.5	92.3	3.8	S1SS2	n/a
92.3	93.3	1.0	S1LL2	n/a
93.3	95.6	2.3	S1SS3	n/a

Mangshan_2 section: MAR (g/m^2/yr) based on TL dating

Note: Mangshan_1 and Mangshan_2 are used to distinguish two different versions of the pedostratigraphy of the section. Section with potential local river Yellow River sources.

Site location: 34.97° N, 113.37° E

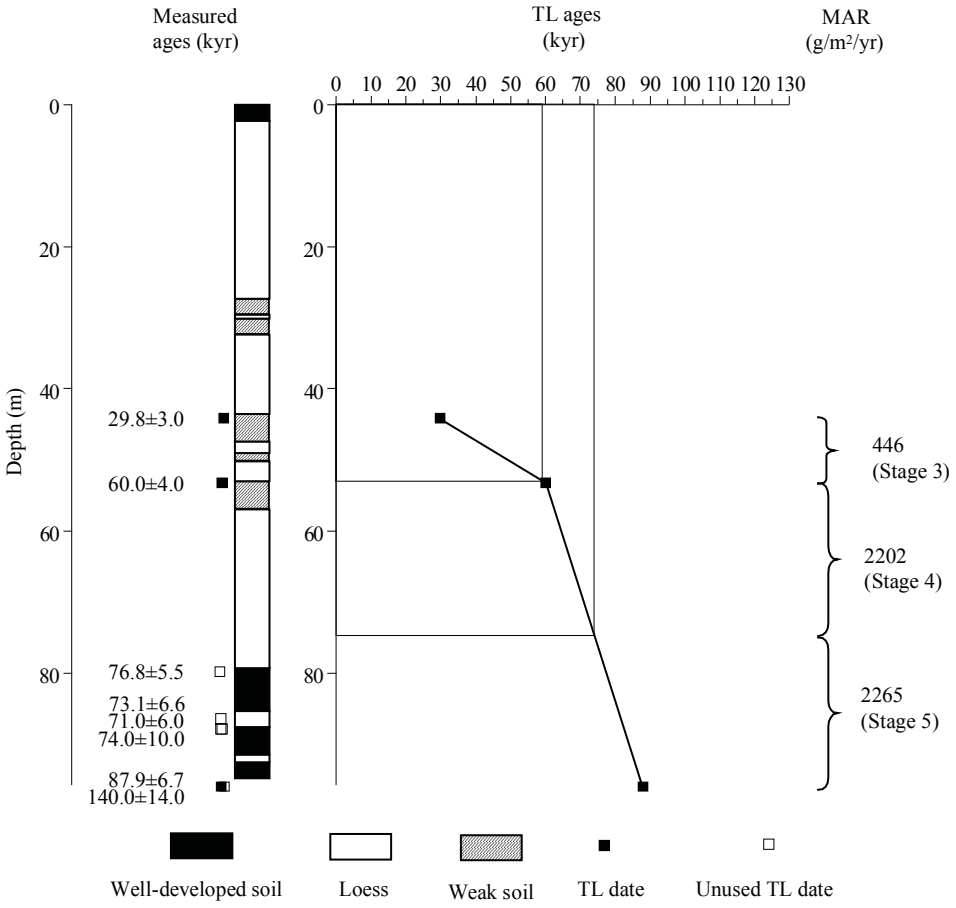

OSL and TL dating: Mangshan_2
(depth given by authors)

Depth (m)	Dating laboratory	Lab. No.	Dating material	TL-method	Age (kyr)	s.d. (kyr)	Reference	Comments
44.1	TL Lab. Geology Institute, SSB and Xi'an Loess Lab.	96106	n/a	n/a	29.8	3.0	Jiang et al. (1998)	OSL sample
53.2	TL Lab. Geology Institute, SSB and Xi'an Loess Lab.	96107	n/a	n/a	60.0	4.0	Jiang et al. (1998)	OSL sample
79.8	TL Lab. Geology Institute, SSB and Xi'an Loess Lab.	96108	n/a	n/a	76.8	5.5	Jiang et al. (1998)	assumed reversal OSL sample
86.4	TL Lab. Geology Institute, SSB and Xi'an Loess Lab.	96109	n/a	n/a	73.1	6.6	Jiang et al. (1998)	overlapping, not used OSL sample
87.8	TL Lab. Geology Institute, SSB and Xi'an Loess Lab.	L93-57	n/a	n/a	71.0	6.0	Jiang et al. (1998)	not used, because conventional TL
87.8	TL Lab. Geology Institute, SSB and Xi'an Loess Lab.	L93-31	n/a	n/a	74.0	10.0	Jiang et al. (1998)	uncertainties > 10%
95.9	TL Lab. Geology Institute, SSB and Xi'an Loess Lab.	90110	n/a	n/a	87.9	6.7	Jiang et al. (1998)	OSL sample
95.9	TL Lab. Geology Institute, SSB and Xi'an Loess Lab.	L93-44	n/a	n/a	140.0	14.0	Jiang et al. (1998)	Not used > 130 kyr
106.1	TL Lab. Geology Institute, SSB and Xi'an Loess Lab.	96111	n/a	n/a	168.8	17.8	Jiang et al. (1998)	Not used > 130 kyr OSL sample

Age model (kyr): Mangshan_2						
Depth (m)	^{14}C	TL	Magnetic susceptibility	Pedostratigraphy (Model III)	Average chronology	Range
0				0.0	0.0	
10				14.2	14.2	
20				17.1	17.1	
30				20.0	20.0	
40				22.9	22.9	
50		49.1		41.0	45.0	41.0-49.1
60		64.5		61.5	63.0	61.5-64.5
70		71.0		67.9	69.4	67.9-71.0
80		77.6		74.0	75.8	74.0-77.6
90		84.0		111.4	97.7	84.0-111.4

MAR (g/m²/yr): Mangshan_2								
Stage (range in kyr)	Assumed DBD (g/cm^3)	^{14}C	TL	MS	Pedostratigraphy			Average MAR
					Model I	Model II	Model III	
Stage 1 (12-0)	1.48				321	0	**214**	214
Stage 2 (24-12)	1.48				5131	5451	**5238**	5238
Stage 3 (59-24)	1.48		**446**		558	385	**500**	473
Stage 4 (74-59)	1.48		**2202**		2220	2625	**2355**	2279
Stage 5 (130-74)	1.48		**2265**		415	345	**395**	1330

References used to generate data report:	
Data used	**Source**
Pedostratigraphy	Jiang et al. (1998)
Magnetic susceptibility	
^{14}C dating	
TL dating	Jiang et al. (1998)
Additional References:	
Data available	**Source**
OSL, magnetic susceptibility, magnetic polarity	Jiang et al. (1999)

Mengdashan section: MAR (g/m^2/yr) based on pedostratigraphy

(Model I: min. glacial, max. interglacial; Model II: max. glacial, min. interglacial; Model III: 2/3 of interglacial soil is aeolian deposit)

Site location: 35.77° N, 102.00° E

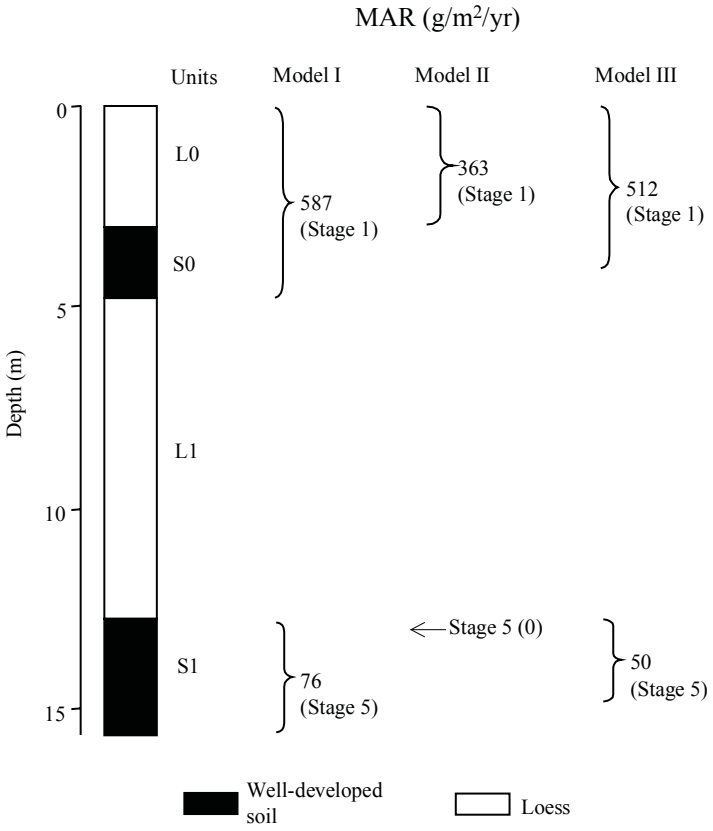

Stratigraphic data: Mengdashan (depth and thickness estimated from diagram, to nearest 1 cm)				
Top depth (m)	Bottom depth (m)	Thickness (m)	Stratigraphic units	DBD (g/cm^3)
0.00	2.94	2.94	L0	n/a
2.94	4.76	1.82	S0	n/a
4.76	12.73	7.97	L1	n/a
12.73	15.59	2.86	S1	n/a

Age model (kyr): Mengdashan						
Depth (m)	^{14}C	TL	Magnetic susceptibility	Pedostratigraphy (Model III)	Average chronology	Range
0				0.0	0.0	
2				5.8	5.8	
4				11.6	11.6	
6						
8						
10						
12						
14				111.2	111.2	

MAR (g/m²/yr): Mengdashan								
Stage (range in kyr)	Assumed DBD (g/cm^3)	^{14}C	TL	MS	Pedostratigraphy			Average MAR
					Model I	Model II	Model III	
Stage 1 (12-0)	1.48				587	363	**512**	512
Stage 2 (24-12)	1.48							
Stage 3 (59-24)	1.48							
Stage 4 (74-59)	1.48							
Stage 5 (130-74)	1.48				76	0	**50**	50

References used to generate data report: Mengdashan	
Data used	**Source**
Pedostratigraphy	Chen and Zhang (1994)
Magnetic susceptibility	-
^{14}C dating	-
TL dating	-
Additional References:	
Data available	**Source**
-	-

Mizhi section: MAR (g/m^2/yr) based on pedostratigraphy

Note: Stage 1 affected by cultivation layer. Last glacial loess (L1) contains sedimentary hiatus.

(Model I: min. glacial, max. interglacial; Model II: max. glacial, min. interglacial; Model III: 2/3 of interglacial soil is aeolian deposit)

Site location: 37.83° N, 110.08° E

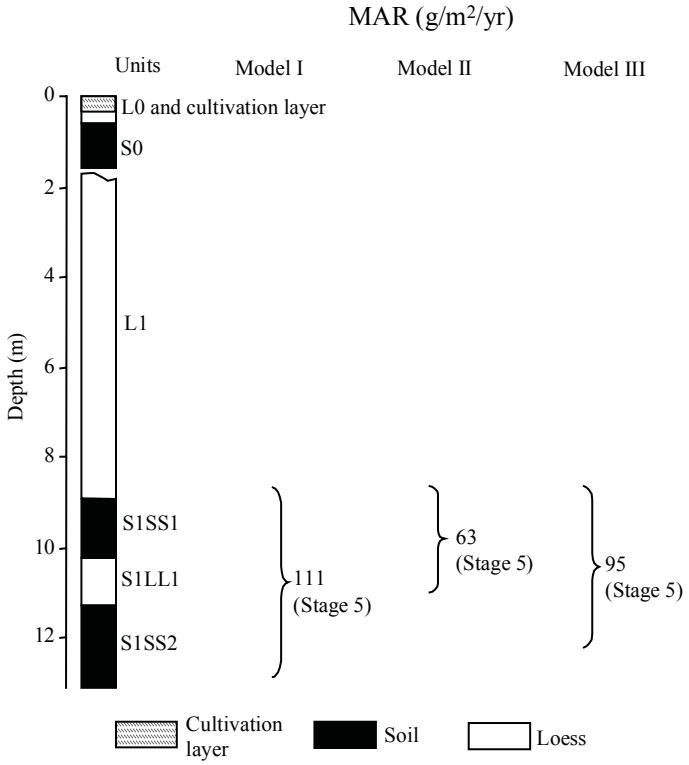

Stratigraphic data: Mizhi (depth and thickness estimated from diagram, to nearest 10 cm)				
Top depth (m)	Bottom depth (m)	Thickness (m)	Stratigraphic units	DBD (g/cm^3)
0.0	0.6	0.6	L0 and cultivation layer	n/a
0.6	1.6	1.0	S0	n/a
1.6	8.7	7.3	L1 with hiatus	n/a
8.7	10.0	1.3	S1SS1	n/a
10.0	11.1	1.1	S1LL1	n/a
11.1	12.9	1.8	S1SS2	n/a

Mizhi section: Magnetic susceptibility

Note: Stage 1 affected by cultivation layer. Last glacial loess (L1) contains sedimentary hiatus. MS MAR not calculated because of hiatus.

Site location: 37.83° N, 110.08° E

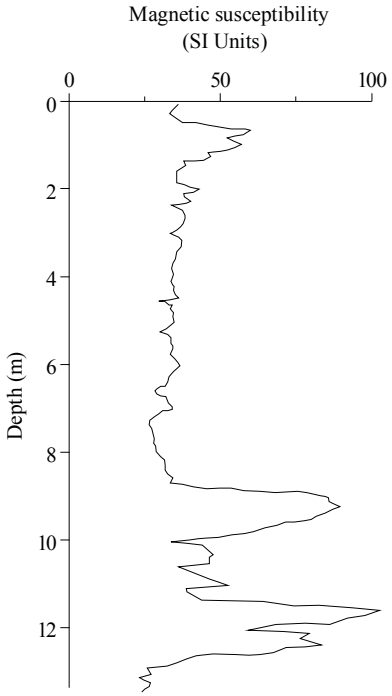

Age model (kyr): Mizhi						
Depth (m)	^{14}C	TL	Magnetic susceptibility	Pedostratigraphy (Model III)	Average chronology	Range
0						
2						
4						
6						
8						
10				94.2	94.2	
12				125.3	125.3	

MAR (g/m²/yr): Mizhi								
Stage (range in kyr)	Assumed DBD (g/cm^3)	^{14}C	TL	MS	Pedostratigraphy			Average MAR
					Model I	Model II	Model III	
Stage 1 (12-0)	1.48							
Stage 2 (24-12)	1.48							
Stage 3 (59-24)	1.48							
Stage 4 (74-59)	1.48							
Stage 5 (130-74)	1.48				111	63	**95**	95

References used to generate data report: Mizhi	
Data used	**Source**
Pedostratigraphy	Sun (unpublished data)
Magnetic susceptibility	Sun (unpublished data)
^{14}C dating	-
TL dating	-
Additional References:	
Data available	**Source**
-	-

Mujiayuan (Wupu) section: MAR (g/m^2/yr) based on magnetic susceptibility

Note: Wupu is the name of the County of Shaaxi Province in which the section is located and was used by Ding et al. (1996) for this section. Mujiayuan is the name of the village where the section is located.

Site location: 37.57° N, 110.72° E

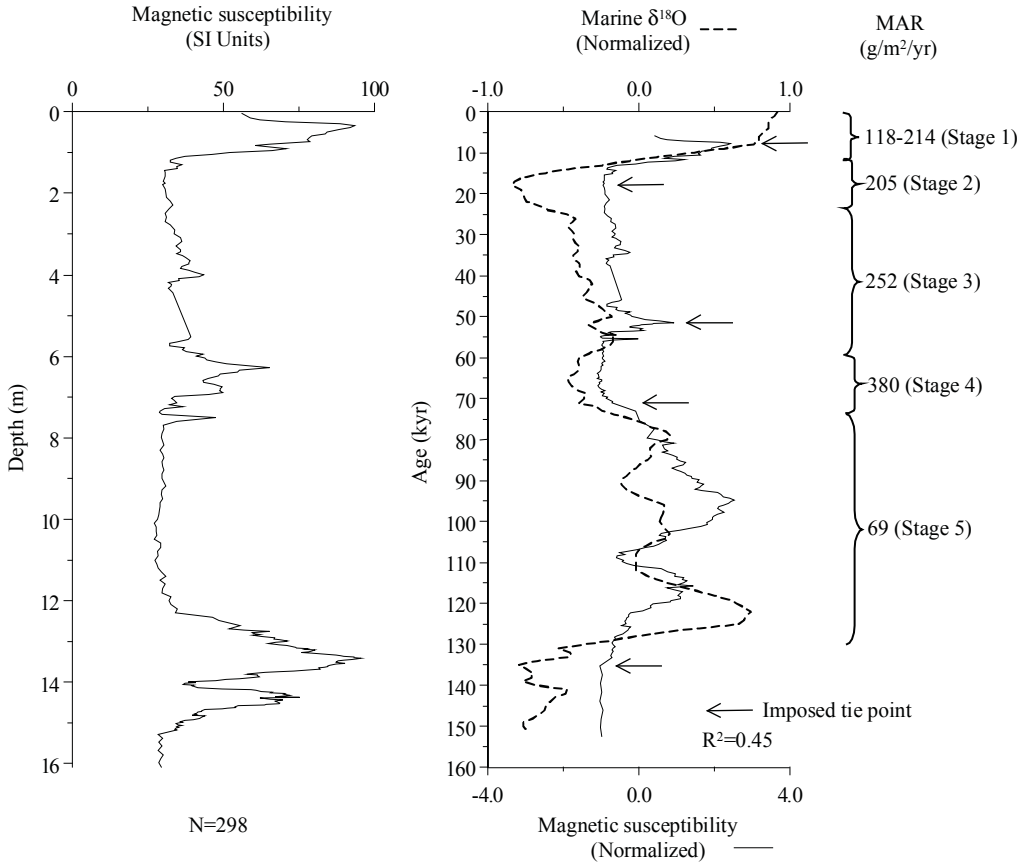

MS age model: Mujiayuan (Wupu)		
Tie-Point	Depth (m)	Age (kyr)
1	0.35	7.81
2	1.80	17.85
3	6.30	51.57
4	12.30	71.12
5	15.28	135.34

Age model (kyr): Mujiayuan (Wupu)						
Depth (m)	^{14}C	TL	Magnetic susceptibility	Pedostratigraphy (Model III)	Average chronology	Range
0			0.0		0.0	
3			26.8		26.8	
6			49.3		49.3	
9			60.4		60.4	
12			70.1		70.1	
15			129.3		129.3	

MAR (g/m²/yr): Mujiayuan (Wupu)								
Stage (range in kyr)	Assumed DBD (g/cm^3)	^{14}C	TL	MS	Pedostratigraphy			Average MAR
					Model I	Model II	Model III	
Stage 1 (12-0)	1.48			**166**				166
Stage 2 (24-12)	1.48			**205**				205
Stage 3 (59-24)	1.48			**252**				252
Stage 4 (74-59)	1.48			**380**				380
Stage 5 (130-74)	1.48			**69**				69

References used to generate data report: Mujiayuan (Wupu)	
Data used	**Source**
Pedostratigraphy	-
Magnetic susceptibility	Sun and Ding (1997)
^{14}C dating	-
TL dating	-
Additional References:	
Data available	**Source**
Magnetic susceptibility	Ding et al. (1999b)

Ningxian section: MAR (g/m^2/yr) based on magnetic susceptibility

Note: Digitized MS data.

Site location: 35.48° N, 107.97° E

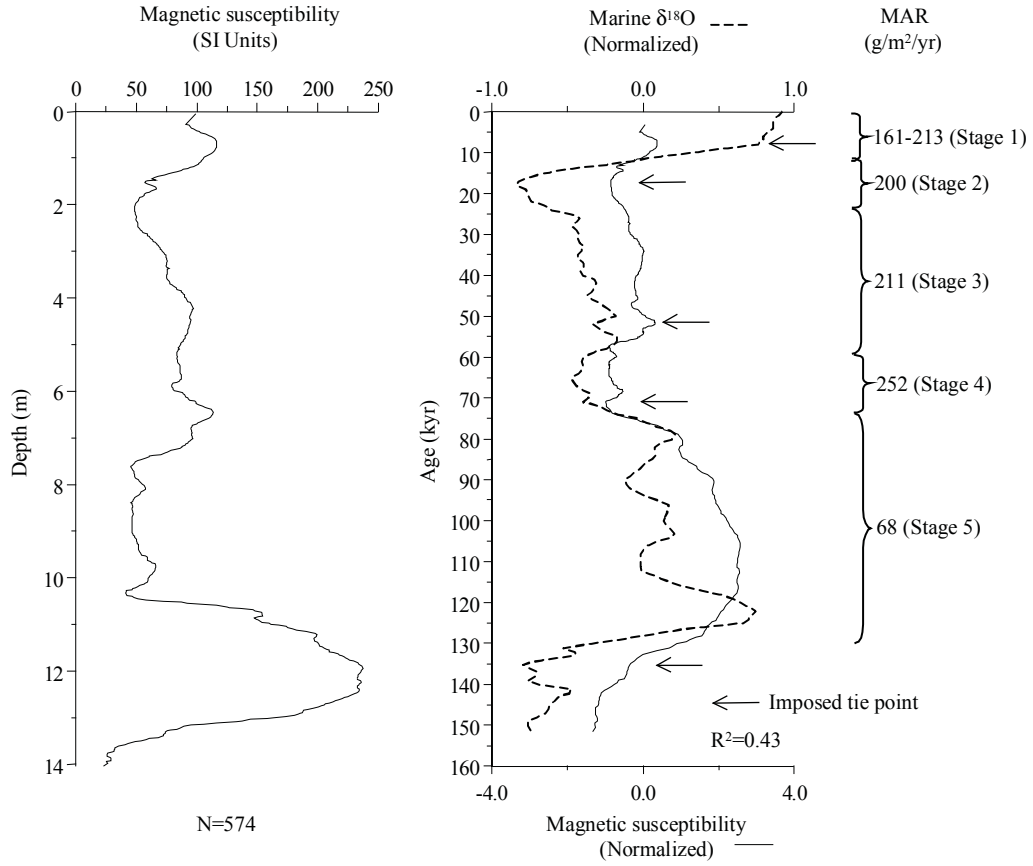

MS age model: Ningxian		
Tie-Point	Depth (m)	Age (kyr)
1	0.70	7.81
2	2.07	17.31
3	6.44	51.57
4	10.34	71.12
5	13.29	135.34

Age model (kyr): Ningxian						
Depth (m)	^{14}C	TL	Magnetic susceptibility	Pedostratigraphy (Model III)	Average chronology	Range
0			0.0		0.0	
2			16.8		16.8	
4			32.5		32.5	
6			48.1		48.1	
8			59.4		59.4	
10			69.4		69.4	
12			107.2		107.2	
14			151.0		151.0	

MAR (g/m²/yr): Ningxian								
Stage (range in kyr)	Assumed DBD (g/cm^3)	^{14}C	TL	MS	Pedostratigraphy			Average MAR
					Model I	Model II	Model III	
Stage 1 (12-0)	1.48			**187**				187
Stage 2 (24-12)	1.48			**200**				200
Stage 3 (59-24)	1.48			**211**				211
Stage 4 (74-59)	1.48			**252**				252
Stage 5 (130-74)	1.48			**68**				68

References used to generate data report: Ningxian	
Data used	**Source**
Pedostratigraphy	-
Magnetic susceptibility	Sun et al. (1995)
^{14}C dating	-
TL dating	-
Additional References:	
Data available	**Source**
-	-

Niuquanzi section: MAR (g/m^2/yr) based on pedostratigraphy

(Model I: min. glacial, max. interglacial; Model II: max. glacial, min. interglacial; Model III: 2/3 of interglacial soil is aeolian deposit)

Site location: 44.18° N, 85.10° E

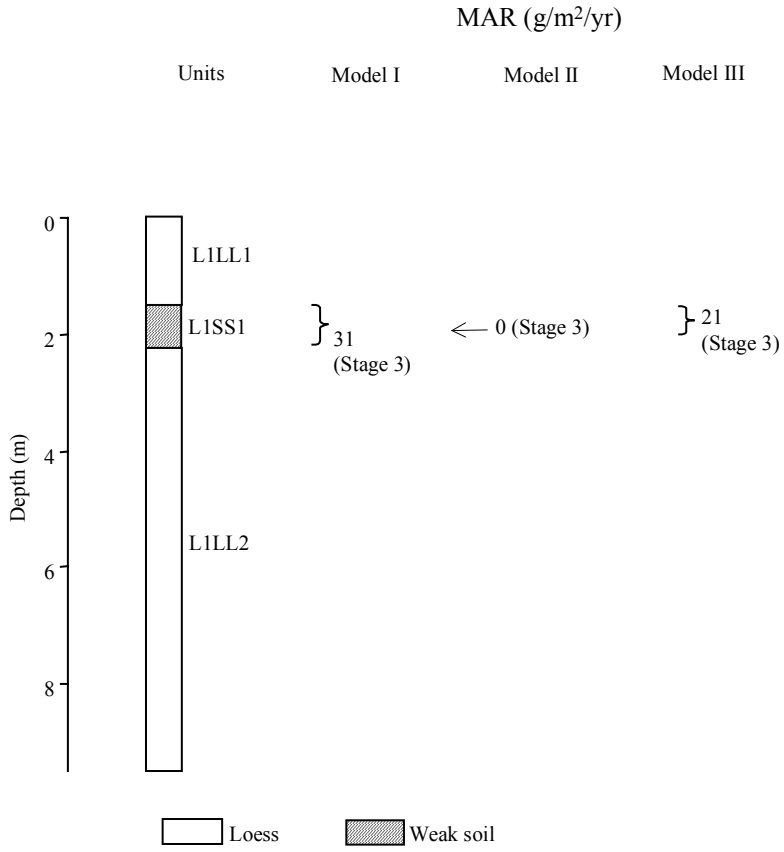

Stratigraphic data: Niuquanzi (depth and thickness estimated from diagram, to nearest 1 cm)				
Top depth (m)	Bottom depth (m)	Thickness (m)	Stratigraphic units	DBD (g/cm^3)
0.00	1.50	1.50	L1LL1	n/a
1.50	2.24	0.74	L1SS1	n/a
2.24	9.50	7.26	L1LL2	n/a

Niuquanzi section: MAR (g/m^2/yr) based on ^{14}C dating

Note: Exact position of ^{14}C sample not indicated although it comes from S0.

(Model I: min. glacial, max. interglacial; Model II: max. glacial, min. interglacial; Model III: 2/3 of interglacial soil is aeolian deposit)

Site location: 44.18° N, 85.10° E

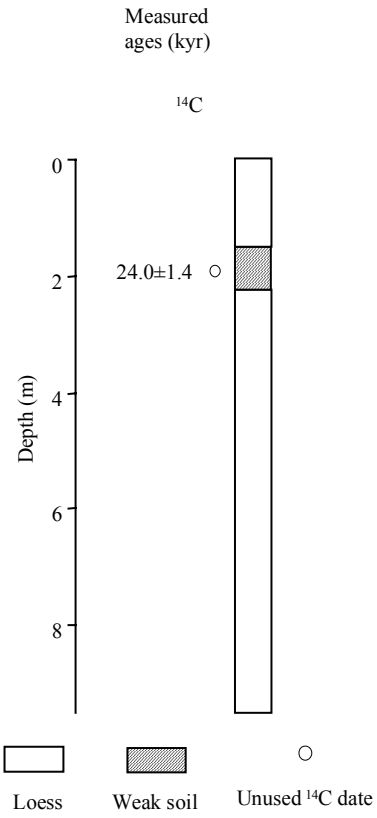

^{14}C dating: Niuquanzi (position of sample not indicated)										
Depth (m)	Dating laboratory	Lab. No.	Dating material	Age (kyr)	s.d. (kyr)	(1σ) Calendar age ranges (kyr)	Relative probability	Assumed calendar age (kyr)	Reference	Comments
-	n/a	n/a	n/a	24	1.4				Wen and Zheng (1987)	beyond calibration range

Age model (kyr): Niuquanzi						
Depth (m)	^{14}C	TL	Magnetic susceptibility	Pedostratigraphy (Model III)	Average chronology	Range
0						
1.5				24.0	24.0	
3						
4.5						
6						
7.5						
9						
10.5						

MAR (g/m²/yr): Niuquanzi								
Stage (range in kyr)	Assumed DBD (g/cm^3)	^{14}C	TL	MS	Pedostratigraphy			Average MAR
					Model I	Modell II	Model III	
Stage 1 (12-0)	1.48							
Stage 2 (24-12)	1.48							
Stage 3 (59-24)	1.48				31	0	**21**	21
Stage 4 (74-59)	1.48							
Stage 5 (130-74)	1.48							

References used to generate data report: Niuquanzi	
Data used	**Source**
Pedostratigraphy	Wen and Zheng (1987)
Magnetic susceptibility	
^{14}C dating	Wen and Zheng (1987)
TL dating	Wen and Zheng (1987)
Additional References:	
Data available	**Source**
-	-

Pucheng section: MAR (g/m^2/yr) based on magnetic susceptibility

Note: Stage 1 affected by cultivation layer.

Site location: 34.97° N, 109.60° E

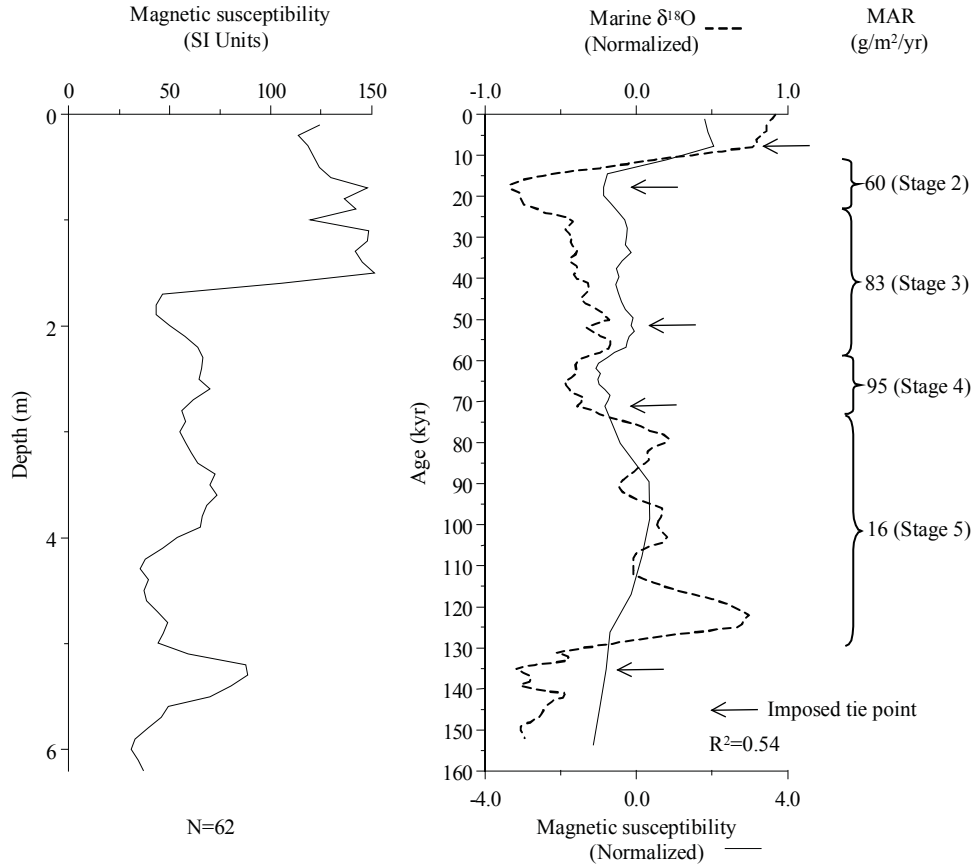

MS age model: Pucheng		
Tie-Point	Depth (m)	Age (kyr)
1	1.50	7.81
2	1.80	17.85
3	3.50	51.57
4	5.00	71.12
5	5.70	135.34

Age model (kyr): Pucheng						
Depth (m)	^{14}C	TL	Magnetic susceptibility	Pedostratigraphy (Model III)	Average chronology	Range
0						
1						
2			21.8		21.8	
3			41.6		41.6	
4			58.1		58.1	
5			71.1		71.1	
6			162.8		162.8	

MAR ($g/m^2/yr$): Pucheng								
Stage (range in kyr)	Assumed DBD (g/cm^3)	^{14}C	TL	MS	Pedostratigraphy			Average MAR
					Model I	Model II	Model III	
Stage 1 (12-0)	1.48							
Stage 2 (24-12)	1.48			**60**				60
Stage 3 (59-24)	1.48			**83**				83
Stage 4 (74-59)	1.48			**95**				95
Stage 5 (130-74)	1.48			**16**				16

References used to generate data report: Pucheng	
Data used	**Source**
Pedostratigraphy	-
Magnetic susceptibility	Ding et al. (1999b)
^{14}C dating	-
TL dating	-
Additional References:	
Data available	**Source**
-	-

Qijidong section

Note: Section not used to estimate MAR, because the stratigraphy cannot be correlated with the CLP stratigraphy, and the section contains sand layers. These four sections (Duobutang, Qijidong, Xietongmen, and Xigaze) are all from the Tibetan Plateau, and were scanned as a unit. The top age on the Xietongmen section is ^{14}C date, all the other ages are TL dates.

Site location: 29.32° N, 89.20° E

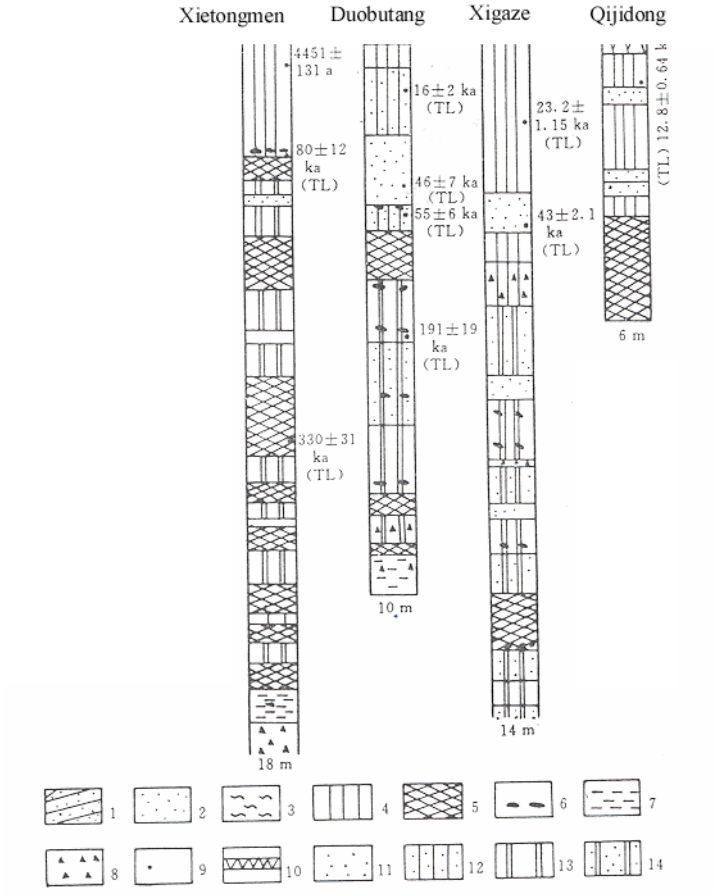

Legend: 1. Bedded sand; 2. Aeolian fine sand, 3. Fluvial layer, 4. Loess, 5. Palaeosol, 6. Nodule
7. Fluvial clay, 8. Gravel layer, 9. Sampling position, 10. Grass layer, 11. Medium sand

References used to generate data report: Qijidong	
Data used	**Source**
Pedostratigraphy	Jin et al. (1998)
Magnetic susceptibility	-
^{14}C dating	-
TL dating	Jin et al. (1998)
Additional References:	
Data available	**Source**
-	-

Qinjiazhai section: MAR (g/m^2/yr) based on pedostratigraphy

Note: Missing Stage 1 deposit.

(Model I: min. glacial, max. interglacial; Model II: max. glacial, min. interglacial; Model III: 2/3 of interglacial soil is aeolian deposit)

Site location: 35.74° N, 109.43° E

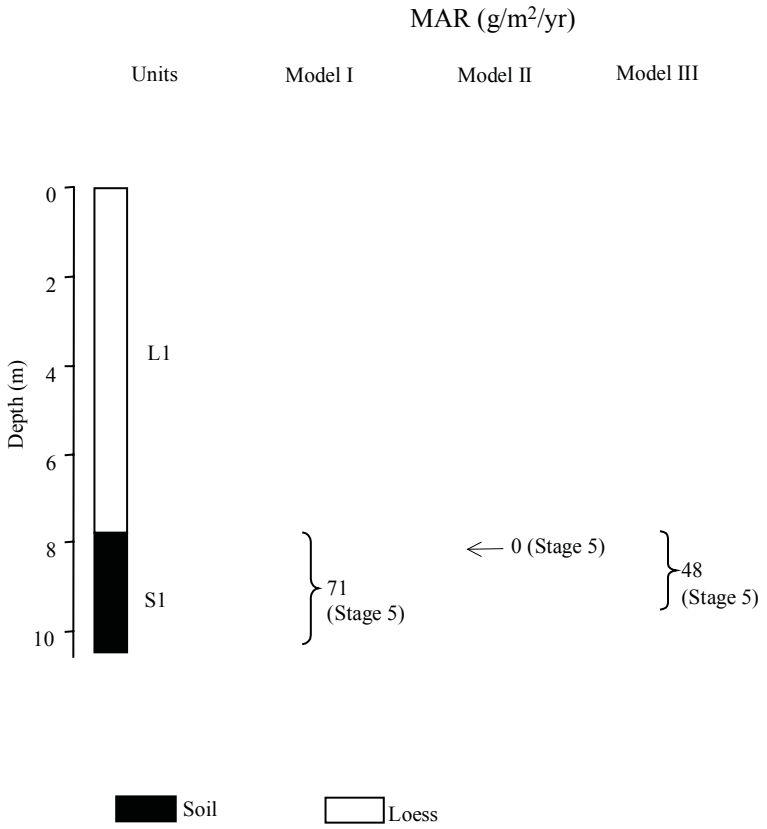

Stratigraphic data: Qinjiazhai (depth and thickness estimated from diagram, to nearest 10 cm)				
Top depth (m)	Bottom depth (m)	Thickness (m)	Stratigraphic units	DBD (g/cm^3)
0.00	7.73	7.73	L1	n/a
7.73	10.43	2.70	S1	n/a

Age model (kyr): Qinjiazhai						
Depth (m)	^{14}C	TL	Magnetic susceptibility	Pedostratigraphy (Model III)	Average chronology	Range
0						
1						
2						
3						
4						
5						
6						
7						
8				82.4		
9				113.5		

MAR (g/m²/yr): Qinjiazhai								
Stage (range in kyr)	Assumed DBD (g/cm^3)	^{14}C	TL	MS	Pedostratigraphy			Average MAR
					Model I	Model II	Model III	
Stage 1 (12-0)	1.48							
Stage 2 (24-12)	1.48							
Stage 3 (59-24)	1.48							
Stage 4 (74-59)	1.48							
Stage 5 (130-74)	1.48				71	0	**48**	48

References used to generate data report: Qinjiazhai	
Data used	**Source**
Pedostratigraphy	Gu et al. (1987)
Magnetic susceptibility	-
^{14}C dating	-
TL dating	-
Additional References:	
Data available	**Source**
^{18}O on quartz	Gu et al. (1987)
Pedostratigraphy, clay minerals	Zhang and Yuan (1987)

Qishan section: MAR (g/m^2/yr) based on pedostratigraphy

Note: Stage 1 affected by cultivation layer.

(Model I: min. glacial, max. interglacial; Model II: max. glacial, min. interglacial; Model III: 2/3 of interglacial soil is aeolian deposit)

Site location: 34.45° N, 107.63° E

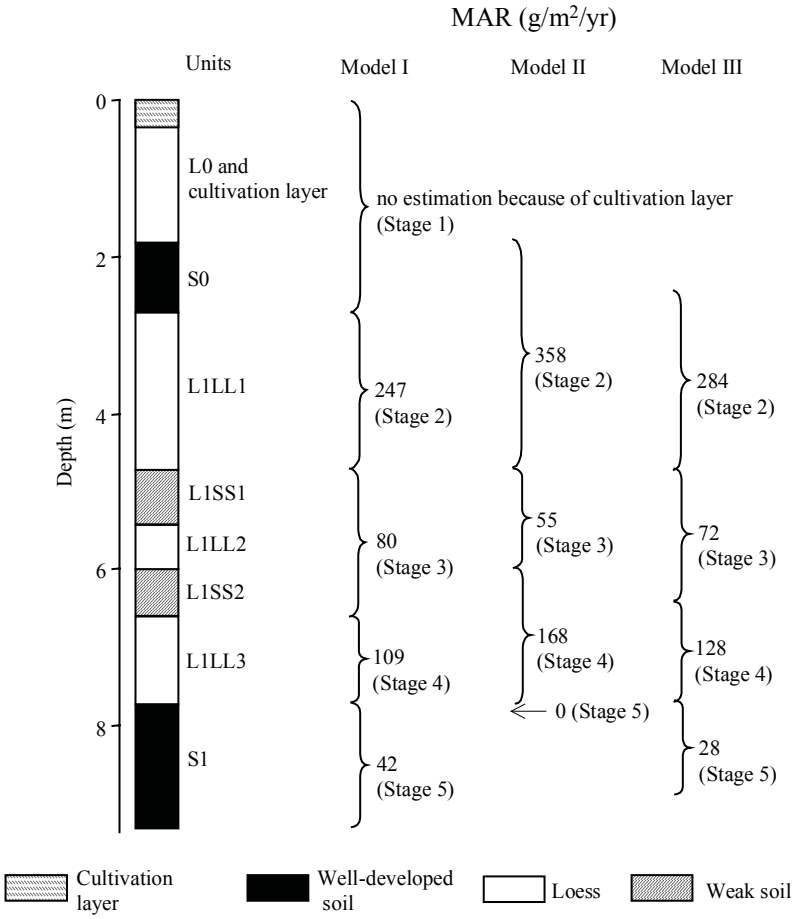

Stratigraphic data: Qishan (depths given by authors, thickness calculated from depths)				
Top depth (m)	Bottom depth (m)	Thickness (m)	Stratigraphic units	DBD (g/cm³)
0.0	1.8	1.8	L0 and cultivation layer	n/a
1.8	2.7	0.9	S0	n/a
2.7	4.7	2.0	L1LL1	n/a
4.7	5.4	0.7	L1SS1	n/a
5.4	6.0	0.6	L1LL2	n/a
6.0	6.6	0.6	L1SS2	n/a
6.6	7.7	1.1	L1LL3	n/a
7.7	9.3	1.6	S1	n/a

Qishan section: MAR (g/m^2/yr) based on magnetic susceptibility

Note: Digitized MS data. Stage 1 affected by cultivation layer.

Site location: 34.45° N, 107.63° E

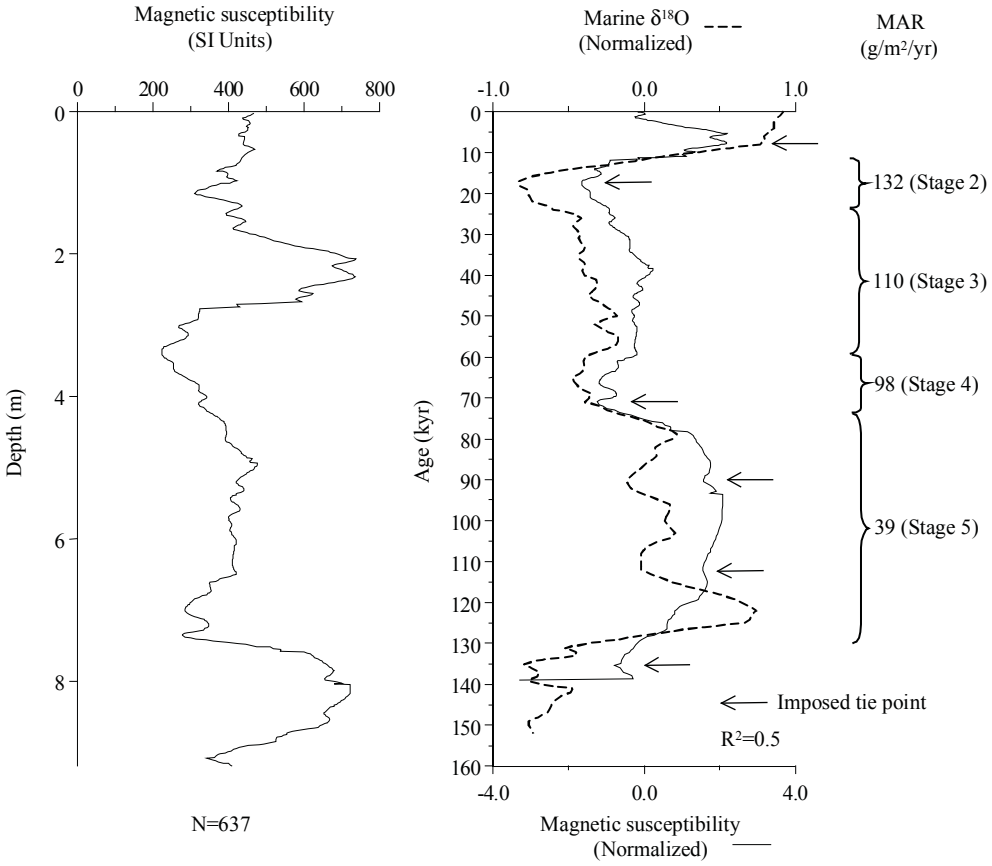

MS age model: Qishan		
Tie-Point	Depth (m)	Age (kyr)
1	2.33	7.81
2	3.36	17.31
3	7.36	71.12
4	7.97	90.10
5	8.46	112.28
6	9.09	135.34

Age model (kyr): Qishan						
Depth (m)	^{14}C	TL	Magnetic susceptibility	Pedostratigraphy (Model III)	Average chronology	Range
0						
1						
2						
3			14.0	15.1	14.5	14.0-15.1
4			26.0	20.4	23.2	20.4-26.0
5			39.4	30.0	34.7	30.0-39.4
6			52.7	50.8	51.7	50.8-52.7
7			66.3	65.7	66.0	65.7-66.3
8			91.4	89.3	90.3	89.3-91.4
9			132.0		132.0	

MAR (g/m²/yr): Qishan								
Stage (range in kyr)	Assumed DBD (g/cm^3)	^{14}C	TL	MS	Pedostratigraphy			Average MAR
					Model I	Model II	Model III	
Stage 1(12-0)	1.48							
Stage 2 (24-12)	1.48			**132**	247	358	**284**	208.0
Stage 3 (59-24)	1.48			**110**	80	55	**72**	91.0
Stage 4 (74-59)	1.48			**98**	109	168	**128**	113.0
Stage 5 (130-74)	1.48			**39**	42	0	**28**	33.5

References used to generate data report: Qishan	
Data used	**Source**
Pedostratigraphy	Chen et al. (1996b)
Magnetic susceptibility	Chen et al. (1996b)
^{14}C dating	-
TL dating	-
Additional References:	
Data available	**Source**
$\delta^{13}C$, $\delta^{18}O$, chemical parameters	Chen et al. (1996b)
Pedostratigraphy, chemical parameters	Li and Wang (1998)

Renjiahutong section: MAR (g/m^2/yr) based on pedostratigraphy

Note: Stage 1 affected by cultivation layer.

(Model I: min. glacial, max. interglacial; Model II: max. glacial, min. interglacial; Model III: 2/3 of interglacial soil is aeolian deposit)

Site location: 35.75° N, 109.42° E

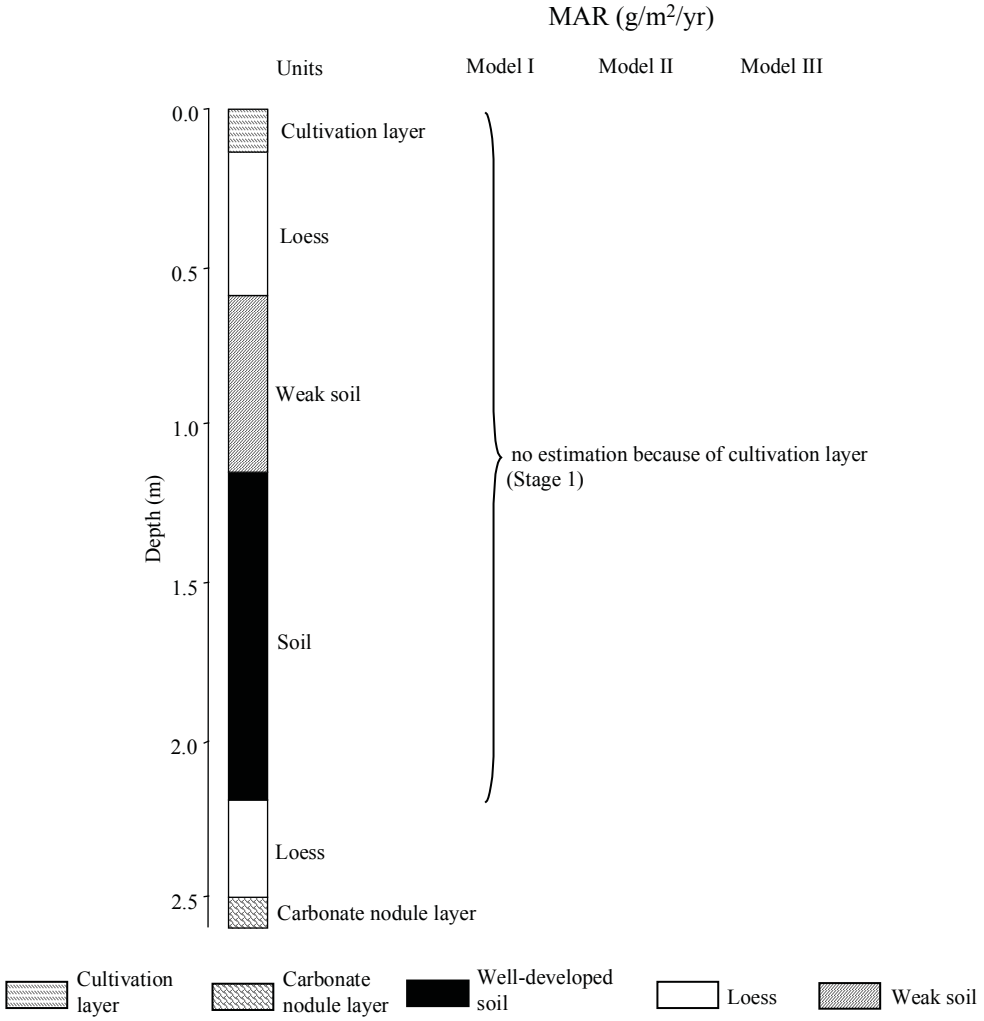

Stratigraphic data: Renjiahutong (thickness given by authors in text, depth calculated from thickness)				
Top depth (m)	Bottom depth (m)	Thickness (m)	Stratigraphic units	DBD (g/cm^3)
0.00	0.60	0.60	cultivation and loess layer	n/a
0.60	1.15	0.55	weak soil	n/a
1.15	2.20	1.05	soil	n/a
2.20	2.50	0.30	loess	n/a
2.50	2.60	0.10	carbonate nodule layer	n/a

Renjiahutong section: MAR (g/m^2/yr) based on ^{14}C dating

Note: Stage 1 MAR calculated excluding cultivation layer, based on available dates.

Site location: 35.75° N, 109.42° E

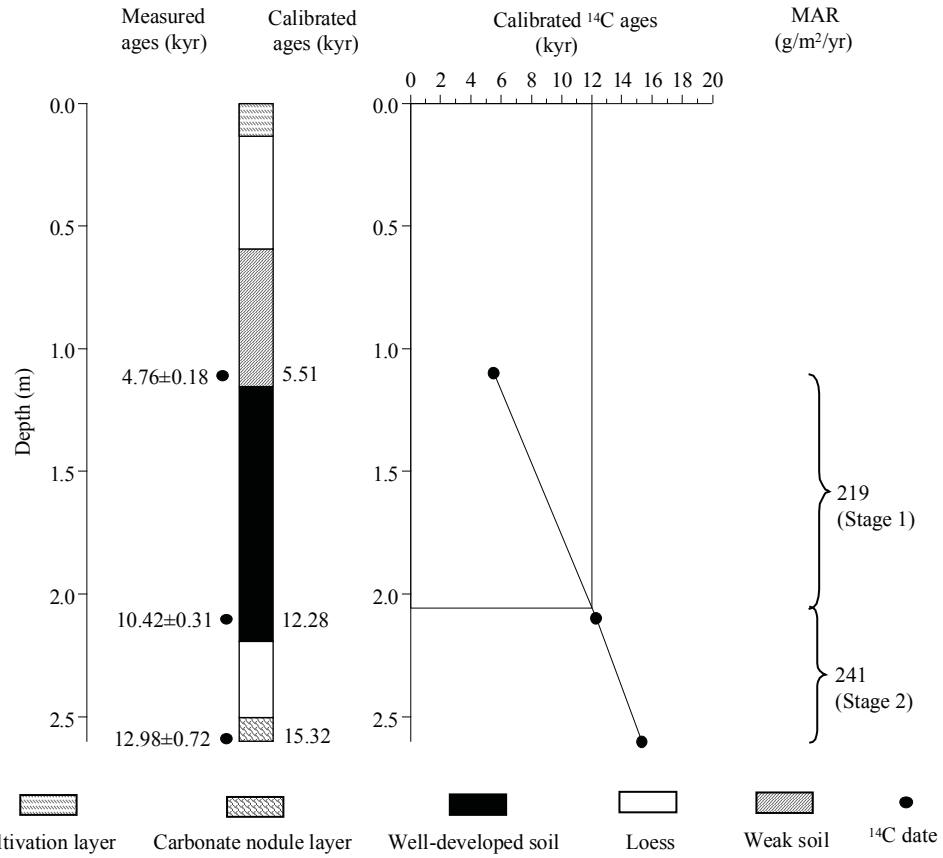

^{14}C dating: Renjiahutong (depth given by the authors)										
Depth (m)	Dating laboratory	Lab. No.	Dating material	Age (kyr)	s.d. (kyr)	(1σ) Calendar age ranges (kyr)	Relative probability	Assumed calendar age (kyr)	Reference	Comments
1.1	Australian National University	ANU-5942	soluble and insoluble organic matter	4.76	0.18	5.29-5.72	1	5.51	Li and Wang (1998)	averaged from two dates
2.1	Australian National University	ANU-5943	insoluble organic matter	10.42	0.31	11.90-12.67	0.795	12.28	Li and Wang (1998)	
						12.71-12.82	0.103			
						11.75-11.86	0.094			
						11.70-11.71	0.008			
2.6	Australian National University	ANU-5944	soluble organic matter	12.98	0.72	14.32-16.31	1	15.32	Li and Wang (1998)	
2.6	Australian National University	ANU-5944	insoluble organic matter	4.18	0.31				Li and Wang (1998)	younger contamination

Renjiahutong section: Magnetic susceptibility

Note: MAR not estimated. Digitized MS data. Stage 1 estimate excluded due to cultivation. Insufficient length of record to estimate Stage 2.

Site location: 35.75° N, 109.42° E

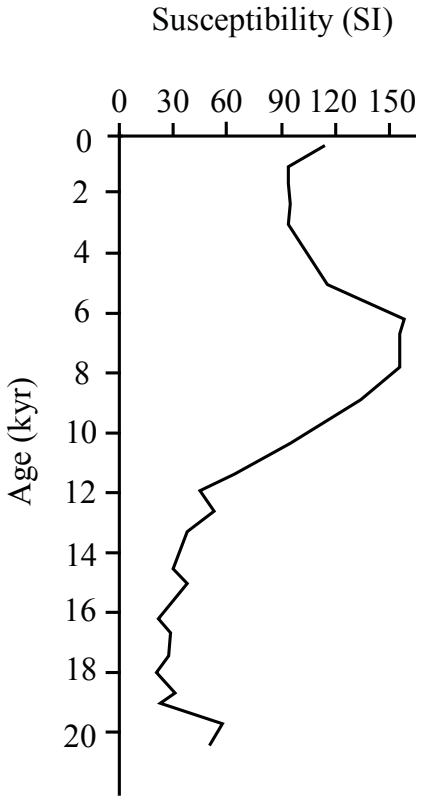

Age model (kyr): Renjiahutong						
Depth (m)	^{14}C	TL	Magnetic susceptibility	Pedostratigraphy (Model III)	Average chronology	Range
0.0						
0.5						
1.0						
1.5	8.2				8.2	
2.0	11.6				11.6	
2.5	14.7				14.7	

MAR (g/m²/yr): Renjiahutong								
Stage (range in kyr)	Assumed DBD (g/cm^3)	^{14}C	TL	MS	Pedostratigraphy			Average MAR
					Model I	Model II	Model III	
Stage 1 (12-0)	1.48	**219**						219
Stage 2 (24-12)	1.48	**241**						241
Stage 3 (59-24)	1.48							
Stage 4 (74-59)	1.48							
Stage 5 (130-74)	1.48							

References used to generate data report: Renjiahutong	
Data used	**Source**
Pedostratigraphy	Zhou et al. (1994)
Magnetic susceptibility	Zhou et al. (1994)
^{14}C dating	Zhou et al. (1994)
TL dating	-
Additional References:	
Data available	**Source**
-	-

Renjiapo section

Note: Section not used in analyses, because only grain size data is available.

Site location: 35.02° N, 107.37° E

References used to generate data report: Renjiapo	
Data used	**Source**
Pedostratigraphy	-
Magnetic susceptibility	-
^{14}C dating	-
TL dating	-
Additional References:	
Data available	**Source**
Grain size	Ding (unpublished data)

Shangjiapo section: MAR (g/m^2/yr) based on pedostratigraphy

Note: Stage 1 affected by cultivation layer.

(Model I: min. glacial, max. interglacial; Model II: max. glacial, min. interglacial; Model III: 2/3 of interglacial soil is aeolian deposit)

Site location: 34.32° N, 108.12° E

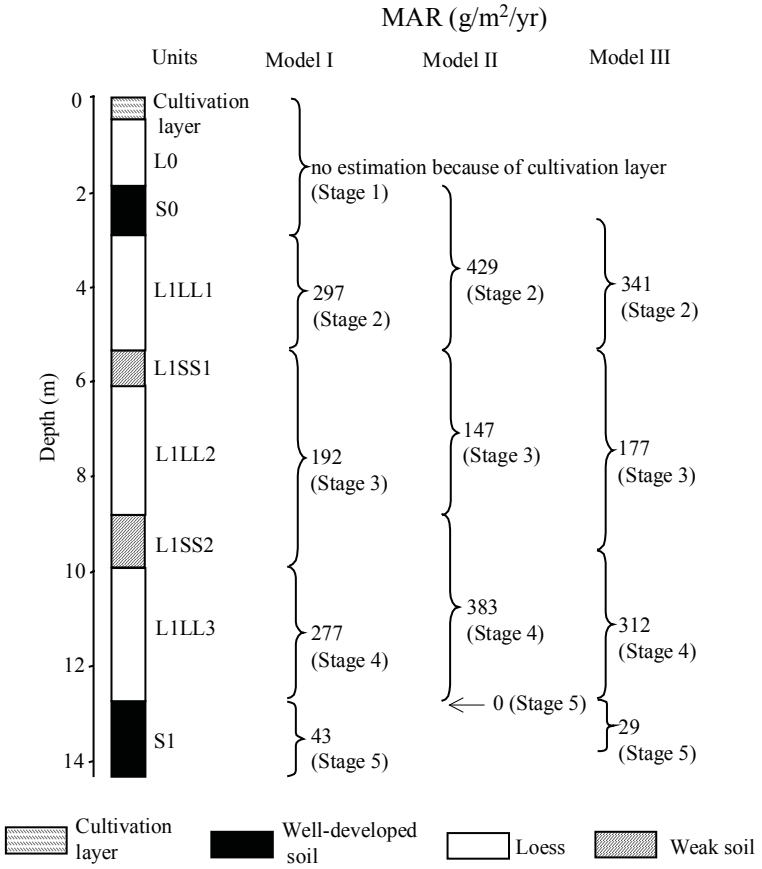

Stratigraphic data: Shangjiapo (thickness given by author, depth calculated from thickness)				
Top depth (m)	Bottom depth (m)	Thickness (m)	Stratigraphic units	DBD (g/cm³)
0.00	0.54	0.54	cultivation layer	n/a
0.54	1.88	1.34	L0	n/a
1.88	2.95	1.07	S0	n/a
2.95	5.36	2.41	L1LL1	n/a
5.36	6.16	0.80	L1SS1	n/a
6.16	8.84	2.68	L1LL2	n/a
8.84	9.91	1.07	L1SS2	n/a
9.91	12.72	2.81	L1LL3	n/a
12.72	14.34	1.62	S1	n/a

Age model (kyr): Shangjiapo						
Depth (m)	^{14}C	TL	Magnetic susceptibility	Pedostratigraphy (Model III)	Average chronology	Range
0						
2						
4				18.0	18.0	
6				29.2	29.2	
8				45.8	45.8	
10				61.0	61.0	
12				70.6	70.6	
14						

MAR (g/m²/yr): Shangjiapo								
Stage (range in kyr)	Assumed DBD (g/cm^3)	^{14}C	TL	MS	Pedostratigraphy			Average MAR
					Model I	Model II	Model III	
Stage 1 (12-0)	1.48							
Stage 2 (24-12)	1.48				297	429	**341**	341
Stage 3 (59-24)	1.48				192	147	**177**	177
Stage 4 (74-59)	1.48				277	383	**312**	312
Stage 5 (130-74)	1.48				43	0	**29**	29

References used to generate data report: Shangjiapo	
Data used	**Source**
Pedostratigraphy	Lei (1992)
Magnetic susceptibility	-
^{14}C dating	-
TL dating	-
Additional References:	
Data available	**Source**
Micromorphology	Lei (1992)

Shenjiazhuang section

Note: Thickness of top loess bed uncertain. No estimation for pedostratigraphy based MAR.

Site location: 36.72° N, 104.13° E

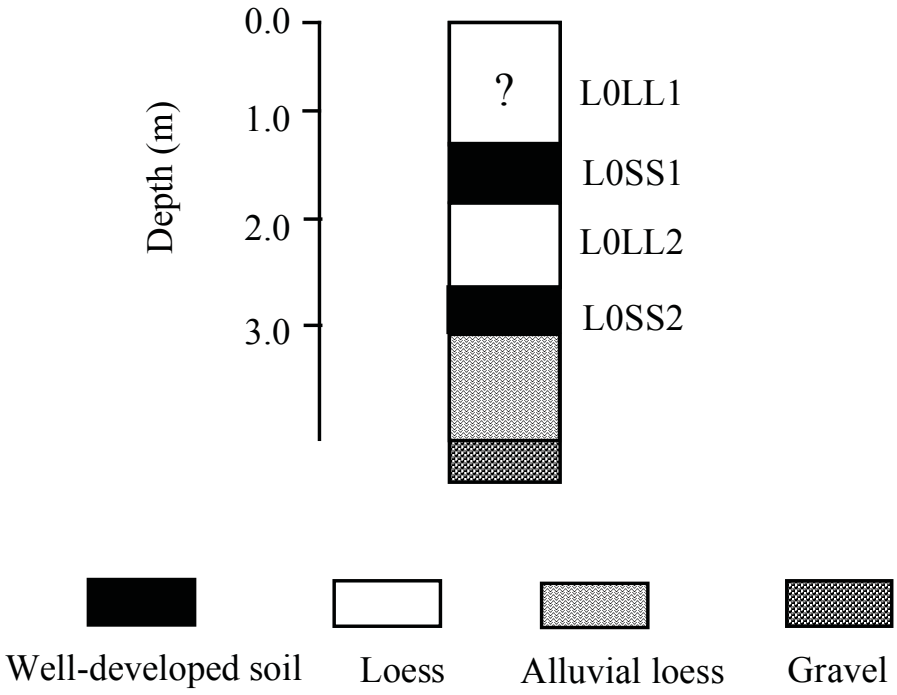

Stratigraphic data: Shenjiazhuang (depth and thickness estimated from diagram, to nearest 1 cm)				
Top depth (m)	Bottom depth (m)	Thickness (m)	Stratigraphic units	DBD (g/cm³)
0.00	1.10	1.10	L0LL1 - thickness uncertain	n/a
1.10	1.65	0.55	L0SS1	n/a
1.65	2.44	0.79	L0LL2	n/a
2.44	2.86	0.42	L0SS2	n/a
2.86	4.17	1.31	alluvial loess	n/a
4.17	4.56	0.39	gravel	n/a

Shenjiazhuang section: MAR (g/m^2/yr) based on ^{14}C dating

Note: Thickness of top loess bed uncertain.

Site location: 36.72° N, 104.13° E

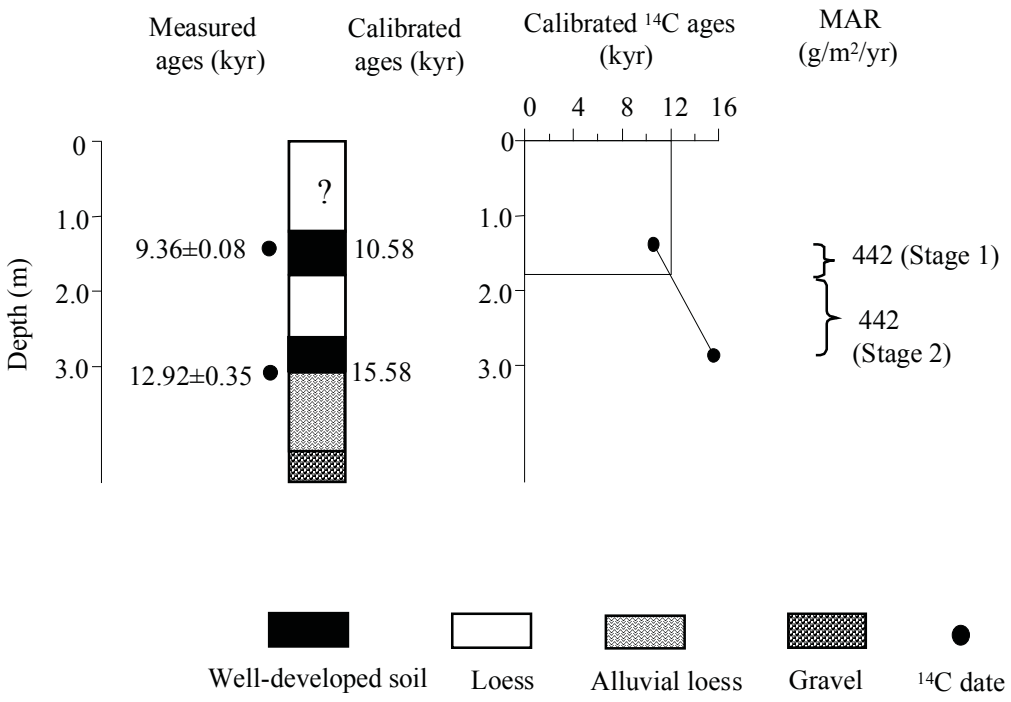

^{14}C dating: Shenjiazhuang (depth estimated from diagram, to nearest 1 cm)										
Depth (m)	Dating laboratory	Lab. No.	Dating material	Age (kyr)	s.d. (kyr)	(1σ) Calendar age ranges (kyr)	Relative probability	Assumed calendar age (kyr)	Reference	Comments
1.38	n/a	n/a	n/a	9.36	0.08	10.69-10.48	0.93	10.58	Chen et al. (1991b)	
						10.45-10.43	0.07			
2.87	n/a	n/a	n/a	12.9	0.35	16.03-15.13	0.748	15.58	Chen et al. (1991b)	
						14.73-14.38	0.252			

Age model (kyr): Shenjiazhuang						
Depth (m)	^{14}C	TL	Magnetic susceptibility	Pedostratigraphy (Model III)	Average chronology	Range
0						
0.5						
1						
1.5	10.6				10.6	
2	12.7				12.7	
2.5	14.3				14.3	

MAR (g/m²/yr): Shenjiazhuang								
Stage (range in kyr)	Assumed DBD (g/cm^3)	^{14}C	TL	MS	Pedostratigraphy			Average MAR
					Model I	Model II	Model III	
Stage 1 (12-0)	1.48	442						442
Stage 2 (24-12)	1.48	442						442
Stage 3 (59-24)	1.48							
Stage 4 (74-59)	1.48							
Stage 5 (130-74)	1.48							

References used to generate data report: Shenjiazhuang	
Data used	**Source**
Pedostratigraphy	Chen et al. (1991b)
Magnetic susceptibility	-
^{14}C dating	Chen et al. (1991b)
TL dating	-
Additional References:	
Data available	**Source**
-	-

Shimao section: MAR (g/m^2/yr) based on pedostratigraphy

Note: Deposits from Stages 1, 2, 3 and 4 contain sedimentary hiatuses**.**

(Model I: min. glacial, max. interglacial; Model II: max. glacial, min. interglacial; Model III: 2/3 of interglacial soil is aeolian deposit)

Site location: 37.92° N, 110.00° E

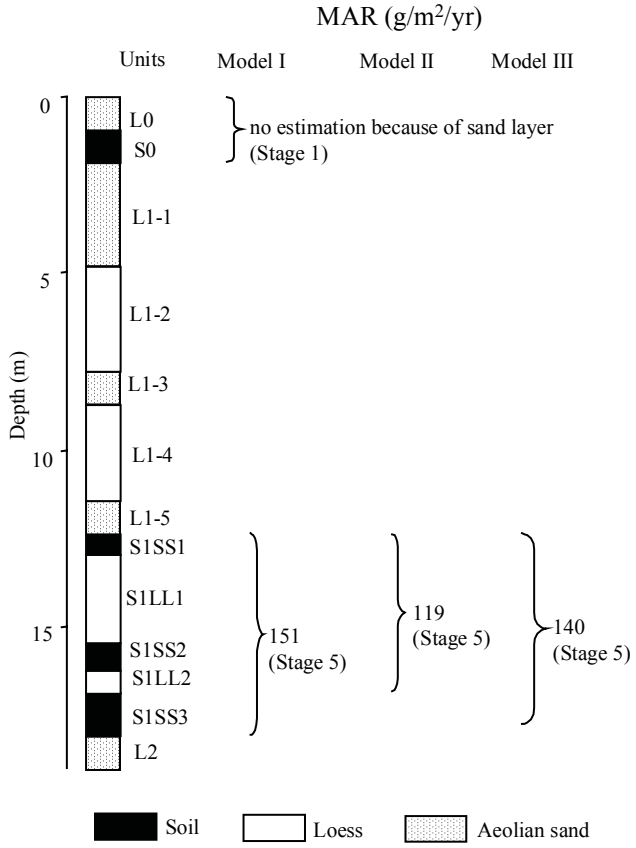

Stratigraphic data: Shimao (depths given by author)				
Top depth (m)	Bottom depth (m)	Thickness (m)	Stratigraphic units	DBD (g/cm³)
0.0	0.9	0.9	L0-sand	n/a
0.9	1.8	0.9	S0	n/a
1.8	4.7	2.9	L1-1-sand	n/a
4.7	7.7	3.0	L1-2	n/a
7.7	8.7	1.0	L1-3-sand	n/a
8.7	11.4	2.7	L1-4	n/a
11.4	12.3	0.9	L1-5-sand	n/a
12.3	12.9	0.6	S1SS1	n/a
12.9	15.4	2.5	S1LL1	n/a
15.4	16.1	0.7	S1SS2	n/a
16.1	16.8	0.7	S1LL2	n/a
16.8	18.0	1.2	S1SS3	n/a
18.0	19.0	1.0	L2	n/a

Shimao section: MAR (g/m^2/yr) based on TL dating

Note: Stages 1, 2, 3 and 4 deposits contain sedimentary hiatuses. Stage 5 MAR calculated based on available dates.

Site location: 37.92° N, 110.00° E

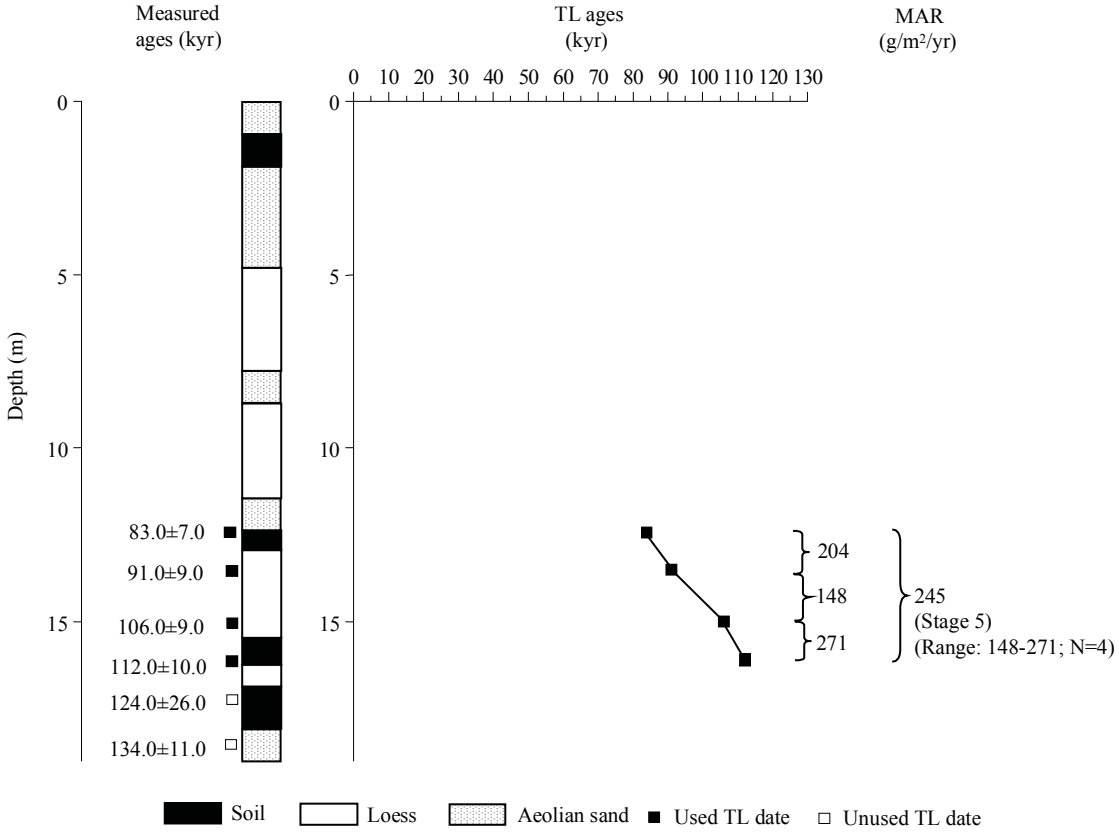

TL dating: Shimao (depth estimated from diagram, to nearest 10 cm)								
Depth (m)	Dating laboratory	Lab. No.	Dating material	TL-method	Age (kyr)	s.d. (kyr)	Reference	Comments
12.4	TL Lab. in Geology Institute, SSB	TL-67	n/a	fine-grain (4-11 µm) technique	83	7	Sun and Ding (1998)	
13.5	TL Lab. in Geology Institute, SSB	TL-16	n/a	fine-grain (4-11 µm) technique	91	9	Sun and Ding (1998)	
15	TL Lab. in Geology Institute, SSB	TL-17	n/a	fine-grain (4-11 µm) technique	106	9	Sun and Ding (1998)	
16.1	TL Lab. in Geology Institute, SSB	TL-68	n/a	fine-grain (4-11 µm) technique	112	10	Sun and Ding (1998)	
17.2	TL Lab. in Geology Institute, SSB	TL-69	n/a	fine-grain (4-11 µm) technique	124	26	Sun and Ding (1998)	uncertainties larger than 10 %
18.6	TL Lab. in Geology Institute, SSB	TL-18	n/a	fine-grain (4-11 µm) technique	134	11	Sun and Ding (1998)	>130 kyr

Shimao section: Magnetic susceptibility

Note: Deposits from Stages 1, 2, 3 and 4 contain sedimentary hiatuses. MS datanot used.

Site location: 37.92° N, 110.00° E

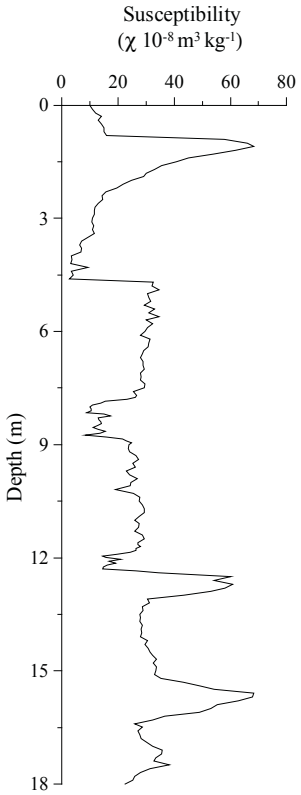

Age model (kyr): Shimao						
Depth (m)	^{14}C	TL	Magnetic susceptibility	Pedostratigraphy (Model III)	Average chronology	Range
0						
3						
6						
9						
12						
15		106		102.7	104.3	102.7-106.0
18		129.5			129.5	

MAR (g/m²/yr): Shimao								
Stage (range in kyr)	Assumed DBD (g/cm^3)	^{14}C	TL	MS	Pedostratigraphy			Average MAR
					Model I	Model II	Model III	
Stage 1 (12-0)	1.48							
Stage 2 (24-12)	1.48							
Stage 3 (59-24)	1.48							
Stage 4 (74-59)	1.48							
Stage 5 (130-74)	1.48		**245**		151	119	**140**	193

References used to generate data report: Shimao	
Data used	**Source**
Pedostratigraphy	Sun and Ding (1998)
Magnetic susceptibility	Sun and Ding (1998)
^{14}C dating	-
TL dating	Sun and Ding (1998)
Additional References:	
Data available	**Source**
CBD-Fe	Sun and Ding (1998)
Pedostratigraphy, TL, magnetic susceptibility	Sun et al. (1998)
Pedostratigraphy, TL, magnetic susceptibility, grain size, magnetic polarity	Sun et al. (1999)

Taishanxincun section: Pedostratigraphy

Note: Section not used, because top part disturbed by colluvium and pedostratigraphy cannot be correlated with that of the CLP.

Site location: 32.17° N, 118.60° E

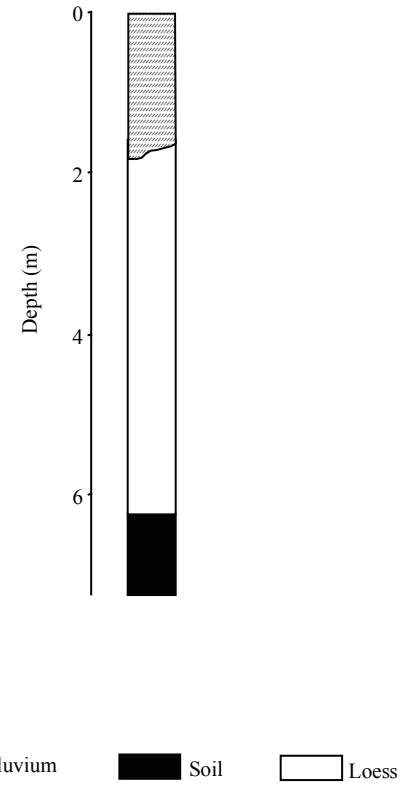

Stratigraphic data: Taishanxincun				
Top depth (m)	Bottom depth (m)	Thickness (m)	Stratigraphic units	DBD (g/cm^3)
0	1.68	1.68	colluvium	n/a
1.68	6.17	4.49	loess	n/a
6.17	7.29	1.12	soil	n/a
7.29	10.09	2.8	loess	n/a
10.09	11.21	1.12	soil	n/a
11.21	15.25	4.04	loess	n/a
15.25	17.38	2.13	soil	n/a
17.38	19.06	1.68	loess	n/a
19.06	21.87	2.81	bedrock	n/a

References used to generate data report: Taishanxincun	
Data used	**Source**
Pedostratigraphy	Zheng et al. (1994)
Magnetic susceptibility	-
^{14}C dating	-
TL dating	-
Additional References:	
Data available	**Source**
-	-

Tuxiangdao section: MAR (g/m^2/yr) based on pedostratigraphy

Note: Last glacial loess (L1) is not subdivided.

(Model I: min. glacial, max. interglacial; Model II: max. glacial, min. interglacial; Model III: 2/3 of interglacial soil is aeolian deposit)

Site location: 36.58° N, 101.73° E

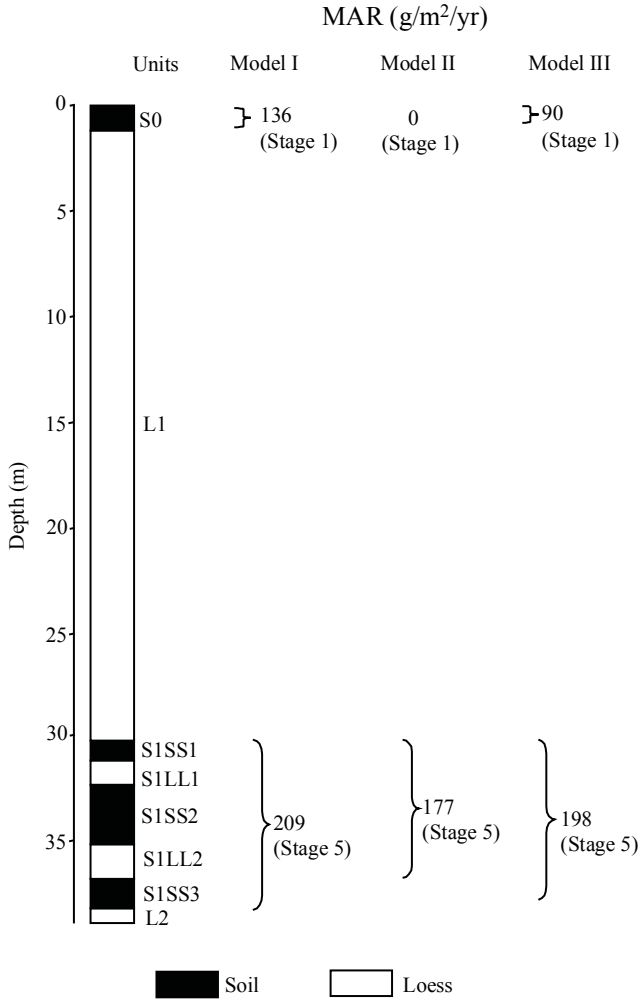

Stratigraphic data: Tuxiangdao (depth and thickness estimated from diagram, to nearest 5 cm)				
Top depth (m)	Bottom depth (m)	Thickness (m)	Stratigraphic units	DBD (g/cm³)
0.00	1.10	1.10	S0	n/a
1.10	30.10	29.00	L1	n/a
30.10	31.10	1.00	S1SS1	n/a
31.10	32.25	1.15	S1LL1	n/a
32.25	35.05	2.80	S1SS2	n/a
35.05	36.80	1.75	S1LL2	n/a
36.80	38.00	1.20	S1SS3	n/a
38.00	38.80	0.80	L2	n/a

Tuxiangdao section: MAR (g/m^2/yr) based on TL dating

Note: Last glacial loess (L1) is not subdivided. Stages 4 and 5 MAR calculated based on available dates.

Site location: 36.58° N, 101.73° E

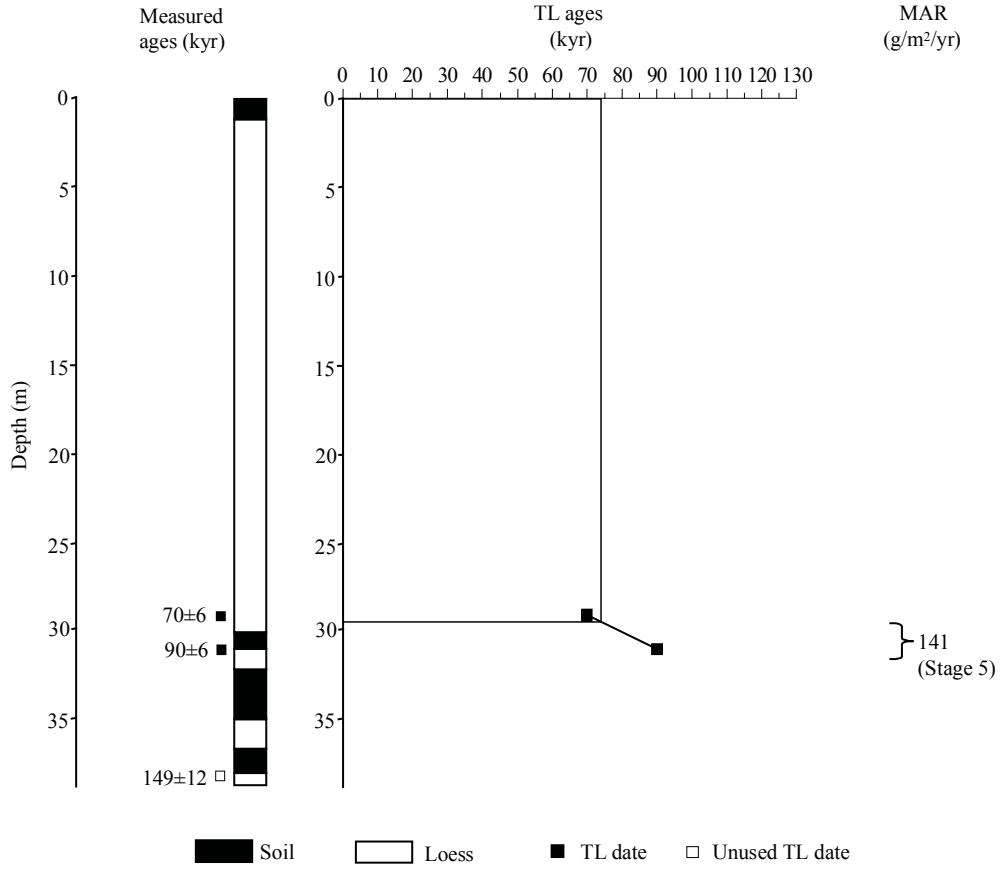

TL dating: Tuxiangdao (depth estimated from diagram, to nearest 10 cm)								
Depth (m)	Dating laboratory	Lab. No.	Dating material	TL-method	Age (kyr)	s.d. (kyr)	Reference	Comments
29.2	Xi'an Loess Lab.	n/a	n/a	n/a	70	6	Chen et al. (1999)	
31.1	Xi'an Loess Lab.	n/a	n/a	n/a	90	6	Chen et al. (1999)	
38.2	Xi'an Loess Lab.	n/a	n/a	n/a	149	12	Chen et al. (1999)	not used, age > 130 kyr

Age model (kyr): Tuxiangdao						
Depth (m)	^{14}C	TL	Magnetic susceptibility	Pedostratigraphy (Model III)	Average chronology	Range
0				0.0	0.0	
6						
12						
18						
24						
30		78.4			78.4	
36				118.1	118.1	

MAR (g/m²/yr): Tuxiangdao								
Stage (range in kyr)	Assumed DBD (g/cm^3)	^{14}C	TL	MS	Pedostratigraphy			Average MAR
					Model I	Model II	Model III	
Stage 1 (12-0)	1.48				136	0	**90**	90
Stage 2 (24-12)	1.48							
Stage 3 (59-24)	1.48							
Stage 4 (74-59)	1.48							
Stage 5 (130-74)	1.48		141		209	177	**198**	170

References used to generate data report: Tuxiangdao	
Data used	**Source**
Pedostratigraphy	Chen et al. (1997) for L1+S0, Chen et al. (1999) for S1+L2
Magnetic susceptibility	-
^{14}C dating	-
TL dating	Chen et al. (1999)
Additional References:	
Data available	**Source**
Magnetic susceptibility, grain size, $CaCO_3$	Chen et al. (1999)

Wangning section: pedostratigraphic information

Note: Section not used, because pedostratigraphy and magnetic susceptibility cannot be easily correlated with that of the CLP.

Site location: 37.02° N, 112.95° E

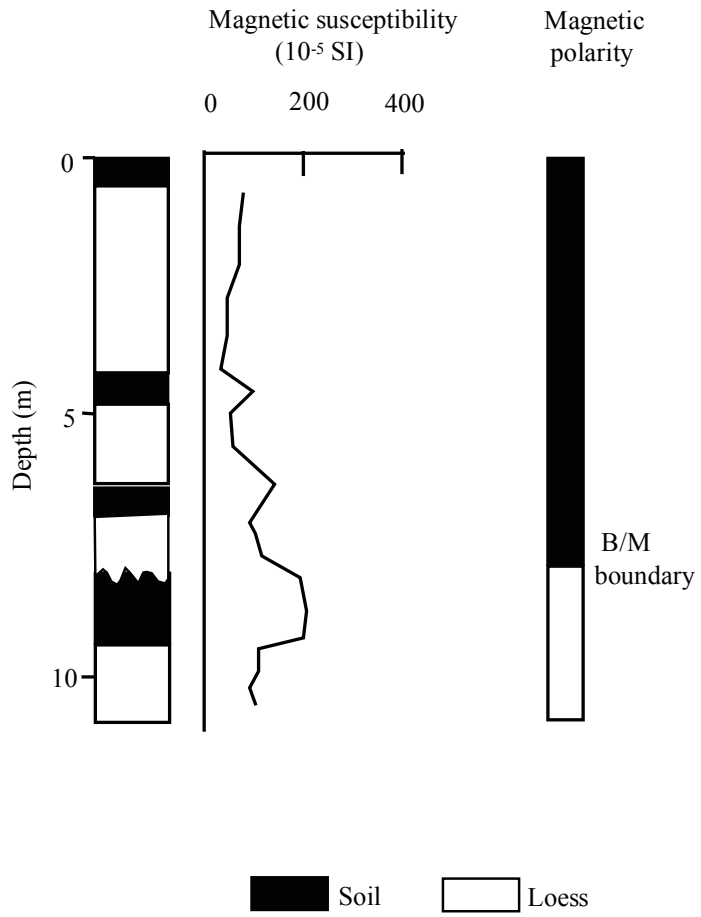

References used to generate data report: Wangning	
Data used	**Source**
Pedostratigraphy	Shi (1994)
Magnetic susceptibility	-
^{14}C dating	-
TL dating	-
Additional References:	
Data available	**Source**
Magnetic susceptibility, magnetic polarity	Shi (1994)

Weinan (Yangguo) section: MAR (g/m^2/yr) based on pedostratigraphy

Note: Liu et al. (1994) used the name of the nearest city for this loess section. Yangguo is the name of the town where the section is located.

(Model I: min. glacial, max. interglacial; Model II: max. glacial, min. interglacial; Model III: 2/3 of interglacial soil is aeolian deposit)

Site location: 34.35° N, 109.52° E

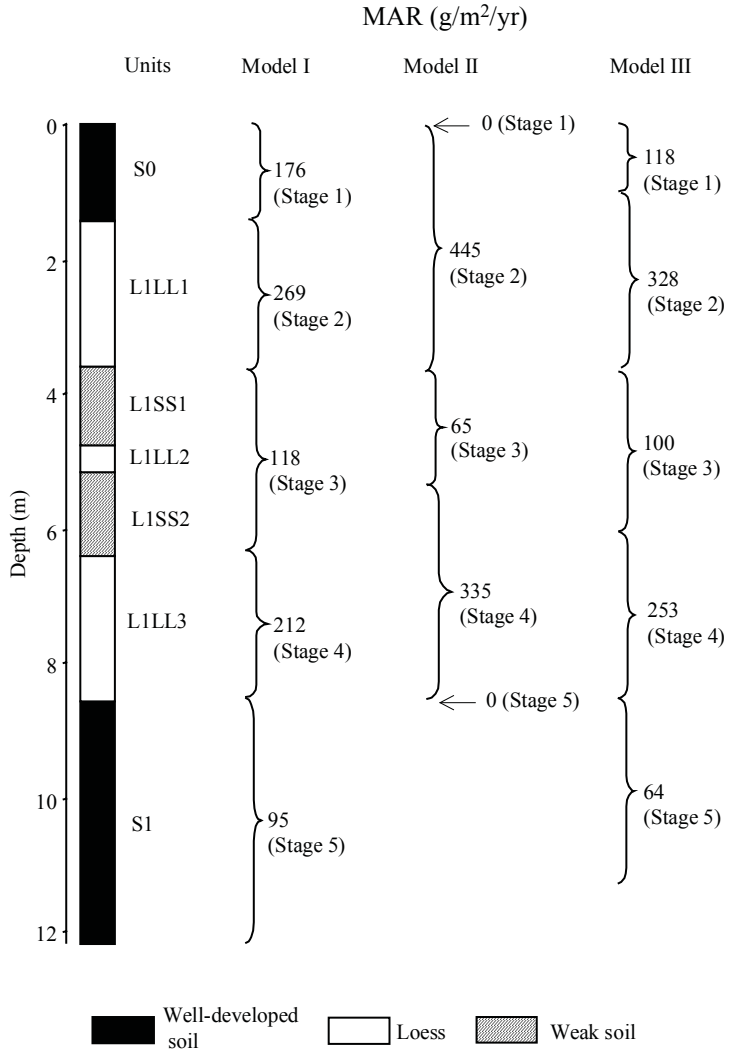

Stratigraphic data: (thickness given by authors in text, depth calculated from thickness)				
Top depth (m)	Bottom depth (m)	Thickness (m)	Stratigraphic units	DBD (g/cm^3)
0.00	1.43	1.43	S0	n/a
1.43	3.61	2.18	L1LL1	n/a
3.61	4.77	1.16	L1SS1	n/a
4.77	5.15	0.38	L1LL2	n/a
5.15	6.40	1.25	L1SS2	n/a
6.40	8.55	2.15	L1LL3	n/a
8.55	12.16	3.61	S1	n/a

Weinan (Yangguo) section: MAR (g/m^2/yr) based on ^{14}C and TL dating

Note: Liu et al. (1994) used the name of the nearest city for this loess section. Yangguo is the name of the town where the section is located.

Site location: 34.35° N, 109.52° E

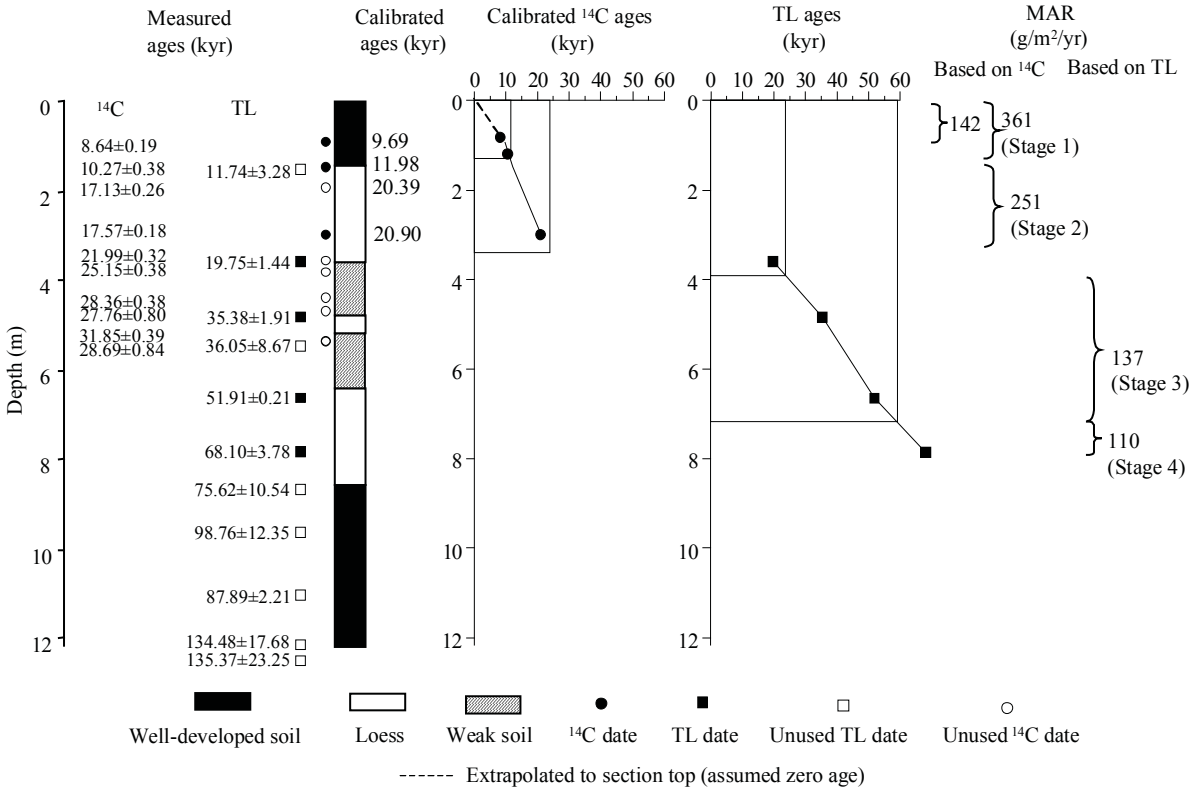

^{14}C dating: Weinan (Yangguo) (depth given by the authors)										
Depth (m)	Dating laboratory	Lab. No.	Dating material	Age (kyr)	s.d. (kyr)	(1σ) Calendar age ranges (kyr)	Relative probability	Assumed calendar age (kyr)	Reference	Comments
0.93	AMS ^{14}C Lab. Peking Univ.	BA92110	humin (insoluble)	8.64	0.2	9.47-9.92	0.957	9.69	Liu et al. (1994a)	
						10.09-10.11	0.043		Liu et al. (1994a)	
0.93	AMS ^{14}C Lab. Peking Univ.	BA92110	Humic acid (soluble)	4.87	0.2	5.46-5.75	0.913	5.60	Liu et al. (1994a)	duplicate sample; soluble fraction; not used, after authors
						5.33-5.37	0.065		Liu et al. (1994a)	
						5.83-5.85	0.022		Liu et al. (1994a)	
1.49	AMS ^{14}C Lab. Peking Univ.	BA92114	humin	10.27	0.4	11.55-12.42	0.748	11.98	Liu et al. (1994a)	
						12.46-12.63	0.139		Liu et al. (1994a)	
						11.41-11.51	0.076		Liu et al. (1994a)	
						11.34-11.39	0.038		Liu et al. (1994a)	
1.95	AMS ^{14}C Lab. Peking Univ.	BA92115	humin	17.13	0.3	19.96-20.82	1	20.39	Liu et al. (1994a)	not used, overlapping

^{14}C dating: Weinan (Yangguo)										
Depth (m)	Dating laboratory	Lab. No.	Dating material	Age (kyr)	s.d. (kyr)	(1σ) Calendar age ranges (kyr)	Relative probability	Assumed calendar age (kyr)	Reference	Comments
3.00	AMS ^{14}C Lab. Peking Univ.	BA92116	humin	17.57	0.2	20.52-21.28	1	20.90	Liu et al. (1994a)	
3.00	AMS ^{14}C Lab. Peking Univ.	BA92116	humic acid	16.85	0.2	19.71-20.42	1	20.07	Liu et al. (1994a)	duplicate sample; soluble fraction; not used, after authors
3.58	AMS ^{14}C Lab. Peking Univ.	BA92118	humin	21.99	0.3				Liu et al. (1994a)	beyond calibration range
3.83	AMS ^{14}C Lab. Peking Univ.	BA92119	humin	25.15	0.4				Liu et al. (1994a)	beyond calibration range
3.83	AMS ^{14}C Lab. Peking Univ.	BA92119	Humic acid	26.91	0.6				Liu et al. (1994a)	duplicate sample; soluble fraction; not used, after authors
4.41	AMS ^{14}C Lab. Peking Univ.	BA92122	humin	28.36	0.4				Liu et al. (1994a)	beyond calibration range
4.41	AMS ^{14}C Lab. Peking Univ.	BA92122	humic acid	33.77	0.4				Liu et al. (1994a)	duplicate sample; soluble fraction; not used, after authors
4.71	AMS ^{14}C Lab. Peking Univ.	BA92124	humin	27.76	0.8				Liu et al. (1994a)	beyond calibration range
4.71	AMS ^{14}C Lab. Peking Univ.	BA92124	Humic acid	29.2	0.7				Liu et al. (1994a)	duplicate sample; soluble fraction; not used, after authors
5.37	AMS ^{14}C Lab. Peking Univ.	BA92127	humin	31.85	0.4				Liu et al. (1994a)	beyond calibration range
5.37	AMS ^{14}C Lab. Peking Univ.	BA92127	humic acid	39.37	0.5				Liu et al. (1994a)	duplicate sample; soluble fraction; not used, after authors
5.39	AMS ^{14}C Lab. Peking Univ.	BA92125	humin	28.69	0.8				Liu et al. (1994a)	not used, after authors
5.39	AMS ^{14}C Lab. Peking Univ.	BA92125	humic acid	34.54	0.8				Liu et al. (1994a)	duplicate sample; soluble fraction; not used, after authors

TL dating: Weinan (Yangguo) (depth given by authors)								
Depth (m)	Dating laboratory	Lab. No.	Dating material	TL-method	Age (kyr)	s.d. (kyr)	Reference	Comments
1.55	TL Lab. Peking U.	HT-17	n/a	fine-grain (20-80 µm) technique	11.7	3.3	Liu et al. (1994a)	not used, error bar >10%
3.60	TL Lab. Peking U.	HT-15	n/a	fine-grain (20-80 µm) technique	19.8	1.4	Liu et al. (1994a)	
4.85	TL Lab. Peking U.	HT-24	n/a	fine-grain (20-80 µm) technique	35.4	1.9	Liu et al. (1994a)	
5.50	TL Lab. Peking U.	HT-18	n/a	fine-grain (20-80 µm) technique	36.1	8.7	Liu et al. (1994a)	not used, error bar >10%
6.65	TL Lab. Peking U.	HT-23	n/a	fine-grain (20-80 µm) technique	51.9	0.2	Liu et al. (1994a)	
7.85	TL Lab. Peking U.	HT-28	n/a	fine-grain (20-80 µm) technique	68.1	3.8	Liu et al. (1994a)	
8.70	TL Lab. Peking U.	HT-19	n/a	fine-grain (20-80 µm) technique	75.6	11	Liu et al. (1994a)	not used, error bar >10%
9.65	TL Lab. Peking U.	HT-26	n/a	fine-grain (20-80 µm) technique	98.8	12	Liu et al. (1994a)	not used, error bar >10%
11.05	TL Lab. Peking U.	HT-29	n/a	fine-grain (20-80 µm) technique	87.9	2.2	Liu et al. (1994a)	reversal (not used by authors)
12.16	TL Lab. Peking U.	HT-21	n/a	fine-grain (20-80 µm) technique	134.5	18	Liu et al. (1994a)	not used, error bar >10%
12.40	TL Lab. Peking U.	HT-30	n/a	fine-grain (20-80 µm) technique	135.4	23	Liu et al. (1994a)	not used, error bar >10%

Weinan (Yangguo) section: MAR (g/m^2/yr) based on magnetic susceptibility

Note: Liu et al. (1994) used the name of the nearest city for this loess section. Yangguo is the name of the town where the section is located.

Site location: 34.35° N, 109.52° E

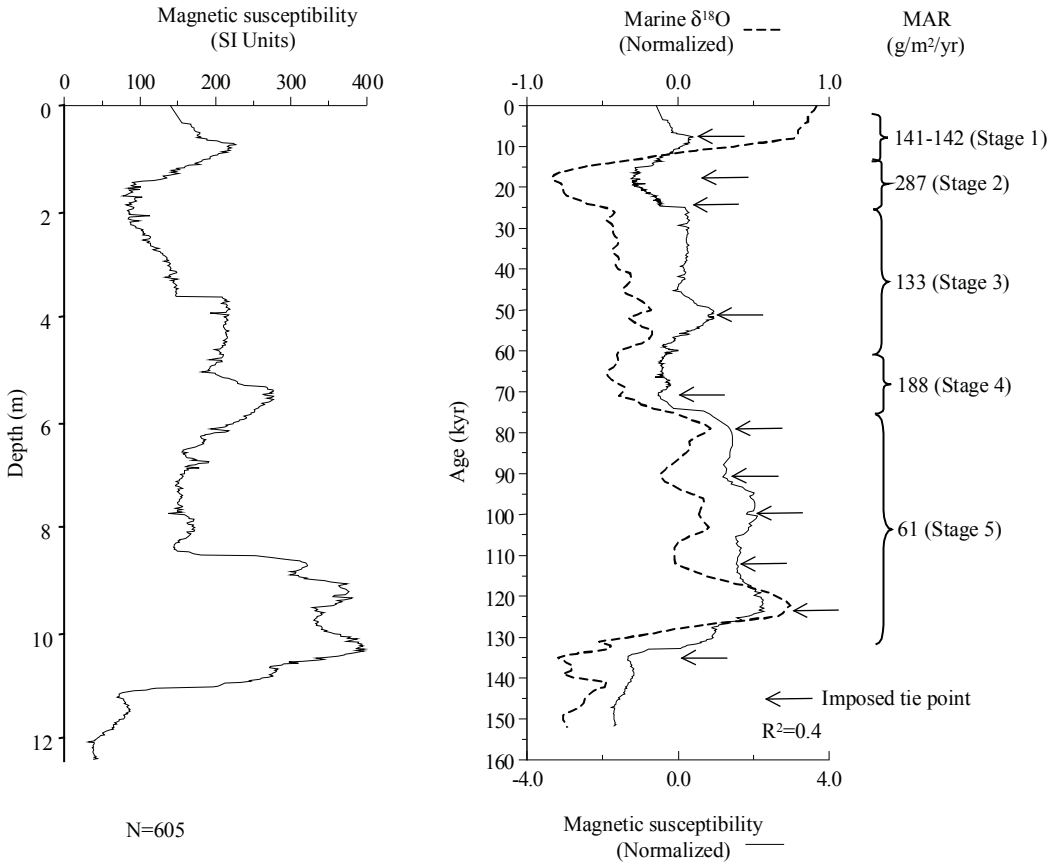

MS age model: Weinan (Yangguo)		
Tie-Point	Depth (m)	Age (kyr)
1	0.74	7.81
2	1.70	17.85
3	3.60	24.46
4	5.50	51.57
5	8.44	71.12
6	8.66	79.25
7	8.90	90.95
8	9.32	99.96
9	9.76	112.28
10	10.36	123.79
11	11.20	135.34

Age model (kyr): Weinan (Yangguo)						
Depth (m)	^{14}C	TL	Magnetic susceptibility	Pedostratigraphy (Model III)	Average chronology	Range
0	0		0	0.0	0.0	-
2	15		18.9	16.8	16.9	15.0-18.9
4		24.5	30..2	29.7	28.1	24.5-30.2
6		45.8	54.9	59.1	53.3	45.8-59.1
8			68.2	70.9	69.5	68.2-70.9
10			116.9	108.1	112.5	108.1-116.9
12			146.3		146.3	

MAR ($g/m^2/yr$): Weinan (Yangguo)								
Stage (range in kyr)	Assumed DBD (g/cm^3)	^{14}C	TL	MS	Pedostratigraphy			Average MAR
					Model I	Model II	Model III	
Stage 1 (12-0)	1.48	**361**		**142**	176	0	**118**	207
Stage 2 (24-12)	1.48	**251**		**287**	269	445	**328**	289
Stage 3 (59-24)	1.48		**137**	**133**	118	65	**100**	123
Stage 4 (74-59)	1.48		**110**	**188**	212	335	**253**	184
Stage 5 (130-74)	1.48			**61**	95	0	**64**	63

References used to generate data report: Weinan (Yangguo)	
Data used	**Source**
Pedostratigraphy	Liu et al. (1994a)
Magnetic susceptibility	Sun and Ding (1997)
^{14}C dating	Liu et al. (1994a)
TL dating	Liu et al. (1994a)
Additional References:	
Data available	**Source**
Pedostratigraphy, magnetic polarity	Ding et al. (1990)
Pedostratigraphy, magnetic polarity	Ding et al. (1991)
Pedostratigraphy, magnetic polarity	Rutter et al. (1991)
Pedostratigraphy, ^{14}C, TL, chemical parameters, micromorphology	Liu et al. (1995)
Pedostratigraphy, magnetic susceptibility, chemical parameters	Guo et al. (1996a)
Micromorphology, chemical parameters	Guo et al. (1996b)
Pedostratigraphy, magnetic susceptibility, ^{14}C, TL, chemical parameters, micromorphology	Guo et al. (1996c)
Magnetic susceptibility	Guo et al. (1998)

Wuyishan section: MAR (g/m^2/yr) based on pedostratigraphy

Note: The stratigraphic section shown by Chen et al. (1991b) shows a break in the L1 loess (Stage 2). No additional information is given about the nature of this section break. MAR was therefore only calculated for Stages 3, 4 and 5.

(Model I: min. glacial, max. interglacial; Model II: max. glacial, min. interglacial; Model III: 2/3 of interglacial soil is aeolian deposit)

Site location: 35.80° N, 103.22° E

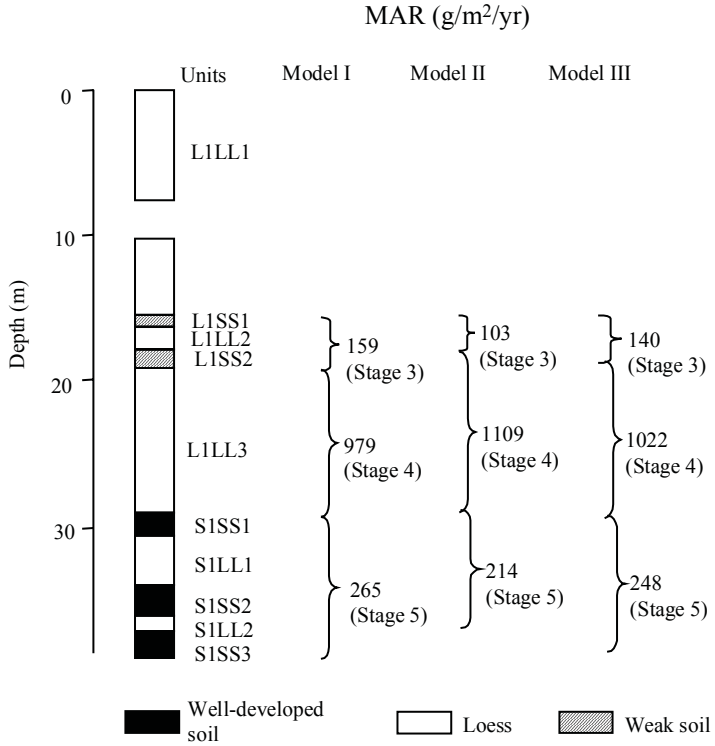

Stratigraphic data: Wuyishan (depth and thickness estimated from diagram, to nearest 1 cm)				
Top depth (m)	Bottom depth (m)	Thickness (m)	Stratigraphic units	DBD (g/cm^3)
0.00	7.59	7.59	L1LL1	n/a
7.59	10.13	section break		n/a
10.13	15.19	5.06	L1LL1	n/a
15.19	16.05	0.86	L1SS1	n/a
16.05	17.62	1.57	L1LL2	n/a
17.62	18.94	1.32	L1SS2	n/a
18.94	28.86	9.92	L1LL3	n/a
28.86	30.63	1.77	S1SS1	n/a
30.63	33.92	3.29	S1LL1	n/a
33.92	35.95	2.03	S1SS2	n/a
35.95	36.96	1.01	S1LL2	n/a
36.96	38.88	1.92	S1SS3	n/a

Age model (kyr): Wuyishan						
Depth (m)	^{14}C	TL	Magnetic susceptibility	Pedostratigraphy (Model III)	Average chronology	Range
0						
5						
10						
15						
20				61.2	61.2	
25				68.4	68.4	
30				80.8	80.8	
35				110.7	110.7	

MAR (g/m²/yr): Wuyishan								
Stage (range in kyr)	Assumed DBD (g/cm^3)	^{14}C	TL	MS	Pedostratigraphy			Average MAR
					Model I	Model II	Model III	
Stage 1 (12-0)	1.48							
Stage 2 (24-12)	1.48							
Stage 3 (59-24)	1.48				159	103	**140**	140
Stage 4 (74-59)	1.48				979	1109	**1022**	1022
Stage 5 (130-74)	1.48				265	214	**62**	62

References used to generate data report: Wuyishan	
Data used	**Source**
Pedostratigraphy	Chen et al. (1991b)
Magnetic susceptibility	-
^{14}C dating	-
TL dating	-
Additional References:	
Data available	**Source**
-	-

Xiadongcun (Jixian) section: MAR (g/m^2/yr) based on pedostratigraphy

Note: Jixian is the name of the County in which the section is located and was used by Han and Jiang (1999) to identify the section. Xiadongcun is the name of the village where the section is located.

(Model I: min. glacial, max. interglacial; Model II: max. glacial, min. interglacial; Model III: 2/3 of interglacial soil is aeolian deposit)

Site location: 36.10° N, 110.67° E

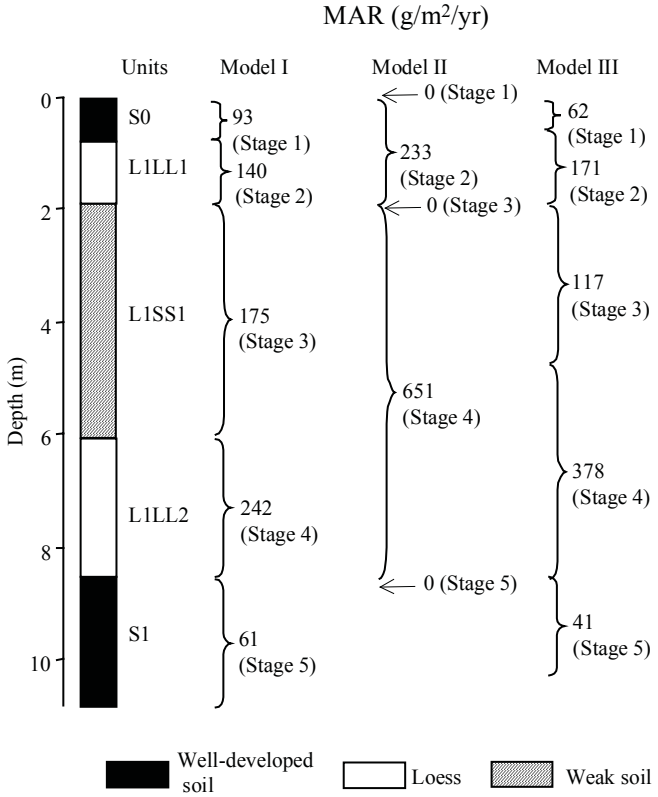

Stratigraphic data: Xiadongcun (Jixian) (depth and thickness estimated from diagram, to nearest 1 cm)				
Top depth (m)	Bottom depth (m)	Thickness (m)	Stratigraphic units	DBD (g/cm^3)
0.000	0.755	0.755	S0	n/a
0.755	1.890	1.135	L1LL1	n/a
1.890	6.040	4.150	L1SS1	n/a
6.040	8.490	2.450	L1LL2	n/a
8.490	10.800	2.310	S1	n/a

Xiadongcun (Jixian) section: MAR (g/m^2/yr) based on magnetic susceptibility

Note: Jixian is the name of the County in which the section is located and was used by Han and Jiang (1999) to identify the section. Xiadongcun is the name of the village where the section is located. There are two versions of the MS data. One (this page) was digitized from Han and Jiang (1999). The other was made available bz Dr. Han Jiamao (see next page).

Site location: 36.10° N, 110.67° E

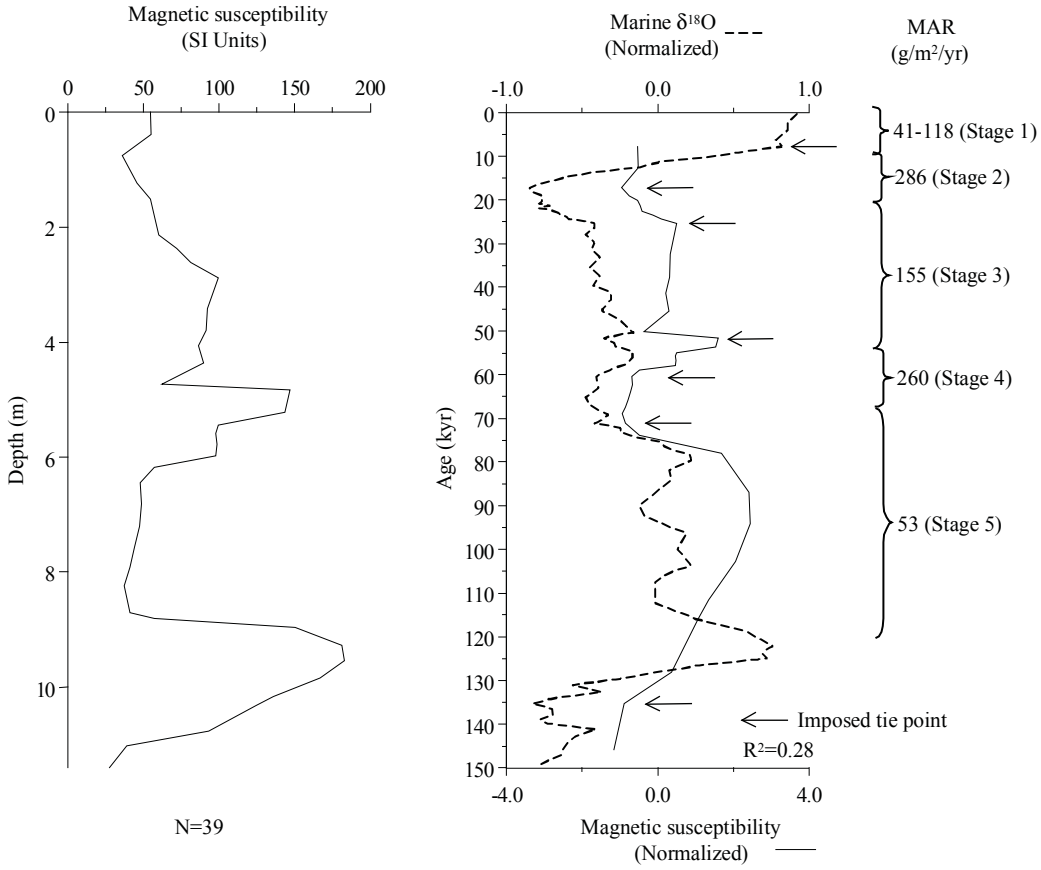

MS age model: Xiadongcun (Jixian)		
Tie-Point	Depth (m)	Age (kyr)
1	0.00	7.81
2	0.76	17.31
3	2.88	25.42
4	4.83	51.57
5	6.44	60.44
6	8.71	71.12
7	11.02	135.34

Xiadongcun (Jixian) section: MAR (g/m^2/yr) based on magnetic susceptibility

Note: Jixian is the name of the County in which the section is located and was used by Han and Jiang (1999) to identify the section. Xiadongcun is the name of the village where the section is located. There are two versions of the MS data. One (previous page) was digitized from Han and Jiang (1999). The other was made available by Dr. Han Jiamao and taken from the data archive at the Institute of Geology, Chinese Academy of Science, P. O. Box 9825, Beijing 100029, China.

Site location: 36.10° N, 110.67° E

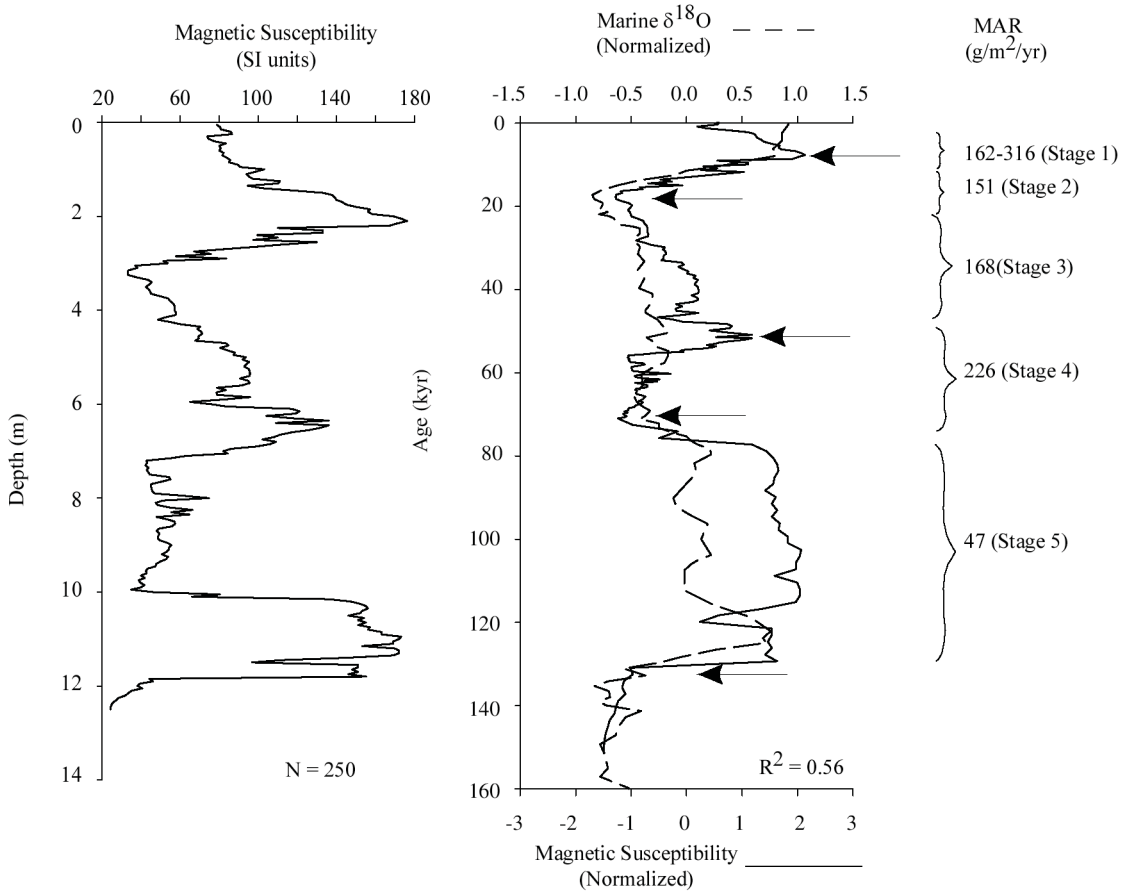

MS age model: Xiadongcun (Jixian)		
Tie-Point	Depth (m)	Age (kyr)
1	2.1	7.81
2	3.2	17.85
3	6.4	51.57
4	9.95	71.12
5	11.85	131.09

Age model (kyr): Xiadongcun (Jixian)							
Depth (m)	^{14}C	TL	Magnetic susceptibility	Magnetic susceptibility (2)	Pedostratigraphy (Model III)	Average chronology	Range
0			0.0	0.0	0.0	0.0	
2			22.1	7.4	25.2	18.2	7.4-25.2
4			40.4	26.3	50.6	39.1	26.3-50.6
6			58.0	49.4	64.1	57.2	49.4-64.1
8			67.9	60.4	71.9	66.7	60.4-71.9
10			107.1	72.7	128.1	102.6	72.7-128.1

MAR ($g/m^2/yr$): Xiadongcun (Jixian)									
Stage (range in kyr)	Assumed DBD (g/cm^3)	^{14}C	TL	MS	MS (2)	Pedostratigraphy			Average MAR
						Model I	Model II	Model III	
Stage 1 (12-0)	1.48			**80**	**239**	93	0	**62**	127
Stage 2 (24-12)	1.48			**286**	**151**	140	233	**171**	203
Stage 3 (59-24)	1.48			**155**	**168**	175	0	**117**	147
Stage 4 (74-59)	1.48			**260**	**226**	242	651	**378**	288
Stage 5 (130-74)	1.48			**53**	**47**	61	0	**41**	47

References used to generate data report: Xiadongcun (Jixian)	
Data used	**Source**
Pedostratigraphy	Han et al. (1991a)
Magnetic susceptibility	Han and Jiang (1999)
^{14}C dating	-
TL dating	-
Additional References:	
Data available	**Source**
Magnetic remanence	Han et al. (1991a)
Pedostratigraphy, magnetic susceptibility, magnetic remanence	Han et al. (1991b)
Pedostratigraphy, magnetic susceptibility, grain size	Han and Jiang (1999)

Xiangyang (Chenshan) section

Note: Stratigraphic division of S1 follows the authors. Section not used, because it contains multiple hiatuses and only the range of thickness is given by the authors.

Site location: 30.87° N, 118.87° E

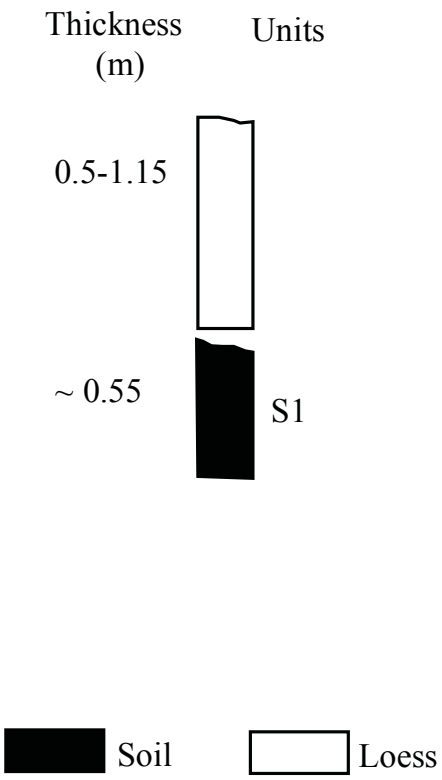

Xiangyang (Chenshan) section: Magnetic susceptibility

Note: MS data not used to estimate MAR, because of sedimentary hiatuses. Digitized MS data.

Site location: 30.87° N, 118.87° E

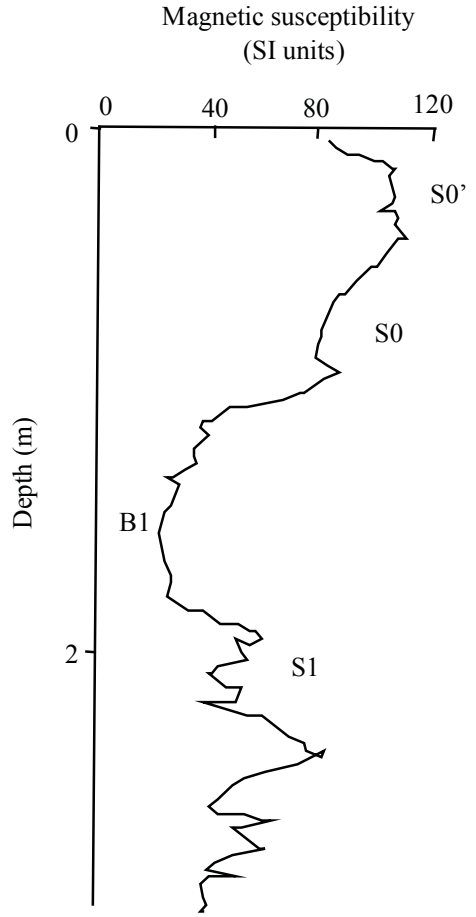

References used to generate data report: Xiangyang (Chenshan)	
Data used	**Source**
Pedostratigraphy	Yang et al. (1991)
Magnetic susceptibility	Li et al. (1997)
^{14}C dating	-
TL dating	-
Additional References:	
Data available	**Source**
Grain size	Yang et al. (1991)
Pedostratigraphy, magnetic susceptibility, grain size	Li et al. (1997)

Xiazhupan section: Pedostratigraphy

Note: Section not used to estimate MAR, because the loess unit contains a gravel layer, and the stratigraphy cannot be correlated with that of the CLP.

Site location: 37.77º N, 120.66º E

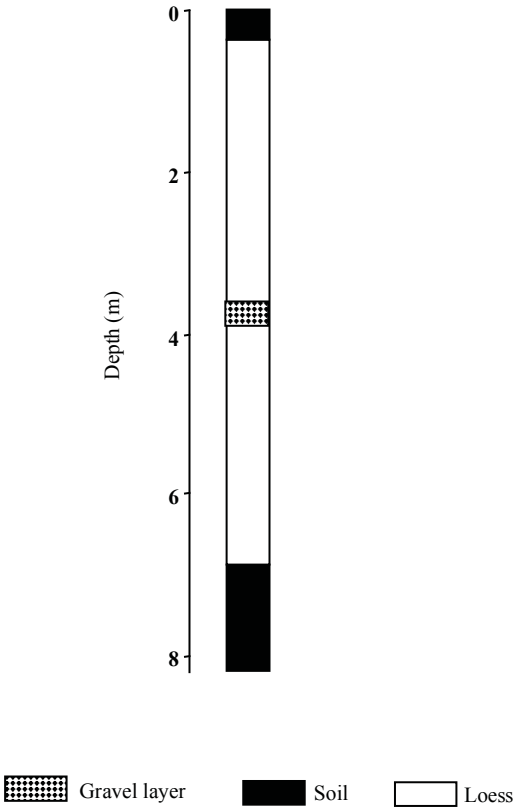

References used to generate data report: Xiazhupan	
Data used	**Source**
Pedostratigraphy	Zheng et al. (1994)
Magnetic susceptibility	-
^{14}C dating	-
TL dating	-
Additional References:	
Data available	**Source**
-	-

Xietongmen section: Pedostratigraphy

Note: Section not used to estimate MAR, because the stratigraphy cannot be correlated with the CLP stratigraphy, and the section contains sand layers. These four sections (Duobutang, Qijidong, Xietongmen, and Xigaze) are all from the Tibetan Plateau, and were scanned as a unit. The top age on the Xietongmen section is ^{14}C date, all the other ages are TL dates.

Site location: 29.43° N, 88.36° E

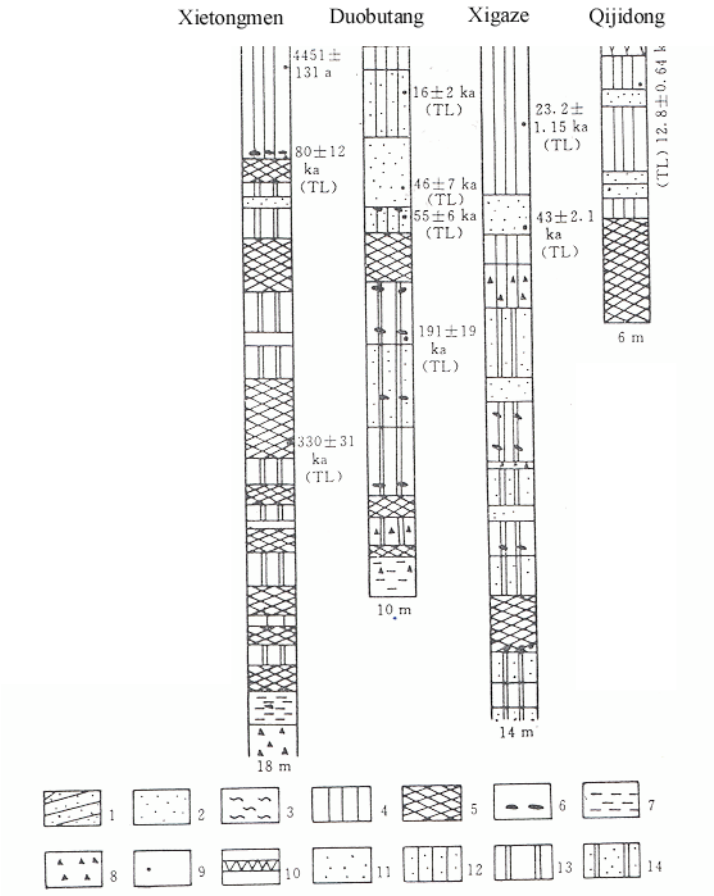

Legend: 1. Bedded sand; 2. Aeolian fine sand, 3. Fluvial layer, 4. Loess, 5. Palaeosol, 6. Nodule
7. Fluvial clay, 8. Gravel layer, 9. Sampling position, 10. Grass layer, 11. Medium sand

References used to generate data report: Xietongmen	
Data used	**Source**
Pedostratigraphy	Jin et al. (1998)
Magnetic susceptibility	-
^{14}C dating	-
TL dating	Jin et al. (1998)
Additional References:	
Data available	**Source**
Magnetic polarity	Jin et al. (1998)

Xifeng section: MAR (g/m^2/yr) based on pedostratigraphy

(Model I: min. glacial, max. interglacial; Model II: max. glacial, min. interglacial; Model III: 2/3 of interglacial soil is aeolian deposit)

Site location: 35.70° N, 107.70° E

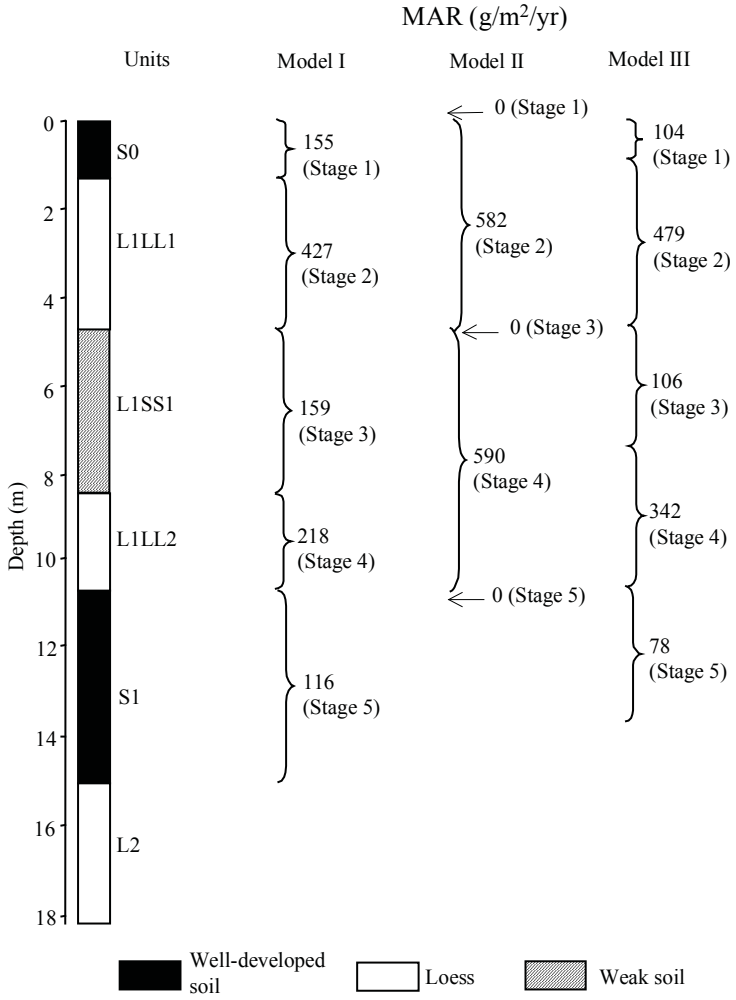

Stratigraphic data: Xifeng (depth and thickness estimated from diagram, to nearest 1 cm)				
Top depth (m)	Bottom depth (m)	Thickness (m)	Stratigraphic units	DBD (g/cm^3)
0.00	1.26	1.26	S0	n/a
1.26	4.72	3.46	L1LL1	n/a
4.72	8.49	3.77	L1SS1	n/a
8.49	10.70	2.21	L1LL2	n/a
10.70	15.10	4.40	S1	n/a
15.10			L2	n/a

Xifeng section: MAR (g/m^2/yr) based on magnetic susceptibility

Note: Digitized MS data.

Site location: 35.70° N, 107.70° E

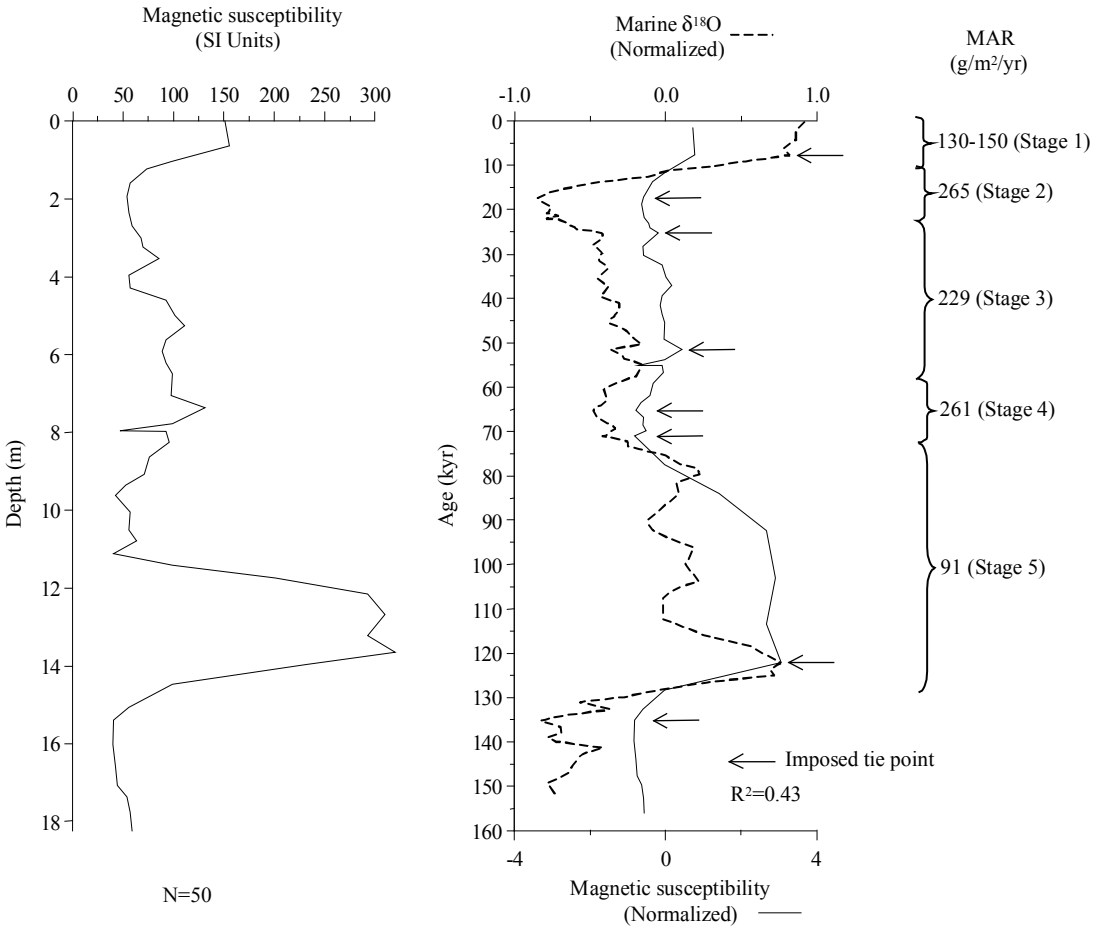

MS age model: Xifeng		
Tie-Point	Depth (m)	Age (kyr)
1	0.63	7.81
2	1.59	17.31
3	3.54	25.42
4	7.38	51.57
5	9.63	65.22
6	11.11	71.12
7	13.65	122.19
8	15.40	135.10

Age model (kyr): Xifeng						
Depth (m)	^{14}C	TL	Magnetic susceptibility	Pedostratigraphy (Model III)	Average chronology	Range
0			0.0	0.0	0.0	
2			19.0	15.5	17.2	15.5-19.0
4			28.5	21.8	25.1	21.8-28.5
6			42.0	41.8	41.9	41.8-42.0
8			55.3	62.1	58.7	55.3-62.1
10			66.8	70.9	68.8	66.8-70.9
12			89.0	98.7	93.8	89.0-98.7
14			124.8		124.8	

MAR (g/m²/yr): Xifeng								
Stage (range in kyr)	Assumed DBD (g/cm^3)	^{14}C	TL	MS	Pedostratigraphy			Average MAR
					Model I	Model II	Model III	
Stage 1 (12-0)	1.48			**140**	155	0	**104**	122
Stage 2 (24-12)	1.48			**265**	427	582	**479**	372
Stage 3 (59-24)	1.48			**229**	159	0	**106**	168
Stage 4 (74-59)	1.48			**261**	218	590	**342**	302
Stage 5 (130-74)	1.48			**91**	116	0	**78**	85

References used to generate data report: Xifeng	
Data used	**Source**
Pedostratigraphy	Liu and Ding (1993)
Magnetic susceptibility	Liu and Ding (1993)
^{14}C dating	-
TL dating	-
Additional References:	
Data available	**Source**
Pedostratigraphy, magnetic susceptibility, magnetic polarity	Liu et al. (1985)
Pedostratigraphy, magnetic susceptibility, magnetic polarity	Liu et al. (1987)
Pedostratigraphy, magnetic susceptibility, magnetic polarity	Liu et al. (1988)
Pedostratigraphy, magnetic susceptibility, magnetic polarity	Liu et al. (1991)
Pedostratigraphy, magnetic susceptibility	Liu et al. (1994b)
Pedostratigraphy, magnetic susceptibility, magnetic polarity	Kukla (1987a)
Pedostratigraphy, magnetic polarity	Kukla (1987b)
Pedostratigraphy, magnetic susceptibility, magnetic polarity	Kukla and An (1989)
Pedostratigraphy, magnetic polarity	Ding et al. (1990)
Pedostratigraphy, magnetic polarity	Ding et al. (1991)
Pedostratigraphy, micromorphology	Guo et al. (1991)
Micromorphology	Guo and Fedoroff (1991)
Micromorphology	Guo et al. (1993)
Micromorphology, chemical parameters	Guo et al. (1996b)
Magnetic susceptibility, micromorphology	Guo et al. (1998)
Magnetic susceptibility	Maher and Thompson (1991)
Pedostratigraphy, magnetic polarity	Rutter et al. (1991)
Magnetic polarity	Zhu et al. (1991)
Pedostratigraphy, magnetic polarity	Rutter (1992)
Magnetic polarity	Liu and Ding (1993)
Pedostratigraphy, magnetic susceptibility, grain size, micromorphology	Han and Jiang (1999)

Xigaze section: Pedostratigraphy

Note: Section not used to estimate MAR, because the stratigraphy cannot be correlated with the CLP stratigraphy, and the section contains sand layers. These four sections (Duobutang, Qijidong, Xietongmen, and Xigaze) are all from the Tibetan Plateau, and were scanned as a unit. The top age on the Xietongmen section is a ^{14}C date, all the other ages are TL dates.

Site location: 29.27° N, 88.85° E

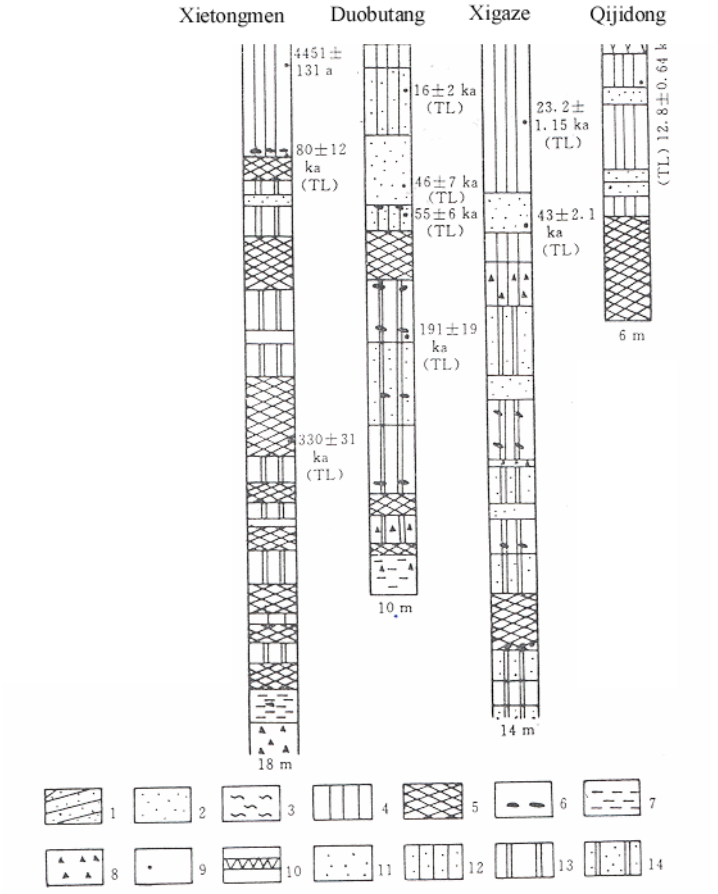

Legend: 1. Bedded sand; 2. Aeolian fine sand, 3. Fluvial layer, 4. Loess, 5. Palaeosol, 6. Nodule
7. Fluvial clay, 8. Gravel layer, 9. Sampling position, 10. Grass layer, 11. Medium sand

References used to generate data report: Xigaze	
Data used	**Source**
Pedostratigraphy	Jin et al. (1998)
Magnetic susceptibility	-
^{14}C dating	-
TL dating	Jin et al. (1998)
Additional References:	
Data available	**Source**
-	-

Xining (Dadunling) section: MAR (g/m^2/yr) based on pedostratigraphy

Note: Han and Jiang (1999) used the name of the capital city of Qinghai Province (i.e. Xining) for the section name. Dadunling (used by Kemp et al., 1997) is the name of a high mountain near the suburb of Xining where the section is located.

(Model I: min. glacial, max. interglacial; Model II: max. glacial, min. interglacial; Model III: 2/3 of interglacial soil is aeolian deposit)

Site location: 36.63° N, 101.80° E

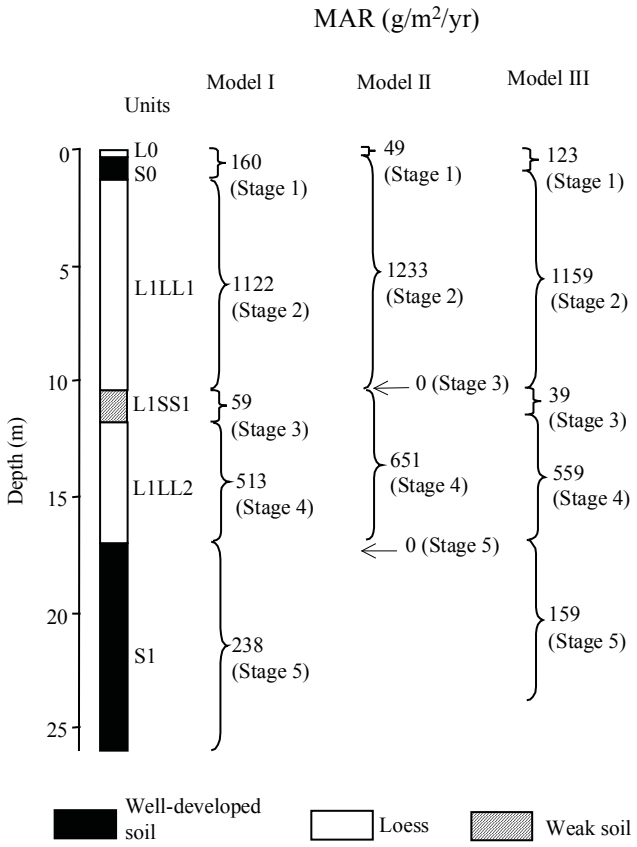

Stratigraphic data: Xining (Dadunling) (depth and thickness estimated from diagram, to nearest 10 cm)				
Top depth (m)	Bottom depth (m)	Thickness (m)	Stratigraphic units	DBD (g/cm^3)
0.0	0.4	0.4	L0	n/a
0.4	1.3	0.9	S0	n/a
1.3	10.4	9.1	L1LL1	n/a
10.4	11.8	1.4	L1SS1	n/a
11.8	17.0	5.2	L1LL2	n/a
17.0	26.0	9.0	S1	n/a

Xining (Dadunling): MAR (g/m^2/yr) based on magnetic susceptibility

Note: Han and Jiang (1999) used the name of the capital city of Qinghai Province (i.e. Xining) for the section name. Dadunling (used by Kemp et al., 1997) is the name of a high mountain near the suburb of Xining where the section is located. Digitized MS data.

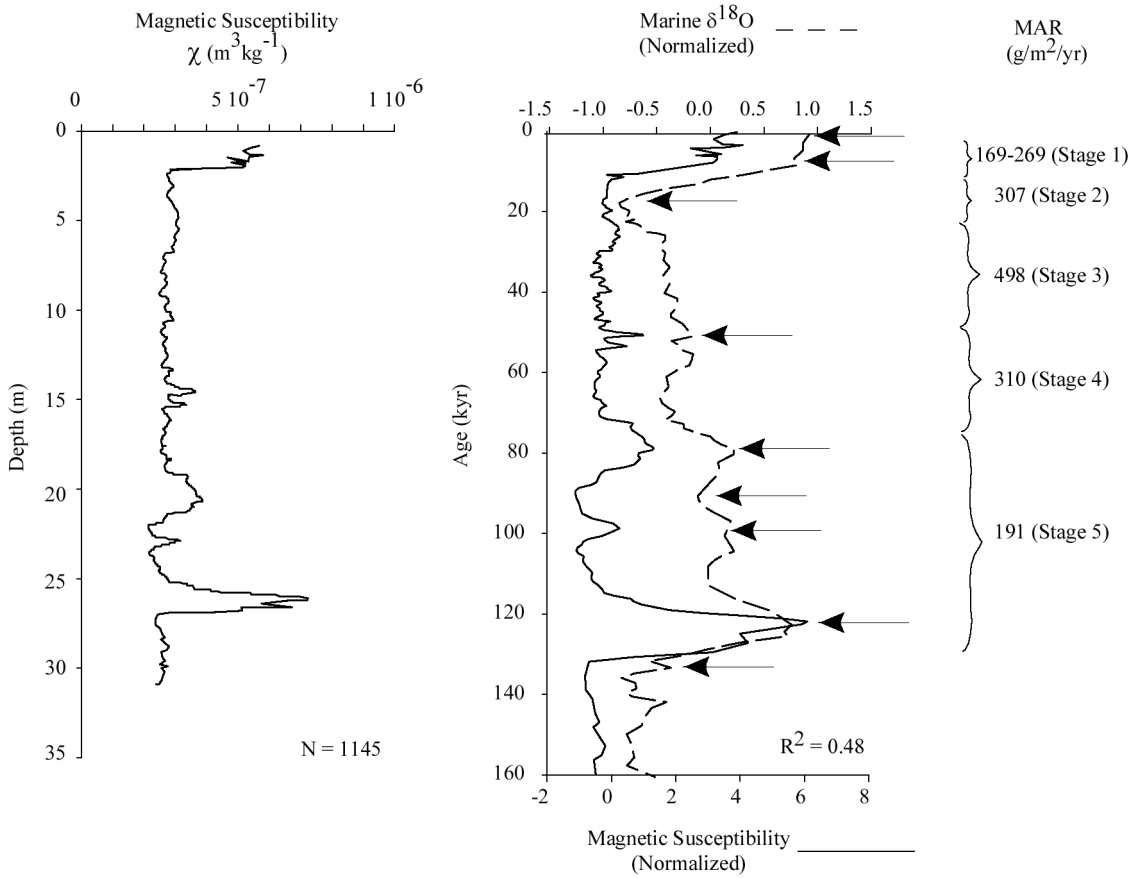

Site location: 36.63° N, 101.80° E

MS age model: Xining (Dadunling)		
Tie-Point	Depth (m)	Age (kyr)
1	0.83	0.21
2	2.03	7.81
3	2.39	17.85
4	14.90	51.57
5	20.70	79.25
6	22.20	90.10
7	23.00	99.96
8	26.20	122.56
9	27.30	135.34

Age model (kyr): Xining (Dadunling)						
Depth (m)	^{14}C	TL	Magnetic susceptibility	Pedostratigraphy (Model III)	Average chronology	Range
0			0.0	0.0	0.0	
4			22.2	15.9	19.1	15.9-22.2
8			33.0	20.9	27.0	20.9-33.0
12			43.8	60.7	52.3	43.8-60.7
16			56.8	71.3	64.1	56.8-71.3
20			75.9	102.0	89.0	75.9-102.0
24			107.0		107.0	

MAR ($g/m^2/yr$): Xining (Dadunling)								
Stage (range in kyr)	Assumed DBD (g/cm^3)	^{14}C	TL	MS	Pedostratigraphy			Average MAR
					Model I	Model II	Model III	
Stage 1 (12-0)	1.48			219	160	49	**123**	171
Stage 2 (24-12)	1.48			307	1122	1233	**1159**	733
Stage 3 (59-24)	1.48			498	59	0	**39**	269
Stage 4 (74-59)	1.48			310	513	651	**559**	435
Stage 5 (130-74)	1.48			191	238	0	**159**	175

References used to generate data report: Xining (Dadunling)	
Data used	**Source**
Pedostratigraphy	Kemp et al. (1997)
Magnetic susceptibility	Han and Jiang (1999)
^{14}C dating	-
TL dating	-
Additional References:	
Data available	**Source**
Magnetic susceptibility, magnetic polarity, pedostratigraphy	Li et al. (1992b)
Grain size, pedostratigraphy	Han and Jiang (1999)

Xinzhuangyuan section: MAR (g/m^2/yr) based on magnetic susceptibility

Note: Digitized MS data.

Site location: 35.63° N, 103.17° E

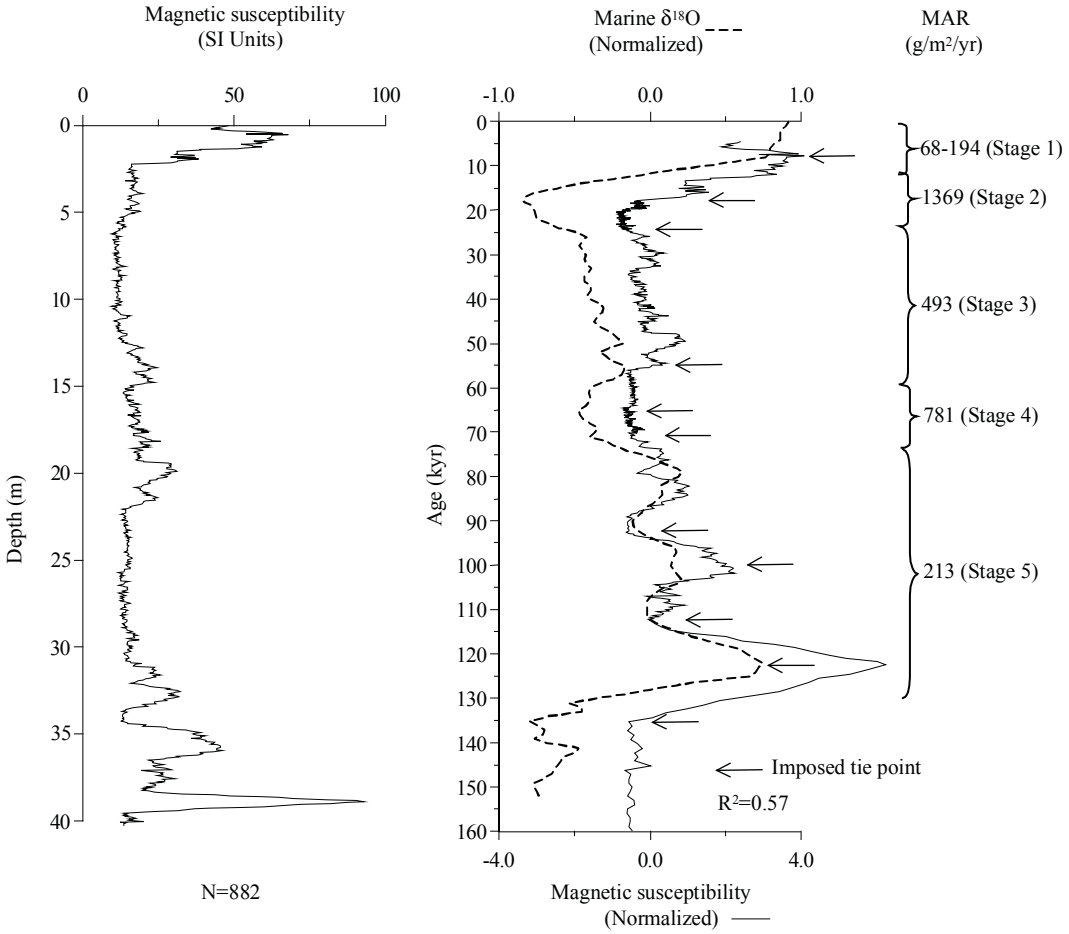

MS age model: Xinzhuangyuan		
Tie-Point	Depth (m)	Age (kyr)
1	0.38	7.81
2	1.78	17.31
3	27.18	71.12
4	31.86	99.96
5	32.85	107.55
6	35.03	125.00
7	35.44	131.09

Age model (kyr): Xinzhuangyuan						
Depth (m)	^{14}C	TL	Magnetic susceptibility	Pedostratigraphy (Model III)	Average chronology	Range
0			0.0		0.0	
6			26.2		26.2	
12			39.0		39.0	
18			51.6		51.6	
24			64.4		64.4	
30			88.5		88.5	
36			139.3		139.3	

MAR (g/m²/yr): Xinzhuangyuan								
Stage (range in kyr)	Assumed DBD (g/cm^3)	^{14}C	TL	MS	Pedostratigraphy			Average MAR
					Model I	Model II	Model III	
Stage 1 (12-0)	1.48			**171**				171
Stage 2 (24-12)	1.48			**486**				486
Stage 3 (59-24)	1.48			**609**				609
Stage 4 (74-59)	1.48			**611**				611
Stage 5 (130-74)	1.48			**204**				204

References used to generate data report: Xinzhuangyuan	
Data used	**Source**
Pedostratigraphy	-
Magnetic susceptibility	Ren (1996)
^{14}C dating	-
TL dating	-
Additional References:	
Data available	**Source**
Grain size	Ren (1996)
Grain size	Ding et al. (1999a)

Xuancheng section: Pedostratigraphy

Note: This section is located in southern China (Anhui Province). It is questionable whether this section and others in this region (e.g. Xuancheng, Lijiagang, Taishanxincun, Xiangyang, Yanziji) are aeolian. It is difficult to relate the pedostratigraphy to that of the CLP sections. Stratigraphic division of S1 follows the authors. Section is not used, because it contains multiple hiatuses, and only the range of thickness is given by authors.

Site location: 30.90° N, 118.85° E

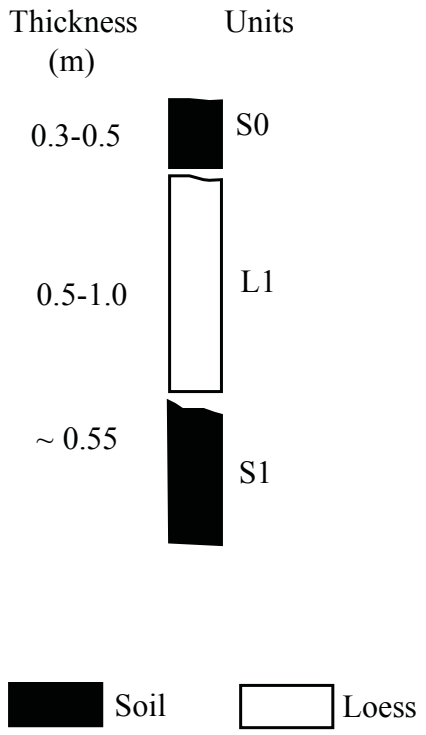

Xuancheng section: Magnetic susceptibility

Note: This section is located in southern China (Anhui Province). It is questionable whether this section and others in this region (e.g. Xuancheng, Lijiagang, Taishanxincun, Xiangyang, Yanziji) are aeolian. It is difficult to relate the pedostratigraphy to that of the CLP sections. Digitized MS data. MS data not used because of sedimentary hiatuses.

Site location: 30.90° N, 118.85° E

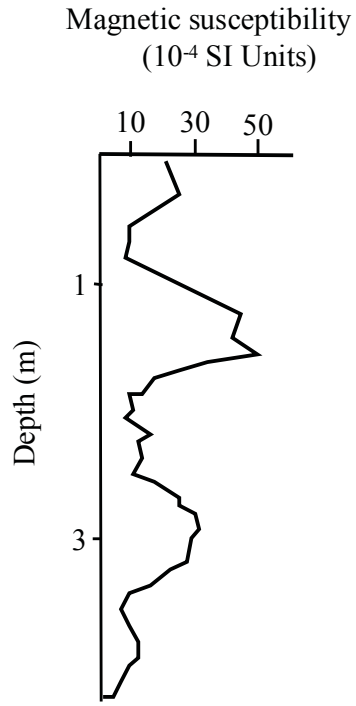

References used to generate data report: Xuancheng	
Data used	**Source**
Pedostratigraphy	Zhao (1995)
Magnetic susceptibility	Zhao (1995)
^{14}C dating	-
TL dating	-
Additional References:	
Data available	**Source**
$\delta^{13}C$, chemical parameters	Zhao (1995)

Xueyuan section: MAR (g/m^2/yr) based on magnetic susceptibility

Note: Digitized MS data.

Site location: 36.92° N, 106.97° E

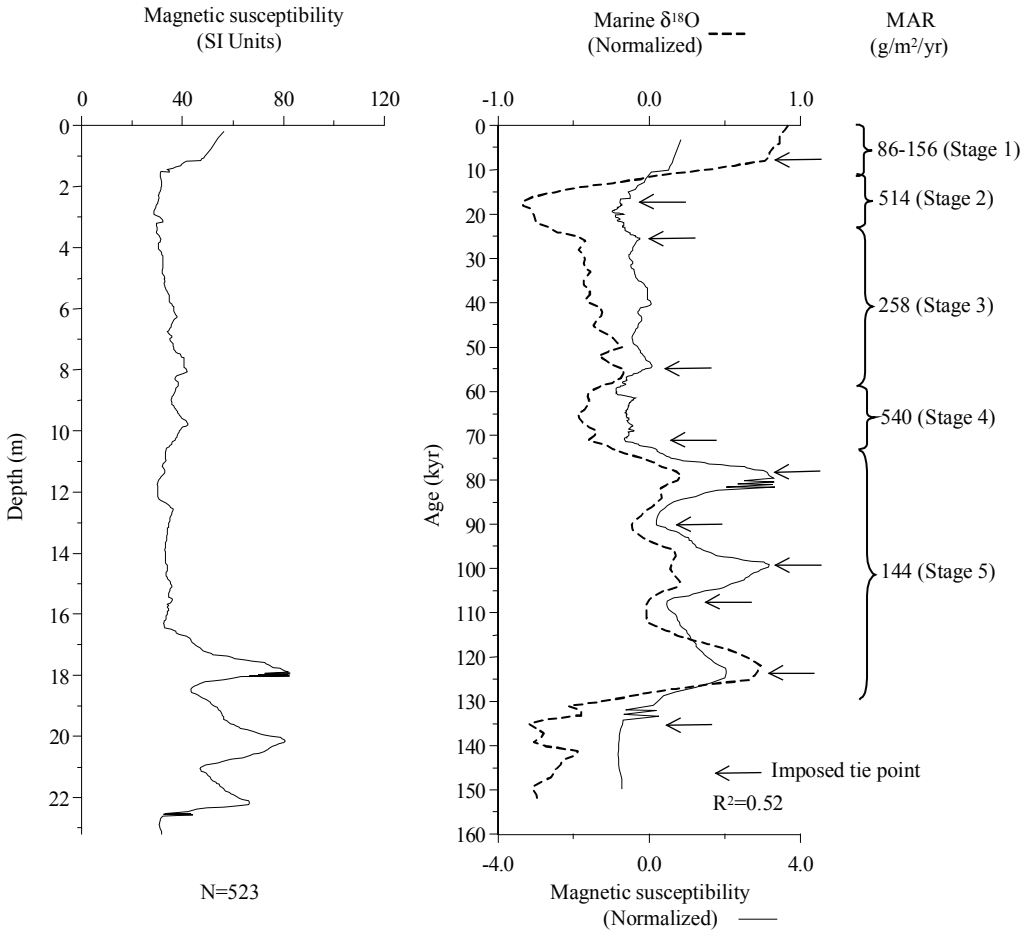

MS age model: Xueyuan		
Tie-Point	Depth (m)	Age (kyr)
1	1.02	7.81
2	1.57	17.31
3	6.25	25.42
4	9.84	54.84
5	16.42	71.12
6	17.84	78.30
7	18.55	90.10
8	20.17	99.38
9	21.02	107.55
10	22.20	123.79
11	22.65	135.34

Age model (kyr): Xueyuan						
Depth (m)	^{14}C	TL	Magnetic susceptibility	Pedostratigraphy (Model III)	Average chronology	Range
0			0.0		0.0	
3			19.8		19.8	
6			25.0		25.0	
9			48.0		48.0	
12			60.2		60.2	
15			67.6		67.6	
18			80.9		80.9	
21			107.5		107.5	

MAR (g/m²/yr): Xueyuan								
Stage (range in kyr)	Assumed DBD (g/cm^3)	^{14}C	TL	MS	Pedostratigraphy			Average MAR
					Model I	Model II	Model III	
Stage 1 (12-0)	1.48			**121**				121
Stage 2 (24-12)	1.48			**514**				514
Stage 3 (59-24)	1.48			**258**				258
Stage 4 (74-59)	1.48			**540**				540
Stage 5 (130-74)	1.48			**144**				144

References used to generate data report: Xueyuan	
Data used	**Source**
Pedostratigraphy	-
Magnetic susceptibility	Sun et al. (1995)
^{14}C dating	-
TL dating	-
Additional References:	
Data available	**Source**
-	-

Xunyi section: MAR (g/m^2/yr) based on magnetic susceptibility

Note: Digitized MS data.

Site location: 35.13° N, 108.33° E

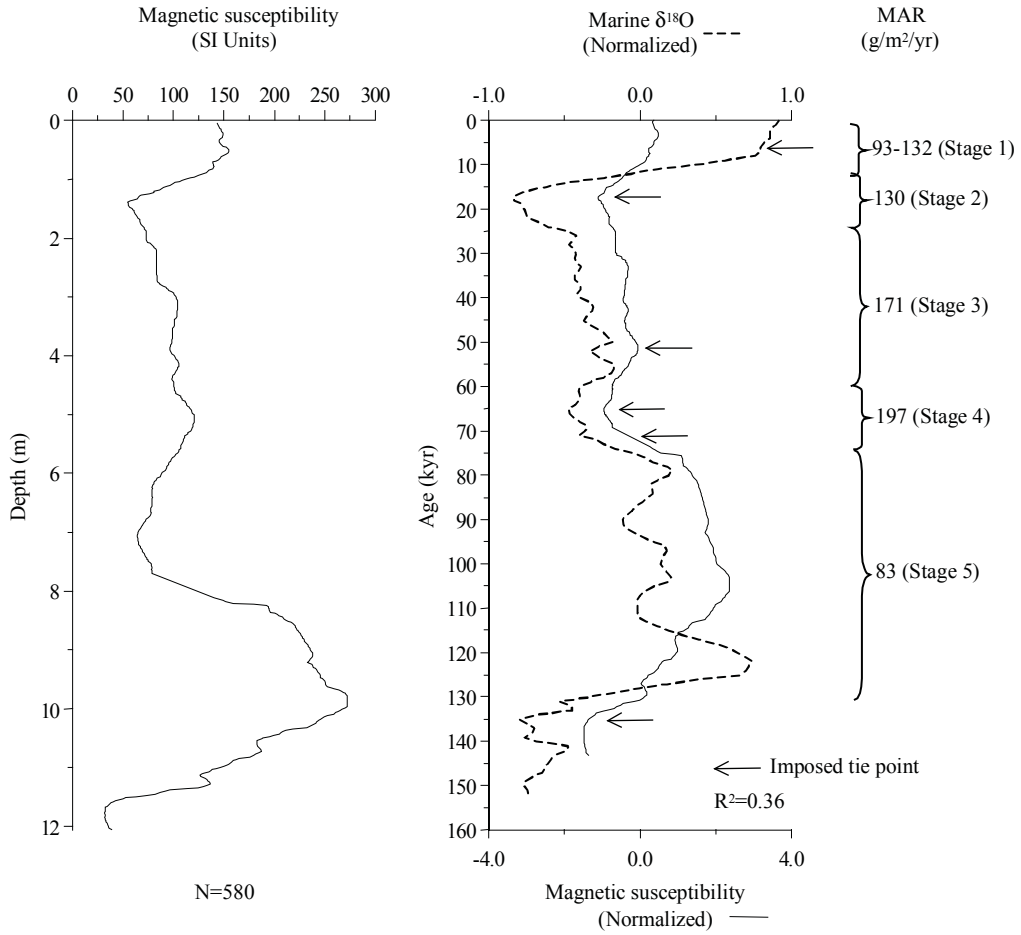

MS age model: Xunyi		
Tie-Point	Depth (m)	Age (kyr)
1	0.71	6.27
2	1.40	17.31
3	5.08	51.57
4	7.05	65.22
5	7.99	71.12
6	11.61	135.34

Age model (kyr): Xunyi						
Depth (m)	^{14}C	TL	Magnetic susceptibility	Pedostratigraphy (Model III)	Average chronology	Range
0			0.0		0.0	
2			23.0		23.0	
4			41.6		41.6	
6			58.0		58.0	
8			71.5		71.5	
10			107.0		107.0	
12			142.2		142.2	

MAR (g/m²/yr): Xunyi								
Stage (range in kyr)	Assumed DBD (g/cm^3)	^{14}C	TL	MS	Pedostratigraphy			Average MAR
					Model I	Model II	Model III	
Stage 1 (12-0)	1.48			**113**				113
Stage 2 (24-12)	1.48			**130**				130
Stage 3 (59-24)	1.48			**171**				171
Stage 4 (74-59)	1.48			**197**				197
Stage 5 (130-74)	1.48			**83**				83

References used to generate data report: Xunyi	
Data used	**Source**
Pedostratigraphy	-
Magnetic susceptibility	Sun et al. (1995)
^{14}C dating	-
TL dating	-
Additional References:	
Data available	**Source**
-	-

Yanchang section: MAR (g/m^2/yr) based on magnetic susceptibility

Site location: 36.60° N, 110.02° E

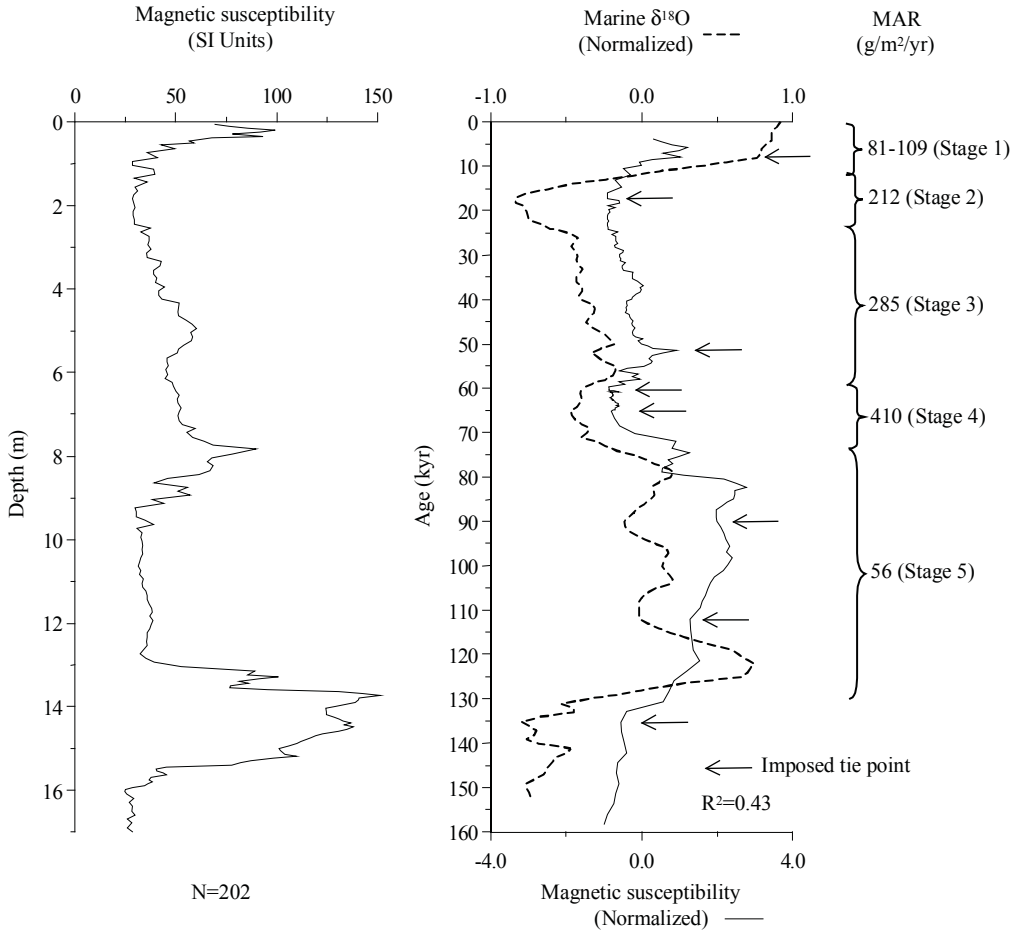

MS age model: Yanchang		
Tie-Point	Depth (m)	Age (kyr)
1	0.35	7.81
2	1.05	17.31
3	7.85	51.57
4	9.35	60.44
5	12.75	65.22
6	14.20	90.10
7	15.00	112.28
8	15.50	135.34

Age model (kyr): Yanchang						
Depth (m)	^{14}C	TL	Magnetic susceptibility	Pedostratigraphy (Model III)	Average chronology	Range
0			0		0.0	
3			27		27.0	
6			42		42.0	
9			58.3		58.3	
12			64.1		64.1	
15			112.3		112.3	

MAR (g/m²/yr): Yanchang								
Stage (range in kyr)	Assumed DBD (g/cm^3)	^{14}C	TL	MS	Pedostratigraphy			Average MAR
					Model I	Model II	Model III	
Stage 1 (12-0)	1.48			**95**				95
Stage 2 (24-12)	1.48			**212**				212
Stage 3 (59-24)	1.48			**285**				285
Stage 4 (74-59)	1.48			**410**				410
Stage 5 (130-74)	1.48			**56**				56

References used to generate data report: Yanchang	
Data used	**Source**
Pedostratigraphy	-
Magnetic susceptibility	Ding et al. (1999b)
^{14}C dating	-
TL dating	-
Additional References:	
Data available	**Source**
Grain size	Ding et al. (1999b)

Yangjiashan (Fengzhou) section: MAR (g/m^2/yr) based on pedostratigraphy

Note: Stage 1 affected by cultivation layer.

(Model I: min. glacial, max. interglacial; Model II: max. glacial, min. interglacial; Model III: 2/3 of interglacial soil is aeolian deposit)

Site location: 34.00° N, 106.65° E

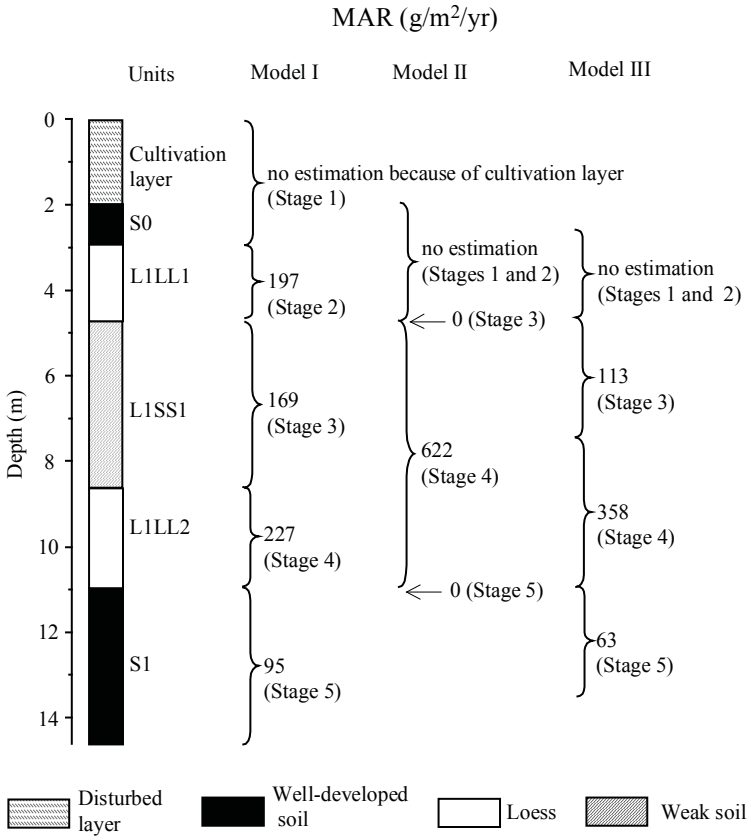

Stratigraphic data: Yangjiashan (Fenzhou) (depth and thickness estimated from diagram, to nearest 10 cm)				
Top depth (m)	Bottom depth (m)	Thickness (m)	Stratigraphic units	DBD (g/cm^3)
0.0	2.0	2.0	cultivation layer	n/a
2.0	3.1	0.9	S0	n/a
3.1	4.7	1.6	L1LL1	n/a
4.7	8.7	4.0	L1SS1	n/a
8.7	11.0	2.3	L1LL2	n/a
11.0	14.6	3.6	S1	n/a

Age model (kyr): Yangjiashan (Fenzhou)						
Depth (m)	^{14}C	TL	Magnetic susceptibility	Pedostratigraphy (Model III)	Average chronology	Range
0						
2						
4				18.9	18.9	
6				35.5	35.5	
8				53.2	53.2	
10				67.6	67.6	
12				89.6	89.6	
14				120.8	120.8	

MAR (g/m²/yr): Yangjiashan (Fenzhou)								
Stage (range in kyr)	Assumed DBD (g/cm^3)	^{14}C	TL	MS	Pedostratigraphy			Average MAR
					Model I	Model II	Model III	
Stage 1 (12-0)	1.48							
Stage 2 (24-12)	1.48				197			
Stage 3 (59-24)	1.48				169	0	**113**	113
Stage 4 (74-59)	1.48				227	622	**358**	358
Stage 5 (130-74)	1.48				95	0	**63**	63

References used to generate data report: Yangjiashan (Fenzhou)	
Data used	**Source**
Pedostratigraphy	Lei (1998)
Magnetic susceptibility	-
^{14}C dating	-
TL dating	-
Additional References:	
Data available	**Source**
Grain size, magnetic polarity	Lei (1998)

Yangmeitang section: Magnetic susceptibility

Note: Section is located in southern China, about 1.0 km SE of Xinshengyu Harbor (or Xinshengyugang). Section not used, because the top of section is missing, magnetic susceptibility curve is digitized but not used.

Site location: 32.17° N, 118.84° E

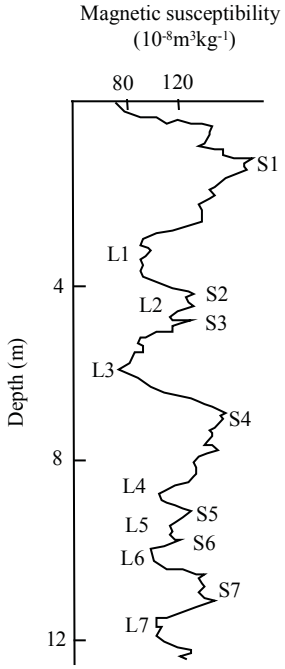

References used to generate data report: Yangmeitang	
Data used	**Source**
Pedostratigraphy	-
Magnetic susceptibility	Zhang et al. (1994)
^{14}C dating	-
TL dating	-
Additional References:	
Data available	**Source**
-	-

Yangtaomao section: Pedostratigraphy

Note: Section not used to estimate MAR because it contains no loess.

Site location: 38.80° N, 110.45° E

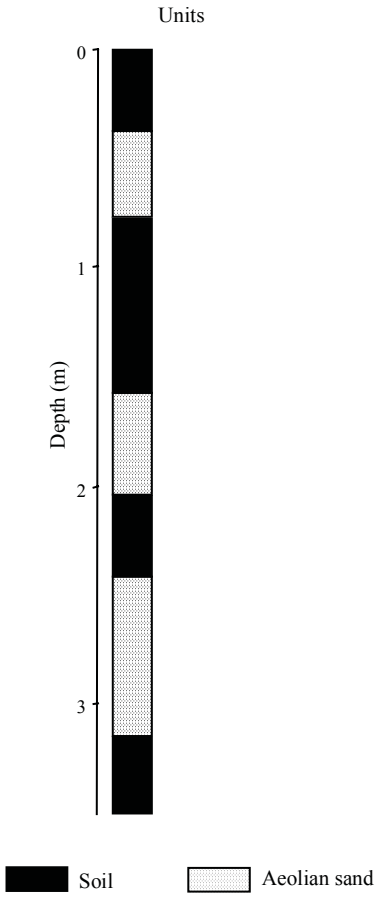

Stratigraphic data: Yangtaomao (depth and thickness estimated from diagram, to nearest 10 cm)				
Top depth (m)	Bottom depth (m)	Thickness (m)	Stratigraphic units	DBD (g/cm³)
0.00	0.38	0.38	sandy palaeosol	n/a
0.38	0.78	0.40	aeolian sand	n/a
0.78	1.57	0.79	sandy palaeosol	n/a
1.57	2.04	0.47	aeolian sand	n/a
2.04	2.42	0.38	sandy palaeosol	n/a
2.42	3.15	0.73	S0LL3	n/a
3.15	3.50	0.35	sandy palaeosol	n/a

Yangtaomao section: Magnetic susceptibility

Note: Section not used to estimate MAR because it contains no loess. Digitized MS data.

Site location: 38.80° N, 110.45° E

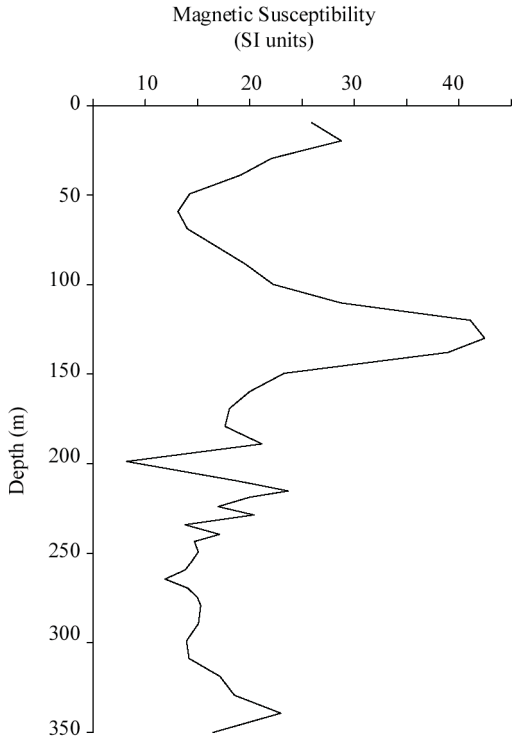

References used to generate data report: Yangtaomao	
Data used	**Source**
Pedostratigraphy	Zhou et al. (1996)
Magnetic susceptibility	Zhou et al. (1996)
^{14}C dating	
TL dating	-
Additional References:	
Data available	**Source**
Grain size, ^{14}C	Zhou et al. (1996)
Pedostratigraphy, ^{14}C	Zhou et al. (1997)
Pedostratigraphy, ^{14}C	Zhou et al. (1998)

Yanziji section: Pedostratigraphy and TL dating

Note: Section not used to estimate MAR because Stage 1 contains colluvium, the loess unit contains a sedimentary hiatus, the S1 lower boundary is not indicated by authors, and only one TL date available.

Site location: 32.15° N, 118.82° E

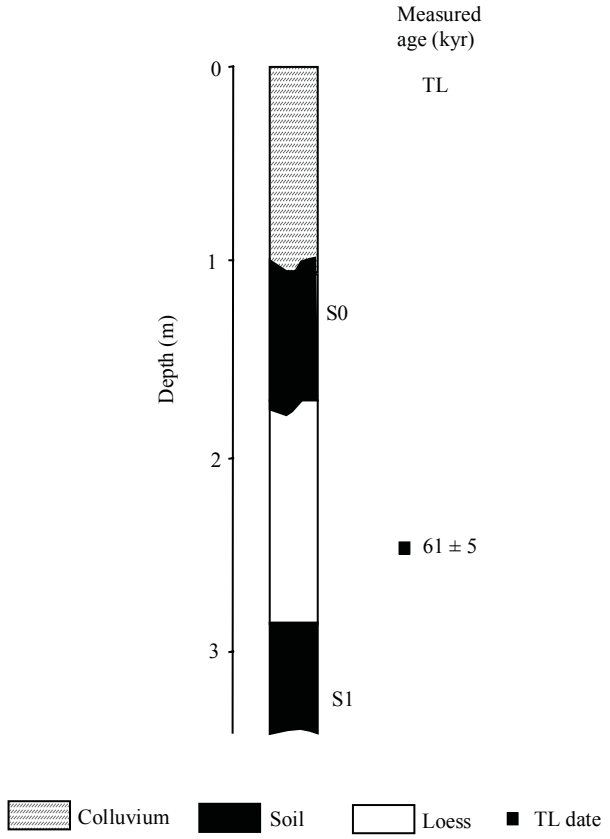

Stratigraphic data: Yanziji (depth and thickness estimated from diagram, to nearest 1 cm)				
Top depth (m)	Bottom depth (m)	Thickness (m)	Stratigraphic units	DBD (g/cm^3)
0	1.12	1.12	colluvium	n/a
1.12	1.68	0.56	S0	n/a
1.68	3.93	2.25	L1	n/a
3.93	4.49	0.56	S1?	n/a

TL dating: Yanziji (depth estimated from diagram, to nearest 10 cm)								
Depth (m)	Dating laboratory	Lab. No.	Dating material	TL-method	Age (kyr)	s.d. (kyr)	Reference	Comments
2.5	n/a	n/a	n/a	n/a	61	5	Zheng et al. (1994)	

References used to generate data report: Yanziji	
Data used	**Source**
Pedostratigraphy	Zheng et al. (1994)
Magnetic susceptibility	-
^{14}C dating	-
TL dating	Zheng et al. (1994)
Additional References:	
Data available	**Source**
-	-

Yichuan section: MAR (g/m^2/yr) based on magnetic susceptibility

Site location: 36.13° N, 110.15° E

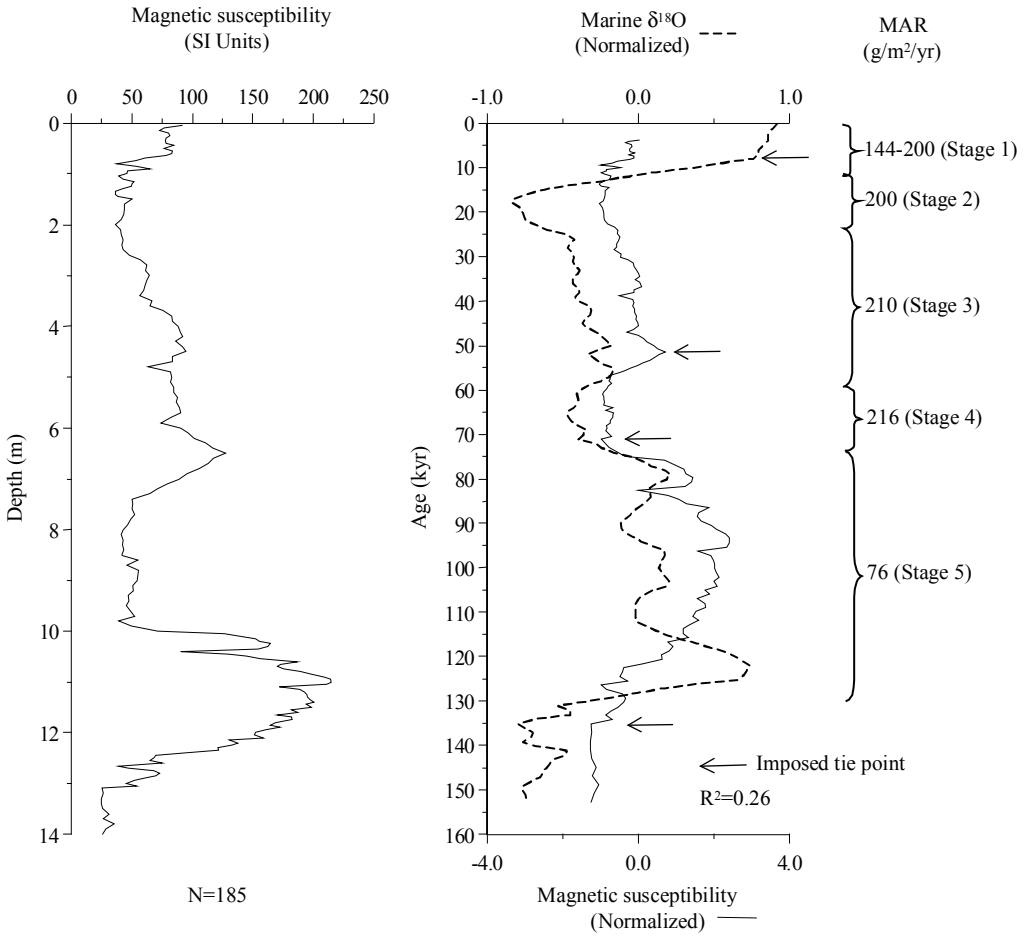

MS age model: Yichuan		
Tie-Point	Depth (m)	Age (kyr)
1	0.60	7.81
2	6.50	51.57
3	9.80	71.12
4	13.10	135.34

Age model (kyr): Yichuan						
Depth (m)	^{14}C	TL	Magnetic susceptibility	Pedostratigraphy (Model III)	Average chronology	Range
0			0.0		0.0	
2			18.2		18.2	
4			33.0		33.0	
6			47.9		47.9	
8			60.4		60.4	
10			75.0		75.0	
12			113.9		113.9	
14			152.8		152.8	

MAR (g/m²/yr): Yichuan								
Stage (range in kyr)	Assumed DBD (g/cm^3)	^{14}C	TL	MS	Pedostratigraphy			Average MAR
					Model I	Model II	Model III	
Stage 1 (12-0)	1.48			**172**				172
Stage 2 (24-12)	1.48			**200**				200
Stage 3 (59-24)	1.48			**210**				210
Stage 4 (74-59)	1.48			**216**				216
Stage 5 (130-74)	1.48			**76**				76

References used to generate data report: Yichuan	
Data used	**Source**
Pedostratigraphy	-
Magnetic susceptibility	Ding et al. (1999b)
^{14}C dating	-
TL dating	-
Additional References:	
Data available	**Source**
Magnetic susceptibility, pedostratigraphy, chemical parameters	Guo et al. (1996c)
Grain size	Ding et al. (1999b)

Yinwan section: MAR (g/m^2/yr) based on pedostratigraphy

Note: Section with potential local river sources. Stage 1 affected by cultivation layer and reworked loess.

(Model I: min. glacial, max. interglacial; Model II: max. glacial, min. interglacial; Model III: 2/3 of interglacial soil is aeolian deposit)

Site location: 34.93° N, 104.17° E

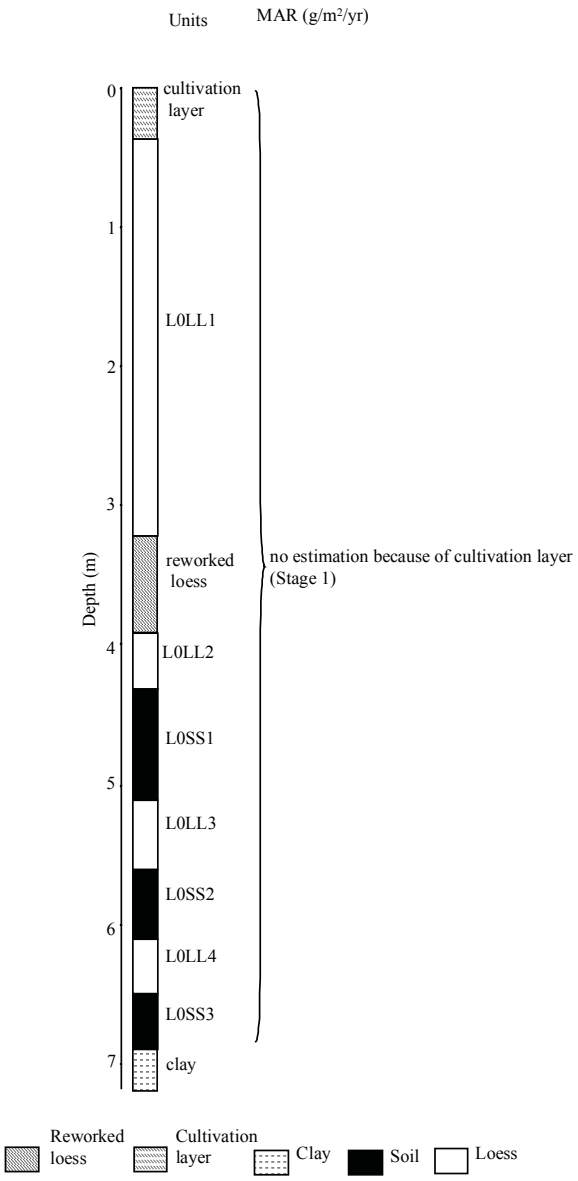

Stratigraphic data: Yinwan
(depth and thickness estimated from diagram, to nearest 10 cm)

Top depth (m)	Bottom depth (m)	Thickness (m)	Stratigraphic units	DBD (g/cm³)
0.0	0.4	0.4	cultivation layer	n/a
0.4	3.2	2.8	L0LL1	n/a
3.2	3.9	0.7	reworked loess	n/a
3.9	4.3	0.4	L0LL2	n/a
4.3	5.1	0.8	L0SS1	n/a
5.1	5.6	0.5	L0LL3	n/a
5.6	6.1	0.5	L0SS2	n/a
6.1	6.5	0.4	L0LL4	n/a
6.5	6.8	0.3	L0SS3	n/a
6.8	7.2	0.4	clay	n/a

Yinwan: MAR (g/m^2/yr) based on ^{14}C and TL dating

Note: Section with potential local river sources. Stage 1 MAR calculated excluding cultivation layer and reworked loess based on available ^{14}C dates. No TL based MAR calculated because only one TL date used.

Site location: 34.93° N, 104.17° E

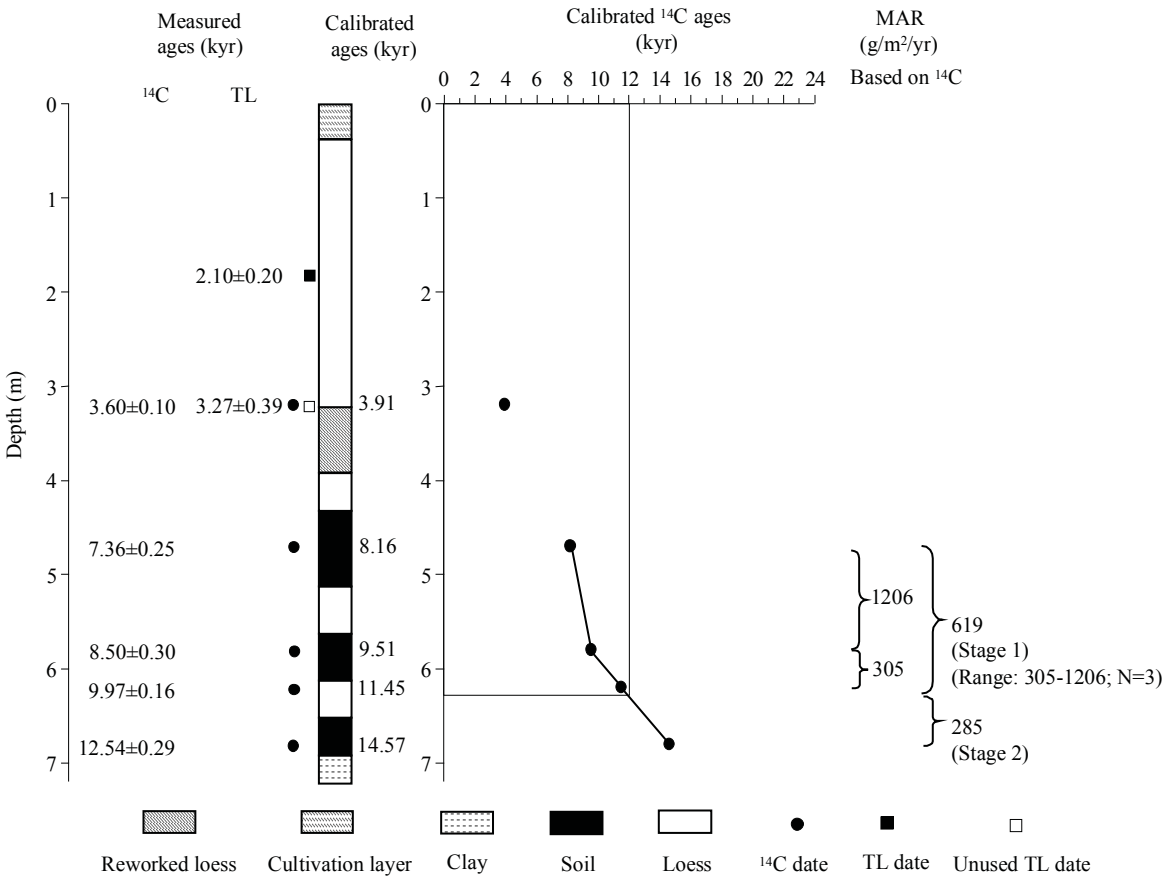

^{14}C dating: Yinwan
(depth estimated from diagram, to nearest 10 cm)

Depth (m)	Dating laboratory	Lab. No.	Dating material	Age (kyr)	s.d. (kyr)	(1σ) Calendar age ranges (kyr)	Relative probability	Assumed calendar age (kyr)	Reference	Comments
3.2	Xi'an Loess Lab.	n/a	insoluble organic matter	3.6	0.1	3.82-3.99	0.695	3.91	Ren et al. (1996)	
						4.03-4.08	0.152			
						3.76-3.79	0.093			
						3.73-3.75	0.06			
4.6	n/a	n/a	n/a	7.36	0.25	7.94-8.39	0.984	8.16	Ren et al. (1996)	Ren et al. (1996) cited Wen (1982) as source
						7.88-7.89	0.016			
5.7	n/a	n/a	n/a	8.5	0.3	9.90-9.12	0.981	9.51	Ren et al. (1996)	Ren et al. (1996) cited Wen (1982) as source
						9.09-9.10	0.019			
6.1	Xi'an Loess Lab.	n/a	insoluble organic matter	9.97	0.16	11.20-11.70	0.962	11.45	Ren et al. (1996)	
						11.72-11.73	0.026			
						11.87-11.88	0.013			
6.7	Xi'an Loess Lab.	n/a	insoluble organic matter	12.5	0.29	14.24-14.90	0.655	14.57	Ren et al. (1996)	
						15.09-15.45	0.289			
						14.15-14.22	0.055			

TL dating: Yinwan
(depth of the top TL date given by authors, depth of the other one estimated from diagram, to nearest 10 cm)

Depth (m)	Dating laboratory	Lab. No.	Dating material	TL-method	Age (kyr)	s.d. (kyr)	Reference	Comments
1.8	Xi'an Loess Lab.	n/a	n/a	n/a	2.1	0.2	Ren et al. (1996)	
3.2	Xi'an Loess Lab.	n/a	n/a	n/a	3.27	0.39	Ren et al. (1996)	uncertainties larger than 10 %

Age model (kyr): Yinwan

Depth (m)	^{14}C	TL	Magnetic susceptibility	Pedostratigraphy (Model III)	Average chronology	Range
0						
1						
2						
3						
4						
5	8.5				8.5	
6	10.5				10.5	

MAR (g/m²/yr): Yinwan								
Stage (range in kyr)	Assumed DBD (g/cm3)	^{14}C	TL	MS	Pedostratigraphy			Average MAR
					Model I	Model II	Model III	
Stage 1 (12-0)	1.48	**619**						619
Stage 2 (24-12)	1.48	**285**						285
Stage 3 (59-24)	1.48							
Stage 4 (74-59)	1.48							
Stage 5 (130-74)	1.48							

References used to generate data report: Yinwan	
Data used	**Source**
Pedostratigraphy	Ren et al. (1996)
Magnetic susceptibility	-
^{14}C dating	Ren et al. (1996)
TL dating	Ren et al. (1996)
Additional References:	
Data available	**Source**
Magnetic susceptibility, grain size, organic matter, $CaCO_3$, ^{14}C	Ren et al. (1996)
Pedostratigraphy, ^{14}C, mineralogy, pollen, magnetic polarity	Wen (1982)

Yuanpu (Yuanbo) section: MAR (g/m^2/yr) based on pedostratigraphy

(Model I: min. glacial, max. interglacial; Model II: max. glacial, min. interglacial; Model III: 2/3 of interglacial soil is aeolian deposit)

Site location: 35.63° N, 103.17° E

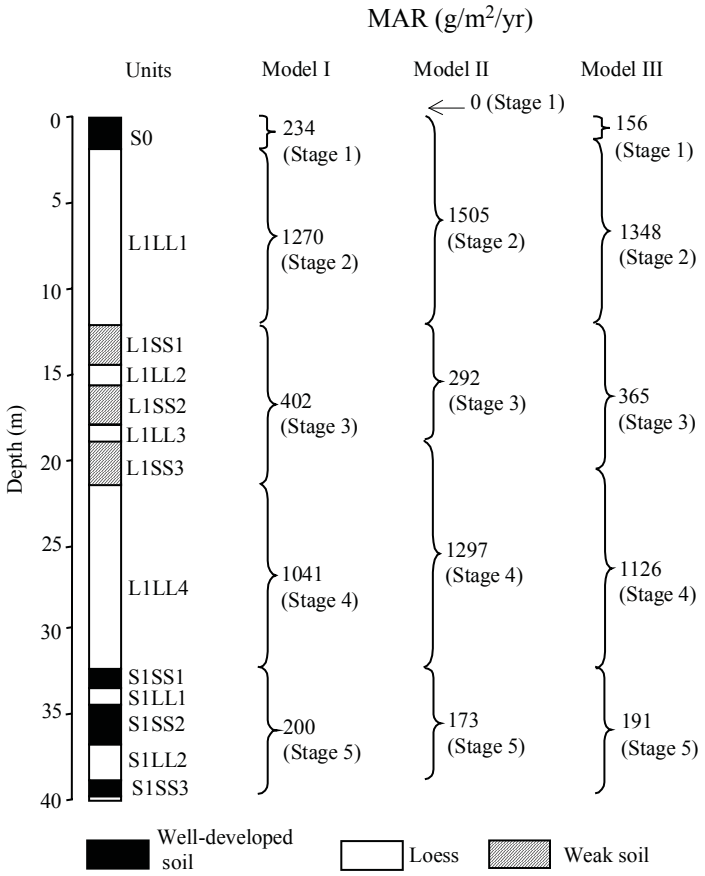

Stratigraphic data: Yuanpu (Yuanbo) (depth and thickness estimated from diagram, to nearest 5 cm)				
Top depth (m)	Bottom depth (m)	Thickness (m)	Stratigraphic units	DBD (g/cm^3)
0.00	1.90	1.90	S0	n/a
1.90	12.20	10.30	L1LL1	n/a
12.20	14.60	2.40	L1SS1	n/a
14.60	15.80	1.20	L1LL2	n/a
15.80	18.20	2.40	L1SS2	n/a
18.20	19.10	0.90	L1LL3	n/a
19.10	21.70	2.60	L1SS3	n/a
21.70	32.25	10.55	L1LL4	n/a
32.25	33.50	1.25	S1SS1	n/a
33.50	34.50	1.00	S1LL1	n/a
34.50	36.80	2.30	S1SS2	n/a
36.80	38.80	2.00	S1LL2	n/a
38.80	39.80	1.00	S1SS3	n/a
39.80			L2	n/a

Yuanpu (Yuanbo) : MAR (g/m^2/yr) based on ^{14}C dating

Note: Only top part of the section is shown.

Site location: 35.63° N, 103.17° E

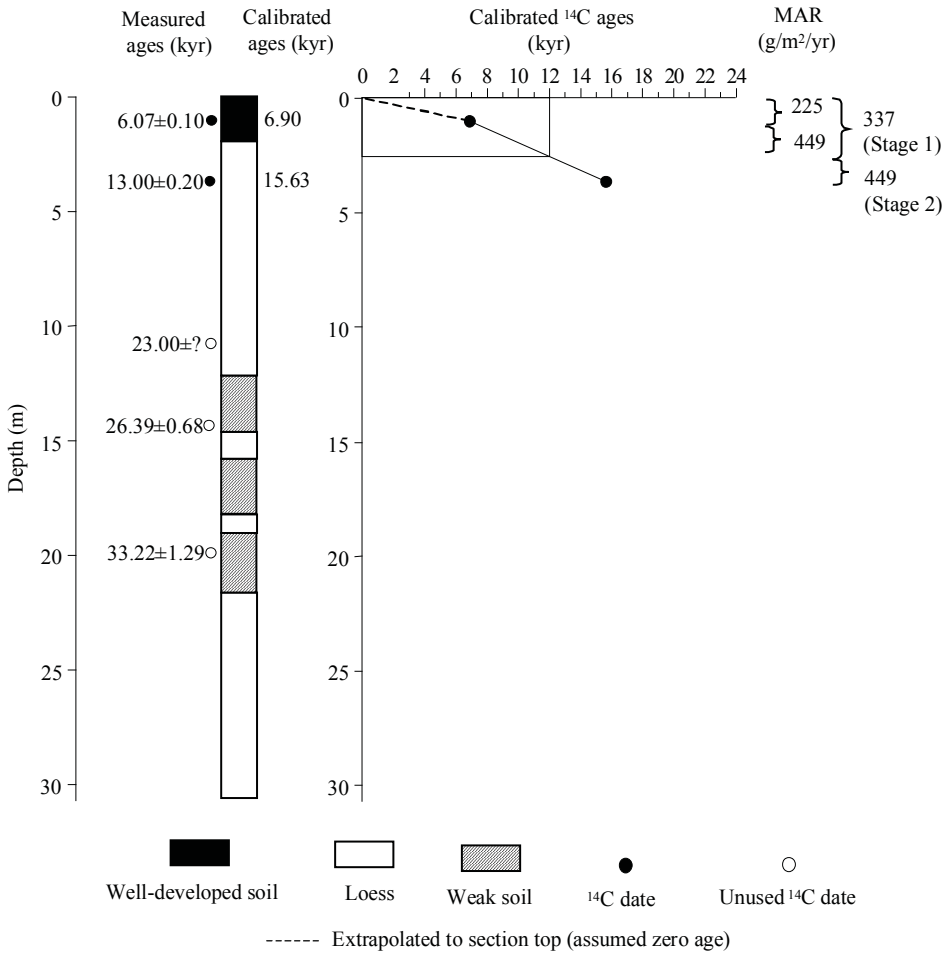

^{14}C dating: Yuanpu (Yuanbo) (depth of four dates given by authors in text; depth of the third date is inconsistent with ist portion on the diagram, so the depth of this date as well as the uppermost date estimated from diagram, to nearest 5 cm)										
Depth (m)	Dating laboratory	Lab. No.	Dating material	Age (kyr)	s.d. (kyr)	(1σ) Calendar age ranges (kyr)	Relative probability	Assumed calendar age (kyr)	Reference	Comments
1.05	n/a	n/a	organic matter	6.07	0.10	6.79-7.02	0.885	6.9	Chen et al. (1996a)	
						7.13-7.15	0.06			
						6.76-6.77	0.055			
3.70	n/a	n/a	organic matter	13.00	0.20	15.18-16.08	0.983	15.63	Chen et al. (1996a)	
						14.54-14.56	0.017			
10.80	n/a	n/a	organic matter	23.00	?				Chen et al. (1996a)	beyond calibration range
14.40	n/a	n/a	organic matter	26.39	0.68				Chen et al. (1996a)	beyond calibration range
20.00	n/a	n/a	organic matter	33.22	1.29				Chen et al. (1996a)	younger contamination

Yuanpu (Yuanbo) section: MAR (g/m^2/yr) based on magnetic susceptibility

Site location: 35.63° N, 103.17° E

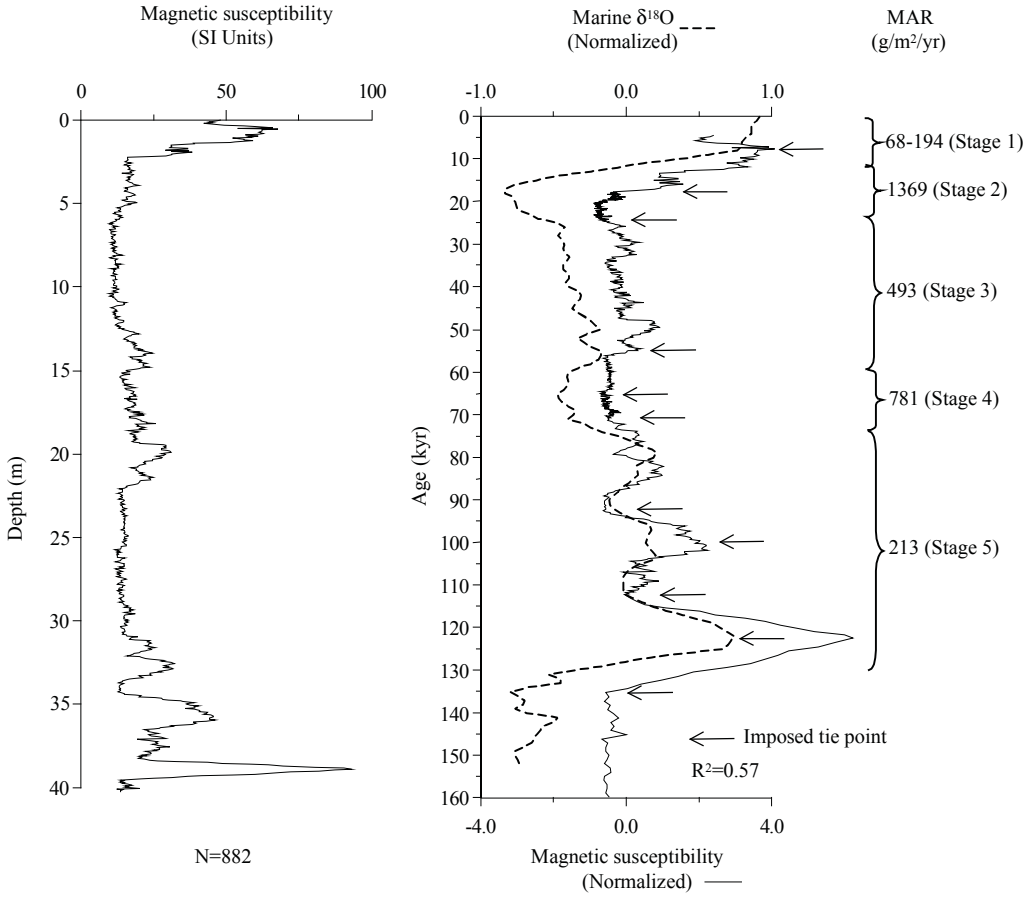

MS age model: Yuanpu (Yuanbo)		
Tie-Point	Depth (m)	Age (kyr)
1	0.55	7.81
2	2.25	17.85
3	12.35	24.46
4	21.50	54.84
5	26.00	65.22
6	30.70	70.82
7	34.20	92.23
8	35.55	99.96
9	38.25	112.28
10	38.90	122.56
11	39.55	135.34

Age model (kyr): Yuanpu (Yuanbo)						
Depth (m)	^{14}C	TL	Magnetic susceptibility	Pedostratigraphy (Model III)	Average chronology	Range
0			0.0.	0.0	0.0	
6			20.3	17.0	18.6	17.0-20.3
12			24.2	23.8	24.0	23.8-24.2
18			43.2	47.4	45.3	43.2-47.4
24			60.6	63.0	61.8	60.6-63.0
30			70.0	71.0	70.5	70.0-71.0
36			102.0	103.0	102.5	102.0-103.0

MAR ($g/m^2/yr$): Yuanpu (Yuanbo)								
Stage (range in kyr)	Assumed DBD (g/cm^3)	^{14}C	TL	MS	Pedostratigraphy			Average MAR
					Model I	Model II	Model III	
Stage 1 (12-0)	1.48	**337**		**131**	234	0	**156**	208
Stage 2 (24-12)	1.48	**449**		**1369**	1270	1505	**1348**	1055
Stage 3 (59-24)	1.48			**493**	402	292	**365**	429
Stage 4 (74-59)	1.48			**781**	1041	1297	**1126**	954
Stage 5 (130-74)	1.48			**213**	200	173	**191**	202

References used to generate data report: Yuanpu (Yuanbo)	
Data used	**Source**
Pedostratigraphy	Chen et al. (1996a), Chen et al. (1999)
Magnetic susceptibility	Chen et al. (1996a) (data provided by author)
^{14}C dating	Chen et al. (1996a)
TL dating	-
Additional References:	
Data available	**Source**
Magnetic susceptibility, pollen, ^{14}C	Chen et al. (1996a)
Pedostratigraphy, magnetic susceptibility, grain size, $CaCO_3$	Chen et al. (1997)
Magnetic susceptibility, grain size	Chen et al. (1999)

Yulin (Yuling) section: MAR (g/m^2/yr) based on pedostratigraphy

Note: The pedostratigraphic units are not labeled because this section is in the marginal desert region and is difficult to correlate with the CLP. Site name spelled as Yuling in Zhou et al. (1998) but the normally accepted spelling is Yulin. Section with potential local sources.

(Model I: min. glacial, max. interglacial; Model II: max. glacial, min. interglacial; Model III: 2/3 of interglacial soil is aeolian deposit)

Site location: 38.35° N, 109.70° E

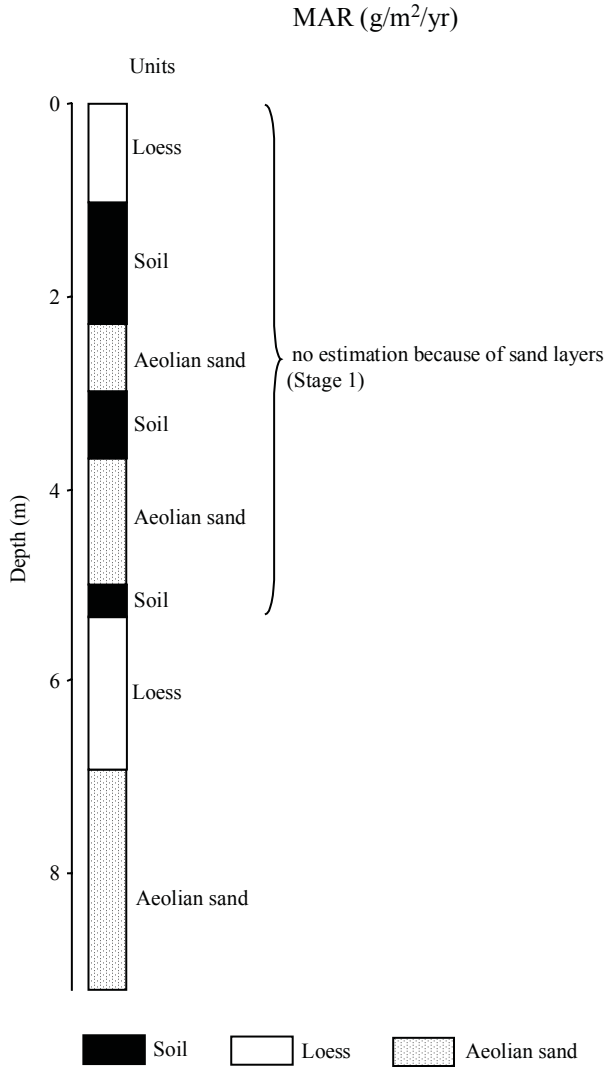

Stratigraphic data: Yulin (Yuling)
(depth and thickness estimated from diagram, to nearest 10 cm)

Top depth (m)	Bottom depth (m)	Thickness (m)	Stratigraphic units	DBD (g/cm³)
0.0	1.0	1.0	loess	n/a
1.0	2.3	1.3	soil	n/a
2.3	3.0	0.7	aeolian sand	n/a
3.0	3.7	0.7	soil	n/a
3.7	5.0	1.3	aeolian sand	n/a
5.0	5.3	0.3	soil	n/a
5.3	6.9	1.6	loess	n/a
6.9	9.2	2.3	aeolian sand	n/a

Yulin (Yuling) section: MAR (g/m^2/yr) based on ^{14}C dating

Note: The pedostratigraphic units are not labeled because this section is in the marginal desert region and is difficult to correlate with the CLP. Site name spelled as Yuling in Zhou et al. (1998) but the normally accepted spelling is Yulin. Section with potential local sources. Stage 1 MAR calculated excluding sand layers based on available dates.

Site location: 38.35° N, 109.70° E

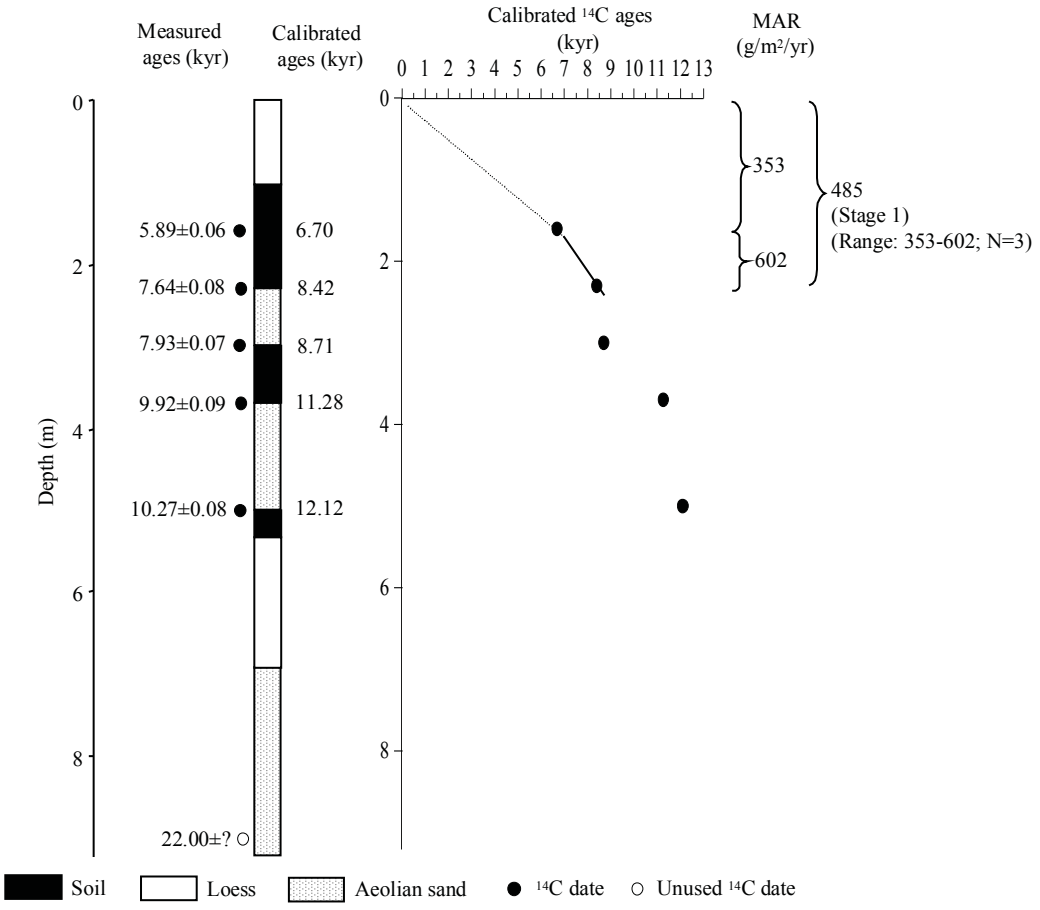

^{14}C dating: Yulin (Yuling)
(depth of the lowest date given by authors, other depths estimated from diagram, to nearest 10 cm)

Depth (m)	Dating laboratory	Lab. No.	Dating material	Age (kyr)	s.d. (kyr)	(1σ) Calendar age ranges (kyr)	Relative probability	Assumed calendar age (kyr)	Reference	Comments
1.6	n/a	n/a	n/a	5.89	0.06	6.64-6.76	0.887	6.70	Zhou et al. (1998)	
						6.77-6.79	0.113			
2.3	n/a	n/a	n/a	7.65	0.09	8.37-8.48	0.787	8.42	Zhou et al. (1998)	
						8.49-8.52	0.163			
						8.53-8.54	0.05			
3.0	n/a	n/a	n/a	7.94	0.07	8.65-8.78	0.543	8.71	Zhou et al. (1998)	
						8.92-8.98	0.262			
						8.83-8.86	0.118			
						8.88-8.90	0.076			
3.7	n/a	n/a	n/a	9.92	0.09	11.20-11.36	0.646	11.28	Zhou et al. (1998)	
						11.50-11.55	0.175			
						11.38-11.43	0.15			
						11.47-11.48	0.029			
5.0	n/a	n/a	n/a	10.27	0.08	11.91-12.32	0.857	12.12	Zhou et al. (1998)	
						11.76-11.82	0.143			
9.0	n/a	n/a	n/a	22.00					Zhou et al. (1998)	beyond calibration range

Age model (kyr): Yulin (Yuling)

Depth (m)	^{14}C	TL	Magnetic susceptibility	Pedostratigraphy (Model III)	Average chronology	Range
0	0				0.0	
1	4.2				4.2	
2	7.6				7.6	
3	8.7				8.7	
4	11.5				11.5	
5	12.1				12.1	
6					-	
7					-	
8					-	

MAR (g/m²/yr): Yulin (Yuling)

Stage (range in kyr)	Assumed DBD (g/cm^3)	^{14}C	TL	MS	Pedostratigraphy			Average MAR
					Model I	Model II	Model III	
Stage 1 (12-0)	1.48	**485**						485
Stage 2 (24-12)	1.48							
Stage 3 (59-24)	1.48							
Stage 4 (74-59)	1.48							
Stage 5 (130-74)	1.48							

References used to generate data report: Yulin (Yuling)	
Data used	**Source**
Pedostratigraphy	Zhou et al. (1998)
Magnetic susceptibility	-
^{14}C dating	Zhou et al. (1998)
TL dating	-
Additional References:	
Data available	**Source**
-	-

Zhaitang section: MAR (g/m^2/yr) based on pedostratigraphy

(Model I: min. glacial, max. interglacial; Model II: max. glacial, min. interglacial; Model III: 2/3 of interglacial soil is aeolian deposit)

Site location: 39.98° N, 115.68° E

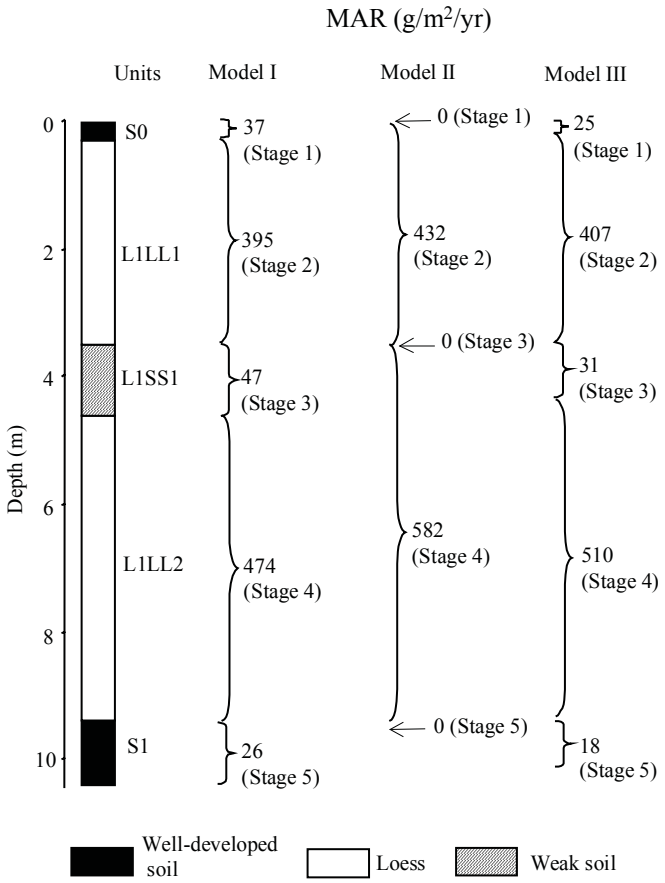

Stratigraphic data: Zhaitang (depth and thickness estimated from diagram, to nearest 10 cm)				
Top depth (m)	Bottom depth (m)	Thickness (m)	Stratigraphic units	DBD (g/cm^3)
0.0	0.3	0.3	S0	n/a
0.3	3.5	3.2	L1LL1	n/a
3.5	4.6	1.1	L1SS1	n/a
4.6	9.4	4.8	L1LL2	n/a
9.4	10.4	1.0	S1	n/a

Zhaitang section: TL and ^{14}C dating

Note: No MAR calculated because only one TL date is used.

Site location: 39.98° N, 115.68° E

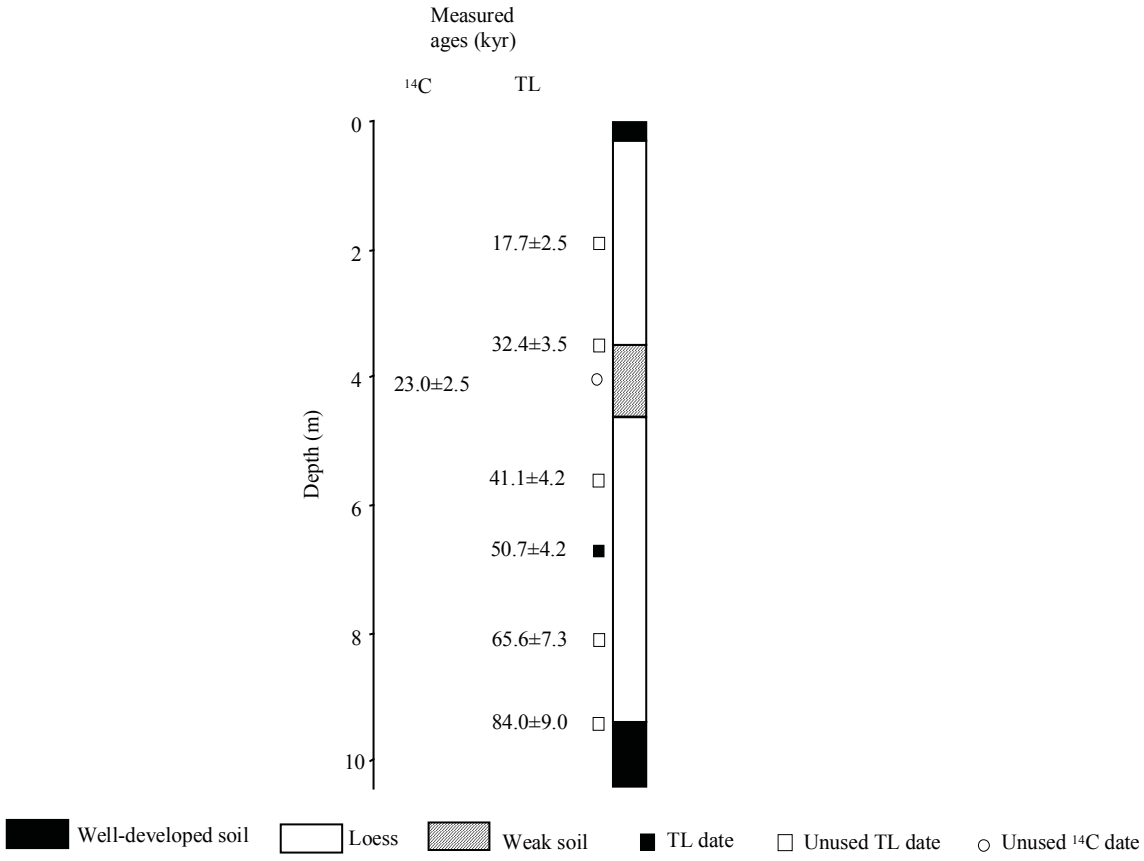

TL dating: Zhaitang
(depth given by authors)

Depth (m)	Dating laboratory	Lab. No.	Dating material	TL-method	Age (kyr)	s.d. (kyr)	Reference	Comments
1.9	Univ. of Adelaide	Z-08	quartz	fine-grain (4-11 µm) technique	17.7	2.5	Lu et al. (1987a)	uncertainties larger than 10 %
3.5	Univ. of Adelaide	Z-06	quartz	fine-grain (4-11 µm) technique	32.4	3.5	Lu et al. (1987a)	uncertainties larger than 10 %
5.6	Univ. of Adelaide	Z-04	quartz	fine-grain (4-11 µm) technique	41.1	4.2	Lu et al. (1987a)	uncertainties larger than 10 %
6.7	Univ. of Adelaide	Z-03	quartz	fine-grain (4-11 µm) technique	50.7	4.2	Lu et al. (1987a)	
8.1	Univ. of Adelaide	Z-02	quartz	fine-grain (4-11 µm) technique	65.6	7.3	Lu et al. (1987a)	uncertainties larger than 10 %
9.4	Univ. of Adelaide	Z-01	quartz	fine-grain (4-11 µm) technique	84	9	Lu et al. (1987a)	uncertainties larger than 10 %

^{14}C dating: Zhaitang
(the authors only state that the sample is from L1SS1)

Depth (m)	Dating laboratory	Lab. No.	Dating material	Age (kyr)	s.d. (kyr)	(1σ) Calendar age ranges (kyr)	Relative probability	Assumed calendar age (kyr)	Reference	Comments
within L1SS1	Xi'an Loess Lab.	n/a	carbonate	23.0	1.5				Lu et al. (1987a)	beyond calibration range; Lu et al. (1987a) cited An and Lu (1984) as source

Age model (kyr): Zhaitang						
Depth (m)	^{14}C	TL	Magnetic susceptibility	Pedostratigraphy (Model III)	Average chronology	Range
0				0.0	0.0	
2				18.5	18.5	
4				46.9	46.9	
6				64.0	64.0	
8				69.9	69.9	
10				130.0	130.0	

MAR (g/m²/yr): Zhaitang								
Stage (range in kyr)	Assumed DBD (g/cm^3)	^{14}C	TL	MS	Pedostratigraphy			Average MAR
					Model I	Model II	Model III	
Stage 1 (12-0)	1.48				37	0	**25**	25
Stage 2 (24-12)	1.48				395	432	**407**	407
Stage 3 (59-24)	1.48				47	0	**31**	31
Stage 4 (74-59)	1.48				474	582	**510**	510
Stage 5 (130-74)	1.48				26	0	**18**	18

References used to generate data report: Zhaitang	
Data used	**Source**
Pedostratigraphy	Lu et al. (1987a)
Magnetic susceptibility	-
^{14}C dating	Original reference is An and Lu (1984) but data taken from Lu et al. (1987a)
TL dating	Lu et al. (1987a)
Additional References:	
Data available	**Source**
Pedostratigraphy, ^{14}C	An and Lu (1984)
Pedostratigraphy, ^{14}C, TL	Lu et al. (1987b)
Pedostratigraphy, ^{14}C	Wen and Zheng (1987)
Grain size	Xiong, S. F. (unpublished data)

Zhangjiayuan section: MAR (g/m^2/yr) based on pedostratigraphy

(Model I: min. glacial, max. interglacial; Model II: max. glacial, min. interglacial; Model III: 2/3 of interglacial soil is aeolian deposit)

Site location: 34.27° N, 107.83° E

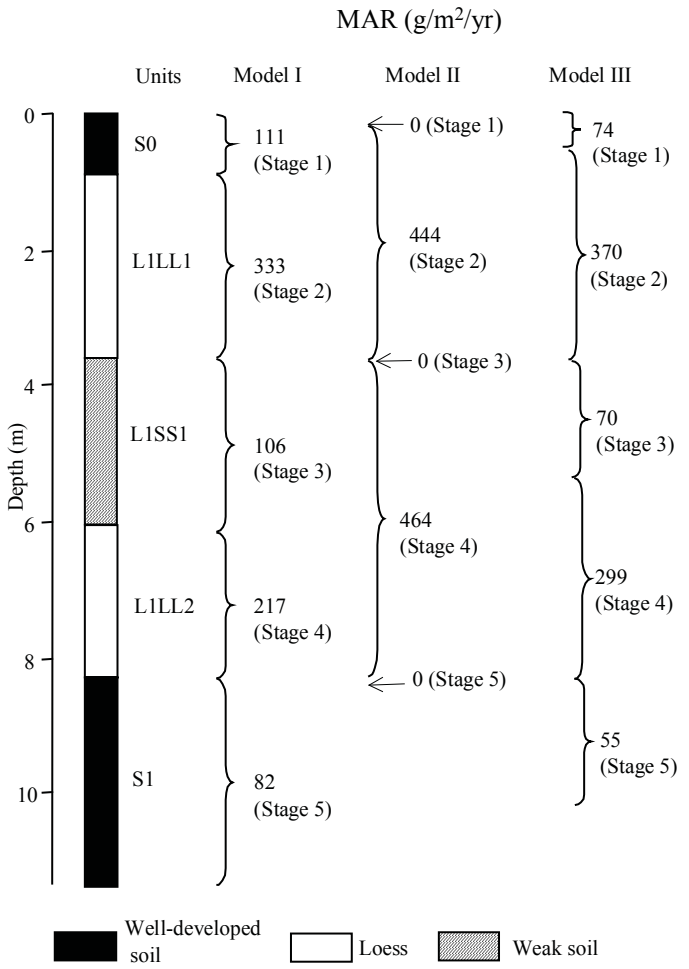

Stratigraphic data: Zhangjiayuan (depths given by the authors)				
Top depth (m)	Bottom depth (m)	Thickness (m)	Stratigraphic units	DBD (g/cm^3)
0.0	0.9	0.9	S0	n/a
0.9	3.6	2.7	L1LL1	1.48
3.6	6.1	2.5	L1SS1	1.48
6.1	8.3	2.2	L1LL2	1.48
8.3	11.4	3.1	S1	1.68

Age model (kyr): Zhangjiayuan						
Depth (m)	^{14}C	TL	Magnetic susceptibility	Pedostratigraphy (Model III)	Average chronology	Range
0				0.0	0.0	
2				17.6	17.6	
4				32.2	32.2	
6				62.5	62.5	
8				72.4	72.4	
10				105.0	105.0	

MAR ($g/m^2/yr$): Zhangjiayuan								
Stage (range in kyr)	Measured DBD (g/cm^3)	^{14}C	TL	MS	Pedostratigraphy			Average MAR
					Model I	Model II	Model III	
Stage 1 (12-0)	1.48				111	0	**74**	74
Stage 2 (24-12)	1.48				333	444	**370**	370
Stage 3 (59-24)	1.48				106	0	**70**	70
Stage 4 (74-59)	1.48				217	464	**299**	299
Stage 5 (130-74)	1.68				82	0	**55**	55

References used to generate data report: Zhangjiayuan	
Data used	**Source**
Pedostratigraphy	Wei et al. (1991)
Magnetic susceptibility	-
^{14}C dating	-
TL dating	-
Additional References:	
Data available	**Source**
Grain size, DBD and other mechanical parameters	Wei et al. (1991)

Zihedian section

Note: Section not used to estimate MAR, because the pedostratigraphy cannot be easily correlated with that of the CLP, and the only TL date > 130 kyr.

Site location: 36.78 ° N, 118.37° E

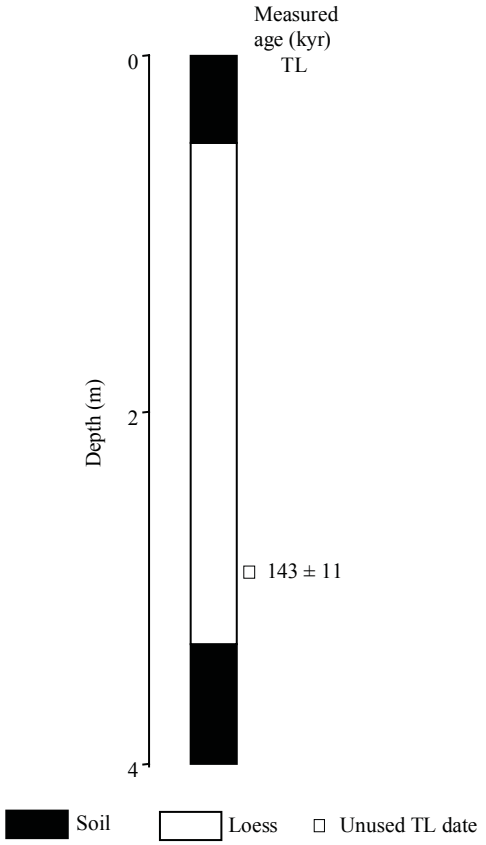

Stratigraphic data: Zihedian (depth and thickness estimated from diagram, to nearest 10 cm)				
Top depth (m)	Bottom depth (m)	Thickness (m)	Stratigraphic units	DBD (g/cm^3)
0	0.57	0.57	S0?	n/a
0.57	3.36	2.79	L1?	n/a
3.36	3.92	0.56	S1?	n/a

TL dating: Zihedian (depth estimated from diagram, to nearest 10 cm)								
Depth (m)	Dating laboratory	Lab. No.	Dating material	TL-method	Age (kyr)	s.d. (kyr)	Reference	Comments
3.0	n/a	n/a	n/a	n/a	143	11	Zheng et al. (1994)	

References used to generate data report: Zihedian	
Data used	**Source**
Pedostratigraphy	Zheng et al. (1994)
Magnetic susceptibility	-
^{14}C dating	-
TL dating	Zheng et al. (1994)
Additional References:	
Data available	**Source**
-	-

117 km milestone site section: pedostratigraphy

Note: S0 is a residual soil, L1 only partially exposed. No estimation for pedostratigraphy based MAR.

(Model I: min. glacial, max. interglacial; Model II: max. glacial, min. interglacial; Model III: 2/3 of interglacial soil is aeolian deposit)

Site location: 44.28° N, 86.25° E

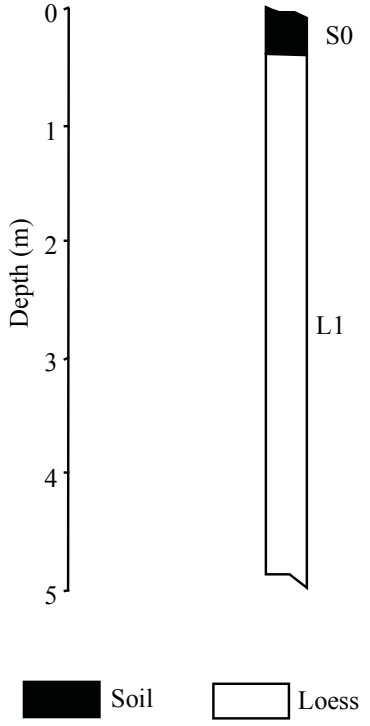

Stratigraphic data: 117 km milestone site (thickness given by author, depth calculated from thickness)				
Top depth (m)	Bottom depth (m)	Thickness (m)	Stratigraphic units	DBD (g/cm^3)
0	0.4	0.4	S0	n/a
0.4		n/a	L1	n/a

117 km milestone site section: MAR (g/m^2/yr) based on ^{14}C dating

Note: S0 is a residual soil, L1 only partially exposed.

(Model I: min. glacial, max. interglacial; Model II: max. glacial, min. interglacial; Model III: 2/3 of interglacial soil is aeolian deposit)

Site location: 44.28° N, 86.25° E

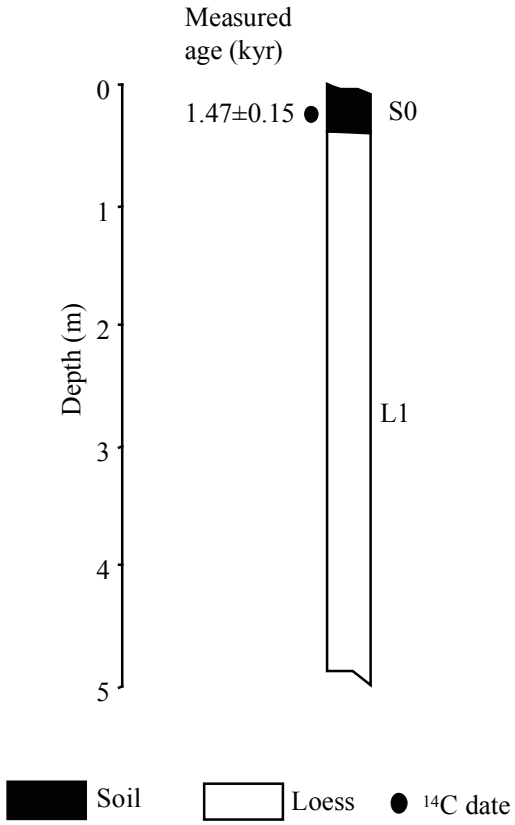

^{14}C dating: (position of ^{14}C not indicated)									
Depth (m)	Dating laboratory	Lab. No.	Dating material	Age ± s.d. (kyr)	(1σ) Calendar age ranges (kyr)	Relative probability	Assumed calendar age (kyr)	Reference	Comments
-	n/a	n/a	n/a	1.47 ± 0.15				Wen and Zheng (1987)	

References used to generate data report: 117 km milestone site	
Data used	**Source**
Pedostratigraphy	Wen and Zheng (1987)
Magnetic susceptibility	-
^{14}C dating	Wen and Zheng (1987)
TL dating	-
Additional References:	
Data available	**Source**
-	-

5. Summary of Results

5.1 Inventory

There are 98 sites in the data base (Table 1). However, MAR estimates could only be made (for at least one MIS stage) at 77 site locations (Table 3). Of these 77 sites, 50 provide estimates based on pedostratigraphic correlation (Table 4), 35 on magnetic susceptibility (Table 5), 12 on TL-dating (Table 6) and 16 on radiocarbon dating (Table 7). From these 77 sites, we made at total of 355 MAR estimates: 66 for MIS 1, 65 for MIS 2, 69 for MIS 3, 65 for MIS 4, and 90 for MIS 5. The majority of these estimates are based pedostratigraphic (149) and magnetic susceptibility (163) chronologies. Only 20 estimates could be made using TL-based chronologies and only 23 using radiocarbon-based chronologies (Figure 3).

The fact that comparatively few MAR estimates could be made using dating techniques that are not based on correlation with MIS reflects, in part, the screening (and rejection) of a large number of dates. Thus, 77 of the 129 TL dates available and 33 of the 102 radiocarbon dates available were rejected. The criteria for rejecting specific dates (see Sections 3.3.1 and 3.3.2) are not draconian: dates were not used to erect chronologies when they exceeded generally accepted maximum limits for each dating technique, when the error bars were >10% of the measured age or when sample contamination was suspected. Only one date was used when pairs of dates were overlapping or reversed in age.

The reliance on chronostratigraphic correlation to derive age models at most sites and for most time intervals imposes significant limitations on the MAR estimates compiled here. First, it is not possible to derive a highly-resolved record of changes in MAR through time; the MAR estimates represent long-term averages in accumulation under interglacial, interstadial or glacial periods. Second, the synchroneity enforced on the records by assuming that intervals of soil formation or loess deposition are coincident with MIS precludes any consideration of possible leads/lags in the timing of global and regional climate changes, or of differences in the timing of events across the CLP itself.

There is no doubt that the CLP is one of the best-studied loess regions in the world. Although there is potential to derive records from nearly 100 sites on the CLP, in reality relatively few sites provide quantitative estimates of aeolian MAR and even then the estimates represent long-term average accumulation. It would be difficult to produce MAR estimates for specific time slices, as is routinely done when compiling other kinds of palaeoenvironmental data for use in earth-system model evaluations (see Kohfeld and Harrison, 2000). There is still much work to be done to improve the chronologies of existing sections, to increase the temporal resolution of the age models, and to extend the spatial coverage of sites from the CLP.

Figure 3. Site Inventory

Sites at which mass accumulation rates can be estimated from any stage using acceptable radiocarbon or luminescence dates. (a) Sites with radiocarbon dates. Solid blue symbols are locations where MARs have been estimated, open symbols are sites with radiocarbon dates, but not enough acceptable dates to estimate MAR for any stage. (b) Sites with luminescence dates. Solid red symbols are sites were MARs for any stage have been estimated; open symbols are sites with luminescence dates, but not enough acceptable dates to calculate MAR. (c) All sites at which MARs could be estimated for at least one stage using either radiocarbon (blue symbols), luminescence dates (red symbols) or both (green squares).

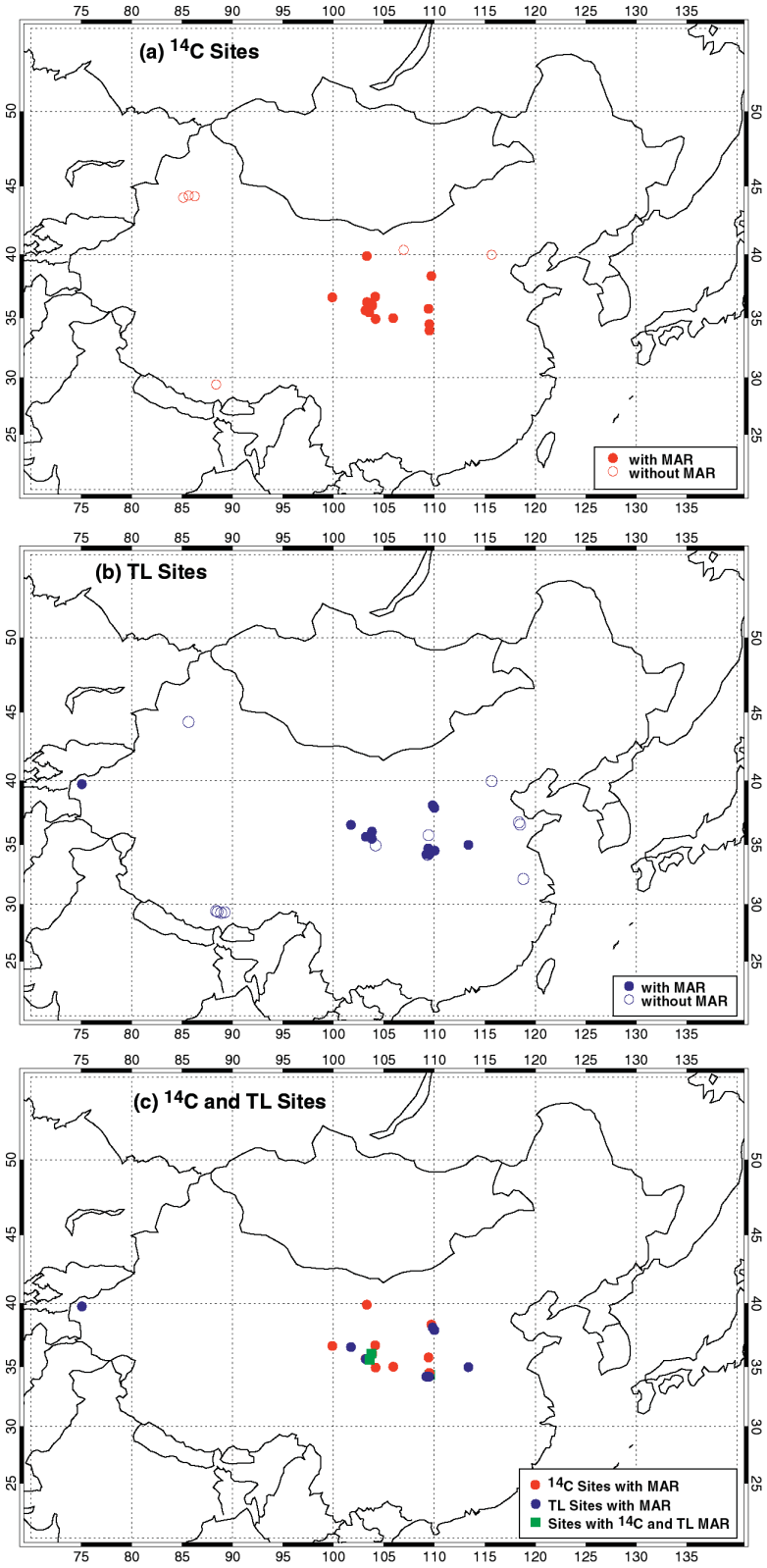

Table 3. Average MAR ($g/m^2/yr$) Estimated for All Data

Site	Latitude (ºN)	Longitude (ºE)	Stage 1	Stage 2	Stage 3	Stage 4	Stage 5
Ancun	35.57	106.87	-	-	180	309	41
Baicaoyuan	36.27	105.10	144	335	470	253	154
Baige	34.80	112.62	-	-	-	-	18
Baimapo	34.17	109.32	-	153	89	131	28
Baishui	35.20	109.59	-	69	62	44	83
Banshan	34.68	105.70	164	366	54	289	76
Baoji (Lingyuan)	34.33	107.00	111	179	128	206	50
Baxie (Dongxiang)	35.58	103.57	1298	944	-	-	-
Beiyuan	35.62	103.20	158	863	491	726	261
Beiyuantou	36.05	107.50	81	468	185	331	75
Beizhuangcun	34.50	109.50	574	-	-	-	-
Caijiagou	38.12	109.83	-	-	345	-	134
Caocun	34.63	111.15	262	-	-	-	70
Caoxian	36.37	104.62	-	-	-	-	153
Chagelebulu_1	39.88	103.30	506	-	-	-	-
Chagelebulu_2	39.88	103.30	387	-	-	-	-
Changqugou	37.45	108.70	-	-	-	-	72
Changwu	35.20	107.82	251	304	39	332	42
Chenjiawo	34.18	109.48	25	345	100	194	21
Chifeng	42.17	119.02	136	237	154	346	139
Chunhua	34.80	108.55	147	168	215	198	67
Dadiwan	35.00	105.92	1048	348	-	-	-
Duanjiapo (Lantian)	34.20	109.20	142	159	71	128	28
Dunwashan	35.85	103.25	-	-	-	2113	223
Fujiazhuang	36.60	118.50	-	-	-	-	18
Ganzi	31.63	99.98	164	514	56	312	53
Gaolanshan	36.00	103.83	294	1277	347	1027	116
Guojialiang	37.50	108.88	-	-	-	-	140
Halali	36.67	99.88	268	-	-	-	-
Heimugou_1	35.75	109.42	116	262	115	259	58
Heimugou_2	35.75	109.42	131	-	-	-	46
Heshui	35.82	108.03	-	-	-	-	49
Huangling	35.60	109.37	-	-	-	-	35
Huanglong	35.62	109.78	67	97	130	187	75
Huanxian	36.58	107.35	169	339	501	565	109
Jiezicun	34.33	109.57	203	210	110	190	84
Jinjiyuan	33.90	109.92	-	-	-	-	11
Jiuzhoutai	36.07	103.75	664	636	472	570	563
Jiyuan	37.15	107.38	-	532	809	692	171
Kansu	39.75	75.05	-	-	-	-	18
Landa	36.05	103.84	296	-	-	-	-
Lijiayuan	36.12	104.85	180	340	455	385	146
Liujiapo_1	34.20	109.20	-	105	127	226	48
Liujiapo_2 (Xian)	34.23	109.12	-	107	55	89	51
Lujiaowan	44.33	85.63	125	-	-	-	6
Majiayuan	36.27	107.50	138	420	340	296	90
Mangshan_1	34.93	113.53	-	-	-	-	30
Mangshan_2	34.97	113.37	214	5238	473	2279	1330
Mengdashan	35.77	102.00	512	-	-	-	50
Mizhi	37.83	110.08	-	-	-	-	95
Mujiayuan (Wupu)	37.57	110.72	166	205	252	380	69
Ningxian	35.48	107.97	187	200	211	252	68
Niuquanzi	44.18	85.10	-	-	21	-	-
Pucheng	34.97	109.60	-	60	83	95	16
Qinjiazhai	35.74	109.43	-	-	-	-	48
Qishan	34.45	107.63	-	208	91	113	34
Renjiahutong	35.75	109.42	219	241	-	-	-
Shangjiapo	34.32	108.12	-	341	177	312	29
Shenjiazhuang	36.72	104.13	442	442	-	-	-
Shimao	37.92	110.00	-	-	-	-	193
Tuxiangdao	36.58	101.73	90	-	-	-	170
Weinan (Yangguo)	34.35	109.52	207	289	123	184	63
Wuyishan	35.80	103.22	-	-	140	1022	62

Site	Latitude (ºN)	Longitude (ºE)	Stage 1	Stage 2	Stage 3	Stage 4	Stage 5
Xiadongcun (Jixian)	36.10	110.67	127	203	147	288	47
Xifeng	35.70	107.70	122	372	168	302	85
Xining (Dadunling)	36.63	101.80	171	733	269	435	175
Xinzhuangyuan	36.20	104.73	171	486	609	611	204
Xueyuan	36.92	106.97	121	514	258	540	144
Xunyi	35.13	108.33	113	130	171	197	83
Yanchang	36.60	110.02	95	212	285	410	56
Yangjiashan	34.00	106.65	-	-	113	358	63
Yichuan	36.13	110.15	172	200	210	216	76
Yinwan	34.93	104.17	619	285	-	-	-
Yuanpu (Yuanbo)	35.63	103.17	208	1055	429	954	202
Yulin (Yuling)	38.35	109.70	485	-	-	-	-
Zhaitang	39.98	115.68	25	407	31	510	18
Zhangjiayuan	34.27	107.83	74	370	70	299	55

Table 4. MAR ($g/m^2/yr$), Pedostratigraphy Model III

Site	Latitude (ºN)	Longitude (ºE)	Stage 1	Stage 2	Stage 3	Stage 4	Stage 5
Ancun	35.57	106.87	-	-	180	309	41
Baicaoyuan	36.27	105.10	132	-	-	-	152
Baige	34.80	112.62	-	-	-	-	18
Baimapo	34.17	109.32	-	-	70	161	19
Banshan	34.68	105.70	164	366	54	289	76
Baoji (Lingyuan)	34.33	107.00	103	225	71	259	32
Beiyuan	35.62	103.20	134	1242	244	1128	127
Caijiagou	38.12	109.83	-	-	345	-	134
Caocun	34.63	111.15	262	-	-	-	70
Caoxian	36.37	104.62	-	-	-	-	153
Changqugou	37.45	108.70	-	-	-	-	72
Changwu	35.20	107.82	251	304	39	332	42
Chenjiawo (Lantian_1)	34.18	109.48	25	345	23	194	21
Dadiwan	35.00	105.92	-	348	-	-	-
Duanjiapo (Lantian)	34.20	109.20	135	177	64	148	26
Dunwashan	35.85	103.25	-	-	-	2113	223
Fujiazhuang	36.60	118.50	-	-	-	-	18
Ganzi	31.63	99.98	164	514	56	312	53
Gaolanshan	36.00	103.83	300	1599	169	1283	85
Guojialiang	37.50	108.88	-	-	-	-	140
Halali	36.67	99.88	267	-	-	-	-
Heimugou_1 (Luochuan)	35.75	109.42	-	-	96	349	45
Heimugou_2	35.75	109.42	131	-	-	-	46
Heshui	35.82	108.03	-	-	-	-	49
Huangling	35.60	109.37	-	-	-	-	35
Jiezicun (Jiezhichun)	34.33	109.57	-	179	155	86	62
Jinjiyuan (Shangzhou)	33.90	109.92	-	-	-	-	11
Jiuzhoutai (Lanzhou)	36.07	103.75	-	851	361	648	197
Kansu	39.75	75.05	-	-	-	-	12
Liujiapo_1	34.20	109.20	-	-	53	226	48
Liujiapo_2 (Xian)	34.23	109.12	-	107	55	89	51
Lujiaowan	44.33	85.63	125	-	-	-	6
Mangshan_1	34.93	113.53	-	-	-	-	30
Mangshan_2	34.97	113.37	214	5238	500	2355	395
Mengdashan	35.77	102.00	512	-	-	-	50
Niuquanzi	44.18	85.10	-	-	21	-	-
Qinjiazhai	35.74	109.43	-	-	-	-	48
Qishan	34.45	107.63	-	284	72	128	28
Shangjiapo	34.32	108.12	-	341	177	312	29
Shimao	37.92	110.00	-	-	-	-	140
Tuxiangdao	36.58	101.73	90	-	-	-	198
Weinan (Yangguo)	34.35	109.52	118	328	100	253	64
Wuyishan	35.80	103.22	-	-	140	1022	62
Xiadongcun (Jixian)	36.10	110.67	62	171	117	378	41
Xifeng	35.70	107.70	104	479	106	342	78
Xining (Dadunling)	36.63	101.80	123	1159	39	559	159
Yangjiashan (Fenzhou)	34.00	106.65	-	-	113	358	63
Yulin (Yuling)	38.35	109.70	156	1348	365	1126	191
Zhangjiayuan	34.27	107.83	25	407	31	510	18
Zihedian	36.78	118.37	74	370	70	299	55

Table 5. MAR ($g/m^2/yr$), Magnetic Susceptibility Age Models

Site	Latitude (ºN)	Longitude (ºE)	Stage 1	Stage 2	Stage 3	Stage 4	Stage 5
Baicaoyuan	36.27	105.10	156	335	470	253	155
Baimapo	34.17	109.32	-	153	108	100	37
Baishui	35.20	109.59	-	69	62	44	83
Baoji (Lingyuan)	34.33	107.00	118	133	184	153	68
Beiyuan	35.62	103.20	183	483	647	569	174
Beiyuantou	36.05	107.50	81	468	185	331	75
Chifeng	42.17	119.02	136	237	154	346	139
Chunhua	34.80	108.55	147	168	215	198	67
Duanjiapo	34.20	109.20	149	141	78	107	30
Gaolanshan	36.00	103.83	270	954	525	771	146
Heimugou_1	35.75	109.42	-	274	152	213	72
Heimugou_1	35.75	109.42	116	250	98	214	57
Huanglong	35.62	109.78	67	97	130	187	75
Huanxian	36.58	107.35	169	339	501	565	109
Jiezicun	34.33	109.57	-	179	155	86	62
Jiuzhoutai	36.07	103.75	-	422	582	491	210
Jiyuan	37.15	107.38	-	532	809	692	171
Lijiayuan	36.12	104.85	180	340	455	385	146
Majiayuan	36.27	107.50	138	420	340	296	90
Mizhi	37.83	110.08	-	-	-	-	95
Mujiayuan	37.57	110.72	166	205	252	380	69
Ningxian	35.48	107.97	187	200	211	252	68
Pucheng	34.97	109.60	-	60	83	95	16
Qishan	34.45	107.63	-	132	110	98	39
Weinan (Yangguo)	34.35	109.52	142	287	133	188	61
Xiadongcun	36.10	110.67	80	286	155	260	53
Xiadongcun	36.10	110.67	239	151	168	226	47
Xifeng	35.70	107.70	140	265	229	261	91
Xining	36.63	101.80	219	307	498	310	191
Xinzhuangyuan	36.20	104.73	171	486	609	611	204
Xueyuan	36.92	106.97	121	514	258	540	144
Xunyi	35.13	108.33	113	130	171	197	83
Yanchang	36.60	110.02	95	212	285	410	56
Yichuan	36.13	110.15	172	200	210	216	76
Yuanpu	35.63	103.17	131	1369	493	781	213

Table 6. MAR ($g/m^2/yr$), TL Ages

Site	Latitude (ºN)	Longitude (ºE)	Stage 1	Stage 2	Stage 3	Stage 4	Stage 5
Baxie (Dongxiang)	35.58	103.57	1449	1449	-	-	-
Beiyuan	35.62	103.20	-	-	582	481	481
Caijiagou	38.12	109.83	-	-	345	-	134
Chenjiawo (Lantian_1)	34.18	109.48	-	-	177	-	-
Jiezicun (Jiezhichun)	34.33	109.57	-	-	-	-	158
Jiuzhoutai (Lanzhou)	36.07	103.75	-	-	-	-	1281
Kansu	39.75	75.05	-	-	-	-	24
Liujiapo_1	34.20	109.20	-	105	201	-	-
Mangshan_2	34.97	113.37	-	-	446	2202	2265
Shimao	37.92	110.00	-	-	-	-	245
Tuxiangdao	36.58	101.73	-	-	-	-	141
Weinan (Yangguo)	34.35	109.52	-	-	137	110	-

Table 7. MAR ($g/m^2/yr$), Radiocarbon Ages (Calendar Years)

Site	Latitude (ºN)	Longitude (ºE)	Stage 1	Stage 2
Baxie (Dongxiang)	35.58	103.57	1147	438
Beizhuangcun (Weinan)	34.50	109.50	574	-
Chagelebulu_1 (Cagelebulu)	39.88	103.30	506	-
Chagelebulu_2 (Cagelebulu)	39.88	103.30	387	-
Dadiwan	35.00	105.92	1048	-
Gaolanshan	36.00	103.83	313	-
Halali	36.67	99.88	269	-
Jiezicun (Jiezhichun)	34.33	109.57	203	203
Jiuzhoutai (Lanzhou)	36.07	103.75	664	-
Landa	36.05	103.84	296	-
Renjiahutong	35.75	109.42	219	241
Shenjiazhuang	36.72	104.13	442	442
Weinan (Yangguo)	34.35	109.52	361	251
Yinwan	34.93	104.17	619	285
Yuanpu (Yuanbo)	35.63	103.17	337	449
Yulin (Yuling)	38.35	109.7	485	-

Table 8. Inventory of Radiocarbon and Thermoluminescence Ages.

	Radiocarbon		Thermoluminescence[#]	
	Dates	Sites*†	Dates	Sites*†
Acceptable	69	16	52	12
Total	102	23	129	24

*Sites where there are enough acceptable dates to allow estimation of a mass accumulation rate

†Five sites contain enough radiocarbon and luminescence dates to estimate MARs from both.

[#]Five dates at Mangshan_2 are optically stimulated luminescence (OSL) dates. (All three acceptable dates at this site are OSL dates.)

5.2 Average Aeolian Mass Accumulation Rates for Stages 1-5

An average aeolian MAR was calculated for each MIS based on all the MARs calculated for a given Stage regardless of the dating technique used to define the Stage boundaries (Figure 4, Table 9). The glacial Stages (MIS 2 and 4) show higher rates of accumulation than the interglacial or interstadial periods. The regionally-averaged accumulation rates are 467 and 438 $g/m^2/yr$ for glacial Stages 2 and 4 respectively. Accumulation rates for the two interglacial Stages (MIS 1 and 5) are lower than the glacial values. The MAR for Stage 5 is 109 $g/m^2/yr$ and the estimate for Stage 1 is 256 $g/m^2/yr$. Thus, aeolian MARs for Stage 2 are on average 4.9 times greater than for Stage 5 and 3.5 times greater than for Stage 1. Thus, the MAR data available support the canonical idea that glacials were times of greater atmospheric dust loading, and hence dust deposition, than interglacials (see e.g. Petit et al., 1981; Heller and Liu, 1982; Hammer et al., 1985; Pye, 1987; Hovan et al., 1989; Rea, 1994).

The average accumulation rate for Stage 1 (256 $g/m^2/yr$) is significantly greater than the average accumulation rate for Stage 5 (109 $g/m^2/yr$), and indeed is rather similar to the value obtained for interstadial Stage 3 (222 $g/m^2/yr$). It is plausible that MAR values for Stage 5 should be lower than those for Stage 1, given other palaeoenvironmental evidence suggesting that the last interglacial was both warmer and wetter than the present interglacial (e.g. Sun et al., 1997). However, the similarity between the average MAR for interglacial Stage 1 and interstadial Stage 3 is surprising and unlikely to be due to a similarity in climatic conditions. There are several possible explanations for this situation.

First, it is possible that the Stage 1 MAR values are artificially inflated because of the long history of human activity on the CLP (Mannion, 1999; Ren, 2000), which may have created conditions of enhanced dust production and deposition (Gill, 1996; Chen et al., 1999a). We are unable to evaluate this hypothesis because the present synthesis does not contain enough information to quantify the magnitude of recent human activities at individual sites.

A second possible explanation is that the difference between the Stage 1 and Stage 5 estimates may be influenced by the methods used to identify and date the two intervals. The estimates for earlier intervals in the loess records are mostly based on correlation methods (i.e. pedostratigraphy or MS), which would tend to reinforce the canonical interpretation of low rates of deposition during interglacial periods. More of the Stage 1 MAR estimates are based on radiocarbon dating. Thus, the large difference between estimates for Stage 1 and Stage 5 may not be real, and the MAR values obtained for Stage 1 may be more typical of interglacial conditions. This would suggest that, although dust deposition is enhanced during the extreme conditions of the glacial periods, the difference is smaller than the 10-fold glacial-interglacial difference suggested by (Broecker, 1995) and (Reader et al., 1999), and more in agreement with the 3-fold differences suggested by (An et al., 1991b) for the central CLP. Furthermore, even the relatively small changes in climate towards interstadial conditions were sufficient to reduce dust deposition rates towards interglacial levels. The present synthesis allows us to explore the impact of different dating methods on the definition of Stage boundaries and MAR estimates for each age (Sections 5.2.1 and 5.2.2).

The MARs for Stage 5 represent average conditions over ca 56 kyr, while the MARs for Stage 1 represent average conditions for only the last 12 kyr. It is possible that the apparent difference between the average MAR values for Stage 1 and Stage 5 may

represent a sampling problem (i.e. that the 12 kyr-record of the current interglacial does not represent the full range of variations in dust deposition within an interglacial). Rates of dust deposition appear to be highly sensitive to climatically-induced changes in source areas (McTainsh, 1989; Goudie and Middleton, 1992; Marticorena and Bergametti, 1996; Mahowald et al., 1999; Tegen et al., in prep; Ginoux et al., submitted), and there is abundant palaeoenvironmental evidence for millenial to multi-millenial climate variability within both Stage 5 (An and Porter, 1997; Chen et al., 1999b; 1999c; Fang et al., 1999; Rasmussen et al., 1999; Eynaud et al., 2000) and Stage 1 (von Grafenstein et al., 1999; Chapman and Shackleton, 2000; deMenocal et al., 2000; Giraudeau et al., 2000; Sarkar et al., 2000; Thompson, 2000). The current synthesis does not allow us to test fully the hypothesis that the difference in the Stage 1 and Stage 5 estimates is a sampling problem, because we have insufficient dating resolution to allow us to reconstruct millennial-scale variations in dust deposition rates within Stage 5. However, we are able to examine the radiocarbon-dated records from Stage 1 and to determine whether millennial-scale climate variability has a significant impact on dust deposition rates within the Holocene (Section 5.2.3).

Figure 4. Regionally-Averaged Aeolian Mass Accumulation Rates

Aeolian mass accumulation rates ($g/m^2/yr$) estimated for each marine isotope stage, averaged across the CLP for all sites with any data (blue bars), compared to sites using only pedostratigraphy (dark red), only magnetic susceptibility (yellow) and only ^{14}C and TL dating (light blue bars). Numbers across the bottom of the graph represent the number of samples used for the average

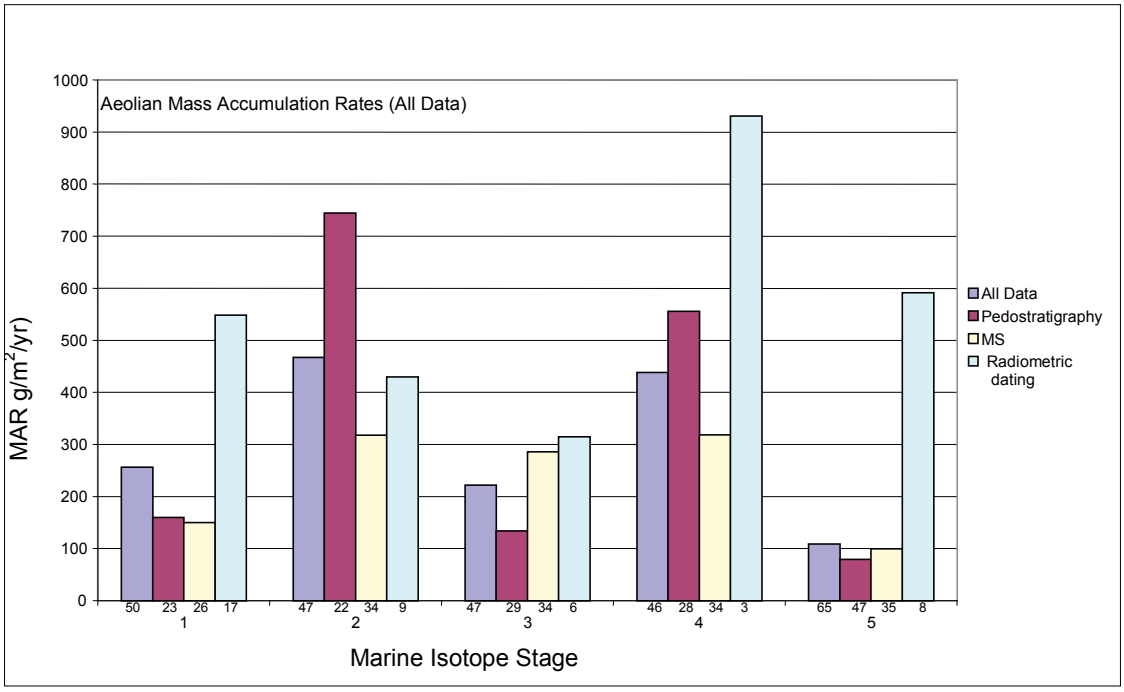

Table 9. MAR Statistics, Comparing Different Dating Methods.

Statistics	Stage 1	Stage 2	Stage 3	Stage 4	Stage 5	Ratio 2/1	Ratio 2/5
			Average, All Data				
Average	256	467	222	438	109	3.5	4.9
S. D.	243	756	175	444	175	4.7	4.2
Max	1298	5238	809	2279	1330	24.5	22.6
Min	25	60	21	44	6	0.3	0.8
N	50	47	47	46	65	39	42
			Pedostratigraphy				
Average	160	745	134	556	79	7.0	8.8
S. D.	106	1090	120	576	74	6.5	5.3
Max	512	5238	500	2355	395	24.5	22.6
Min	25	107	21	86	6	1.2	2.1
N	23	22	29	28	47	16	21
			Magnetic Susceptibility				
Average	149	318	286	318	99	2.4	3.3
S. D.	48	257	196	201	55	2.0	1.4
Max	270	1369	809	781	213	10.5	6.5
Min	67	60	62	44	16	0.6	0.8
N	26	34	34	34	35	26	34
			^{14}C and TL				
Average	548	429	315	931	591	0.9	1.3
S. D.	352	401	175	1116	787	0.3	
Max	1449	1449	582	2202	2265	1.3	1.3
Min	203	105	137	110	24	0.5	1.3
N	17	9	6	3	8	5	1
Range of Averages	150-548	318-745	134-315	318-931	79-591	0.9-7.0	1.3-8.8

5.2.1 Comparison of Averages Based on Different Dating Techniques

We have estimated average aeolian MARs for each MIS based on all of the MARs calculated for a given Stage using each dating technique (i.e. pedostratigraphy, magnetic susceptibility, TL and radiocarbon dating) separately, in order to explore the impact of using different dating techniques to define stage boundaries and hence to calculate MAR. We have also made comparisons of the age models, and of the inferred MARs for individual Stages, at the limited number of sites (24) for which we have estimates based on multiple different dating techniques.

The regionally-averaged MAR estimates based on different dating techniques are very different (Figure 4, Table 9). The average MAR for the CLP for Stage 1, for example, ranges from 149 $g/m^2/yr$ (using magnetic susceptibility) to 548 $g/m^2/yr$ (using radiocarbon dating). For Stage 2, the regionally-averaged MAR ranges from 318 $g/m^2/yr$ (magnetic susceptibility) to 745 $g/m^2/yr$ (pedostratigraphy). The Stage 2/Stage 1 MAR ratio varies from 0.9 to 7.0, depending on which dating technique was used to define the stage boundaries.

The pedostratigraphy and magnetic susceptibility age models are based on correlation with the marine isotope stratigraphy of Martinson et al. (1987). Both chronologies assume that processes on the CLP (i.e. soil formation or magnetic susceptibility enhancement) and changes in global ice volume as recorded in the marine isotope stratigraphy were contemporaneous. Thus, both techniques should effectively reinforce the canonical view that high accumulation is characteristic of glacial periods and low accumulation of interglacial periods. Uncertainties in the marine isotope chronology itself will impart uncertainties in our estimates of MAR based on these two dating methods (as much as ± 5 kyr: Martinson et al., 1987). However, we would expect these two age models to produce similar average MAR results.

The MARs generated using pedostratigraphic correlation show glacial-interglacial differences in MAR significantly larger than are shown by the average estimates for all data (Table 9). Stage 2 accumulation rates are 7 times greater than Stage 1 and 8.8 times greater than Stage 5 accumulation rates. The MARs calculated from the magnetic susceptibility age models also show more deposition during glacial periods than during interglacial periods (Table 9). However, the glacial-interglacial differences are smaller, with Stage 2 MARs only 2.4 times greater than Stage 1 MARs and 3.3 times greater than Stage 5 MARs. Furthermore, the differences in the regionally-averaged accumulation rates for Stages 2, 3 and 4 are smaller than shown by MARs based on the pedostratigraphic age model.

These differences between the MAR estimates based on pedostratigraphic and magnetic susceptibility methods can also be seen at individual sites. At some sites (e.g. Baicoayuan, Baimapo and Duanjiapo (Lantian_2)) the two age models yield age estimates for specific depths that are within the ± 5 kyr uncertainty inherent in the marine isotope chronology itself (Martinson et al., 1987). However, there are several sites where the discrepancies in the age estimates are significantly larger and result in significant differences in the MAR estimates. At Gaolanshan, for example, the MAR estimates for Stages 2 and 4 based on magnetic susceptibility and pedostratigraphy differ by more than $600g/m^2/yr$.

One reason why the pedostratigraphic and magnetic susceptibility records show different magnitudes for changes in MAR, despite both methods being based on

correlation with the marine isotope stratigraphy, is that the available magnetic susceptibility records do not show particularly good correlations with the Martinson et al. (1987) marine isotope stratigraphy. At 18 of the sites the correlation coefficients (R^2) between the MS curves and the Martinson et al. (1987) stratigraphy were < 0.5. Only three of the remaining 16 sites had R^2 values > 0.6. No R^2 values exceed 0.8. The correlation coefficients exhibit no distinct spatial pattern across the CLP (Figure 5). The three sites with R^2 values > 0.6 all occur in the northwestern CLP. However, they are close to sites with some of the lowest correlation coefficients. The poor correlation between the marine isotope stratigraphy and magnetic susceptibility suggest that the use of magnetic susceptibility as a dating method in this region is questionable.

Figure 5. Correlation Coefficients between Magnetic Susceptibility Records and the Marine Isotope Stratigraphy.

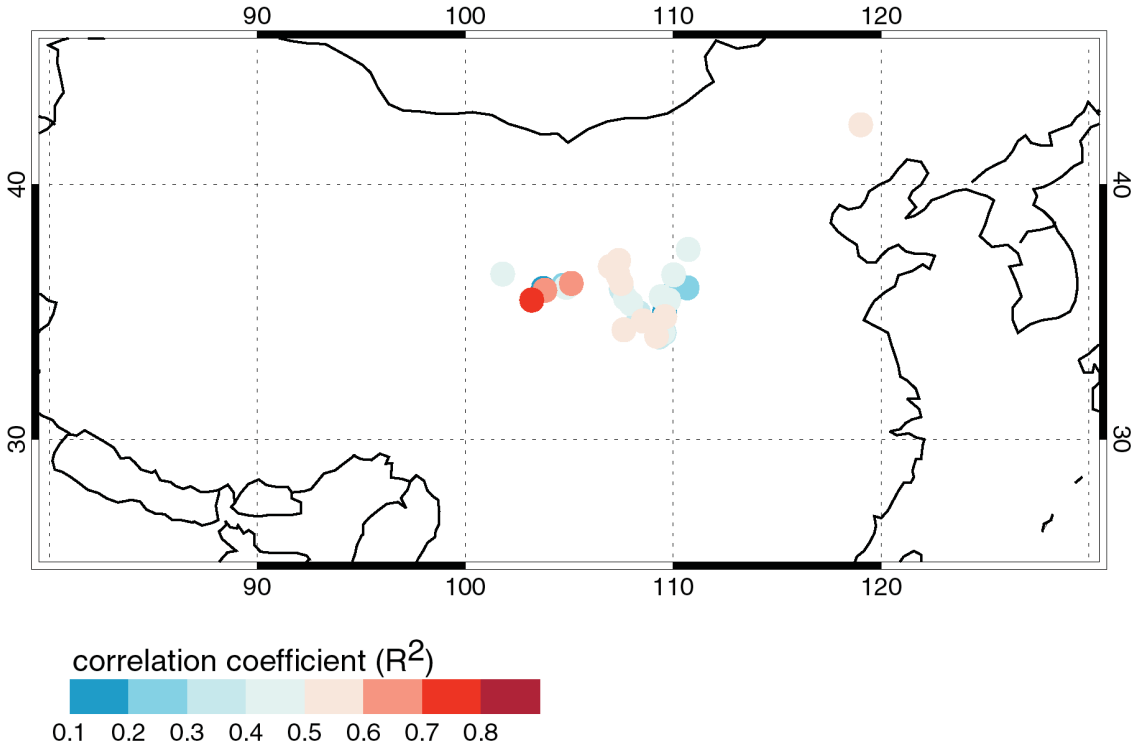

Both radiocarbon and luminescence are independent dating techniques and *a priori* should lead to more realistic estimates of changes in MAR. However, the estimates for Stages 1, 4, and 5 based on radiocarbon or luminescence dating are 2-7 times greater than estimates for these intervals made using either pedostratigraphy or magnetic susceptibility. Furthermore, the data available show *lower* accumulation rates during Stage 2 than during either Stage 1 or Stage 5 (Figure 4). Similar results are seen in

comparisons at individual sites. Thus, luminescence-based estimates for Stage 5 at Jiuzhoutai are 1000 g/m^2/yr *greater* than the estimates based on both pedostratigraphy and magnetic susceptibility dating. This results in Stage 5 TL-based accumulation rates appearing to be larger than accumulation rates during the glacial (i.e. Stage 2) period.

These counterintuitive results could, of course, simply reflect problems with the dating techniques or dating samples. However, it could simply be due to sampling biases in the estimates available to make these calculations of MARs. There are, in fact, very few sites with sufficient dates to make radiocarbon- or luminescence-based MAR estimates (see section 5.1). The ratio of Stage 1 to Stage 2 MARs can be calculated at only 5 individual sites; the Stage 2/Stage 5 ratio can be determined at only one site. Furthermore, the sites which have either radiocarbon or luminescence dating do not appear to represent a random-sampling of the data set: 60% of the sites with radiocarbon- or luminescence-based Stage 1 MARs are loess terraces but only 35% of the sites for which it is possible to derive Stage 1 MARs are loess terraces. If aeolian MARs from loess terraces are different from the MARs generated on other types of loess (see Section 5.2.3) our radiocarbon- and luminescence-based MAR estimates will be biased. An additional bias may have been introduced by the methods used to calculate MARs: when there are hiatuses within a given Stage but it was possible to calculate MAR values for dated portions of a stage with continuous sedimentation, we allowed these estimates to represent the Stage MAR values. This will tend to overestimate the accumulation rates for the Stage as a whole.

5.2.2 Millennial-Scale Variability in Aeolian Accumulation Rates during Stage 1

One of the hypotheses proposed to explain the apparent differences in average accumulation rates between Stage 1 and 5 is that the duration of Stage 1 (12 kyr) is not sufficient to capture the full range of interglacial conditions (and hence interglacial variability in dust deposition rates) when compared with Stage 5 (56 kyr). The records assembled here have insufficient dating control to examine millennial-scale variability in Stage 5. However, sufficient radiocarbon dates are available from 10 sites to reconstruct changes in dust accumulation rates during MIS 1. The records (Figure 6) show high rates of accumulation between ca 12-8 kyr BP, with minimum dust accumulation rates between 6 and 3 kyr BP. Although the number of sites is limited, there is a suggestion of increased dust accumulation rates after 3 kyr. The changes in dust accumulation rates are significant. Average accumulation rates at 9 kyr BP (i.e. during the initial phase of high accumulation rates) are 764 g/m^2/yr, while average accumulation rates at 4 kyr BP (i.e. during the phase of minimum dust accumulation) are only 478 g/m^2/yr. Thus, even within the Holocene, aeolian accumulation rates have varied by almost a factor of 2.

These results, although based on relatively few sites and therefore preliminary in nature, have important implications. First, since there are significant millennial-scale changes in dust accumulation rates within Stage 1, it is possible that the differing estimates obtained for Stages 1 and 5 could be influenced by differences in the length of the sampling period involved. Perhaps more importantly, these results suggest that averages in dust accumulation rates over entire marine isotope stages are not appropriate tools to evaluate the output of dust-cycle model experiments focussing on specific time slices, such as the LGM (21 kyr) or the mid-Holocene (6 kyr). However, a considerable effort will be required to improve the dating resolution of existing records in order to be able

to extract information on dust accumulation rates for specific time windows. Until this is done, the usefulness of loess records for evaluation of simulations of the palaeodust cycle will necessarily be limited.

Figure 6. Variability in MAR as estimated from radiometric dating, 0-16,000 years.

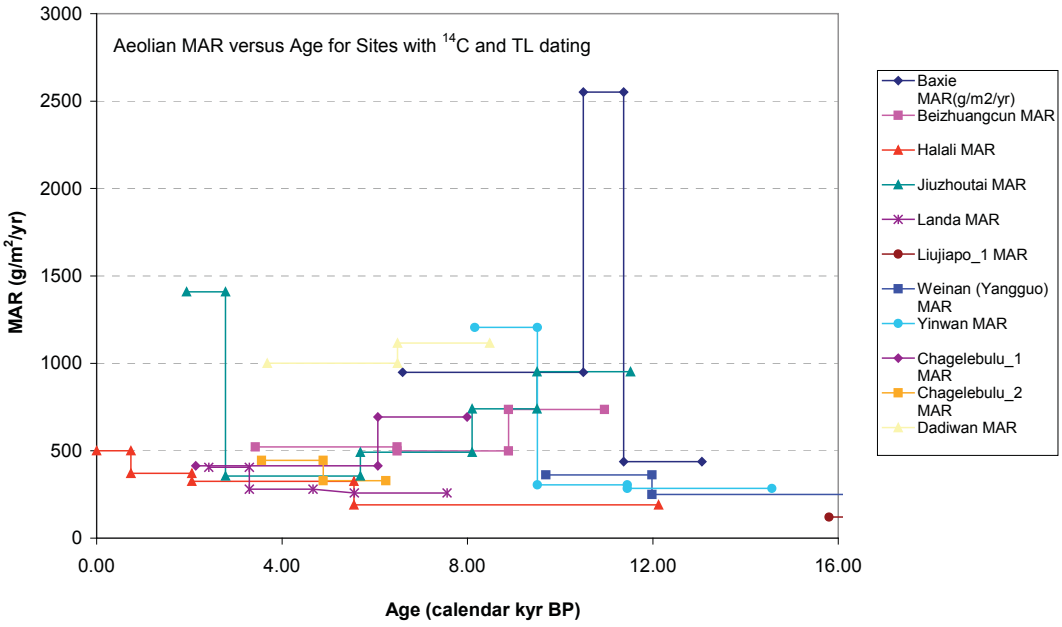

5.2.3 Impact of Geomorphological Setting on MAR Averages

The variability in MAR estimates across the CLP is affected not only by the dating methods employed to define stage boundaries but also by the geomorphological setting of each site. The regionally-averaged MAR for the CLP based on loess and river terrace sites (Table 10) is consistently larger than the estimate based on non-terrace sites (Table 11; Figure 7). The largest differences between the estimates from these two types of site occur during the glacial Stages 2 and 4. Thus, the average accumulation rate based on non-terrace sites is 286 g/m^2/yr for Stage 2 and 300 g/m^2/yr for Stage 4, compared with estimates of respectively 1062 and 935 g/m^2/yr for terrace sites. Differences between estimates from the two types of sites for interglacial stages are smaller. As a result, the apparent glacial-interglacial changes in MAR are also greatly amplified at the terrace sites compared with other sites (Figure 8). The Stage 2/1 and Stage 2/5 ratios for terrace sites (5.6 and 8.0, respectively) are approximately twice as large as those for non-terrace sites (2.6 and 4.3, respectively). Terrace sites occur close to local riverine sources of dust. It is not therefore surprising that the rates of dust accumulation are significantly higher during all Stages and very much higher during glacial periods. However, these results indicate a further possible source of bias in the estimates of glacial-interglacial changes in dust accumulation rates.

Figure 7. Comparison of Regionally-Averaged MAR for Different Geomorphological Settings.

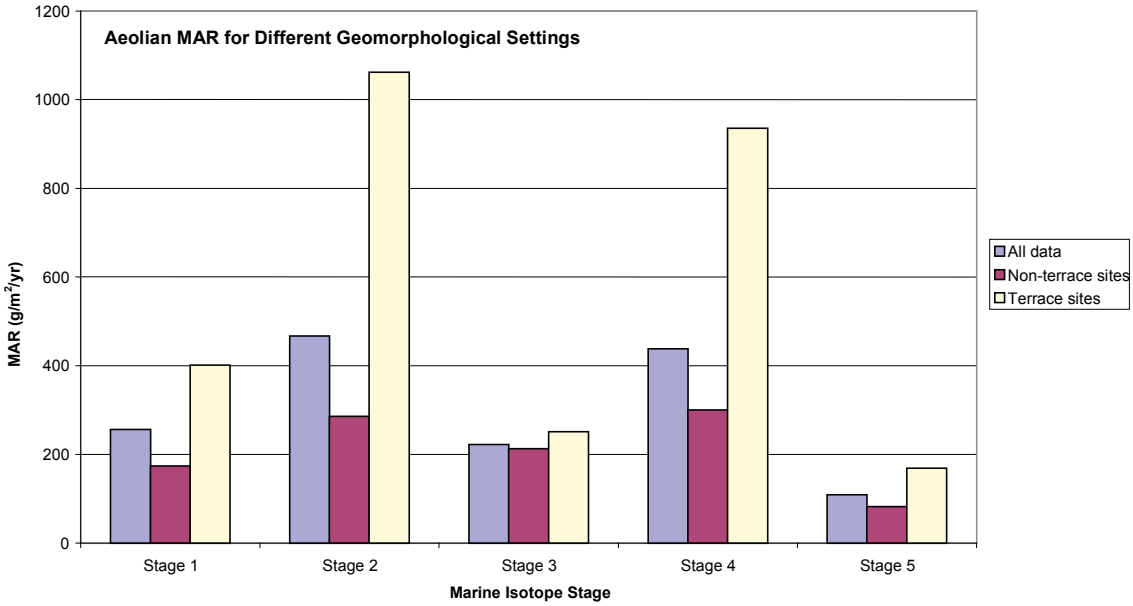

Figure 8. Impact of Geomorphological Setting on Flux Ratios

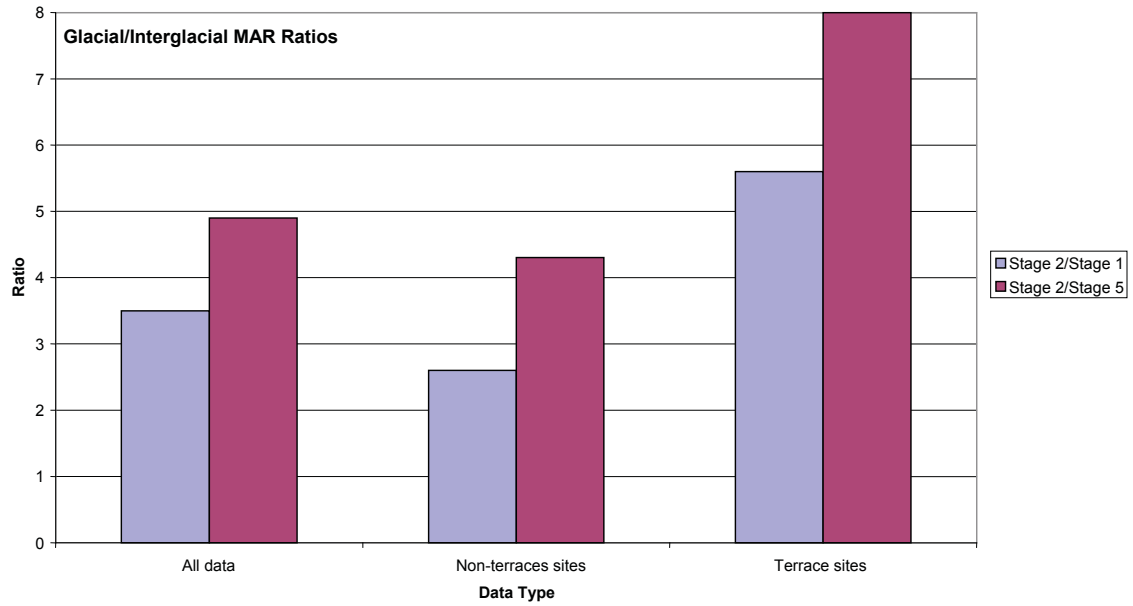

Table 10. MAR Statistics, Only Loess and River Terrace Sites.

Statistics	Stage 1	Stage 2	Stage 3	Stage 4	Stage 5	Ratio 2/1	Ratio 2/5
			Average, All Data				
Average	401	1062	251	935	169	5.6	8.0
S.D.	340	1416	186	710	303	7.7	7.4
Maximum	1298	5238	491	2279	1330	24.5	22.6
Minimum	25	285	21	312	6	0.3	1.1
N	18	11	11	10	20	11	7
			Pedostratigraphy				
Average	193	1315	180	961	97	10.4	11.5
SD	130	1534	161	748	98	7.6	6.4
Max	512	5238	500	2355	395	24.5	22.6
Min	25	348	21	312	6	3.1	4.3
N	12	9	11	10	20	7	8
			Magnetic Susceptibility				
Average	224	542	563	535	180	2.5	3.2
SD	44	285	66	191	27	1.1	2.3
max	270	954	647	771	210	3.5	6.5
min	183	307	498	310	146	1.4	1.6
N	3	4	4	4	4	3	4
			^{14}C and TL				
Average	682	654	458	1342	721		
S.D.	404	535	119	1217	886		
Max	1449	1449	582	2202	2265		
Min	269	285	345	481	24		
N	10	4	3	2	6		

Table 11. MAR Statistics, from Yuan, Mao and Liang-type Sites

Statistics	Stage 1	Stage 2	Stage 3	Stage 4	Stage 5	Ratio 2/1	Ratio 2/5
			Average, All Data				
Average	174	286	213	300	82	2.6	4.3
S. D.	106	182	174	184	50	2.6	3.0
Max	506	1055	809	954	204	13.8	16.4
Min	25	60	39	44	16	1.0	0.8
N	32	36	36	36	45	28	35
			Pedostratigraphy				
Average	114	362	101	307	64	5.5	8.1
S. D.	61	291	77	220	46	5.2	5.4
Max	251	1348	365	1126	191	16.3	22.6
Min	25	107	23	86	18	1.2	2.1
N	13	15	20	20	29	11	15
			Magnetic Susceptibility				
Average	140	288	249	290	89	2.4	3.3
S. D.	39	242	177	187	49	2.1	1.4
Max	239	1369	809	781	213	10.5	6.4
Min	67	60	62	44	16	0.6	0.8
N	23	30	30	30	31	23	30
			^{14}C and TL				
Average	357	250	172	110	202		
S. D.	117	125	32		62		
Max	506	449	201	110	245		
Min	203	105	137	110	158		
N	7	5	3	1	2		
Range of Averages	114-357	250-362	101-249	110-307	64-202	2.4-5.5	3.3-8.1

5.3 Spatial Patterns in Accumulation Rates and Glacial-Interglacial Flux Ratios

Maps showing MAR values at individual sites across the CLP during each of the MIS (Figure 9) confirm the results of the analyses of average MAR values (Section 5.2) in showing that Stages 2 and 4 have higher accumulation rates than 1, 3, and 5. Stage 5 is characterised by the lowest accumulation rates everywhere. The same patterns are shown on maps based only on non-terrace sites (Figure 10).

Highest MARs consistently occur in the northwestern CLP and lowest MARs in the southeastern CLP during Stages 2, 3, 4 and 5 (Figure 9). This pattern becomes somewhat clearer when only non-terrace sites are considered (Figure 10), largely because values from individual terrace sites show considerable variability (as might be expected given that they are influenced by local sources). The spatial gradient (from northwest to southeast) in dust accumulation is least clear in Stage 1 (Figures 9 and 10). This may reflect the influence of agriculture and human interference on local sources and accumulation rates at some sites. The lowest glacial-to-interglacial stage ratios are found in the northwestern CLP and the highest glacial-interglacial ratios in the southeastern CLP (Figures 11 and 12). This pattern is particularly obvious in the Stage 2/Stage 5 ratio. The observed spatial gradients in the magnitude of dust accumulation and the glacial-interglacial differences in accumulation indicate that the dust source region lies to the northwest of the CLP, and has not changed significantly over the past 130,000 years.

Observations of modern dust storms indicate that the Gobi Desert and the semi-arid regions of northwestern China are the main sources of dust to the CLP today (Liu et al., 1981). Provenance studies on the loess from the CLP are consistent with the material originating in these regions (Liu et al., 1985; Liu et al., 1994; Derbyshire et al., 1998) and suggest no substantial differences between different intervals (Gallet et al., 1996; Biscaye et al., 1997). Thus, our conclusions about the source of the CLP loess are consistent with other lines of evidence.

6. Conclusions

We have compiled descriptions of 98 individual sections with sediments covering part or all of the last 150,000 years, from the CLP, the surrounding desert margins, and Tibet. This compilation provides the most comprehensive documentation of loess stratigraphies from China currently available. Age models and aeolian mass accumulation rates (MAR) for one or more of the Marine Isotope Stages (MIS) could be determined at 77 sites using independent chronologies based on pedostratigraphy, magnetic susceptibility, luminescence dating or radiocarbon dating. Altogether, we were able to derive 355 MAR estimates. Analyses of these data support the following conclusions:

- Aeolian MARs (based on averaging all available data) for Stage 2 are 4.9 times greater than Stage 5 and 3.5 times greater than Stage 1. Stage 5 exhibits the lowest accumulation rates (109 $g/m^2/yr$).
- Pedostratigraphic age models show the most marked glacial-interglacial changes across the CLP, but have been tuned to the marine isotope stratigraphy to produce this result.

Figure 9. Spatial Patterns of Aeolian Mass Accumulation Rates, All Data.

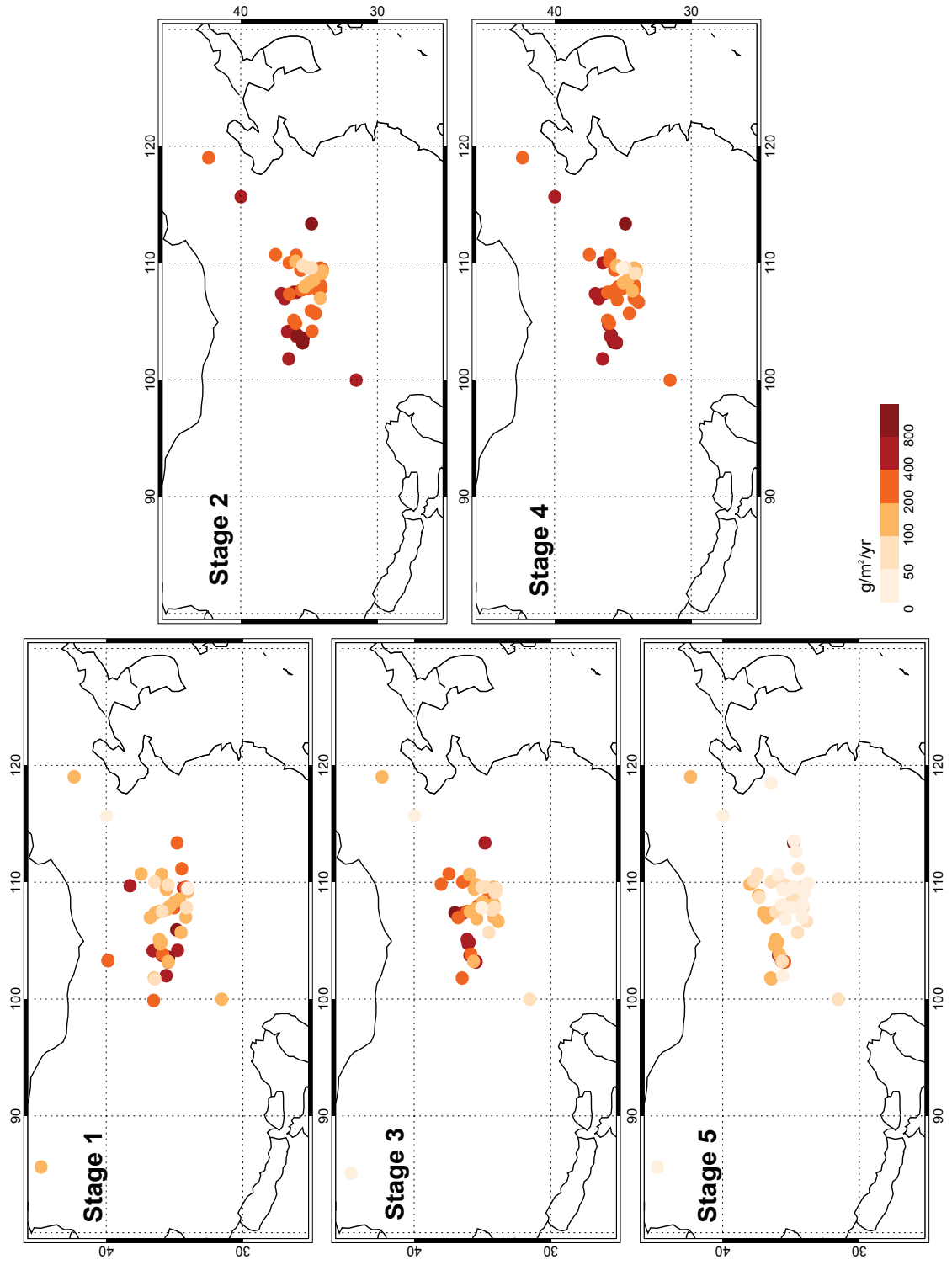

Figure 10. Spatial Patterns of Aeolian Mass Accumulation Rates, Excluding Terraces.

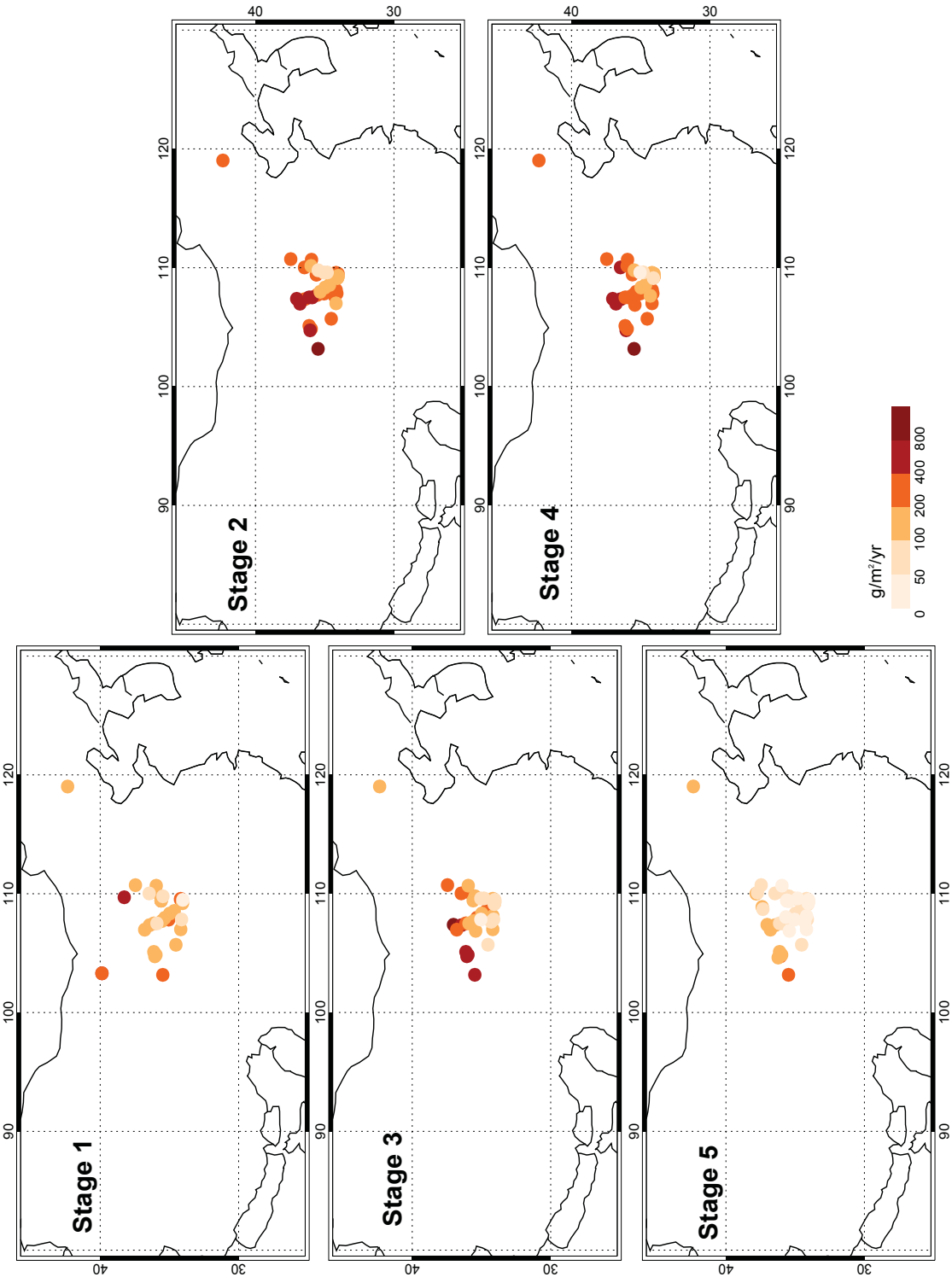

Figure 11. Glacial-Interglacial Aeolian Accumulation Rate Ratios, All Data.

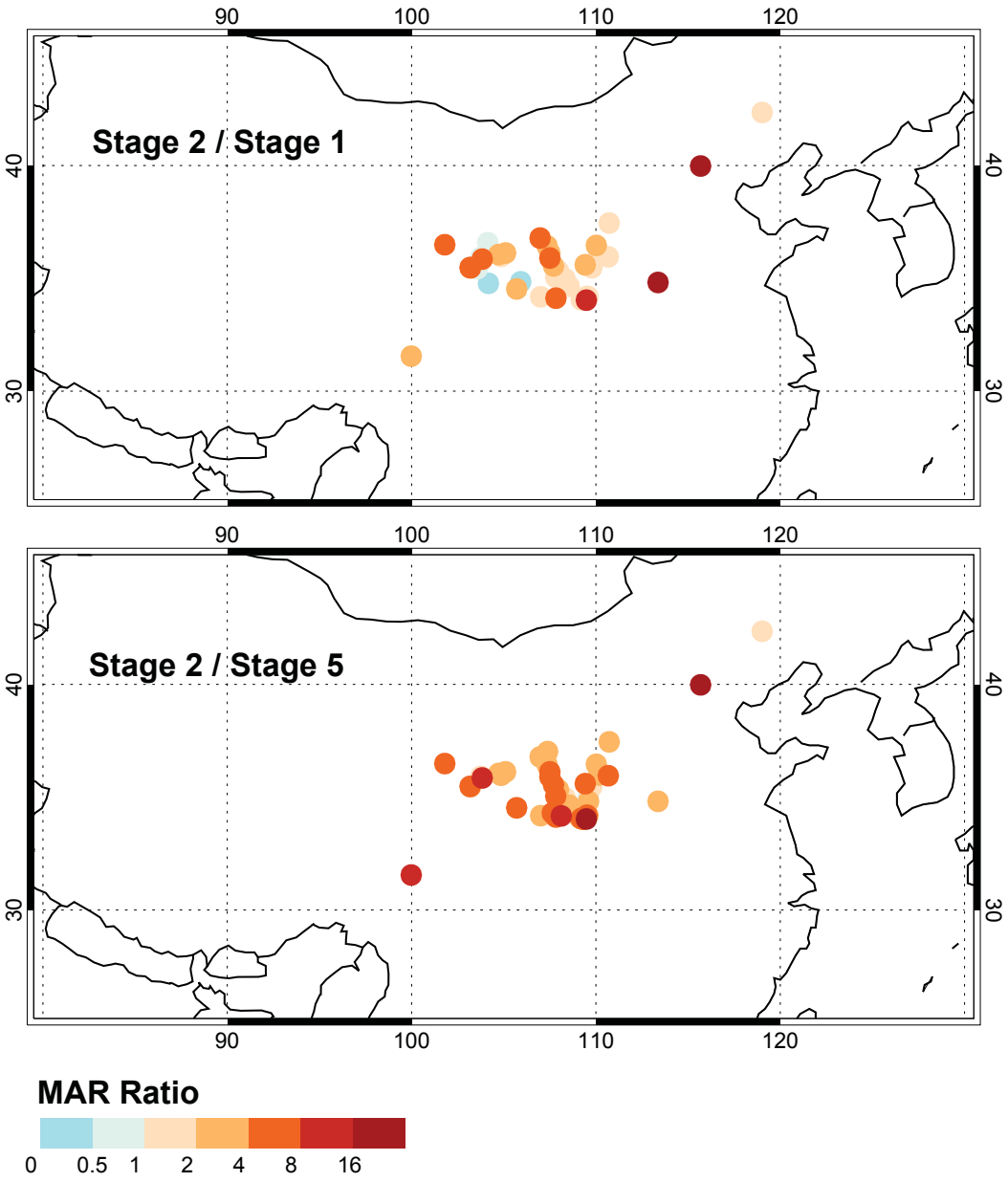

Figure 12. Glacial-Interglacial Aeolian Accumulation Rate Ratios, Excluding Terraces.

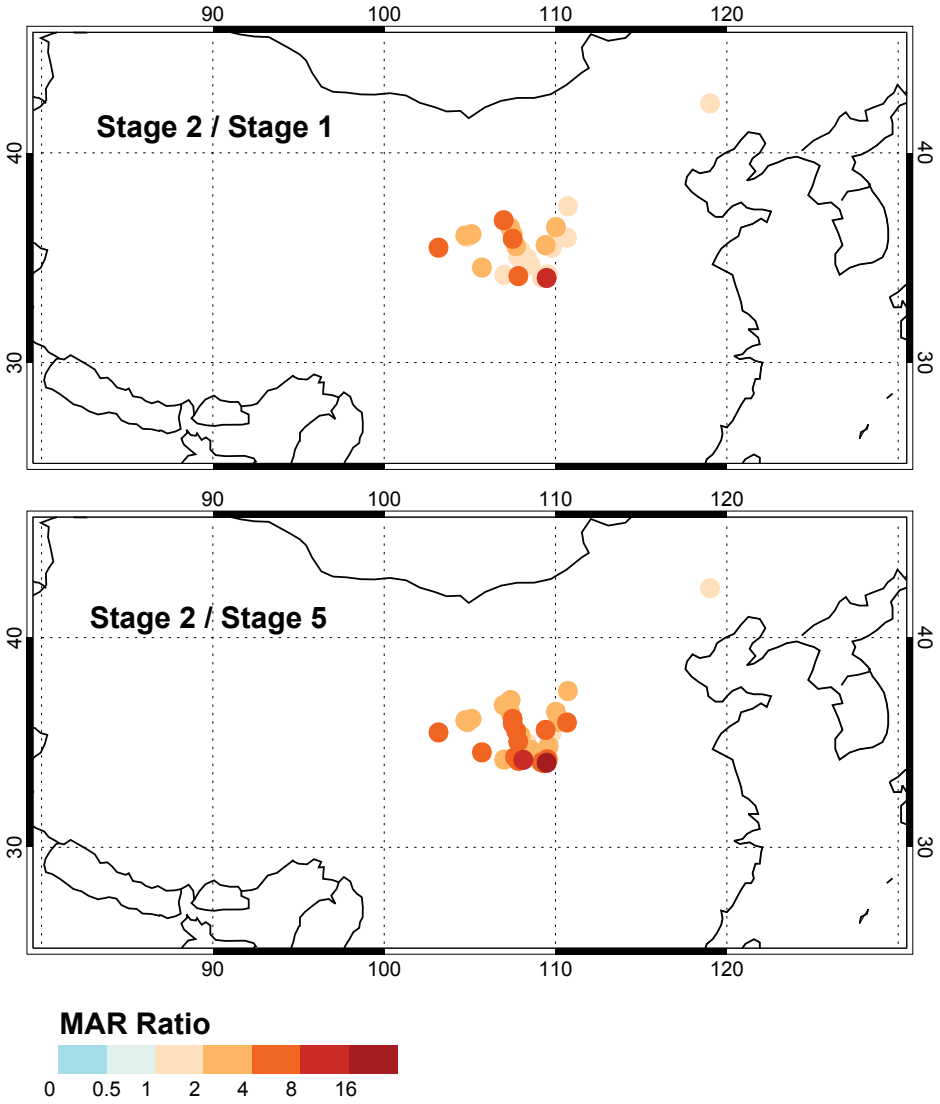

- Glacial-interglacial differences are not as pronounced with MAR estimates made using magnetic susceptibility age models. The reliability of bulk magnetic susceptibility as a chronostratigraphic tool is questionable; most magnetic susceptibility records from the CLP are poorly-correlated (< 0.5) with the marine isotope stratigraphy.
- Glacial-interglacial patterns were more difficult to determine using independent dating techniques, because so few dates are available. Furthermore, most of the radiocarbon- or luminescence-dated sections are from sites with local dust sources.
- MAR estimates for specific stages are also influenced by geomorphological setting. The regionally-averaged MAR for Stages 2 and 4 are 3 times greater at loess terrace sites than MARs from other sites. Rates estimated from terrace sites were twice that of MARs from non-terrace sites for Stage 1. Glacial-interglacial ratios (Stage 2/Stage 1, Stage 2/Stage 5) were also significantly amplified in the loess terrace sites.
- MAR values during all stages were highest in the northwestern CLP and lowest in the southeastern CLP. This observation is consistent with the suggestion that dust for the entire CLP is derived consistently from the northwest. The pattern is more pronounced when loess terrace sites (which show considerable inter-site variability) were not considered.

Analyses of available data from the CLP thus show some interesting and potentially diagnostic patterns in both time and space. However, the fact that the patterns are significantly affected by geomorphological setting and by the specific method used to erect chronologies means that the data would require careful screening before they could be used for model evaluation. There are insufficient sites with independent and well-resolved chronologies to be able to construct detailed records of the spatial patterns of changes in aeolian MAR for specific time windows (shorter than individual marine isotope stages). Thus, although the CLP represents perhaps the best-studied loess region in the world, there is still much work to be done to quantify changes in the aeolian mass accumulation rates, and an urgent need to develop better and more complete chronologies.

7. Acknowledgements

We thank An Chengbang, Chen Fahu, Ding Zhongli, Dong Guangrong, Xiong Shangfa, and Zhou Weijian for help with both published and unpublished data. We gratefully acknowledge Susi Stanek for her valuable assistance with assembling the report, and also Silvana Schott and Gerhard Boenisch for their contributions to the graphics and data calculations. Ni Jian assisted with translations. This data synthesis was completed as part of the DIRTMAP Data Base, which is funded through the MPI-BGC. MPI-BGC also provided financial support to JMS from March-October, 1999. The DIRTMAP data base (http://www.bgc-jena.mpg.de/bgc_prentice) is endorsed and supported by the INQUA Loess Commission, the IGBP/GAIM Paleo Trace Gas and Mineral Aerosol Challenge (TRACES), the IGBP/PAGES PaleoMApping Project (PMAP), and the International Geological Correlation Programme (IGCP) #413. The members of the DIRTMAP Steering Committee are E. Derbyshire, S. P. Harrison, D. Muhs, A. Wintle, and L. Zhou.

8. References Cited in Text

Aitken MJ (1998) An Introduction to Optical Dating: The Dating of Quaternary Sediments by the Use of Photon-stimulated Luminescence. Oxford University Press, Oxford, UK, pp 280

An ZS, Wang J, Li H (1977) Palaeomagnetic research of the Luochuan loess section (in Chinese). Geochemica 4: 239-249

An Z, Kukla GJ, Porter SC, Xiao J (1991a) Magnetic susceptibility evidence of monsoon variation on the Loess Plateau of Central China during the last 130,000 years. Quaternary Research 36: 29-36

An ZS, Kukla G, Porter SC, Xiao JL (1991b) Late Quaternary dust flow on the Chinese Loess Plateau. Catena 18: 125-132

An Z, Porter SC (1997) Millennial-scale climatic oscillations during the last interglaciation in central China. Geology 25: 603-606

Andreae MO (1995) Climatic effects of changing atmospheric aerosol levels. In: Henderson-Sellers A (ed) World Survey of Climatology: Future Climates of the World. Elsevier, Amsterdam, pp 341-392

Anonymous (1986) Maps of Gansu Province (in Chinese). Mapping Bureau of Gansu Province, Lanzou, China.

Anonymous (1992) Maps of Shaanxi Province (in Chinese). Xi'an Mapping Press, Xi'an, China, pp 264

Anonymous (1995) Maps of Xizang Autonomous Region (in Chinese). Mapping Bureau of Xizang Autonomous Region, China Mapping Press, Beijing, China, pp 166

Begét J (1990) Middle Wisconsin climate fluctuations recorded in central Alaskan loess. Géographie physique et Quaternaire 44: 3-13

Berger GW (1988) TL dating studies of tephra, loess and lacustrine sediments. Quaternary Science Reviews 7: 295-303

Berger GW, Pillans BJ, Palmer AS (1992) Dating loess up to 800 ka by thermoluminescence. Geology 20: 403-406

Biscaye PE, Grousset FE, Revel M, Van der Gaast S, Zielinski GA, Vaars A, Kukla G (1997) Asian provenance of glacial dust (Stage 2) in the GISP2 ice core, Summit, Greenland. Journal of Geophysicial Research 102: 26315-26886

Bradley RS (1985) Quaternary Paleoclimatology: Methods of Paleoclimatic Reconstruction. Allen and Unwin, Inc, Boston, pp 472

Broecker WS (1995) The Glacial World According to Wally. Eldigio Press, Lamont-Doherty Earth Observatory of Columbia University, Palisades, NY, pp

Bronk Ramsey C (1998) Probability and dating. Radiocarbon 40: 461-474

Chapman M, Shackleton N (2000) Evidence of 550-year and 1000-year cyclicities in North Atlantic circulation patterns during the Holocene. Holocene 10: 287-291

Chen F, Shi Q, Wang J (1999a) Environmental changes documented by sedimentation of Lake Yiama in arid China since the Late Glaciation. Journal of Paleolimnology 22: 159-169

Chen FH, Bloemendal J, Feng ZD, Wang JM, Parker E, Guo ZT (1999b) East Asian monsoon variations during Oxygen Isotope Stage 5: Evidence from the northwestern margin of the Chinese Loess Plateau. Quaternary Science Reviews 18: 1127-1135

Chen Y, Chen M, Fang T (1999c) Biogenic sedimentation patterns in the northern South China Sea: An ultrahigh-resolution record MD972148 of the past 150,000 years

from the IMAGES III-IPHIS cruise. Terrestrial, Atmospheric, and Oceanic Sciences 10: 215-224

Chlachula J, Evans ME, Rutter NW (1998) A magnetic investigation of a Late Quaternary loess/palaeosol record in Siberia. Geophysical Journal International 132: 128-132

deMenocal P, Ortiz J, Guilderson T, Sarnthein M (2000) Coherent high- and low-latitude climate variability during the Holocene warm period. Science 288: 2198-2202

Derbyshire E (1984) Granulometry and fabric of the loess at Jiuzhoutai, Lanzhou, People's Republic of China. In: Pecsi M (ed) Lithology and Stratigraphy of Loess and Paleosols. Hungarian Academy of Sciences, Budapest, pp 97-103

Derbyshire E, Kemp R, Meng X (1995) Variations in loess and palaeosol properties as indicators of palaeoclimatic gradients across the Loess Plateau of North China. Quaternary Science Reviews 14: 681-697

Derbyshire E, Meng X, Kemp RA (1998) Provenance, transport and characteristics of modern aeolian dust in western Gansu Province, China, and interpretation of the Quaternary loess record. Journal of Arid Environments 39: 497-516

Ding ZL, Liu TS, Liu XM, Chen XY (1990) Thirty-seven climatic cycles in the last 2.5 Ma. Chinese Science Bulletin 35: 668-672

Ding ZL, Xiong SF, Sun JM, Yang SL, Gu ZY, Liu TS (1999) Pedostratigraphy and paleomagnetism of a similar to 7.0 Ma eolian loess-red clay sequence at Lingtai, Loess Plateau, north-central China and the implications for paleomonsoon evolution. Palaeogeography, Palaeoclimatology, Palaeoecology 152: 49-66

Duchaufour P (1982) Pedology: Pedogenesis and Classification (English Edition). George Allen and Unwin, London, pp 448

Eynaud F, Turon J, Sanchez-Goni M, Gendreau S (2000) Dinoflagellate cyst evidence of 'Heinrich-like events' off Portugal during the Marine Isotopic Stage 5. Marine Micropaleontology 40: 9-21

Fang X, Li J, Banerjee S, Jackson M, Oches E, Van der Voo R (1999) Millennial-scale climatic change during the last interglacial period: Superparamagnetic sediment proxy from paleosol S1, western Chinese Loess Plateau. Geophysical Research Letters 26: 2485-2488

Gallet S, Jahn BM, Torii M (1996) Geochemical characterization of the Luochuan loess-paleosol sequence, China, and paleoclimatic implications. Chemical Geology 133: 67-88

Gill T (1996) Eolian sediments generated by anthropogenic disturbance of playas: Human impacts on the geomorphic system and geomorphic impacts on the human system. Geomorphology 17: 207-228

Ginoux P, Chin M, Tegen I, Prospero J, Holben B, Dubovik O, SJ L (submitted) Global simulations of dust in the troposphere: model description and assessment. Journal of Geophysical Research

Giraudeau J, Cremer M, Manthé S, Labeyrie L, Bond G (2000) Coccolith evidence for instabilities in surface circulation south of Iceland during Holocene times. Earth and Planetary Science Letters 179: 257-268

Goudie AS, Middleton NJ (1992) The changing frequency of dust storms through time. Climatic Change 20: 197-225

Guo Z, Fedoroff N, An ZS, Liu TS (1993) Interglacial dustfall and origin of iron oxides-hydroxides in the paleosols of the Xifeng loess section, China. Scientia Geologica Sinica 2: 91-100

Hammer CU, Clausen HB, Dansgaard W, Neftel A, Kristinsdottor P, Johnson E (1985) Continuous impurity analysis along the Dye 3 deep core. In: CC Langway Jr, Oeschger H, Dansgaard W (eds) Greenland Ice Core: Geophysics, Geochemistry, and the Environment. AGU, Washington DC, pp 90-94

Han JM, Hus JJ, Liu TS, Paepe R, Vandenberghe RE (1991) Magnetic properties of the Malan and Lishi Formations (in Chinese). Quaternary Sciences 4: 310-325

Harrison SP, Kohfeld KE, Roelandt C, Claquin T (in press) The role of dust in climate changes today, at the last glacial maximum and in the future. Earth Science Reviews

Heller F, Liu T-S (1982) Magnetostratigraphical dating of loess deposits in China. Nature 300: 431-433

Heller F, Evans ME (1995) Loess magnetism. Reviews of Geophysics 33: 211-240

Hovan SA, Rea DK, Pisias N, Shackleton NJ (1989) A direct link between the China loess and marine $\delta^{18}O$ records: aeolian flux to the North Pacific. Nature 340: 296-298

Hovan SA, Rea DK, Pisias NG (1991) Late Pleistocene continental climate and oceanic variability recorded in Northwest Pacific sediments. Paleoceanography 6: 349-370

Kemp RA, Derbyshire E, Meng XM, Chen FH, Pan BT (1995) Pedosedimentary reconstruction of a thick loess-paleosol sequence near Lanzhou in North-Central China. Quaternary Research 43: 30-45

Kohfeld KE, Harrison SP (2000) How well can we simulate past climates? Evaluating the models using global palaeoenvironmental datasets. Quaternary Science Reviews 19: 321-347

Kohfeld KE, Harrison SP (in press) DIRTMAP: The geologic record of dust. Earth Science Reviews

Kukla G (1987) Loess stratigraphy in Central China. Quaternary Science Reviews 6: 191-219

Kukla G, Heller F, Ming LX, Chun XT, Sheng LT, Sheng AZ (1988) Pleistocene climates in China dated by magnetic susceptibility. Geology 16: 811-814

Liu CQ, Masuda A, Okada A, Yabuki S, Fan ZL (1994) Isotope geochemistry of Quaternary deposits from the arid lands in northern China. Earth and Planetary Science Letters 127: 25-38

Liu JQ, Chen TM, Nie GZ, Song CY, Guo ZT, Li K, Gao SJ, Qiao YL, and Ma, Z. B. (1994) Datings and reconstruction of the high resolution time series in the Weinan loess section of the last 150,000 years (in Chinese). Quaternary Sciences 193-202

Liu TS (1964) Loess on the Middle Reaches of the Yellow River (in Chinese). Science Press, Beijing, pp 143-146

Liu TS (1965) The Loess Deposits in China (in Chinese). Science Press, Beijing, pp 244

Liu TS (1966) Composition and Texture of Loess (in Chinese). Science Press, Beijing, pp 132

Liu TS, Gu XF, An ZS, Fan YX (1981) The dust fall in Beijing, China on April 18, 1980. Geological Society of America Special Paper 186: 149-157

Liu TS (1985) Loess and the Environment (in Chinese). China Ocean Press, Beijing, pp 481

Liu T, An Z, Yuan B, Han J (1985) The loess-paleosol sequence in China and climatic history. Episodes 8: 21-28

Liu TS, Guo ZT, Liu JQ, Han JM, Ding ZL, Gu ZY, Wu NQ (1995) Variations of eastern Asian monsoon over the last 140,000 years. Bulletin de la Societé geologique de France 166: 221-229

Liu XM, Liu TS, Shaw J, Heller F, Xu TC, Yuan BY (1991) Paleomagnetic and paleoclimatic studies of Chinese loess. In: Liu TS (ed) Loess, Environment and Global Change. Science Press, Beijing, China, pp 61-81

Liu X, Shaw J, Liu T, Heller F, Yuan B (1992) Magnetic mineralogy of Chinese loess and its significance. Geophysical Journal International 108: 301-308

Maher BA, Thompson R (1991) Mineral magnetic record of the Chinese loess and paleosols. Geology 19: 3-6

Mahowald N, Kohfeld KE, Hansson M, Balkanski Y, Harrison SP, Prentice IC, Schulz M, Rodhe H (1999) Dust sources and deposition during the Last Glacial Maximum and current climate: A comparison of model results with palaeodata from ice cores and marine sediments. Journal of Geophysical Research 104: 15895-15916

Mannion A (1999) Domestication and the origins of agriculture: an appraisal. Progress in Physical Geography 23: 37-56

Marticorena B, Bergametti G (1996) Two-year simulations of seasonal and interannual changes of the Saharan dust emissions. Geophysical Research Letters 23: 1921-1924

Martin CW, Johnson WC (1995) Variation in radiocarbon ages of soil organic matter fractions from Late Quaternary buried soils. Quaternary Research 43: 232-237

Martinson DG, Pisias NG, Hays JD, Imbrie J, Moore TC, Shackleton NJ (1987) Age dating and the orbital theory of the ice ages: development of a high-resolution 0 to 300,000-year chronostratigraphy. Quaternary Research 27: 1-29

McTainsh GH (1989) Quaternary aeolian dust processes and sediments in the Australian region. Quaternary Science Reviews 8: 235-253

Murray AS, Wintle AG (2000) Luminescence dating of quartz using an improved single-aliquot regenerative-dose protocol. Radiation Measurements 32: 57-73

Overpeck J, Rind D, Lacis A, Healy R (1996) Possible role of dust-induced regional warming in abrupt climate change during the last glacial period. Nature 384: 447-449

Paillard D, Labeyrie L, Yiou P (1996) Macintosh Program Performs Time-Series Analysis. Eos Transactions AGU 77: 379

Petit JR, Briat M, Royer A (1981) Ice age aerosol content from East Antarctic ice core samples and past wind strength. Nature 293: 391-394

Petit JR, Mounier L, Jouzel J, Korotkevich YS, Kotlyakov VI, Lorius C (1990) Paleoclimatological and chronological implications of the Vostok core dust record. Nature 343: 56-58

Petit JR, Jouzel J, Raynaud D, Barkov NI, Barnola JM, Basile I, Bender M, Chappellaz J, Davis M, Delaygue G, Delmotte M, Kotlyakov VM, Legrand M, Lipenkov VY, Lorius C, Pepin L, Ritz C, Saltzman E, Stievenard M (1999) Climate and atmospheric history of the past 420,000 years from the Vostok ice core, Antarctica. Nature 399: 439-436

Prescott JR, Robertson GB (1997) Sediment dating by luminescence: a review. Radiation Measurements 27: 893-922

Pye K (1987) Aeolian Dust and Dust Deposits. Academic Press, San Diego, pp 334

Rasmussen T, Balbon E, Thomsen E, Labeyrie L, van Weering T (1999) Climate records and changes in deep outflow from the Norwegian Sea similar to 150-55 ka. Terra Nova 11: 61-66

Rea DK (1994) The paleoclimatic record provided by eolian deposition in the deep sea: the geologic history of wind. Reviews of Geophysics 32: 159-195

Reader MC, Fung I, McFarlane N (1999) The mineral dust aerosol cycle during the Last Glacial Maximum. Journal of Geophysical Research - Atmospheres 104: 9381-9398

Ren G (2000) Decline of the mid- to late Holocene forests in China: climatic change or human impact? Journal of Quaternary Science 15: 273-281

Rutter N, Ding Z (1993) Paleoclimates and monsoon variations interpreted from micromorphogenic features of the Baoji paleosols, China. Quaternary Science Reviews 12: 853-862

Sarkar A, Ramesh R, Somayajulu BLK, Agnihotri R, Jull AJT, Burr GS (2000) High resolution Holocene monsoon record from the eastern Arabian Sea. Earth and Planetary Science Letters 177: 209-218

Stuiver M, Kra RS (1986) Calibration Issue, Proceedings of the 12th International ^{14}C conference. Radiocarbon 28: 805-1030

Stuiver M, Reimer PJ (1993) Extended ^{14}C data base and revised Calib 3.0 ^{14}C age calibration program. Radiocarbon 35: 215-230

Stuiver M, Reimer PJ, Bard E, Beck JW, Burr GS, Hughen KA, Kromer B, McCormac G, van der Plicht J, Spurk M (1998a) INTCAL98 Radiocarbon Age Calibration, 24000-0 cal BP. Radiocarbon 40: 1041-1083

Stuiver M, Reimer PJ, Braziunas TF (1998b) High-precision radiocarbon age calibration for terrestrial and marine samples. Radiocarbon 40: 1127-1151

Sun XJ, Song CQ, Wang FY, Sun MR (1997) Vegetation history of the Loess Plateau of China during the last 100,000 years based on pollen data. Quaternary International 37: 25-36

Tegen I, Lacis A, Fung I (1996) The influence on climate forcing of mineral aerosols from disturbed soils. Nature 380: 419-422

Tegen I, Lacis AA (1996) Modeling of particle size distribution and its influence on the radiative properties of mineral dust aerosol. Journal of Geophysical Research 101: 19237-19244

Tegen I, Harrison SP, Kohfeld KE, Prentice IC, Coe MT, Heimann M (in prep) Impact of vegetation and preferential source areas on the dust aerosol cycle. Journal of Geophysical Research

Thompson LG (2000) Ice core evidence for climate change in the Tropics: Implications for our future. Quaternary Science Reviews 19: 19-35

Verosub KL, Fine P, Singer ML, Tenpas J (1993) Pedogenesis and paleoclimate: Interpretation of the magnetic susceptibility record of Chinese loess-paleosol sequences. Geology 21: 1011-1014

Vlag PA, Oches EA, Banerjee SK, Solheid PA (1999) The paleoenvironmental-magnetic record of the Gold Hill Steps loess section in central Alaska. Physics and Chemistry of the Earth Part A - Solid Earth and Geodesy 24: 779-783

von Grafenstein U, Erlenkeuser H, Brauer A, Jouzel J, Johnsen SJ (1999) A Mid-European decadal isotope-climate record from 15,500 to 5000 years B. P. Science 284: 1654-1657

Watts WA (1988) Late-Tertiary and Pleistocene vegetation history - 20 My to 20 ky. In: Huntley B, Webb III T (eds) Vegetation history. Kluwer Academic Publishers, Dordrecht, pp 155-193

Wintle AG (1990) A review of current research on TL dating of loess. Quaternary Science Reviews 9: 385-397

Wintle AG (1997) Luminescence dating: laboratory procedures and protocols. Radiation Measurements 27: 769-817

Wintle AG, Questiaux DG, Roberts RG, Spooner NA (1993) Dating loess up to 800 ka by thermoluminescence: Comment and reply. Geology 21: 568-569

Zheng H, Oldfield F, Yu L, Shaw J, An Z (1991) The magnetic properties of particle-sized samples from the Luo Chuan loess sections: evidence for pedogenesis. Physics of the Earth and Planetary Interiors 68: 250-258

Zhou LP, Oldfield F, Wintle AG, Robinson SG, Wang JT (1990) Partly pedogenic origin of magnetic variations in Chinese loess. Nature 346: 737-739

Zhou LP, Shackleton NJ (in press) Photon-stimulated luminescence of quartz from loess and effects of sensitivity change on palaeodose determination. Quaternary Science Reviews

Zhou WJ, An ZS, Head MJ (1994) Stratigraphic division of Holocene loess in China. Radiocarbon 36: 37-45

9. References for Section 4

An ZS, Lu YC (1984) A climatostratigraphic subdivision of late Pleistocene strata named Malan formation in north China (in Chinese). Kexue Tongbao 29: 1239-1241

An ZS, Liu TS, Kan XF, Sun JZ, Wang JD, Kao WY, Zhu YZ, Wei MJ (1987) Loess-paleosol sequences and chronology at Lantian Man Localities. In: Liu TS (ed) Aspects of Loess Research. China Ocean Press, Beijing, China, pp 192-203

An ZS, Xiao JL (1990) A real example about the study of dust sedimentary flux in the Loess Plateau. Geoderma 45: 123-143

An ZS, Kukla GJ, Porter SC, Xiao JL (1991a) Magnetic susceptibility evidence of monsoon variation on the Loess Plateau of central China during the last 130,000 years. Quaternary Research 36: 29-36

An ZS, Kukla G, Porter SC, Xiao JL (1991b) Late Quaternary dust flow on the Chinese Loess Plateau. Catena 18: 125-132

An ZS, Wu XH, Wang PX, Wang SM, Dong GR, Sun XJ, Zhang DE, Lu YC, Zheng SH, Zhao SL (1991c) Changes in the monsoon and associated environmental changes in China since the last interglacial. In: Liu TS (ed) Loess, Environment and Global Change. Science Press, Beijing, China, pp 1-29

An ZS, Porter SC, Zhou WJ, Lu YC, Donahue DJ, Head MJ, Wu XH, Ren JZ, Zheng HB (1993) Episode of strengthened summer monsoon climate of Younger Dryas age on the Loess Plateau of central China. Quaternary Research 39: 45-54

An ZS, Porter SC, Kutzbach JE, Wu XH, Wang SM, Liu XD, Li XQ, Zhou WJ (2000) Asynchronous Holocene optimum of the East Asian monsoon. Quaternary Science Reviews 19: 743-762

Burbank DW, Li JJ (1985) Age and palaeoclimatic significance of the loess of Lanzhou, north China. Nature 316: 429-431

Cao JX (1988) The study of environmental changes and loess-paleosol sequences of Jiuzhoutai, Lanzhou (in Chinese). Journal of Lanzhou University (Natural Science) 24: 108-122

Chang YP, Huang WB, Tang YJ, Ji HX, Ding SY (1964) The discussion of Cenozoic formation from Lantian, Shensi Province (in Chinese). Vertebrata PalAsiatica 8: 134-148

Chen FH, Li JJ, Zhang WX, Pan BT (1991a) The loess profile of South Bank, climate information and lake-level fluctuation of Qinghai Lake during the Holocene (in Chinese). Scientia Geographica Sinica 11: 76-85

Chen FH, Li JJ, Zhang WX (1991b) Loess stratigraphy of the Lanzhou profile and its comparison with deep-sea sediment and ice core record. GeoJournal 24: 201-209

Chen FH, Zhang WX (1994) Climatic changes and Neolithic Culture since LGM (in Chinese). In: Chen FH, Zhang WX (ed) Loess stratigraphy and the Quaternary glacial in Gansu and Qinghai Provinces. Science Press, Beijing, China, pp 139-149

Chen FH, Ma YZ, Li JJ (1996) High resolution record of Malan Loess in the Longxi Loess Plateau and rapid climate changes during the last glaciation (in Chinese). Journal of Glaciology and Geocryology 18: 111-118

Chen FH, Bloemendal J, Wang JM, Li JJ, Oldfield F (1997) High-resolution multi-proxy climate records from Chinese loess: evidence for rapid climatic changes over the last 75 kyr. Palaeogeography, Palaeoclimatology, Palaeoecology 130: 323-335

Chen FH, Bloemendal J, Feng ZD, Wang JM, Parker E, Guo ZT (1999) East Asian monsoon variations during the Oxygen Isotope Stage 5: evidence from the northwestern margin of the Chinese loess Plateau. Quaternary Science Reviews 18: 1127-1135

Chen Y, Li ZH, Ye H, Wang YH (1996) Carbon, oxygen isotope records on climatic changes in the central Loess Plateau since 130 ka B. P. (in Chinese). Marine Geology and Quaternary Geology 16: 17-22

Cheng GL, Lin JL, Li SZ (1978) A discussion on the ages of bearing Lantian Man strata (in Chinese). In: Society CP (ed) Proceedings of selected papers from the First Symposium of China Palynology Society. Science Press, Beijing, China, pp 151-157

Chu J (1998) Loess accumulation and palaeoclimate records since the last glacial period in Baicaoyuan, Gansu Province (in Chinese). Ms. Thesis, Chinese Academy of Sciences, Beijing, China, pp 11-17

Derbyshire E, Wang JT, Shaw J, Rolph T (1987) Interim results of studies of the sedimentology and remanent magnetization of the loess succession at Jiuzhoutai, Lanzhou, China. In: Liu TS (ed) Aspects of Loess Research. China Ocean Press, Beijing, China, pp 175-191

Derbyshire E, Kemp RA, Meng XM (1995a) Variations in loess and palaeosol properties as indicators of palaeoclimatic gradients across the Loess Plateau of north China. Quaternary Science Reviews 14: 681-697

Derbyshire E, Keen DH, Kemp RA, Rolph TA, Shaw J, Meng XM (1995b) Loess-palaeosol sequences as recorders of palaeoclimatic variations during the last glacial-interglacial cycle: some problems of correlation in north-central China. Quaternary Proceedings 4:7-18

Derbyshire E, Kemp RA, Meng XM (1997) Climate change, loess and palaeosols: proxy measures and resolution in North China. Journal of the Geological Society 154: 793-805

Ding ZL, Liu DS, Liu XM, Chen MY, An ZS (1990) 37 climatic cycles in the last 2.5 Ma. Chinese Science Bulletin 35: 667-671

Ding ZL, Rutter N, Liu TS, Evans ME, Wang YC (1991) Climatic correlation between Chinese loess and deep-sea cores: A structural approach. In: Liu TS (ed) Loess, Environment and Global Change. Science Press, Beijing, China, pp 168-186

Ding ZL, Rutter N, Han JT, Liu TS (1992) A coupled environmental system formed at about 2.5 Ma in East Asia. Palaeogeography, Palaeoclimatology, Palaeoecology 94: 223-242

Ding ZL, Yu Z, Rutter NW, Liu T (1994) Towards an orbital time scale for Chinese loess deposits. Quaternary Science Reviews 13: 39-70

Ding ZL, Liu TS, Rutter NW, Yu ZW, Guo ZT, Zhu RX (1995) Ice-volume forcing of East Asia winter monsoon variations in the past 800,000 years. Quaternary Research 44: 149-159

Ding ZL, Ren JZ, Liu TS, Sun JM, Zhou XQ (1996) Climatic changes on millennial time scales-Evidence from a high-resolution loess record (in Chinese). Science in China (Series D) 26: 385-391

Ding ZL, Rutter NW, Liu TS, Sun JM, Ren JZ, Rokosh D, Xiong SF (1998) Correlation of Dansgaard-Oeschger cycles between Greenland ice and Chinese loess. Paleoclimates 2: 281-291

Ding ZL, Ren JZ, Yang SL, Liu TS (1999a) Climate instability during the penultimate glaciation: Evidence from two high-resolution loess records, China. Journal of Geophysical Research-Solid Earth 104: 20123-20132

Ding ZL, Sun JM, Rutter NW, Rokosh D, Liu TS (1999b) Changes in sand content of loess deposits along a north-south transect of the Chinese Loess Plateau and the implications for desert variations. Quaternary Research 52: 56-62

Dong GR, Gao QZ, Zou XY, Li BS, Yan MC (1995a) Climatic changes in the southern marginal zone of the Badain Jaran Desert since the late Pleistocene (in Chinese). Chinese Science Bulletin 40: 1214-1218

Dong GR, Chen HZ, Wang GY, Li XZ, Shao YJ, Jin JN (1995b) The evolution of deserts on northern China and its relationship with the climatic changes since 150 kyr. Science in China (Series D) 25: 1302-1312

Fan SX, Tong GB, Zheng HR (1998) Evolution of paleoclimate and plant community in the last 800 ka B. P. in Datong area (in Chinese). Journal of Geomechanics 4: 64-68

Fang XM, Li JJ, Derbyshire E, Fitzpatrick EA, Kemp RA (1994) Micromorphology of the Beiyuan loess paleosol sequence in Gansu Province, China: Geomorphological and paleoenvironmental significance. Palaeogeography, Palaeoclimatology, Palaeoecology 111: 289-303

Fang XM, Chen FB, Shi YF, Li JJ (1996) Ganzi loess and the evolution of the cryosphere on the Tibetan Plateau (in Chinese). Journal of Glaciology and Geocryology 18: 193-200

Fang XM, Banerjee S, Van Der Voo R (1998) Last interglacial sharp monsoon fluctuations: Rock magnetic and paleomagnetic evidence from high resolution loess-paleosol sequence, Lanzhou, China. PAGES Newsletter 6: 6

Forman SL (1991) Late Pleistocene chronology of loess deposition near Luochuan, China. Quaternary Research 36: 19-28

Gallet S, Jahn BM, Torii M (1996) Geochemical characterization of the Luochuan loess-paleosol sequence, China, and paleoclimatic implications. Chemical Geology 133: 67-88

Gu ZY, Liu TS, Zheng SH (1987) A preliminary study on quartz oxygen isotope in Chinese loess and soils. In: Liu TS (ed) Aspects of Loess Research. China Ocean Press, Beijing, China, pp 291-302

Gu ZY, Liu RM, Liu Y (1991) Response of the stable isotopic composition of loess-paleosol carbonate to paleoenvironmental changes (in Chinese). In: Liu TS (ed) Loess, Environment and Global Change. Science Press, Beijing, China, pp 82-92

Guo ZT, Fedoroff N (1991) Paleoclimatic and stratigraphic implications of the paleosol S1 in the loess sequence in China. In: Liu TS (ed) Loess, Environment and Global Change. Science Press, Beijing, China, pp 187-198

Guo ZT, Fedoroff N, An ZS (1991) Genetic types of the Holocene soil and the Pleistocene paleosols in the Xifeng loess section in central China (in Chinese). In: Liu TS (ed) Loess, Environment and Global Change. Science Press, Beijing, China, pp 93-111

Guo ZT, Fedoroff N, An ZS, Liu TS (1993) Interglacial dustfall and origin of iron oxides-hydroxides in the paleosols of the Xifeng loess section, China. Scientia Geologica Sinica 2: 91-100

Guo ZT, Ding ZL, Liu DS, Liu TS (1996a) Pedosedimentary events in loess of China and Quaternary climatic cycles. Chinese Science Bulletin 41: 1189-1193

Guo ZT, Fedoroff N, Liu DS (1996b) Micromorphology of the loess-paleosol sequence of the last 130 ka in China and paleoclimatic events. Science in China (Series D) 39: 468-477

Guo Z, Liu T, Guiot J, Wu N, Lu H, Han J, Liu J, Gu Z (1996c) High frequency pulses of East Asian monsoon climate in the last two glaciations: link with the North Atlantic. Climate Dynamics 12: 701-709

Guo ZT, Liu TS, Fedoroff N, Wei LY, Ding ZL, Wu NQ, Lu HY, Jiang WY, An ZS (1998) Climate extremes in loess of China coupled with the strength of deep-water formation in the North Atlantic. Global and Planetary Change 18: 113-128

Han JM, Hus JJ, Paepe R, Vandenberghe RE, Liu TS (1991a) The rock magnetic properties of the Malan and Lishi Formation in the loess Plateau of China. In: Liu TS (ed) Loess, Environment and Global Change. Science Press, Beijing, China, pp 33-47

Han JM, Hus JJ, Liu TS, Paepe R, Vandenberghe RE (1991b) Magnetic properties of the Malan and Lishi Formations (in Chinese). Quaternary Sciences 1991: 310-325

Han JM, Jiang WY (1999) Particle size contributions to bulk magnetic susceptibility in Chinese loess and paleosol. Quaternary International 62: 103-110

Heller F, Liu TS (1982) Magnetostratigraphical dating of loess deposits in China. Nature 300: 431-433

Heller F, Liu TS (1984) Magnetism of Chinese loess deposits. Geophysical Journal of the Royal Astronomical Society 77: 125-141

Heller F, Meili B, Wang JD, Li HM, Liu TS (1987) Magnetization and sedimentation history of loess in the central Loess Plateau of China. In: Liu TS (ed) Aspects of Loess Research. China Ocean Press, Beijing, pp 147-163

Jia LP (1965) A discovery of Lantian skull and stratigraphy from which it came (in Chinese). Kexue Tongbo 6: 477-481

Jia LP (1966) The Cenozoic formation in Lantian of Shaanxi Province (in Chinese). In: Proceedings of field symposium on Lantian Cenozoic in Shaanxi Province. Science Press, Beijing, China, pp 1-31

Jiang FC, Wu XH, Sun DH, Xiao HG, Wang SM, An ZS, Tian GQ, Liu K, Yin WD, Xue B (1998) Mangshan loess section in Central China (in Chinese). Journal of Geomechanics 4: 12-18

Jiang FC, Wu XH, Xiao HG, Xue B, Wang SM, Sun DH, An ZS (1999) Mangshan loess in China central plains and the coupling effect between tectonics and climate (in Chinese). Marine Geology and Quaternary Geology 19: 45-51

Jin HL, Dong GR, Liu YQ, Zhang CL (1998) The sandfield evolution and climatic changes in the middle course area of Yarlung Zangbo River in Tibet, China since 0.80 Ma B. P. (in Chinese). Journal of Desert Research 18: 97-104

Kang JC, Li JJ (1993) The 150,000-year environmental records of loess sections near Linxia, Gansu Province (in Chinese). Geological Review 39: 165-175

Kemp RA, Derbyshire E, Meng XM, Chen FH, Pan BT (1995) Pedosedimentary reconstruction of a thick loess-paleosol sequence near Lanzhou in north-central China. Quaternary Research 43: 30-45

Kemp RA, Derbyshire E, Meng XM (1997) Micromorphological variation of the S1 paleosol across northwest China. Catena 31: 77-90

Kukla G (1987a) Loess stratigraphy in Central China. Quaternary Science Reviews 6: 191-219

Kukla G (1987b) Correlation of Chinese, European and American loess series with deep-sea sediments. In: Liu TS (ed) Aspects of Loess Research. China Ocean Press, Beijing, China, pp 27-38

Kukla G, An Z (1989) Loess stratigraphy in central China. Palaeogeography, Palaeoclimatology, Palaeoecology 72: 203-225

Lei XY (1992) Stratigraphic division, microfabric and mechanical characteristics of the late Pleistocene loess in the southern Loess Plateau of China (in Chinese). Quaternary Sciences 1992: 128-135

Lei XY (1998) Preliminary studies on origin and grain size of Qinling loess (in Chinese). Acta Geologica Sinica 72: 178-187

Li JJ, Zhu JJ, Kang JC, Chen FH, Fang XM, Mu DF, Cao JX, Tang LY, Zhang YT, Pan BT (1990) Correlation between the loess record near Lanzhou and the Vostok ice core during the last glacial-interglacial cycle (in Chinese). Science in China (Series B) 10: 1086-1094

Li JJ, Zhu JJ, Kang JC, Chen FH, Fang XM, Mu DF, Cao JX, Tang LY, Zhang YT, Pan BT (1992a) The comparison of Lanzhou loess profile with Vostok ice core in Antarctica over the last glaciation cycle. Science in China (Series B) 35: 476-488

Li XS, Yang DY, Lu HY, Han HY (1997) Climatic changes inferred from grain size variations of aeolian sequences in South Anhui Province (in Chinese). Marine Geology and Quaternary Geology 17: 74-81

Li Z, Ma HZ, Zeng YN (1992b) A preliminary study on the Dadunling loess profile of Xining (in Chinese). Qinghai Geology 1: 26-31

Li ZH, Wang YH (1998) The geochemical records and the palaeoclimatic changes of loess deposits (in Chinese). Marine Geology and Quaternary Geology 18: 41-47

Lin BH, Liu RM, An ZS (1991) Preliminary research on stable isotopic compositions of Chinese loess (in Chinese). In: Liu TS (ed) Loess, Environment and Global Change. Science Press, Beijing, China, pp 124-131

Liu JF, Su Y (1994) Changes of vegetation and climate during the last 0.8 Ma in Pingling, Gansu Province (in Chinese). Geographical Research 13: 90-97

Liu JQ, Chen TM, Nie GZ, Song CY, Guo ZT, Li K, Gao SJ, Qiao YL, Ma ZB (1994) Datings and reconstruction of the high resolution time series in the Weinan loess section of the last 150,000 years (in Chinese). Quaternary Sciences 1994: 193-202

Liu TS (1964) Loess on the Middle Reaches of the Yellow River (in Chinese). Science Press, Beijing, China, pp 234

Liu TS, Ding ML (1984) A tentative chronological correlation of early human fossil horizons in China with the loess-deep sea records (in Chinese). Acta Anthroplogica Sinica 3: 93-101

Liu TS, Yuan BY (1987) Paleoclimatic cycles in northern China (Luochuan loess section and its environmental implications). In: Liu TS (ed) Aspects of Loess Research. China Ocean Press, Beijing, China, pp 1-26

Liu TS, Ding ZL (1993) Stepwise coupling of monsoon circulations to global ice volume variations during the late Cenozoic. Global and Planetary Change 7: 119-130

Liu TS, Guo ZT, Liu JQ, Han JM, Ding ZL, Gu ZY, Wu NQ (1995) Variations of eastern Asian monsoon over the last 140,000 Years. Bulletin de la Societé Geologique de France 166: 221-229

Liu XM, Liu TS, Xu TC, Liu C, Chen MY (1987) A preliminary study on magnetostratigraphy of a loess profile in Xifeng area, Gansu Province. In: Liu TS (ed) Aspects of Loess Research. China Ocean Press, Beijing, China, pp 164-174

Liu XM, Liu TS, Xu TC, Liu C, Chen MY (1988) The Chinese loess in Xifeng .1. the primary study on magnetostratigraphy of a loess profile in Xifeng area, Gansu Province. Geophysical Journal-Oxford 92: 345-348

Liu XM, Liu TS, Shaw J, Heller F, Xu TC, Yuan BY (1991) Paleomagnetic and paleoclimatic studies of Chinese loess (in Chinese). In: Liu TS (ed) Loess, Environment and Global Change. Science Press, Beijing, China, pp 61-81

Liu XM, Rolph T, Bloemendal J, Shaw J, Liu TS (1994b) Remanence characteristics of different magnetic grain-size categories at Xifeng, central Chinese loess plateau. Quaternary Research 42: 162-165

Lu HY, Wu NQ, Nie GZ, Wang YJ (1991) Phytolith in loess and its bearing on paleovegetation (in Chinese). In: Liu TS (ed) Loess, Environment and Global Change. Science Press, Beijing, China, pp 112-123

Lu YC (1981) Pleistocene climatic cycles and variation of $CaCO_3$ contents in a loess profile. Scientia Geologica Sinica 2: 122-131

Lu YC, Prescott JR, Robertson GB, Hutton JT (1987a) Thermoluminescence dating of the Malan loess at Zhaitang, China. Geology 15: 603-605

Lu YC, Prescott JR, Hutton JT (1987b) Thermoluminescence dating of the Zhaitang section of the Malan Loess, China (in Chinese). In: Liu TS (ed) Aspects of Loess Research. China Ocean Press, Beijing, China, pp 259-273

Lu YC, Zhang JZ, Xie J (1988) Thermoluminescence dating of loess and palaeosols from the Lantian section, Shaanxi Province, China. Quaternary Science Reviews 7: 245-250

Lu YC, Zhao H (1991) Thermoluminescence dating for loess at Jiezicun, Weinan, Shaaxi Province (in Chinese). Geological Review 37: 356-362

Ma XH, Qian F, Li P, Ju WQ (1978) Paleomagnetic dating of Lantian Man (in Chinese). Vertebrate PalAsiatica 16: 238-243

Maher BA, Thompson R (1991) Mineral magnetic record of the Chinese loess and paleosols. Geology 19: 3-6

Musson FM, Clarke ML, Wintle AG (1994) Luminescence dating of loess from the Liujiapo section, central China. Quaternary Science Reviews 13: 407-410

Porter SC, An ZS (1995) Correlation between climate events in the North Atlantic and China during the last glaciation. Nature 375: 305-308

Ren JZ (1996) Late Quaternary climate instability in east Asia recorded in Chinese loess (in Chinese). Ph.D. thesis, Chinese Academy of Sciences, Beijing, China, pp 54-85

Ren JZ, An ZS, Head J (1996) The environmental evolution in Longxi Basin during the last 13 kyr (in Chinese). In: Liu TS, An ZS, Wu XJ (ed) Loess, Quaternary and Global Change. Science Press, Beijing, China, pp 90-98

Rutter N, Ding ZL, Evans ME, Liu TS (1991) Baoji-type pedostratigraphic section, Loess Plateau, north-central China. Quaternary Science Reviews 10: 1-22

Rutter N (1992 XIII INQUA Congress 1991-Chinese loess and global change-Presidential address. Quaternary Science Reviews 11: 275-281

Rutter N, Ding ZL (1993) Paleoclimates and monsoon variations interpreted from micromorphogenic features of the Baoji paleosols, China. Quaternary Science Reviews 12: 853-862

Shen CD, Liu TS, Beer J, Oeschger H, Bonani H, Suter G, Wolfli W (1987) ^{10}Be in loess. In: Liu TS (ed) Aspects of Loess Research. China Ocean Press, Beijing, China, pp 277-282

Shen CD, Beer J, Liu TS, Oeschger H, Bonani G, Suter M, Wolfli W (1991) ^{10}Be in loess. In: Liu TS (ed) Loess, Environment and Global Change. Science Press, Beijing, China, pp 48-60

Shi N, Liu, HF, Lu, WS (1994) Study of magnetism on Wangning red loam section in Yushe Basin, Shanxi Province: Its age and sedimentary environment (in Chinese). Quaternary Sciences 1994: 183-191

Sun DH, Zhou J, Jiang FC, Porter SC (1995) Preliminary study on the summer monsoon variations on the Loess Plateau since the last interglacial period. Chinese Science Bulletin 40: 1873-1876

Sun JM (1994) Paleoenvironmental reconstruction in the desert-loess transitional zone of north China (in Chinese). Ph. D. thesis, Chinese Academy of Sciences, Beijing, China, pp 97-99

Sun JM, Ding ZL (1997) Spatial and temporal changes of dry and wet climate during the last 130,000 years in the Loess Plateau (in Chinese). Quaternary Sciences 1997: 168-175

Sun JM, Ding ZL (1998) Deposits and soils of the past 130,000 years at the desert-loess transition in northern China. Quaternary Research 50: 148-156

Sun JM, Yin GM, Ding ZL, Liu TS, Chen J (1998) Thermoluminescence chronology of sand profiles in the Mu Us Desert, China. Palaeogeography, Palaeoclimatology, Palaeoecology 144: 225-233

Sun JM, Ding ZL, Liu TS, Rokosh D, Rutter N (1999) 580,000 year environmental reconstruction for eolian deposits at the Mu Us desert margin, China. Quaternary Science Reviews 18: 1351-1364

Teng ZH (1998) Loess sequences and environment evolution on the southern bank of Yellow River between Zhengzhou and Luoyang (in Chinese). In: An ZS (ed) Loess, Yellow River and Yellow River Culture. Yellow River Hydrology Press, Zhengzhou, China, pp 8-12

Wang YY, Hsueh HH, Ho JC, Chang KW (1966) Quaternary stratigraphy of northern Shanxi and eastern Gansu loess district (in Chinese). Acta Geologica Sinica 46: 102-117

Wang YY, Li P, Wu ZB, Yue LP, Ja WM (1978) The date of formation of loess in Lanzhou on the base of palaeomagnetic analysis (in Chinese). Geological Science and Geotechnical Journal 4: 76-81

Wang YY (1982) Loess and Quaternary Geology (in Chinese). People´s Press, Shaanxi, China, pp 20-47

Wei LY, Cui JX, Lu YC (1991) A preliminary study of the physicomechanic properties of loesses and paleosols of different ages at Weibei Yuan, Shaanxi Province. In: Liu TS (ed) Loess, Environment and Global Change. Science Press, Beijing, China, pp 245-259

Wen QZ (1982) Loess in the Longxi Basin, Gansu Province (in Chinese). Geography Science 2: 202-209

Wen QZ, Zheng HH (1987) Paleoclimatic records in the loess section of North Xinjiang, China. In: Liu TS (ed) Aspects of Loess Research. China Ocean Press, Beijing, China, pp 59-69

Woo JK (1964) Mandible of the *sinanthropus*-type discovered at Lantian, Shensi (in Chinese). Vertebrate PalAsiatica 8: 1-17

Woo JK (1966) The Hominid skull of Lantian, Shensi (in Chinese). Vertebrate PalAsiatica 10: 1-22

Xiao HG, Jiang FC, Wu XH, Tian GQ, Liu K (1998) Loess stratigraphy in the region of San Men Xia (in Chinese). In: An ZS (ed) Loess, Yellow River and Yellow River Culture. Yellow River Hydrology Press, Zhengzhou, China, pp 1-7

Xu L, Liu TS, Chen MY, Maher BA, Banerjee SK (1991) Origin of magnetic minerals and magnetic susceptibility variations in Chinese loess. In: Liu TS (ed) Loess, Environment and Global Change. Science Press, Beijing, China, pp 279-288

Yang DY, Han HY, Zhou LF (1991) Eolian deposit and environmental change of Middle-Late Pleistocene in Xuancheng, Anhui Province south of the lower reachs of the Changjiang River (in Chinese). Marine Geology and Quaternary Geology 11: 97-103

Yu ZW, Nie GZ, Ding ZL (1991) Application of the walsh transform to periodicity analysis of loess-paleosol sequence. In: Liu TS (ed) Loess, Environment and Global Change. Science Press, Beijing, China, pp 235-244

Yuan BY, Bater B, Chai JJ, Cui JX (1987) The division of the paleoclimatic cycles of Luochuan loess section by the reflective spectrum. In: Liu TS (ed) Aspects of Loess Research. China Ocean Press, Beijing, China, pp 322-327

Yue LP (1989) Study on magnetostratigraphy of Duanjiapo loess section (in Chinese). Geological Review 35: 479-488

Zhang JX, Cai ML, Zhang ZQ, Wang YJ (1994) The preliminary studies on the paleoclimate records of Xiashu Loess, Nanjing (in Chinese). Jiangsu Geology 18: 189-194

Zhang LY (1989) Landslide history and late Cenozoic environmental factors in the Sa Le Shan area, Dongxiang County, Gansu Province, China (in Chinese). Journal of Lanzhou University 25: 81-93

Zhang NX, Yuan BY (1987) Study on clay minerals in Luochuan section and their paleoenvironment significance. In: Liu TS (ed) Aspects of Loess Research. China Ocean Press, Beijing, China, pp 348-361

Zhao JB (1994) Development of the loess 'terrain' in Xi'an and Changwu (in Chinese). In: Zhao JB (ed) Quaternary Soils and Environment in Loess Area of Northwestern China. Shaanxi Science and Technology Press, Xi'an, China, pp 1-11

Zhao QG, Yang H (1995) A preliminary study on red earth and changes of Quaternary environment in south China (in Chinese). Quaternary Sciences 1995: 107-116

Zheng HB, An ZS, Shaw J, Liu TS (1991a) A detailed terrestrial geomagnetic record for the interval 0-5.0 Ma. In: Liu TS (ed) Loess, Environment and Global Change. Science Press, Beijing, China, pp 147-156

Zheng HB, Oldfield F, Yu LH, Shaw J, An ZS (1991b) The magnetic-properties of particle-sized samples from the Luo Chuan loess section: evidence for pedogenesis. Physics of the Earth and Planetary Interiors 68: 250-258

Zheng HH, Zhu ZY, Huang BL, Lu LC (1994) A study on loess geochronology of Shandong Peninsula and northern part of Jiangsu and Anhui Provinces (in Chinese). Marine Geology and Quaternary Geology 14: 63-68

Zhou LP, Shackleton NJ (1999) Misleading positions of geomagnetic reversal boundaries in Eurasian loess and implications for correlation between continental and marine sedimentary sequences. Earth and Planetary Science Letters 168: 117-130

Zhou WJ, An ZS (1991) ^{14}C chronology of Loess Plateau in China. In: Liu TS (ed) Quaternary Geology and Environment in China. Science Press, Beijing, China, pp 192-200

Zhou WJ, An ZS, Lin BH, Xiao JL, Zhang JZ, Xie J, Zhou MF (1992) Chronology of the Baxie loess profile and the history of monsoon climates in China between 17,000 and 6000 years BP. Radiocarbon 34: 818-825

Zhou WJ, An ZS, Head MJ (1994) Stratigraphic division of Holocene loess in China. Radiocarbon 36: 37-45

Zhou WJ, Donahue DJ, Porter SC, Jull TA, Li XQ, Stuiver M, An ZS, Matsumoto E, Dong GR (1996) Variability of monsoon climate in East Asia at the end of the last glaciation. Quaternary Research 46: 219-229

Zhou WJ, Donahue D, Jull AJ (1997) Radiocarbon AMS dating of pollen concentrated from eolian sediments: implications for monsoon climate change since the late Quaternary. Radiocarbon 39: 19-26

Zhu RX, Ding ZL, Nie GZ, Wei XF, Jin ZX (1991) Records of Matuyama-Brunhes transitional field from Xifeng, Gansu Province. In: Liu TS (ed) Loess, Environment and Global Change. Science Press, Beijing, China, pp 142-146